Presented Before the Division of Fuel Chemistry
American Chemical Society
Chicago, Ill., August 1964

The Production of Nonagglomerating Char from Caking Coal in a Continuous Fluid-Bed Reactor

A. J. Forney, R. F. Kenny, S. J. Gasior, and J. H. Field

U. S. Bureau of Mines, 4800 Forbes Avenue,
Pittsburgh, Pennsylvania 15213

INTRODUCTION

The goal of this investigation is to develop a method of producing a nonagglomerating fuel from strongly caking coals. This fuel then could be used in a fluidized-bed gasifier or hydrogenator to make methane. The strongly caking coals, found mainly in Eastern United States where the large market for gas exists, become plastic and cake when heated to gasification temperatures.

An earlier paper described a method of operating with a batch charge of coal in a fluid-bed system.[1/] The caking properties of Pittsburgh seam coal and other highly caking coals were destroyed at 400° to 425° C by fluidizing fine coal (18-100 mesh) with steam or nitrogen which contain at least 0.2 percent oxygen. In the batch system a thoroughly nonagglomerating char could be produced in about 5 minutes. The surface of the char was made noncaking in about 1 minute. It was found that the coal must be heated by the fluidizing gas and not through the reactor wall to avoid agglomerating in the pretreating vessel.

The criteria adopted to indicate that the pretreatment was successful in these continuous tests are:

1. Good fluidization must be maintained in the pretreating reactor at the temperature employed.

2. The free-swelling index (FSI) of the resulting char must be less than 2.

3. The char must be noncaking when subjected to a hydrogen treatment at 600° C.

All three conditions must be satisfied before the char is considered noncaking. The free-swelling index, while not a direct measurement of agglomeration properties, does indicate the change in this property. For example, the FSI of Pittsburgh seam coal, a high-volatile A bituminous coal, is about 8, and after successful pretreatment, less than 2.

To optimize the pretreatment, the following information was to be derived from the experiments with continuous feed of coal and discharge of char:

1. The minimum residence time of the coal.
2. The minimum temperature.
3. The minimum oxygen-to-coal feed ratio.
4. The minimum weight loss.
5. The optimum mesh size of coal.
6. The effect of pressure.
7. The quality of the offgas.

APPARATUS AND EXPERIMENTATION

The flowsheet of the continuous unit is shown in figure 1. Nitrogen or steam plus air was used as the fluidizing medium. Coal feed is semicontinuous in that the feeder delivers batches at the rate of about 8 to 20 per minute, producing a feed rate of 120 to 900 grams per hour. This coal is conveyed to the bottom of the reactor by the feed gas. The char is discharged from the lower side arm while the gases, tars, and dusts are discharged from the upper one. The reactor is a stainless steel tube of 1-inch diameter, with the expanded section at the top 2 inches in diameter. The 29-inch section containing the bed of coal is heated electrically. A manometer indicates the pressure drop developed over the coal bed. Because the height of the bed is fixed, the residence time of the coal depends on the rate of coal feed.

DISCUSSION OF RESULTS

More drastic pretreatment was required to destroy the caking properties of coal in the unit with continuous feed and discharge of solids than in comparable batch operations reported previously. Due to the back-mixing of fresh and treated material, some particles remain in the reaction zone a relatively short time and others for a much longer time. Thus the treatment must be severe enough to convert those particle which are in the reactor for a very short time.

Figure 2 shows the results of tests in which the temperature of the bed was varied from 410° to 450° C and the oxygen content of the inert gas used for pretreating was 1.4 and 2.3 percent during pretreatment. Nonagglomerating char was produced in only two of these tests. These employed an oxygen content of 2.3 percent and temperatures of 440° to 450° C, whereas only 0.2 percent oxygen in the fluidizing gas was needed in the batch tests. With a lower oxygen content of 1.4 percent, the chars produced at 440° C caked in the reactor. The higher oxygen content is necessary in the continuous tests because there is a constant feed of raw coal and a greater inventory of coal in the bed tests.

The reason the chars cake during pretreatment at the higher temperatures but not at the lower ones, as demonstrated in figure 2 by the 1.4-percent oxygen parameter, may be explained with the photographs of chars shown in figure 3. At 410° C the particles are discrete, but at 435° C the smaller particles stick to the larger ones. It is believed that more of the viscous,

tarry material exudes from the inside of the large particles at the higher temperature. Once the limited amount of oxygen in the gas has been consumed, there is none to oxidize this additional viscous material and the particles stick together. The smaller particles are rendered noncaking more rapidly than the larger particles, so they did not stick to each other, but only to the large particles.

Figure 4 shows the effect on the FSI of varying the residence time from 9 to 34 minutes while holding the oxygen-to-coal ratio constant at about 0.2 cubic foot per pound of coal. Temperature parameters were 420°, 430°, 440°, and 450° C. At this oxygen content, a minimum of about 25 minutes is needed to make noncaking char at 440° C. The time could not be decreased at this oxygen-to-coal ratio by increasing the temperature because at 450° C the char caked in the reactor during treatment. Figure 5 shows the same type plot using an oxygen-to-coal ratio of about 0.3. A residence time of only 7 minutes was adequate to render the coal noncaking at 440° C, and less than 7 minutes at 450° C.

As shown in figure 5, the percentage of volatile matter in the char decreases with increasing pretreatment temperature and residence time. At 14 minutes the volatile matter content of the char is 29 percent at 420° C, and is 23 percent at 450° C. After 34 minutes the volatile matter is 26 percent at 420° C and 21 percent at 450° C.

Since the char from Pittsburgh seam coal is noncaking when its FSI is decreased to 1-1/2, all the data yielding this FSI at 420°, 430°, and 440° C obtained at various residence times and oxygen-to-coal ratios were cross-plotted as shown in figure 6. If a residence time of 5 minutes is desired, the required oxygen-to-coal ratio is about 0.40 when operating at 430° C. Lower temperatures resulted in a much higher oxygen-to-coal ratio or a longer residence time.

Figure 7 shows the effect of temperature on the FSI and volatile matter of char from Pittsburgh seam coal for four different particle sizes at a constant residence time of 14 minutes. The oxygen-to-coal feed ratio was constant at 0.3 cubic foot oxygen per pound of coal. For the 18-48 mesh size the FSI decreased rapidly from 6-1/2 at 410° to 1 at 440° C. Lower free-swelling values were obtained with decreasing sizes of particles treated at similar temperatures; for example, for the 150-200 mesh the indices were 1 at 410° C and noncaking (NC) at 450° C. These results show how much more readily the finer coal sizes can be pretreated.

Loss of volatile matter is more rapid for the small particles than the coarser sizes. Also, as anticipated, the loss of volatiles increases with increasing temperatures. The loss of volatile matter of 18-48 and 48-100 mesh sizes for satisfactory decaking of coal is about 10 percent. This is roughly equivalent to the weight loss and to the loss in heating value of the coal.

Since the finer size particles require less drastic treatment, an attempt was made to show that the oxygen needed for pretreatment varied with the particle diameter. As shown in figure 8, the oxygen-to-coal ratio varied from 0.42 for the 18-48 mesh to 0.06 for the 150-200 mesh. This theory was partially successful, but the finer mesh sizes caked in the reactor when the bed temperature was raised above 430° C. The mesh sizes finer than 100 mesh were more difficult to fluidize.

Figure 9 shows the effect of temperature on the quality of offgas made during pretreatment with steam plus air. The oxygen-to-coal feed ratio was 0.4 cubic foot per pound. The quantity of methane and higher hydrocarbons increased with increasing temperatures. The yields of carbon oxides increased slightly, but the hydrogen yield remained constant at about 0.2 cc/gram. Similar results were obtained in the batch tests except that the yield of hydrogen (about 66 cc/gram in the batch tests) is lower in the continuous operation, probably because the oxygen needed to treat the coal reacted with the hydrogen.

Table 1 shows analysis of coal and chars used in the above tests. As in the batch tests, the oxygen content is greater in the raw coal than in the chars.

TABLE 1.- Analysis of coal and chars from the tests to study the effect of temperature on the offgas made during steam-air treatment of Pittsburgh seam coal of 48-100 mesh size

Analysis (as received)	Coal	Chars				
		410° C	420° C	430° C	440° C	450° C
Proximate, percent						
Moisture	1.5	0.1	0.1	0.3	0.0	0.3
Volatile matter	36.0	27.2	26.9	25.9	23.4	22.7
Fixed carbon	54.4	64.4	64.6	66.9	68.6	67.9
Ash	8.1	8.3	8.4	6.9	8.0	9.1
Ultimate, percent						
Hydrogen	5.2	4.5	4.4	4.4	4.2	4.1
Carbon	75.2	77.3	76.9	78.0	77.0	76.1
Nitrogen	1.5	1.6	1.3	1.6	1.6	1.6
Oxygen	7.9	6.4	7.1	7.4	7.4	7.2
Sulfur	2.1	1.9	1.9	1.7	1.8	1.9
Ash	8.1	8.3	8.4	6.9	8.0	9.1
Heating value, Btu/lb	13,410	--	13,240	13,470	--	13,130

The effect of pressure was studied at 1, 5, 10, and 20 atmospheres using steam plus air as the fluidizing gas. A mesh size of 150-200 was used so that a lower fluidization gas velocity could be employed. Generally there was no great change due to pressure. Using a fluidizing gas mixture of steam plus air with an oxygen-to-coal ratio of 0.3 cubic foot per pound at 430° C, as the pressure was increased the yield of carbon oxide gases decreased, but the hydrocarbon yield increased. The amount of coal throughput increased as the pressure was increased, but at a rate less than linearly. Again, as in the batch tests, the particles seemed to explode when the pressure was released, probably because trapped gas in the particles escaped on depressurization.

CONCLUSION

The tests have demonstrated the operability of a small-scale continuous unit designed to pretreat highly caking coal to remove its caking quality. The principal difference between results of continuous and batch operation is the need for a higher oxygen content of the feed gas in continuous flow. The minimum residence time required for the coal to be in the reactor is about 5 minutes at 430° C. About 0.4 cubic foot of oxygen is needed in the treating gas for each pound of coal to destroy the caking quality of Pittsburgh seam coal. Although the optimum mesh size is 18-100, finer mesh sizes permit less drastic treatment. However, finer mesh sizes are more difficult to fluidize. Minimum weight loss was 10 percent, which is equivalent to 10 percent loss of heating value of the original coal. The effect of pressure is negligible compared to atmospheric pressure. However, higher throughputs can be achieved at higher pressures.

Steam plus oxygen is the desired fluidizing medium if both the char and the offgas are to be utilized in a gasifier. This results in an advantage over other methods of treatment because the volatile matter evolved during the pretreatment is not removed from the system.

Reference Cited

1. Forney, A. J., R. F. Kenny, S. J Gasior, and J. H. Fiéld. The Destruction of the Caking Properties of Coal by Pretreatment in a Fluidized Bed. Ind. and Eng. Chem. Product Research and Development, v. 3, No. 1, March 1964, pp. 48-53.

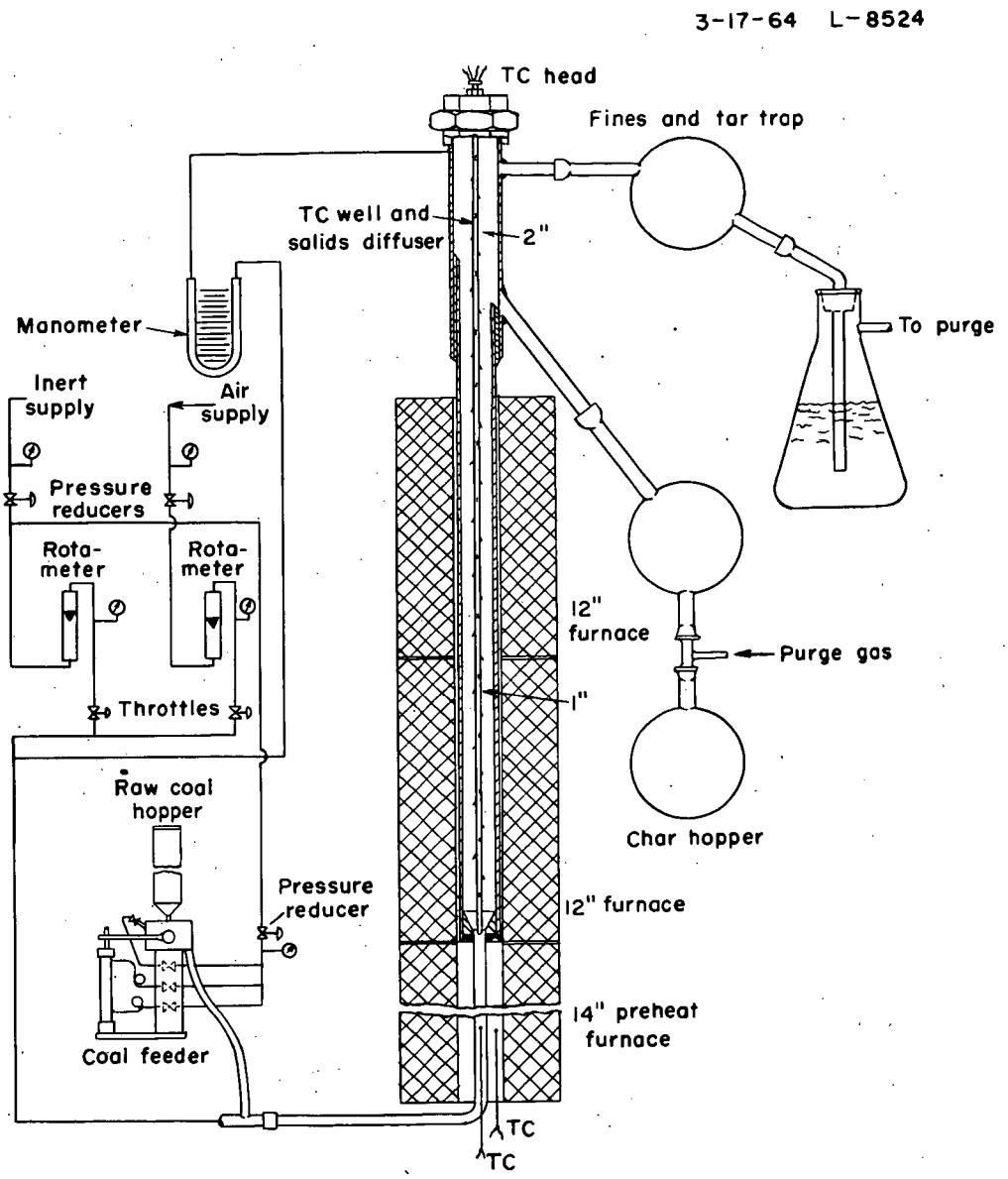

Figure 1. Continuous fluidized-bed coal pretreater.

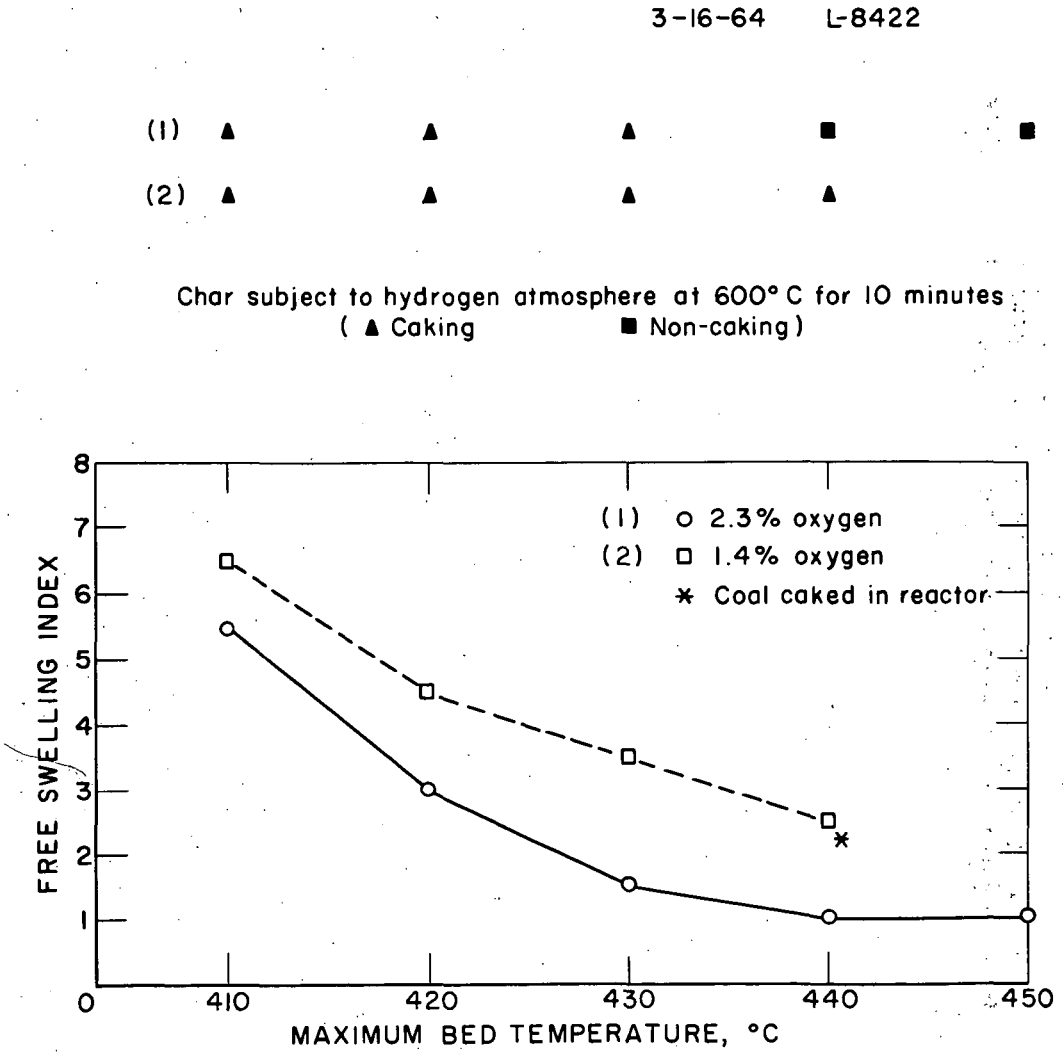

Figure 2. The effect of oxygen content of the fluidizing gas and of temperature on the caking properties of Pittsburgh seam coal (18-100 mesh). The fluidizing gas is inert gas with oxygen content as noted. The average residence time of the char in the reactor is 19 minutes.

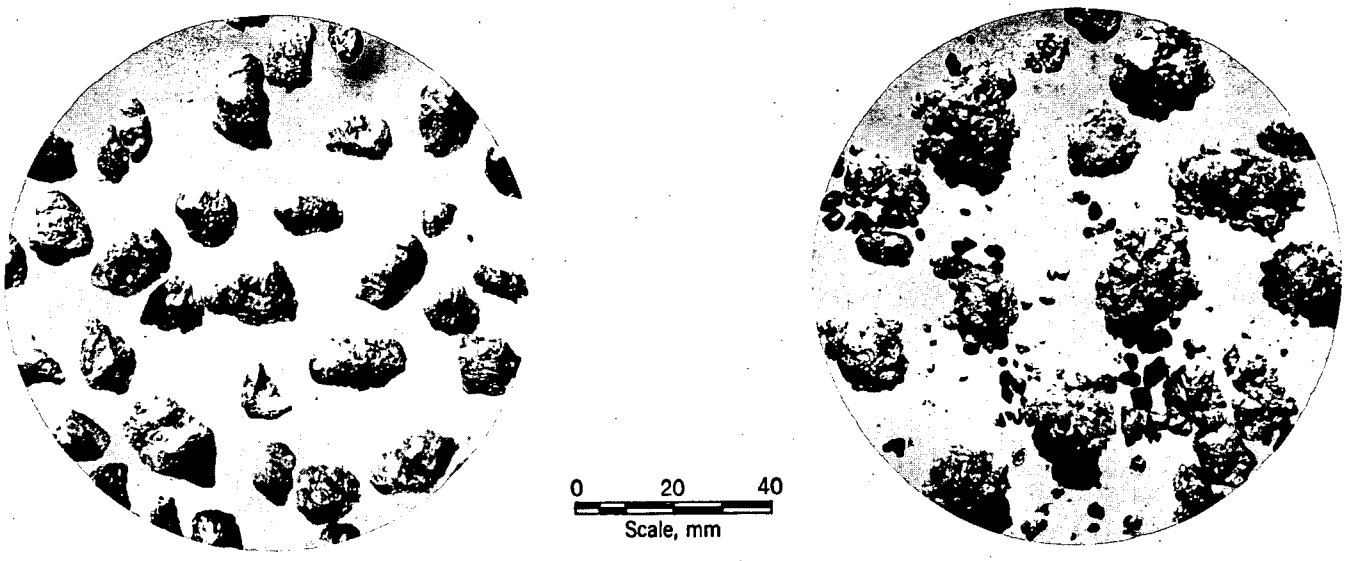

Figure 3. The effect of increased temperature on the caking property of char made from Pittsburgh seam coal (18-100 mesh), 1.4 percent oxygen in the feed gas.

H-91086-P

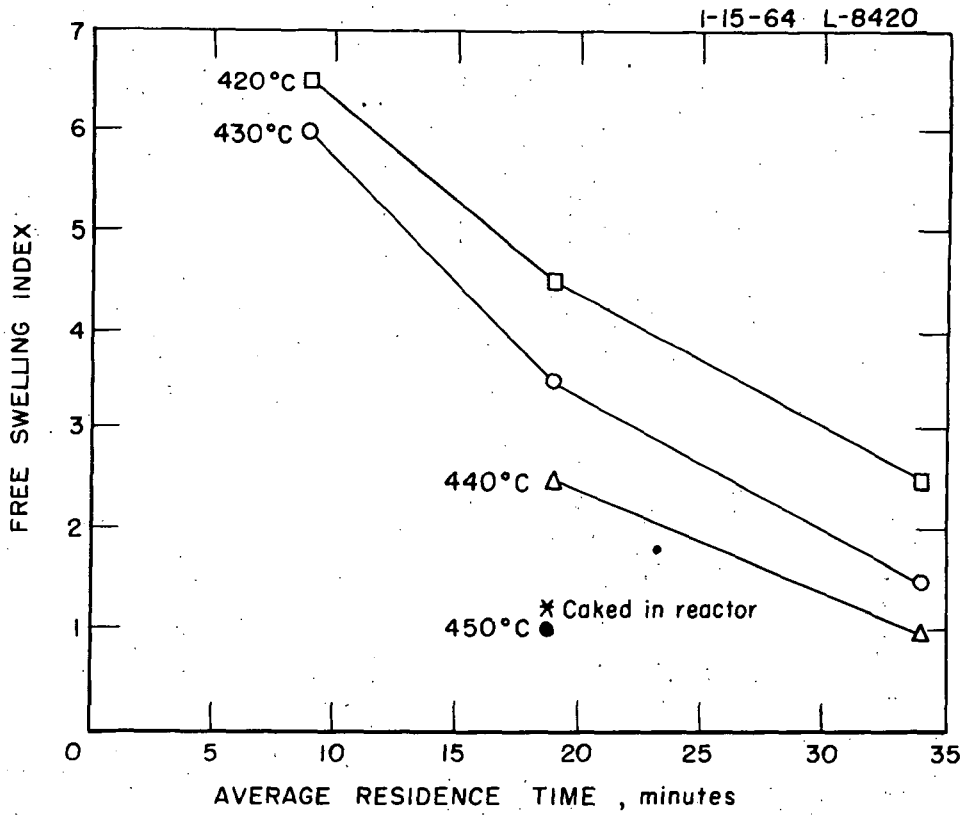

Figure 4. The effect of residence time and of temperature of pretreatment on the free-swelling index of char from Pittsburgh seam coal (18-100 mesh) 0.18-0.20 ft.^{3} oxygen/lb coal feed.

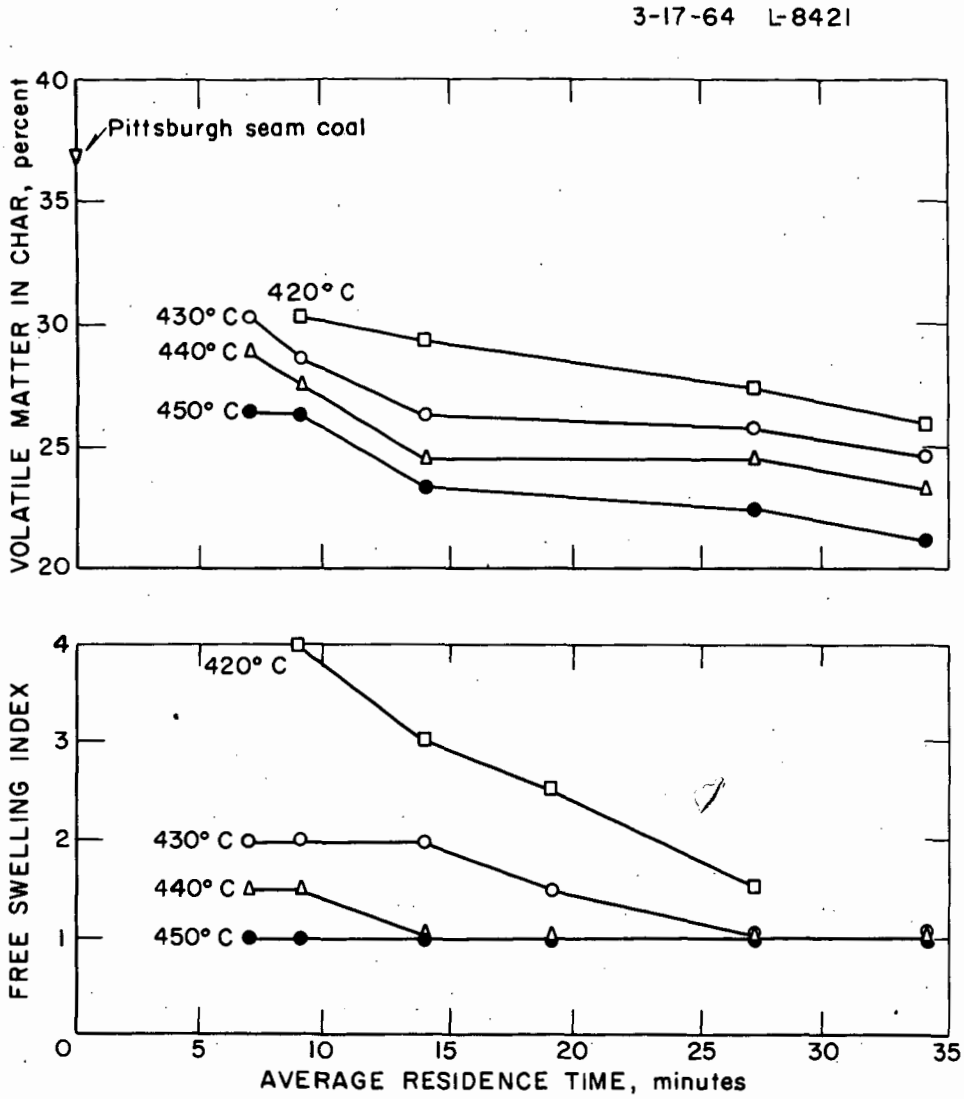

Figure 5. The effect of residence time and of temperature of pretreatment on the free-swelling index and the volatile matter of the char from Pittsburgh seam coal (18-100 mesh; 0.28-0.33 cu ft oxygen/lb coal feed).

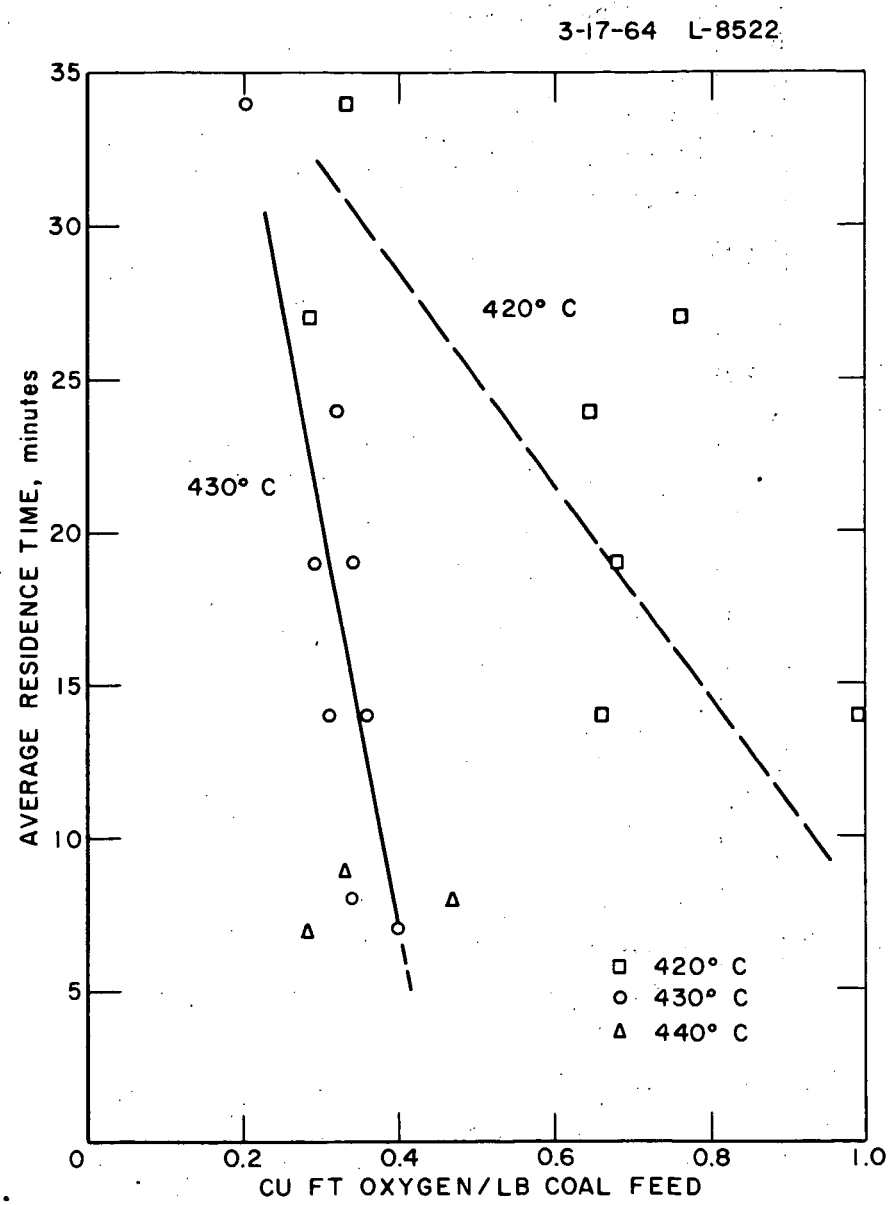

Figure 6. The effect of temperature and oxygen-coal ratio on the residence time of Pittsburgh seam coal of 18-100 mesh (FSI = 1-1/2).

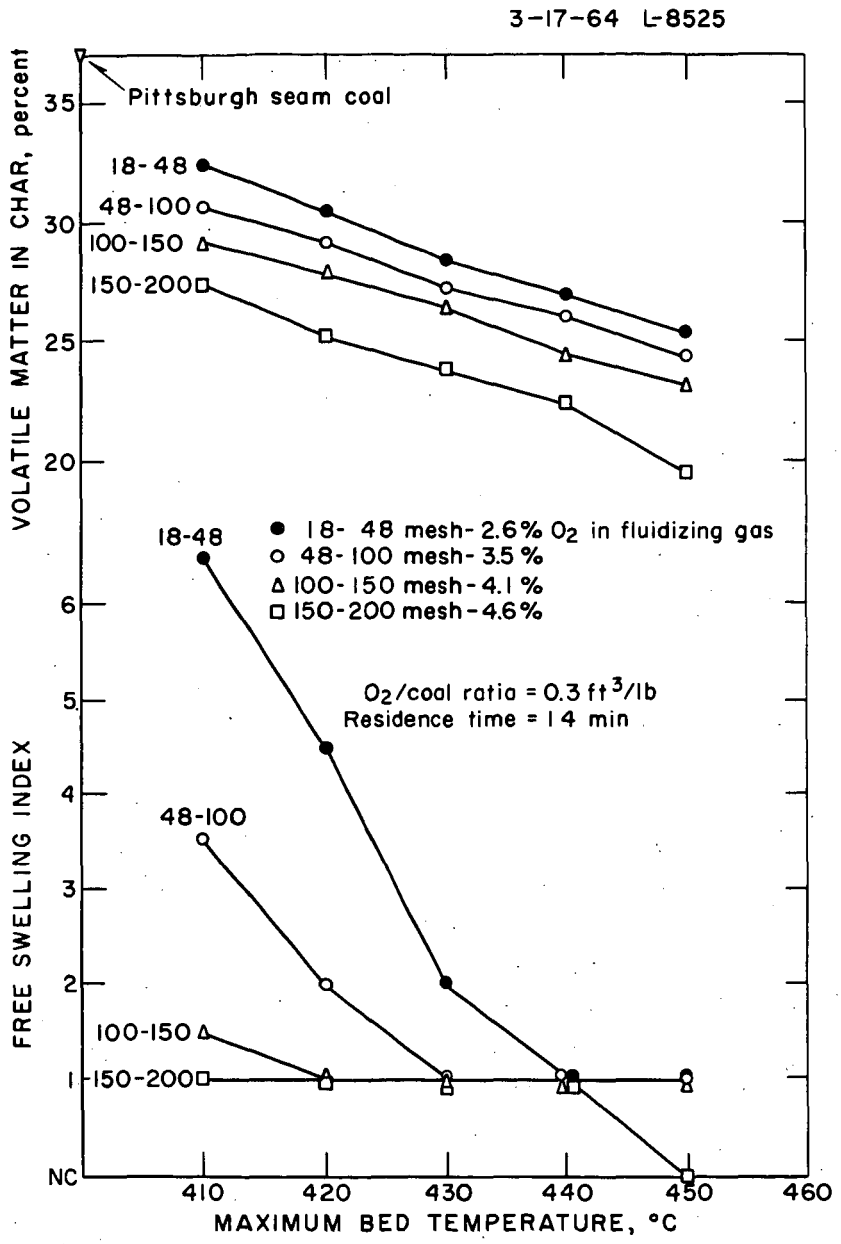

Figure 7. The effect of mesh-size and temperature on the free-swelling index and volatile matter content of the char made from Pittsburgh seam coal.

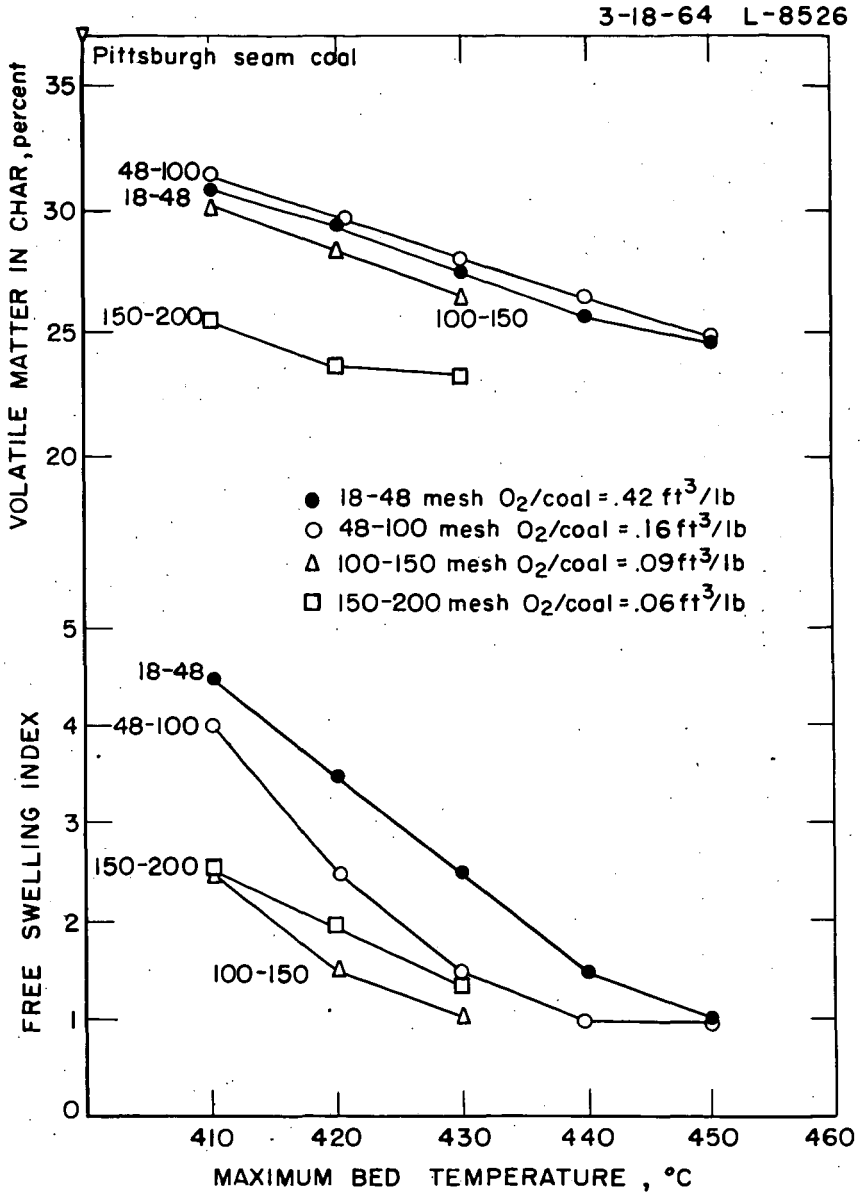

Figure 8. The effect of mesh size and temperature on the free-swelling index of char made from Pittsburgh seam coal. (The oxygen/coal feed ratio varied as noted; residence time is 14 minutes.)

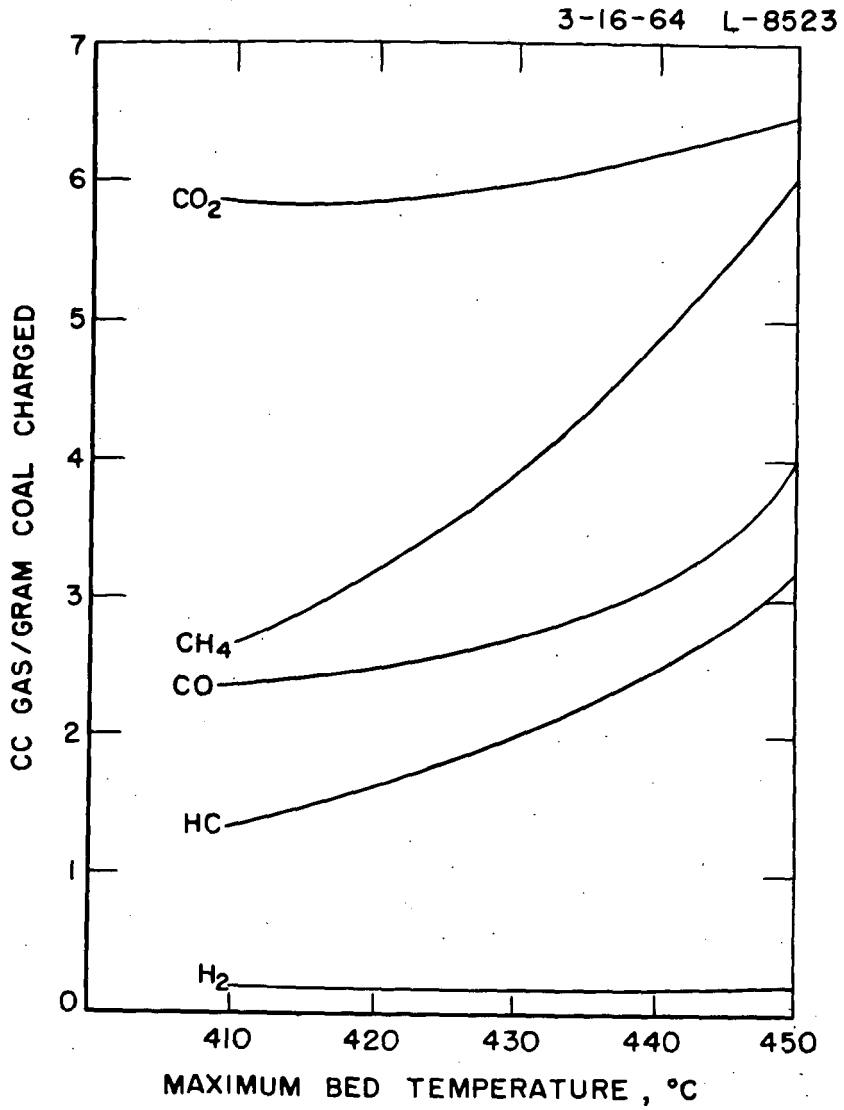

Figure 9. The effect of temperature on off gas made during steam-air treatment of Pittsburgh seam coal of 48-100 mesh (O_2-coal ratio = 0.4 cu ft/lb; residence time is 14 minutes).

Presented Before the Division of Fuel Chemistry
American Chemical Society
Chicago, Ill., August 30 - September 4, 1964

LABORATORY SCALE CARBONIZATION OF NORTH DAKOTA LIGNITE: INFLUENCE OF TEMPERATURE AND ATMOSPHERE ON PRODUCT DISTRIBUTION AND ACTIVITY

Robert B. Porter and Robert C. Ellman

U. S. Department of the Interior, Bureau of Mines
Grand Forks Lignite Research Laboratory
Grand Forks, N. Dak.

INTRODUCTION

The purpose of this investigation has been to study the effect of temperature and atmosphere on carbonization characteristics of lignite. An objective has been to produce a char with minimum sulfur and maximum reactivity toward air, with minimum loss of heating value. Research in carbonization has been extensive on higher rank solid fuels, including efforts to reduce sulfur and control reactivity of chars and cokes (1, 2). For North Dakota lignite, previous attention has been focused upon yield and composition of byproducts.

The considerable influence of atmosphere and temperature on the proportion of sulfur volatilized during carbonization of coal from Illinois and Indiana has been reported by Snow (3) and Mangelsdorf and Broughton (4). Significant differences in sulfur removal were found, depending upon atmosphere during carbonization. More recently, Draycott (5), of the University of Sydney, Australia, reported studies of desulfurization of metallurgical coke in a variety of atmospheres. Best desulfurization occurred at 1,000°C in oil gas with intermittent blasts of steam. Ninety-two percent of the sulfur was removed with a coke loss of about forty percent.

CARBONIZATION EQUIPMENT

The test apparatus was essentially a tube furnace with three separately controlled electric heaters to provide a reproducible and uniform temperature distribution within the unit during carbonization. The carbonization tube was constructed of 1-1/2-inch, schedule 40, stainless steel pipe. Three thermocouples were mounted in the 14-1/2-inch length which held the sample, a fourth in an end heater section, and a fifth was imbedded in the sample; these provided for temperature measurement and control. The tube was charged externally and then placed in the furnace.

The arrangement of the carbonization equipment, including the modifications for various atmospheres, is shown in figure 1. A collection train was provided for the byproduct tar, water, hydrogen sulfide, ammonia, light hydrocarbons, and gas.

PROCEDURE

Each charge consisted of 200 grams (0.441 lb) of lignite, sized 4 x 8 mesh, from the Kincaid mine, Burke County, North Dakota. Nitrogen was passed through the carbonization tube at the rate of 0.6 cubic feet per hour. In the tests in which

carbonization gas was recycled, its flow was regulated to give a superficial space velocity of one-half foot per second, and in the tests in which carbonization was done in a steam atmosphere, steam was injected at the rate of about 500 grams (1.102 lb) per hour. The average heating rate was 400°F per hour, and the sample was held at temperature for 2 hours.

All products except gas were weighed. Gas volume was measured, the gas analyzed, and the weight of the nitrogen-free gas calculated. The condensate contained most of the tar and water and part of the ammonia and hydrogen sulfide product. These components were separated, and their weights were added to those collected in the remainder of the product collection train.

In nitrogen and carbonization gas atmospheres, the test temperatures were 500°, 800°, 900°, 1,000°, 1,300°, and 1,700°F. Three individual tests were performed at each temperature for material balance plus one test to produce char for reactivity measurements.

For carbonization in steam, similar tests were performed at a lower range of temperatures, 500° to 1,100°F, at 100°F intervals because of the significant gasification that occurred at higher temperatures. Char for reactivity measurements was made at 1,200° and 1,300°F in steam, and for comparison purposes, in nitrogen atmosphere at 800°, 900°, and 1,000°F, using the same lignite feed sample.

LIGNITE FEED SAMPLES

Three different batches of lignite from the Kincaid mine were used in these tests. Feed number 1 was used for the nitrogen atmosphere material balance tests. Feed number 2 was used for the nitrogen atmosphere char production tests, and all of the tests in recycled carbonization gas atmosphere. Feed number 3 was used for steam atmosphere tests, and the three comparison tests that were made in nitrogen atmosphere. Analyses of these feeds are shown in table 1. The much higher sulfur content of feed number 3 is of special interest.

TABLE 1. - Analyses of lignite feed for carbonization experiments[1/]

Feed number	1	2	3
Proximate analysis, percent:			
Moisture	31.9	26.9	32.3
Volatile matter	26.6	29.5	29.6
Fixed carbon	32.2	34.7	30.6
Ash	9.3	8.9	7.5
Ultimate analysis, percent:			
Hydrogen	6.5	5.9	6.7
Carbon	42.7	46.7	44.2
Nitrogen	.4	.8	.7
Oxygen	40.7	37.3	38.8
Sulfur	.4	.4	2.1
Ash	9.3	8.9	7.5
Heating value, Btu/lb	7,200	7,780	7,660

1/ Kincaid lignite "as-charged."

PRODUCT YIELDS

The product yields obtained by carbonizing in nitrogen and carbonization gas atmospheres were very similar. As carbonization temperature increased, yields of gas, tar, and water product increased at the expense of the char; the rate of increase became less as temperature advanced. Product yields as a function of carbonization temperature are shown in figures 2 and 3.

The product yields obtained from steam carbonization, as shown in figure 4, were similar to the others below 900°F. Above this temperature the yield of char product continued to decline steeply with advancing temperature, and the yield of gas product increased very rapidly. Figure 5 compares the char yields obtained from nitrogen and steam carbonization to illustrate the effect of gasification.

TESTS OF CHARS

Crossing-Point Temperature

The reactivity of each char in air was determined in a crossing-point-temperature apparatus. The apparatus was constructed of a length of 1/2-inch stainless steel pipe placed in a small vertical tube furnace. A 1-1/2-inch deep charge sized 40 x 60 mesh was supported on a screen in the middle of the tube. The wall temperature and the temperature at the center of the charge were recorded. The wall temperature was increased at a rate of 27°F per minute, while air was diffused through the sample at the rate of 0.45 cubic feet per hour. The crossing-point temperature was defined as the temperature at which the inside temperature overtook the wall temperature which means the lower the crossing-point temperature the more reactive the char towards air.

The crossing-point temperatures for chars are shown in figure 6. The lowest crossing-point temperatures were found for the chars carbonized in the 800° to 1,000°F region. Both recycled carbonization gas and steam decrease char activity toward air. Char produced from feed number 3 gave higher crossing points than char produced from feed number 2 under similar conditions.

Acetic Acid Adsorption

The chars produced in steam atmosphere were tested for their ability to adsorb acetic acid. After evidence of soluble alkali in the chars was found, each char was treated in a Soxhlet extractor with water for 60 hours and then dried. The acetic acid adsorption test procedure was to mix a half gram of 40 x 60-mesh soluble-alkali-free char with 50 milliliters of 5 millinormal acetic acid in a closed container and shake mechanically for 2 hours. The final acid strength was determined, and an adsorption constant calculated. This constant was the ratio of acid concentration in the char to that in the liquid at equilibrium.

Figure 7 shows the acetic acid adsorption constants of the chars tested as functions of the carbonization temperatures. Activity shows a rapid increase as the carbonization temperature increases from 1,000°F.

Low crossing-point temperatures and low acetic acid adsorption constants occur in the same carbonization temperature region. These two types of activity seem to

be quite distinct. The opposite trends of the two char activities with carbonization temperature were confirmed by a statistical rank test.

Sulfur Removal Relationships

The criteria used for a well desulfurized char was low sulfur and high heating value. The sulfur content of the chars was therefore compared in this report on the basis of pounds of sulfur per million Btu. Figure 8 shows the sulfur contents of the various chars on this basis as a function of carbonization atmosphere and temperature.

The chars carbonized in nitrogen show the lowest sulfur content at 900°F carbonization temperature. The chars carbonized in recycled carbonization gas were similar except that the 900°F char was higher in sulfur than the 800° or 1,000°F chars.

The sulfur contents of the chars carbonized in steam were different: increasing from 500° to 700°F, dropping to 1,000°F, holding fairly constant to 1,200°F, and rising rapidly to 1,300°F. The higher sulfur in feed number 3 is reflected in the chars produced from it.

The criterion used for a good desulfurization process was a high ratio of sulfur loss to heating value loss. This function, the loss ratio, was obtained by dividing the percentage sulfur lost by the percentage Btu lost, and it depends upon the sulfur content and heating value of the feed, the char yield, and the sulfur content and heating value of the char produced.

The loss ratios as functions of carbonization atmosphere and temperature are shown in figure 9. The highest loss ratios were at 900°F for chars produced in nitrogen atmospheres and best at 800°F for chars produced in recycled carbonization gas. For chars produced in steam, two peaks were found, the highest loss ratio was at 500°F, and the second highest was at 1,000°F.

SUMMATION

The highest reactivities of chars toward air were found in chars produced by carbonizing in the region of 800° to 1,000°F. Carbonization in either recycled carbonization gas or steam produced chars less reactive than those carbonized in nitrogen.

The reactivity measured by acetic acid adsorption was not the same reactivity as that measured by crossing-point temperature. The acetic acid adsorption value varies with carbonization temperature in the opposite manner as compared to crossing-point values for the chars that were produced by carbonization in steam.

The lowest char sulfur content and highest loss ratio occurred at 900°F when carbonizing in a nitrogen atmosphere. For carbonization in recycled carbonization gas, the lowest sulfur content occurred at 1,000°F and the highest loss ratio at 800°F. The desulfurization by carbonizing in steam was quite different. The lowest sulfur content occurred at 1,200°F, the highest loss ratio was found at 500°F, and the next best at 1,000°F. Differences in lignite feed were reflected in the char produced, both in reactivity toward air and in sulfur removal.

REFERENCES

(1) Thiessen, Gilbert, Forms of Sulfur in Coal, Ch. in Chemistry of Coal Utilization, ed. by H. H. Lowry, John Wiley & Sons, New York, N. Y., 1, 425-449 (1945).

(2) Wilson, Philip J., Jr., and Clendenin, J. D., Low-Temperature Carbonization, Ch. in Chemistry of Coal Utilization, ed. by H. H. Lowry, John Wiley & Sons, New York, N. Y., Supp. v., 395-460 (1963).

(3) Snow, R. D., Conversion of Coal Sulfur to Volatile Sulfur Compounds During Carbonization in Streams of Gases, Ind. and Eng. Chem., 24 903-909 (1932).

(4) Mangelsdorf, A., and Broughton, F. B., Effect of Atmosphere on Desulfurization of Coal During Carbonization, Ind. and Eng. Chem., 24, 1136-1137 (1932).

(5) Draycott A., Production of Low Sulphur Coke from High Sulphur Coals. Chem. Ind. & Eng. 3, No. 7, 17-30 (1954).

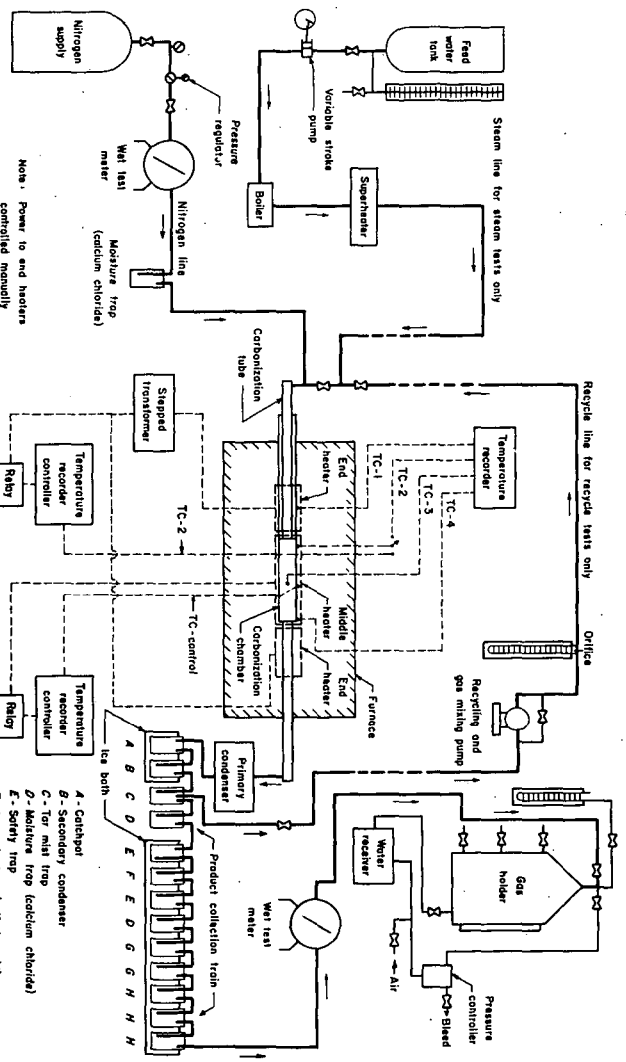

Fig 1 Flow sheet, carbonizer and auxiliary equipment.

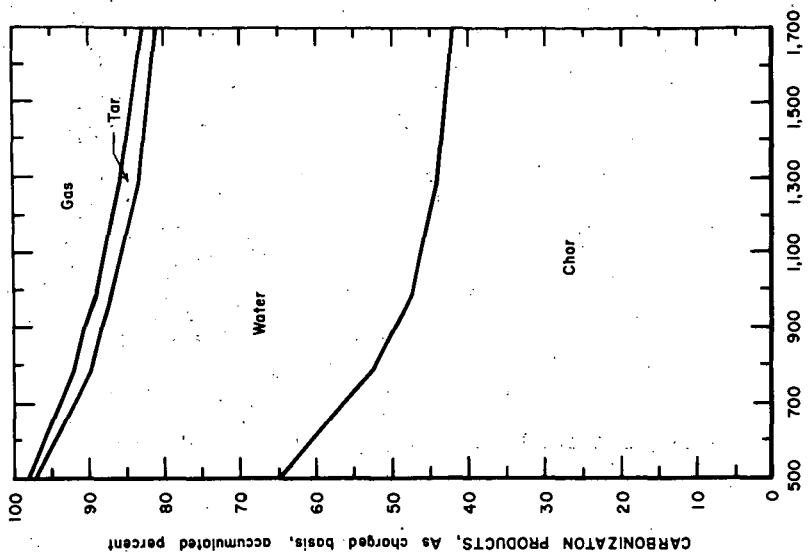

Fig 3 Product yields, carbonization in recycled carbonization gas atmosphere.

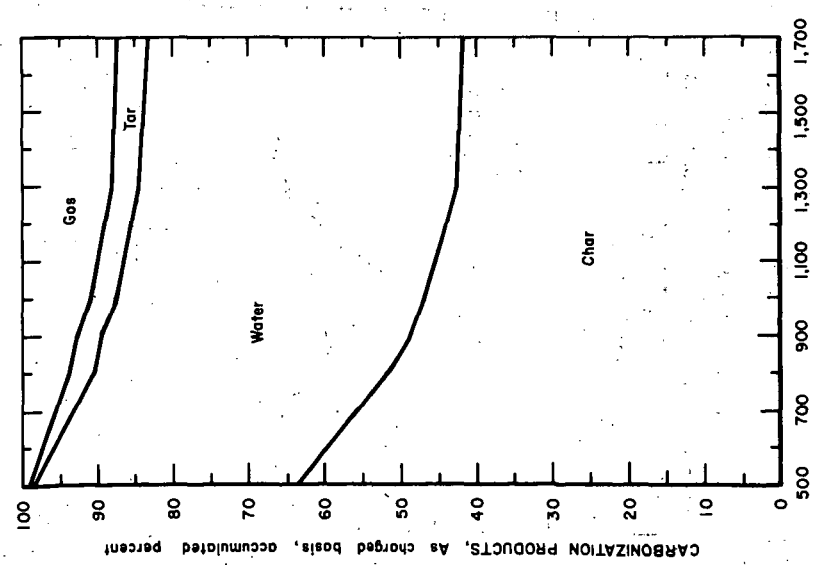

Fig 2 Product yields, carbonization in nitrogen atmosphere.

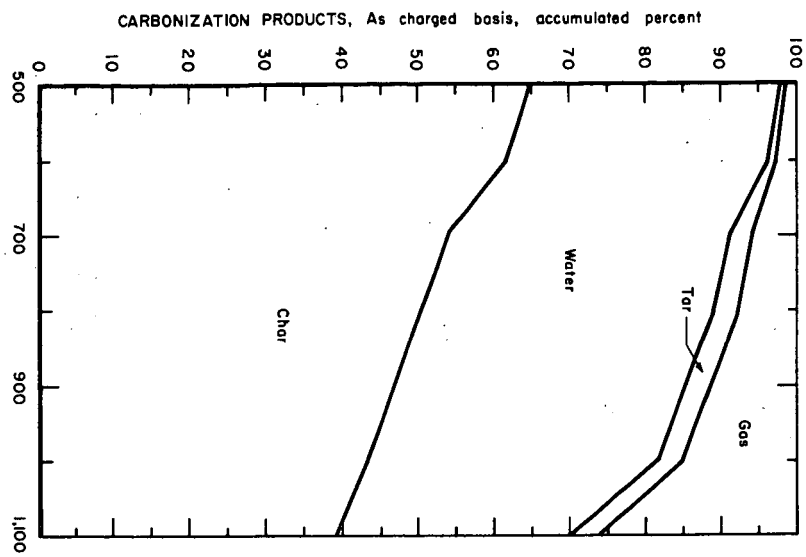

Fig. 4 Product yields, carbonization in steam atmosphere.

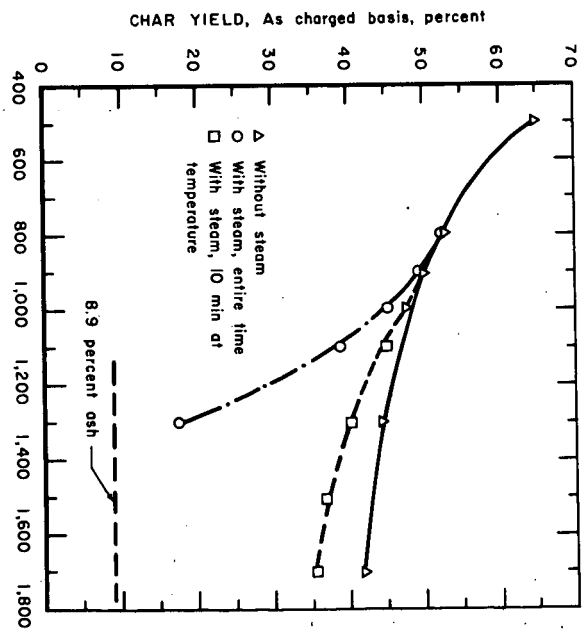

Fig 5 Effect of steam on char yield.

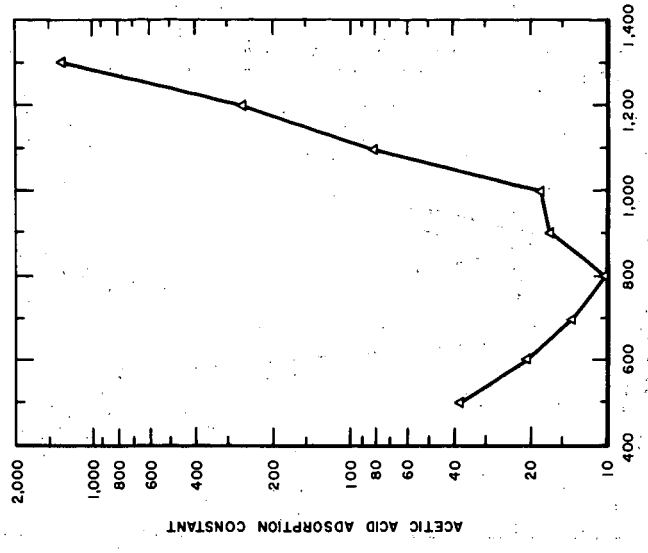

Fig 7 Acetic acid adsorption of chars as a function of carbonization temperature in steam atmosphere.

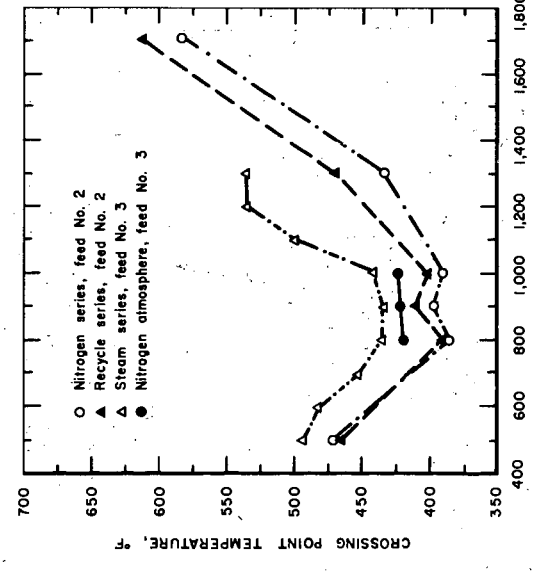

Fig 6 Crossing-point temperatures of chars as a function of carbonization temperature and atmosphere.

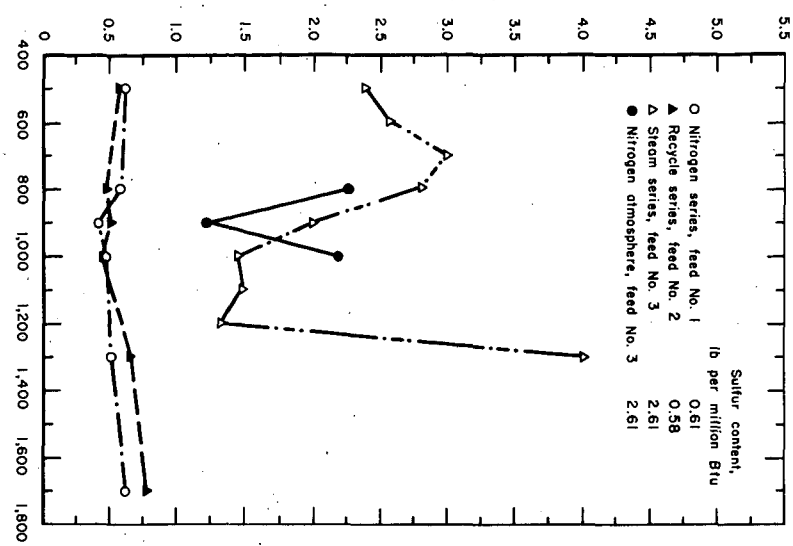

Fig 8 Sulfur contents of chars as a function of carbonization temperature and atmosphere.

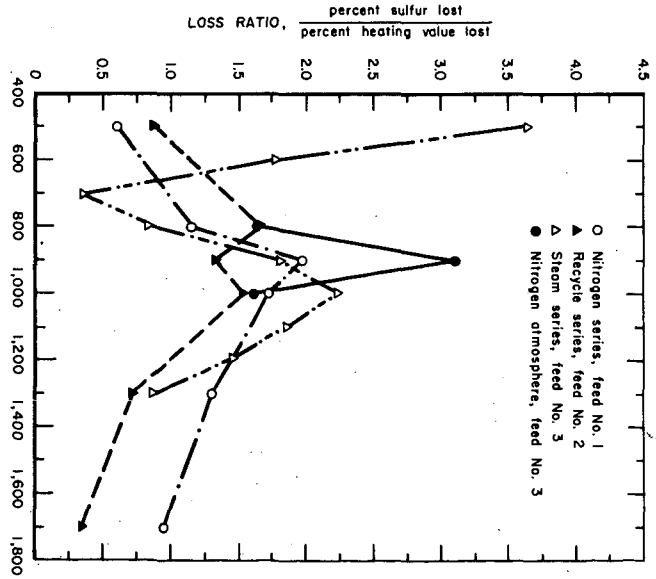

Fig 9 Sulfur-heating value loss ratio as a function of carbonization temperature and atmosphere.

Presented Before the Division of Fuel Chemistry
American Chemical Society
Chicago, Ill., August 30 - September 4, 1964

ETHYLENE AND AROMATICS BY CARBONIZATION OF CANNEL COAL

R. S. Montgomery and D. L. Decker

The Dow Chemical Company, Midland, Michigan

The low-temperature carbonization of coal is a possible alternative to the cracking of crude oil for the production of ethylene and aromatics. The previous investigations reported by this laboratory were concerned with the carbonization of lignites.[1] It was found that if lignites were carbonized at a low temperature in order to obtain the maximum yield of tar and this tar cracked without being allowed to condense, acceptable yields of ethylene, propylene and aromatics could be obtained. Once the low temperature tar is allowed to condense, however, large amounts of char and heavy residue are formed in the cracker and the yields of the desired products are small. It was concluded from this work that this process could be commercially important if the cost of crude oil increases enough to offset the high initial capital cost.

The present investigation was concerned with the use of West Virginia and Kentucky cannel coals in this process. Cannel coal is a high volatile, non-coking coal and occurs in lenticular pockets in bituminous coal beds. It was hoped that the higher yields which would certainly be obtained with these coals, and therefore the lower capital investment required for the same production, would more than offset the increased cost of the coal.

EXPERIMENTAL

Equipment

The equipment used in this work is very similar to that used in the earlier work. The evolved volatile matter passed from a batch carbonizer through the cracker into the collection train, which consisted of a water-jacketed receiver, condenser, and two low-temperature absorbers. These absorbers consisted of jacketed pyrex columns packed with steel wool. The noncondensable gas passed through a cotton trap and then through a wet-test gas meter, which measured the volume of the evolved gas. After leaving the wet-test gas meter, the gas passed into a solenoid-actuated valve which allowed a fraction of the gas to be collected in a gas holder. The remainder was vented to the atmosphere.

The carbonizer used in these experiments was similar to that used in the lignite experiments, except that it was modified so that superheated steam could be blown through the coal during carbonization. It was made from a two inch stainless steel pipe, 24 inches in length. Near the top of the retort, a one-half inch pipe was provided as a take-off for the volatile matter. A one inch plug fitted with a thermocouple well was used at the top of the carbonizer for the introduction of the coal. A removable steel sparger was provided at the bottom of the carbonizer for the introduction of the superheated steam and the removal of the char. Heat for the carbonizer was provided by electric furnaces controlled by means of Variacs.

The cracking reactors were 36 inches long and were fabricated of Vycor tubing of 31 mm outside diameter. A concentric 9 mm Vycor tube, through the entire length of the cracking tube, allowed a thermocouple to be placed inside the tube and the cracking temperature to be measured for any point in the tube. The cracking temperature was controlled by the temperature near the exit of the reactor. The cracker was heated with resistance tape wound directly on the tubing and the electric current controlled by a Variac. Different average retention times were obtained by using two, three or four of these reactors in series.

Coals Used

Samples of four different cannel coals were used in this work. Three were from West Virginia - Gay Mine, Logan County; Stollings Mine, Madison County; and Dorothy Mine, Boone County; one was from the Big Chief Mine, Letcher County, Kentucky. The samples which were received as 6 to 8 inch lumps were crushed, and the fraction which passed through a 3-1/2 mesh and remained on a 10 mesh screen was used in the experiments.

Table 1

Proximate Analysis	Gay	Stollings	Dorothy	Big Chief
Moisture	0.31%	0.56%	0.63%	0.46%
Net Volatile	48.46	54.86	61.05	53.07
Fixed Carbon	37.42	34.26	32.52	41.49
Ash	13.81	10.32	5.80	4.98
Ultimate Analysis				
Hydrogen	6.56	7.04	7.71	7.29
Carbon	74.52	74.79	78.84	80.96
Nitrogen	0.67	1.22	0.88	1.23
Sulfur	0.52	1.24	0.86	0.77
Oxygen	3.92	5.39	5.91	4.77
Fisher Assay				
Oil, gal/ton	85.8	90.6	104.2	86.5
Water, gal/ton	2.4	3.6	3.8	3.4
Gas and loss, %	9.1	9.2	10.9	6.7
Sp. Gr. oil 60/60°F	0.9056	0.9106	0.9079	0.9022

PROCEDURE

Cannel Coal (500 grams) was charged into the carbonizer and the cracker temperature brought up to the predetermined level. Then the temperature of the carbonizer was slowly and uniformly raised from room temperature to a maximum of 550°C. When the carbonizer reached 300°, superheated steam at 500° was introduced into it. After the experiment, the carbonizer was allowed to cool to room temperature and the train disassembled, and the contents of the receiver and two absorbers steam distilled. The steam-distilled oil was then fractionated, and the fractions examined by mass spectrometry. The residual oil and tar in the distillation pot plus any increase in weight of the absorbers was designated as

heavy oil. The volume of gas produced was measured with the wet-test gas meter and samples of the gas examined by mass spectrometry.

Exploratory experiments indicated that the primary process variables were cracking temperature, retention time and the steam-coal ratio. Therefore the effect of these three process variables at three different levels were investigated on the cannel coal from the Gay Mine, using nine experiments in a "Latin Square" arrangement. With this arrangement, the effect of a single variable can be determined with the effects, first order at least, of the other variables confounded or cancelled out. The levels of the process variables that were chosen were:

Cracking temperature - 800°, 850°, and 900°.

Average retention time - 0.5, 0.7, and 0.9 seconds.

Steam-to-coal ratio - 1.0, 1.25, and 1.5.

The "average retention time" deserves some comment. Since a batch carbonizer was used in these experiments, the rate of volatile generation in the carbonizer varied within rather wide limits as the carbonizer temperature was raised from 300° to 550°. Because of this, the gas velocity through the crackers, and therefore the retention time in the cracker also, varied within rather wide limits. "The average retention time" was calculated on the basis of the total volume of volatiles generated and volume of the crackers used in the experiment. These "average retention times" can only be used as guides; all that can be said for certain is that the retention times are in the ratios two, three and four.

Another problem which arises with regard to the interpretation of the effects of retention time is that the actual retention time is affected by the steam-coal ratio used. When more steam is passed through the carbonizer, the space velocity is increased, and therefore the retention time in the cracker correspondingly decreased. Because of this, the effects of average retention time and steam-coal ratio are interrelated despite the Latin Square arrangement of the data. This must be taken into account when interpreting the retention time data.

RESULTS

Analysis of the products obtained in these experiments makes it possible to evaluate the effects of the process variables on the yields of the various products. Since all of the volatile matter passed through the cracker, the volume and composition of the evolved gases and oils was affected by all the process variables, that is, cracking temperature, retention time, and steam-coal ratio. The character of the char produced, however, could only be affected by the steam-coal ratio.

Effect of Process Variables on Gas Produced

The composition of the gas evolved from the coal varies as different levels of the process variables are employed. Some constituents of the gas are affected greatly by the process variables, others, very little.

The chief components of the gas are ethylene, ethane, acetylene, propylene, butadiene, methane, hydrogen, and carbon monoxide and dioxide. These comprise at least 98% of the total gas produced.

The process variables have little or no effect on the total yield of gas, at least at the levels investigated. It might be expected that

the higher cracking temperatures and longer retention times would produce more gas, but this is not the case.

The yield of ethylene, too, is not particularly affected by the process variables. However, the best yield was produced at a cracking temperature of 850°, an average retention time of 0.5 seconds, and a steam-coal ratio of 1.25.

The lowest cracking temperature and the shortest retention time investigated result in the production of the largest amount of ethane. Apparently more of the ethane is converted to ethylene at the more rigorous cracking conditions. At a cracking temperature of 800°, 24.8 pounds/ton is obtained, while at 900°, only 9.9 pounds/ton is obtained. The steam-coal ratio, however, does not seem to have any significant effect.

As might be expected, the highest yield of acetylene is obtained at the highest cracking temperature. At a cracking temperature of 800°, only 8.1 pounds/ton is obtained, but this is raised to 22.3 pounds/ton by increasing the cracking temperature to 900°. The steam-coal ratio is not nearly so important, but the production of acetylene is favored by the higher ratio. Perhaps surprisingly, the retention time has only little effect.

There is a substantial decrease in the yield of propylene when the higher cracking temperatures and longer retention times are employed. At a cracking temperature of 800°, 64.6 pounds/ton is obtained, but this falls to only 23.8 pounds/ton at 900°. Similarly, increasing the average retention time from 0.5 to 0.9 seconds resulted in a decrease in the yield of propylene from 59.8 to 32.1 pounds/ton. The steam-coal ratio, however, had comparatively little effect.

The yield of butadiene decreases rapidly as the cracking temperature and retention time are increased. At a cracking temperature of 800°, 22.0 pounds/ton is obtained, but at 900° only 11.2 pounds/ton is obtained. Similarly, increasing the retention time from 0.5 to 0.9 seconds decreases the yield of butadiene from 20.9 to 12.7 pounds/ton. The best steam-coal ratio for the production of butadiene is 1.25.

The process variables do not greatly affect the yield of methane. On the average, the methane yield is about 150 pounds/ton.

As might be expected, greater quantities of hydrogen are produced at the more rigorous cracking conditions. At a cracking temperature of 800°, a ton yields 12 pounds of hydrogen, at 900°, 19.4 pounds. Increasing the retention time from 0.5 to 0.9 seconds, similarly raises the yield of hydrogen from 13.5 to 17.1 pounds/ton. An increase in the steam-coal ratio from 1.0 to 1.5 decreases the amount of hydrogen obtained from a yield of 17 pounds/ton to 14 pounds/ton, probably because of its effect on the retention time.

The yield of carbon dioxide is quite constant at 15 pounds/ton at all levels of the process variables studied, and only cracking temperature has much effect on the yield of carbon monoxide. When the cracking temperature is raised from 800° to 900°, the yield of carbon monoxide increases from 40.9 to 72.2 pounds/ton.

Effect of Process Variables on Light Oil Produced

The process variables at the levels studied have no significant effect on the total yield of light oil. It might be expected that higher

temperatures and longer retention times would favor the production of light oil owing to the conversion of heavy oil to light oil at the more rigorous conditions, but this is not true. Evidently, if more light oil is produced, more light oil is also converted into gaseous hydrocarbons. At all the conditions studied, the yield of light oil was about 115 pounds/ton.

The light oil contains a large number of compounds. The more easily identifiable components of the mixture are benzene, toluene, styrene, C_2 benzenes, indene, indan, and/or methylstyrene, naphthalene, and methyl naphthalene. These components comprise 58 to 73% of the total. The remainder is made up of more highly substituted benzenes, styrenes, and naphthalenes. Only the effects of the process variables on the production of benzene, toluene, styrene, and naphthalene will be discussed, since these are the most commercially important components.

The yield of benzene as a function of retention time shows a definite maximum at 0.7 seconds; and as a function of steam-coal ratio, a definite minimum at a ratio of 1.25. However, the levels of cracking temperature employed seem to have no significant effect.

The yield of toluene as a function of steam-coal ratio shows, like the yield of benzene, a definite minimum at a ratio of 1.25, although in this case neither the cracking temperature nor the retention time seem to be important.

The process variables have very little effect on the yield of styrene. It is relatively constant at about 6.0 pounds/ton.

The highest cracking temperatures and the longest retention times investigated favored the production of naphthalene. At a cracking temperature of 800°, the yield was 9.3 pounds/ton, while at 900° it increased to 13.9 pounds/ton. In the same way, increasing the retention time from 0.5 to 0.9 seconds increased the yield from 9.0 to 13.6 pounds/ton. The steam-coal ratio, on the other hand, seemed to have little effect.

Effect of Process Variables on Heavy Oil Produced

As expected, the higher cracking temperatures favored the conversion of the heavy oil to light oil and volatile gases. Surprisingly, however, there was a definite maximum in the yield at the intermediate retention time and the intermediate steam-coal ratio, that is, 0.7 seconds and a ratio of 1.25.

Some analytical work was done on the heavy oil, but due to its complex nature, no individual components were determined. The heavy oil is mainly aromatic in character and is composed of polynuclear aromatic hydrocarbons of high molecular weight. An ultimate analysis was made on the heavy oil from each run, but there was little difference. The average analysis is:

Carbon	90.35%
Hydrogen	5.03
Nitrogen	1.46
Sulfur	0.67
Ash	1.36
Oxygen (by diff.)	1.13

Comparison of the Different Cannel Coals

In view of the fact that the yields of the commercially important products are, in general, not particularly sensitive to the process conditions in the ranges investigated, the four different cannel coals were compared at only a single set of conditions. A cracking temperature of 850°, an average retention time of 0.9 seconds, and a steam-coal ratio of 1.0 was chosen. While these conditions are not optimum, it seems unlikely that the comparison would be drastically different at any other generally-similar conditions. The results of these experiments are given in Tables 2, 3, 4, 5 and 6.

There is a good correlation between the yields of total gas, ethylene, total light oil, benzene, toluene, etc., and the gas and oil yield in the Fisher assay. When more gas and oil is obtained in the Fisher assay, a similar increase is noticed in the yields of the more valuable products. This is not, however, true with the yields of heavy oil. There is probably a tendency for the high assaying coals to produce more heavy oil, but the correlation is not nearly as high as it is for the light oils and gases.

DISCUSSION

The low-temperature carbonization of cannel coal immediately followed by a thermal cracking of the volatile products produces excellent yields of ethylene, benzene, and other aromatic hydrocarbons. As expected, the yields of these products are much higher than could be obtained from lignite; over five times as much ethylene and benzene can be obtained. This did indeed result in a lower capital investment for a commercial plant producing the same amount of ethylene and aromatics as the lignite plant, and undoubtedly more than offset the increased cost of the cannel coal. A preliminary economic analysis, however, indicated that this process is still probably not competitive with the conventional crude oil cracking process. If the cost of crude oil should increase significantly, or if significant engineering improvements could be made to lower the capital cost, the commercial use of this process would be a possibility.

REFERENCE

[1] R. S. Montgomery, D. L. Decker and J. C. Mackey, Ind. Eng. Chem., 51, p. 1293 (1959).

TABLE 2

Cracking Temperature: 850°C Average retention time: 0.9 sec.
Steam-coal ratio: 1.0

Charge: 500 gms. of 3-1/2 - 10 mesh "Gay" cannel coal

Yield of Gas:	107.9 gms.	431.0 lbs/ton	502.6 lbs/ton(MAF)
Ethylene	42.3	169.0	197.0
Acetylene	2.2	8.8	10.2
Propylene	4.3	17.2	20.0
Butadiene	1.7	6.8	7.9
Butene-2	0.5	2.0	2.3
Methane	35.6	142.0	166.0
Ethane	3.1	12.4	14.4
Hydrogen	3.7	14.8	17.2
Carbon monoxide	11.2	44.8	52.2
Carbon dioxide	3.3	13.2	15.4
Yield of Light Oil:	23.7	94.8	110.3
Benzene		18.2	21.2
Toluene		10.4	12.1
Styrene		5.7	6.6
C_2 Benzenes		2.5	2.9
Indene		4.9	5.7
Indan/or methylstyrene		1.7	2.0
Naphthalene		9.7	11.3
Methyl naphthalenes		3.4	4.0
Yield of Heavy Oil:	53.0	212.0	247.0
Yield of Char	290.1	1160.0	

Heat Content of Gas: 747 BTU/cu.ft. (ethylene-free)

TABLE 3

Cracking Temperature: 850°C Average retention time: 0.9 sec.
Steam-coal ratio: 1.0

Charge: 500 gms. of 3-1/2 - 10 mesh "Big Chief" cannel coal

Yield of Gas:	121.1 gms.	484.0 lbs/ton	509.4 lbs/ton(MAF)
Ethylene	45.3	181.4	191.0
Acetylene	1.6	6.4	6.7
Propylene	6.6	26.4	27.8
Butadiene	2.7	10.8	11.4
Butene-2	0.5	2.0	2.1
Methane	35.7	143.0	150.5
Ethane	2.9	11.6	12.2
Hydrogen	4.2	16.8	17.7
Carbon monoxide	16.7	66.0	69.4
Carbon dioxide	4.9	19.6	20.6
Yield of Light Oil:	26.6	106.2	111.5
Benzene		29.9	31.4
Toluene		11.9	12.5
Styrene		4.5	4.7
C_2 Benzenes		3.1	3.3
Indene		6.0	6.3
Indan/or methylstyrene		2.0	2.1
Naphthalene		7.3	7.7
Methyl naphthalene		3.0	3.2
Yield of Heavy Oil:	60.7	242.8	254.0
Yield of Char:	272.2	1088.0	

Heat Content of Gas: 728 BTU/cu.ft. (ethylene-free)

TABLE 4

Cracking Temperature: 850°C Average retention time: 0.9 sec.
Steam-coal ratio: 1.0

Charge 500 gms. of 3-1/2 - 10 mesh "Stollings" cannel coal

Yield of Gas:	123.0 gms.	491.8 lbs/ton	549.7 lbs/ton(MAF)
Ethylene	46.5	186.0	208.8
Acetylene	2.7	10.8	12.1
Propylene	8.6	34.4	38.6
Butadiene	2.9	11.6	13.0
Butene-2	0.5	2.0	2.2
Methane	33.9	135.6	152.3
Ethane	3.9	15.6	17.5
Hydrogen	3.7	14.8	16.6
Carbon monoxide	14.1	56.2	63.0
Carbon dioxide	5.7	22.8	25.6
Yield of Light Oil:	28.0	112.0	126.0
Benzene		35.8	40.2
Toluene		14.1	15.8
Styrene		5.4	6.1
C_2 Benzenes		4.3	4.8
Indan/or methylstyrene		2.6	2.9
Naphthalene		8.1	9.1
Methyl naphthalene		3.6	4.0
Yield of Heavy Oil:	71.4	284.0	309.0
Yield of Char:	265.8	1063.0	

Heat Content of Gas: 784 BTU/cu.ft. (ethylene-free)

TABLE 5

Cracking Temperature: 850°C Average retention time: 0.9 sec.
Steam-coal ratio: 1.0

Charge: 500 gms. of 3-1/2 - 10 mesh "Dorothy" cannel coal

Yield of Gas:	138.0 gms.	552.2 lbs/ton	587.9 lbs/ton(MAF)
Ethylene	57.5	230.0	245.0
Acetylene	4.1	16.4	17.5
Propylene	9.6	38.4	40.8
Butadiene	3.4	13.6	14.5
Butene-2	0.5	2.0	2.1
Methane	37.6	150.6	160.2
Ethane	5.0	20.0	21.3
Hydrogen	4.6	18.4	19.6
Carbon monoxide	9.2	36.8	39.2
Carbon dioxide	6.5	26.0	27.7
Yield of Light Oil:	33.5	133.8	142.3
Benzene		43.8	46.6
Toluene		16.7	17.8
Styrene		6.3	6.7
C_2 Benzenes		3.9	4.2
Indene		7.7	8.2
Indan/or methylstyrene		11.1	11.8
Methyl naphthalenes		4.5	4.8
Yield of Heavy Oil:	65.1	260.2	277.0
Yield of Char:	236.1	944.0	

Heat Content of Gas: 794 BTU/cu.ft. (ethylene-free)

TABLE 6

	"Gay"	"Stollings"	"Big Chief"	"Dorothy"
Ultimate Analysis of Heavy Oil:				
Carbon	90.26%	89.58%	87.42%	88.40%
Hydrogen	5.00	4.94	5.51	4.98
Nitrogen	1.35	1.57	1.38	1.74
Sulfur	.62	.74	.74	.84
Ash	2.01	1.60	1.30	.66
Oxygen (by diff.)	.76	1.57	3.65	3.38
Proximate Analysis of Char:				
Moisture	0.67%	0.75%	0.63%	0.76%
Net volatile	8.69	9.90	9.43	11.06
Fixed carbon	66.95	70.56	80.84	76.89
Ash	23.70	18.79	9.10	11.29
Ultimate Analysis of Char:				
Hydrogen	2.82	2.91	3.09	3.05
Carbon	68.70	71.73	81.63	79.59
Nitrogen	0.69	1.46	1.46	1.53
Sulfur	0.37	1.12	0.62	0.83
Oxygen (by diff.)	3.72	4.29	4.00	3.71
BTU/lb. of Char (MAF)	14,350	14,680	14,865	14,900

Presented Before the Division of Fuel Chemistry
American Chemical Society
Chicago, Ill., August 30 - September 4, 1964

CHANGES IN THE ULTRAFINE STRUCTURE OF ANTHRACITE UPON HEAT TREATMENT

S. P. Nandi, V. Ramadass, and P. L. Walker, Jr.

Department of Fuel Technology, Pennsylvania State University, University Park, Pennsylvania

It is well known that the ultrafine structure of anthracite exhibits molecular-sieve properties (1-6). It has further been shown that upon using appropriate activation procedures (during the reaction of anthracite with carbon dioxide at elevated temperatures), a large increase in adsorption capacity and rate of adsorption can be obtained in the ultrafine structure while still retaining its molecular-sieve behavior (6). Little quantitative data are available, however, on the changes produced in the ultrafine structure of anthracite upon thermal treatment to elevated temperatures in the absence of oxidizing gases. In this paper, the change in the ultrafine structure of three anthracites upon heat treatment has been followed using conventional techniques (gas adsorption and density measurements) and the newer technique (unsteady-state diffusion of gases from the ultrafine structure).

EXPERIMENTAL

Anthracites Used

Three Pennsylvania anthracites of 200x325 Tyler mesh were used in this study. The analyses of the anthracites used are given in Table I.

Heat Treatment

Heat treatment up to 1000°C was carried out in a tubular furnace, with the power input to the furnace controlled by a Leeds-Northrup duration-adjusting type program controller. A desired linear heating rate of 5.0 ± 0.1°C/min and maximum temperatures during soaking within 2°C could be maintained. Nitrogen of 99.96% purity was passed over the sample (ca. 25g held in a quartz boat) throughout the heating and cooling cycle, after it was first circulated over copper turnings at 550°C to remove traces of oxygen.

In selected cases, heat treatments at temperatures in the range 1200-1700°C were performed in an induction furnace under an atmosphere of helium of 99.98% purity. Desired heating rates and maximum temperatures were obtained by manually adjusting the power input.

Apparatus to Measure Properties of Anthracites

The apparatus and procedures used to measure the properties of anthracite have been completely described previously: gas adsorption (7,8), mercury density (9), helium density (8), crystallite height measurements (10,11), and unsteady-state diffusion (12). Considering the unsteady-state diffusion measurements briefly, a differential experimental system was used to avoid errors caused by small temperature fluctuations. In principle, the procedure consisted of charging the particle sample under investigation with the selected gas up to some pressure in excess of atmospheric (by exposure to the gas at the diffusion temperature for

24 hr) and then measuring the unsteady-state release of the gas after sudden reduction of the pressure outside the particles back to atmospheric. The charging pressure never exceeded 2 atm. and usually was ca. 1.7 atm. Prior to charging the samples with gas, they were outgassed at 450°C for 24 hr.* It was essential that the outgassing temperature be higher than the maximum temperature of diffusion measurement, since removal of water and/or occluded gases during the measurement would invalidate the experiment.

Detailed studies have been made on the kinetics of VM release from anthracites (13, 14). The volume and analysis of the VM release, as a function of temperature, have been measured. Where appropriate, these results will be presented in this paper. The experimental apparatus and procedure have been fully described (13).

RESULTS AND DISCUSSION

Volatile Matter Release From Anthracites

Prior to examining the change in ultrafine structure of the anthracites upon heat treatment, results on the liberation of VM and the accompanying weight loss during heat treatment should be examined. Samples were heated to maximum temperature at 5°C/min and soaked for 24 hr. Table II summarizes the results. Three separate heating runs were made on St. Nicholas and Dorrance anthracites to 800 and 900°C. Weight losses agreed to within ±2%.

For the St. Nicholas and Dorrance anthracites, relatively small decreases in weight occurred upon heating to 500°C. In fact, the VM release remained small up to 650°C for the St. Nicholas anthracite, as seen in Figure 1. Figure 2 shows that a sharp increase in VM release from the St. Nicholas anthracite coincided with the occurrence of substantial amounts of hydrogen and methane in the recovered gas. At heat treatment temperatures (HTT) up to 650°C, the VM primarily consisted of carbon dioxide and carbon monoxide. For the Treverton anthracite, a substantial weight loss occurred upon heating to 500°C. This is believed to be a result of release of much greater quantities of the oxides of carbon from this anthracite relative to St. Nicholas and Dorrance.

It is of interest that the weight losses for St. Nicholas and Dorrance anthracites were higher for maximum HTT of 700 and 800°C than for a HTT of 900°C, for the particular heating cycle selected. This is thought to be a result of the sharp increase in the H_2-CH_4 ratio in the product gas with increasing temperatures above ca. 750°C, as seen in Figure 2. The equilibrium H_2-CH_4 ratio for the reaction, $C + 2H_2 \rightleftharpoons CH_4$, is ca. 10 at 1000°K and 1 atm. total pressure (15). It is seen from Figure 2 that the H_2-CH_4 ratio in the VM at this liberation temperature is ca. 0.3. This indicates either that a sizeable amount of methane is being produced as a primary product by desorption of functional groups on the coal and then slowly decomposing to produce hydrogen or that the gas pressure within the ultrafine structure of the anthracite is very high. For example, at 1000°K and a total pressure of 100 atm., the H_2-CH_4 equilibrium ratio is ca. 0.3. Heat treatment runs were made on St. Nicholas anthracite up to 800 and 900°C, but with no soak-time at maximum temperature. In this case, the weight losses were 2.7 and 3.1% respectively. With increasing soak time (and at a value of less than 2 hr.), the weight loss for the

* Outgassing at 450°C is thought to have produced a negligible change in the ultrafine structure of the St. Nicholas and Dorrance anthracites, as will be seen later from the surface area results. In the case of the higher volatile matter Treverton anthracite, this outgassing temperature apparently produced a significant change in the raw coal.

900°C HTT eventually falls below that for the 800°C HTT, since the difference in average molecular weight of the total VM produced for these HTT will more than compensate for the larger volume of VM released in the 900°C heat treatment run.

It is noteworthy that the weight loss for the Treverton anthracite did not go through a maximum with increasing HTT. This could be a result of the oxides and carbon making a greater contribution to the total VM for this anthracite and thus reducing the effect of an increase in the H_2-CH_4 ratio on the average molecular weight of the VM. Confirming results are not available on this point.

Surface Areas

Table III summarizes the surface area results obtained from nitrogen and carbon dioxide adsorption. As suggested by Walker and Geller (2) and later supported by Anderson, Hofer, and Bayer (16), areas calculated from carbon dioxide adsorption at 195°K represent closely the total surface area of coal. On the other hand, nitrogen at 77°K diffuses slowly into pores less than ca. 4.5A in diameter and thus is not adsorbed by most of the ultrafine structure in coals. For heat treatment temperatures up to 800°C, the anthracites retained their large surface areas. In fact, for the Dorrance and Treverton samples (and probably St. Nicholas) the surface areas went through a maximum with increasing HTT. The increase in surface area upon heat treatment at the lower temperatures can be attributed to the release of gaseous oxides of carbon, resulting in the opening up of pores which were closed to carbon dioxide adsorption in the raw anthracites. As expected, the Treverton anthracite, which showed the greatest VM release at lower temperatures, also showed the greatest increase in surface area. At HTT above 800°C, the total surface area of the anthracites decreased sharply as the ultrafine pores decreased in size and ultimately became inaccessible to carbon dioxide. This model will be further clarified by the unsteady-state diffusion results. A sizeable activation energy can be attributed to the process which decreased the size of the ultrafine pores. That is, for the 900°C heat treatment run on St. Nicholas anthracite, with no soak time, the area was still 206 m^2/g.

It is seen, from the nitrogen adsorption results, that the amount of area in pores greater than ca. 4.5A varied widely. These areas also went through a maximum with increasing HTT. For a HTT of 900°C the areas were particularly low for the Dorrance and Treverton anthracites.

Densities and Pore Volumes

Table IV presents the helium and mercury density values on a m.m.f.b. The helium and mercury density of the mineral matter in all samples was taken as 2.7 g/cc (17). The helium densities increased with increasing HTT. At low HTT, the helium density would be expected to increase because the release of the gaseous oxides of carbon would open up closed pores. In the intermediate range up to ca. 800°C, the release of methane would remove carbon atoms and unblock pores. Further, the release of the low density species, hydrogen, would increase the helium density. At HTT above 800°C, it is suggested that most of the increase in helium density is attributed to a decrease in average size of the closed pores and their ultimate elimination.

As expected from the helium density results, the mercury densities also increased with increasing HTT as seen in Table IV. From the helium and mercury densities, the total open pore volume and porosity of the samples can be calculated. The results are summarized in Table V. In spite of the large increases in densities with increasing HTT, the total open pore volumes and porosities

showed erratic and relatively little change. This indicates that most of the pore volume which was eliminated upon heat treatment was located in pores already closed to helium.

Crystallite Heights

As shown by transmission electron microscopy studies, pore volume in carbons can be produced by the irregular packing of crystallites (17). Therefore, it is of interest to compare changes in crystallographic parameters upon heat treatment with changes in ultrafine pore structure. Unfortunately, the obtaining of quantitative data on crystallite diameter and interlayer spacing is laborious (11) and probably, in any case, not meaningful for samples relatively high in mineral matter. Quantitative crystallite height values can be obtained relatively simply (11), (even on impure samples); they are presented in Table VI. No apparent relation exists between the change in crystallite height upon heat treatment and changes in the ultrafine pore structure. As showed previously for other raw carbonaceous solids (18), the crystallite height of the raw anthracites decreased upon heat treatment at temperatures between 500-900°C. Possible reasons for this have been discussed (19).

It has previously been shown that the closed pore volume in calcined petroleum cokes decreases sharply with increase in crystallite alignment (20). The relative degree of crystallite alignment can be measured for carbons of essentially the same crystallite size from the relative intensity of their (002) x-ray diffraction peak (20,21). I(002) values for the anthracites are presented in Table VI, normalized to 100 for the raw St. Nicholas sample. Relatively minor changes in I(002) occurred with increasing heat treatment temperature for the anthracites, showing that significant improvement in crystallite alignment did not occur. Therefore, the substantial increase in helium density upon heat treatment to 900°C (part of which is caused by a decreasing closed pore volume) cannot be attributed to enhanced crystallite alignment.

Diffusion Parameters

As considered theoretically by Kington and Laing for the diffusion of gases through molecular sieve zeolites (22), when the size of the diffusing species closely approaches the size of the aperture through which it passes, the diffusion becomes activated. Under these conditions a further small decrease in aperture size produces a large increase in activation energy for diffusion. Nelson and Walker showed the validity of this concept experimentally for the diffusion of propane through 4 and 5A Linde zeolites, obtaining activation energies of 8.7 and 0.5 kcal/mole respectively (12). The kinetic dimension* of propane, calculated using the Lennard-Jones potential and viscosity data is 5.1A (23).

As indicated previously the parameter, $D^{\frac{1}{2}}/r_o$, has been calculated from the diffusion results. The diffusion coefficient, D, has not been given since the value of the diffusion path length, r_o, is unknown at present. Studies on the change of $D^{\frac{1}{2}}/r_o$ with anthracite particle size clearly shows that r_o is not the particle radius (24). In any case, we were primarily interested in the activation energy for the diffusion coefficient. Since r_o should be independent of diffusion temperature, values of $D^{\frac{1}{2}}/r_o$ will be sufficient for this purpose.

A thorough study was made of the diffusion of gases from St. Nicholas anthracite heat treated up to 1700°C. For samples heated to 900°C, the diffusion of nitrogen, ethane, and argon was studied. For samples heated to

*The kinetic dimension is the distance of approach where the potential energy of interaction equals zero.

higher temperatures, it was necessary to use smaller diffusing species in order to have a rate of diffusion which was sufficiently rapid to be measurable in a convenient period of time. Hydrogen and helium were used.

Figure 3 presents Arrhenius plots for the diffusion of nitrogen and ethane out of St. Nicholas anthracite samples heated to a maximum temperature of 900°C. The plots of nitrogen and ethane diffusing from the raw anthracite are not shown, since they fall very close to the 700°C sample. Large decreases in the diffusion parameters of both nitrogen and ethane resulted, however, when the HTT was increased from 700 to 900°C. There also was a significant increase in the activation energy for diffusion of both gases in going from a HTT of 700 to 900°C, indicating a decrease in the average size of the ultrafine pore structure which is determining the diffusion rate. As expected ethane had a higher activation energy for diffusion from comparable St. Nicholas samples than did nitrogen. That is, the kinetic dimensions of ethane and nitrogen are 4.41 and 3.68A respectively (23). It is noted that there was some increase in the difference in activation energy for ethane and nitrogen diffusion when the St. Nicholas sample was heated to higher temperatures. That is, the difference in activation energy was ca. 1.2 kcal/mole for the raw anthracite and ca. 2.7 kcal/mole for samples heat treated to 800 and 900°C. This indicates the possibility of producing sharper molecular sieve effects for different gases by heat treating anthracites.

Figure 4 presents Arrhenius plots for the diffusion of helium and hydrogen out of St. Nicholas samples heated at temperatures between 1200 and 1700°C. Considerable experimental difficulties were encountered in these diffusion rate measurements. The ultrafine pore volume of these samples was low; and, hence, the volume of gas released was low (ca. 0.4 cc at S.T.P. for 25g samples). A slight variation in room temperature affected the rate measurements. Even though the precision of these measurements was less than that obtained for samples heated to temperatures below 900°C, the Arrhenius plots are reasonably good. There was an increase in the activation energy for the diffusion of helium with increasing HTT. The sample heated to 1400°C had the same activation energy for helium diffusion as the sample heated to 900°C had for nitrogen diffusion. This is strong evidence for a continued decrease in the size of the ultrafine pores with increasing HTT in this temperature range. As expected, hydrogen had a higher activation energy for diffusion out of the 1400°C heat treated sample than did helium. That is, the kinetic dimensions of hydrogen and helium are 2.97 and 2.58A respectively (23). It is of interest that the activation energy for helium diffusion from the 3A Linde zeolite is less than 1 kcal/mole (24). This suggests that the ultrafine pores in the St. Nicholas samples heated to 1400 and 1700°C had a size less than 3A.

Figures 5-7 present Arrhenius plots for the diffusion of argon from St. Nicholas, Dorrance, and Treverton samples heat treated up to 900°C. Again, increases in the activation energy for diffusion occurred with increasing HTT. It is of interest, however, that the Dorrance anthracite showed a greater increase in activation energy for argon diffusion than did Treverton or St. Nicholas. Further, the activation energy for the diffusion of argon from Treverton was appreciably higher than the values for the other anthracites, when the samples were heated only to 600°C. Since nitrogen has a kinetic dimension close to that of argon (3.41A), this is consistent with the fact that the nitrogen surface area of Treverton heat treated to 600°C was considerably less than the nitrogen area of the Dorrance sample.

CONCLUSIONS

Heat treatment of Pennsylvania anthracites in an oxygen-free atmosphere above ca. 700°C is seen to decrease the average size of the ultrafine pores. The result is a sharp decrease in total surface area, as measured by carbon dioxide adsorption for HTT at or above 900°C and a continuous increase in the activation energy for diffusion of gases from the ultrafine pores with increasing HTT.

We appreciate the financial support of the Coal Research Board of the Commonwealth of Pennsylvania which made this work possible.

REFERENCES

1. Kini, K. A., Nandi, S. P., Sharma, H. N., Iyengar, M. S., and Lahiri, A., Fuel, 1956, 35, 71.
2. Walker, P. L. Jr. and Geller, Irwin, Nature, 1956, 178, 1001.
3. Anderson, R. B., Hall, W. K., Lecky, J. A., and Stein, K. C., J. Phys. Chem., 1956, 60, 1548.
4. Joy, A. S., Conference on Science in the Use of Coal, Institute of Fuel, 1958, pp. A-67 to A-71.
5. Gregg, S. J. and Pope, M. I., Fuel, 1959, 38, 501.
6. Metcalfe, J. E. III, Kawahata, M., Walker, P. L. Jr., Fuel, 1963, 42, 233.
7. Emmett, P. H., A. S. T. M. Tech. Publ., No. 51, 1941, pp. 95-105.
8. Kotlensky, M. V., Ph. D. Thesis, The Pennsylvania State University, 1959.
9. Walker, P. L., Jr., Rusinko, F. Jr., and Raats, E., J. Phys. Chem., 1955, 59, 245.
10. Scherrer, P., Nachr. Ges. Wissensch. Gottingen, 1918, 2, 98.
11. Short, M. A. and Walker, P. L. Jr., Carbon, 1963, 1, 3.
12. Nelson, E. T. and Walker, P. L. Jr., J. Appl. Chem., 1961, 11, 358.
13. Nelson, E. T., Young, G. J., and Walker, P. L. Jr., Special Research Report #3, Coal Research Board, Commonwealth of Pennsylvania, 1958.
14. Worrall, Jean and Walker, P. L. Jr., Special Research Report #16, Coal Research Board, Commonwealth of Pennsylvania, 1959.
15. Walker, P. L. Jr., Rusinko, Frank Jr., and Austin, L. G., Advances in Catalysis, Vol. XI, Academic Press, Inc., 1959, pp. 133-221.
16. Anderson, R. B., Hofer, L. J. E., and Bayer, J., Fuel, 1962, 41, 559.
17. Walker, P. L. Jr., Amer. Scientist, 1962, 50, 259.
18. Gibson, J., Holohan, M., and Riley, H. L., J. Chem. Soc., 1946, 456.
19. Kinney, C. R., Nunn, R. C., and Walker, P. L. Jr., Ind. Eng. Chem., 1957, 49, 880.
20. Walker, P. L. Jr., Rusinko, F. Jr., Rakszawski, J. F., and Liggett, L. M., Proceedings of the Third Carbon Conference, Pergamon Press, 1958, pp. 643-658.
21. Walker, P. L. Jr., Gardner, R. P., Short, M. A., and Austin, L. G., Proceedings of the Fifth Carbon Conference, Volume 2, Pergamon Press, 1963, pp. 483-492.
22. Kington, G. L. and Laing, W., Trans. Faraday Soc., 1955, 51, 287.
23. Hirschfelder, J. O., Curtiss, C. F., and Bird, R. B., "Molecular Theory of Gases and Liquids", John Wiley and Sons, Inc., 1954, p. 1110.
24. Nandi, S. P., Ph. D. Thesis, The Pennsylvania State University, 1964.

TABLE I

ANALYSES OF ANTHRACITES

Coal	% Carbon (d. m. f.)	% Volatile (d. m. f.)	% Ash
St. Nicholas	94.0	4.5	9.1
Dorrance	92.7	5.8	9.9
Treverton	92.0	9.0	9.7

TABLE II

WEIGHT LOSSES UPON HEAT TREATMENT OF THE ANTHRACITES

Anthracite	Heat Treatment Temperature, °C	Loss In Weight, %
St. Nicholas	500	1.7
	700	3.7
	800	4.0
	900	3.6
	1000	4.5
Dorrance	500	0.79
	600	4.2
	700	5.2
	800	6.8
	900	4.6
Treverton	500	4.8
	600	6.6
	700	8.4
	800	9.5
	900	10.2

TABLE III

EFFECT OF HEAT TREATMENT ON THE SURFACE AREAS OF THE ANTHRACITES

Anthracite	Heat Treatment Temperature, °C	Surface Areas, m^2/g N_2	CO_2
St. Nicholas	raw	32.3	220
	700	24.9	215
	800	9.6	198
	900	5.1	104
	1000	3.7	23.6
Dorrance	raw	34.2	215
	500	38.8	235
	600	23.4	250
	700	10.2	273
	800	6.8	187
	900	1.0	25.9
Treverton	raw	1.5	131
	500	2.8	222
	600	7.2	243
	700	11.5	216
	800	2.3	208
	900	0.8	61.1

TABLE IV

EFFECT OF HEAT TREATMENT ON THE HELIUM AND MERCURY DENSITIES OF THE ANTHRACITES

Anthracite	Heat Treatment Temperature, °C	Helium Density g/cc	Mercury Density g/cc
St. Nicholas	raw	1.66	1.47
	700	1.73	1.49
	800	1.80	1.50
	900	1.86	1.56
	1000	2.08	1.61
Dorrance	raw	1.63	1.27
	500	1.64	1.35
	600	1.65	1.42
	700	1.79	----
	800	1.85	1.57
	900	2.06	1.65
Treverton	raw	1.58	1.21
	500	1.63	1.27
	600	1.67	1.36
	700	1.75	1.43
	800	2.05	1.54
	900	2.08	1.65

TABLE V

EFFECT OF HEAT TREATMENT ON THE SPECIFIC OPEN PORE VOLUME AND PERCENTAGE POROSITY OF THE ANTHRACITES

Anthracite	Heat Treatment Temperature, °C	V_t, cc/g	Porosity %
St. Nicholas	raw	0.07	10.6
	700	0.10	14.2
	800	0.11	16.5
	900	0.10	16.1
	1000	0.14	22.6
Dorrance	raw	0.17	22.1
	500	0.13	17.7
	600	0.10	13.9
	800	0.10	15.2
	900	0.11	18.7
Treverton	raw	0.19	23.2
	500	0.09	11.2
	600	0.14	18.6
	700	0.13	18.3
	800	0.16	25.0
	900	0.13	20.6

TABLE VI

X-RAY DIFFRACTION RESULTS ON THE HEAT TREATED ANTHRACITES

Anthracite	Heat Treatment Temperature, °C	Crystallite Height, A	I(002)
St. Nicholas	raw	15.6	100
	700	10.8	105
	800	10.8	97
	900	11.1	103
	1000	13.0	106
Dorrance	raw	18.0	131
	500	15.8	122
	600	13.2	117
	700	11.3	100
	800	15.2	131
	900	13.0	122
Treverton	raw	18.4	100
	500	14.9	96
	600	11.2	80
	700	11.2	78
	800	11.2	86
	900	10.6	94

FIGURE CAPTIONS

Fig. 1 Relationship Between the Volume of Volatile Matter Evolved and Temperature for St. Nicholas Anthracite

Fig. 2 Relationship Between Volatile Matter Composition and Temperature for St. Nicholas Anthracite

Fig. 3 Activation Energy Plots for the Diffusion of Nitrogen and Ethane from Heat Treated St. Nicholas Anthracite

Fig. 4 Activation Energy Plots for the Diffusion of Helium and Hydrogen from Heat Treated St. Nicholas Anthracite

Fig. 5 Activation Energy Plots for the Diffusion of Argon from Heat Treated St. Nicholas Anthracite

Fig. 6 Activation Energy Plots for the Diffusion of Argon from Heat Treated Dorrance Anthracite

Fig. 7 Activation Energy Plots for the Diffusion of Argon from Heat Treated Treverton Anthracite

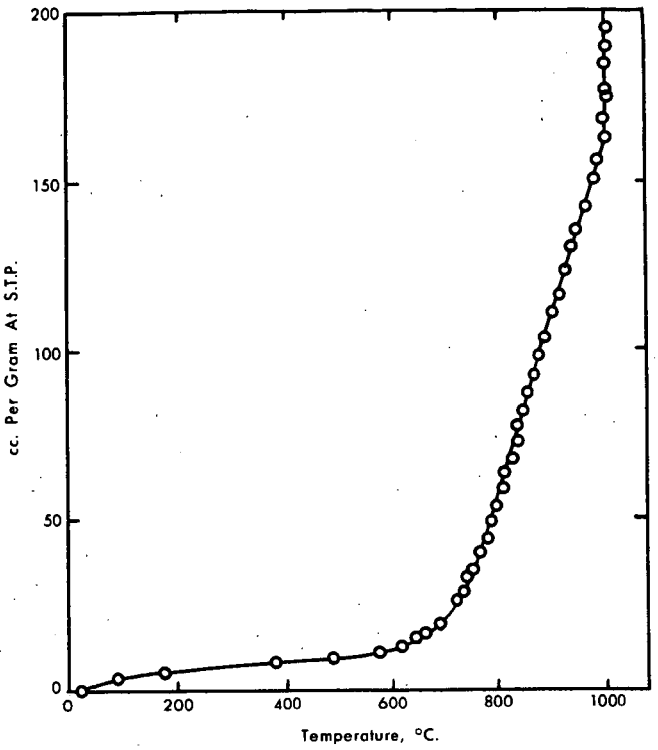

FIGURE 1

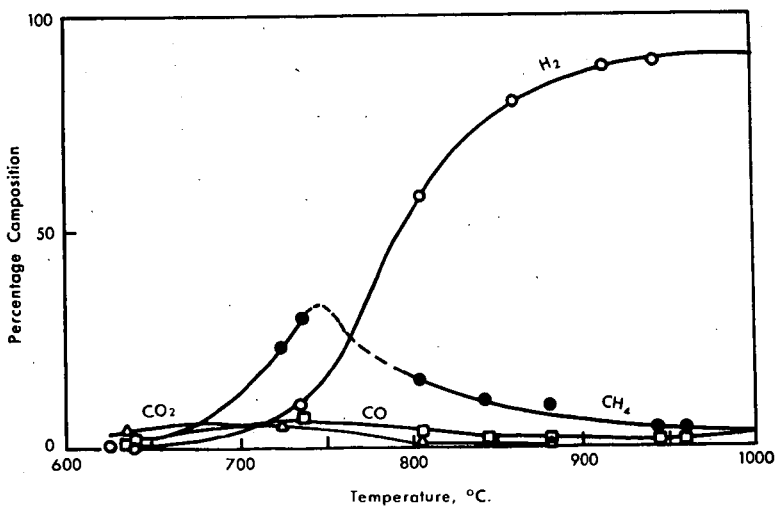

FIGURE 2

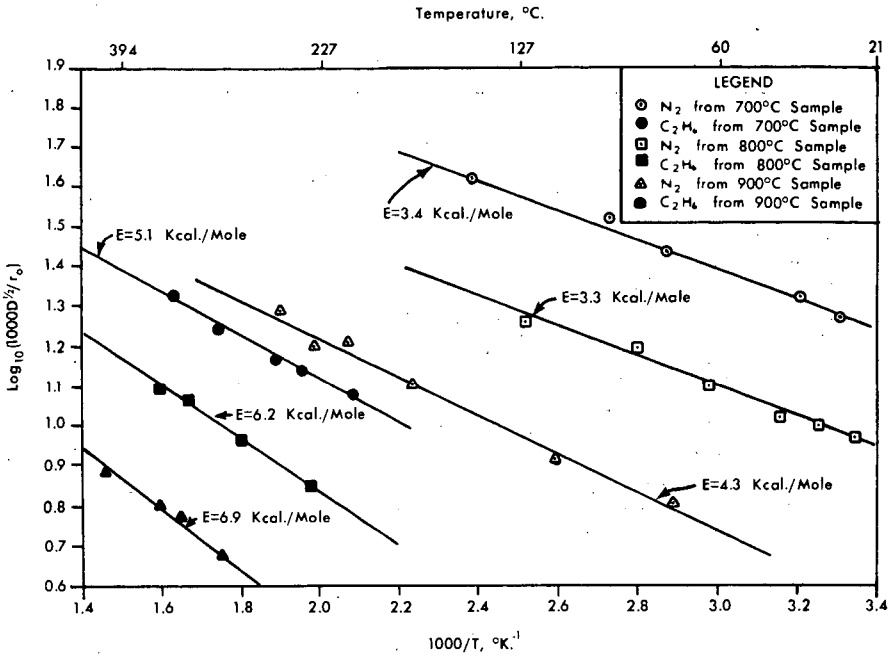

FIGURE 3

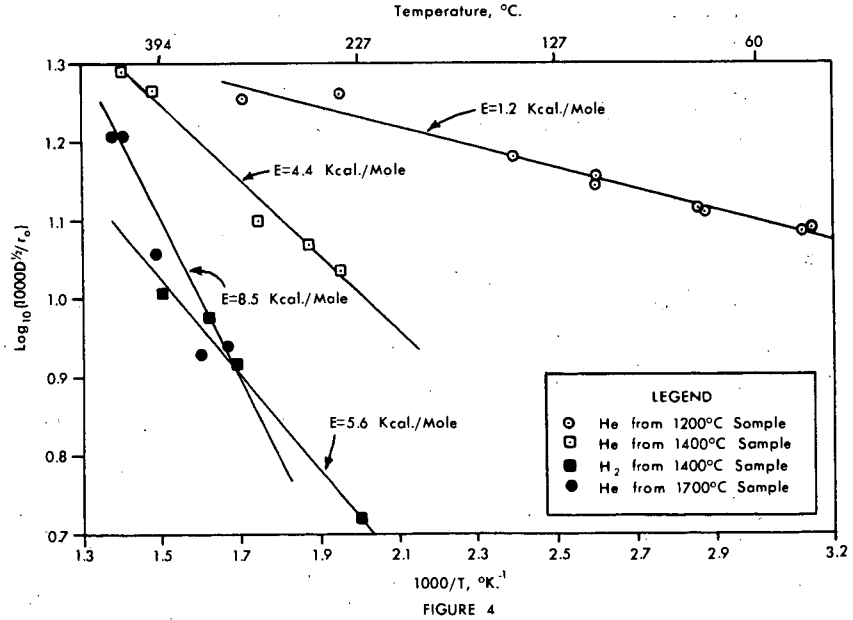

FIGURE 4

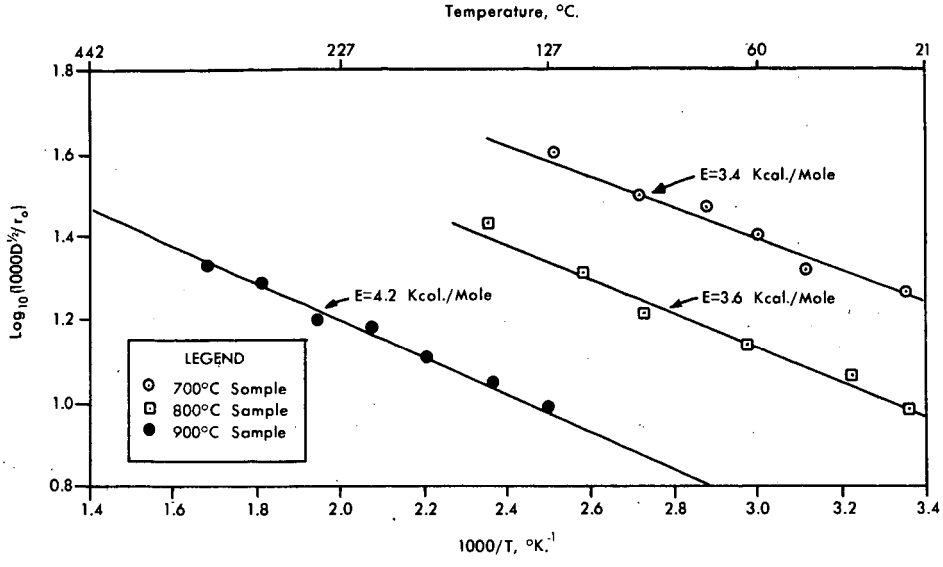

FIGURE 5

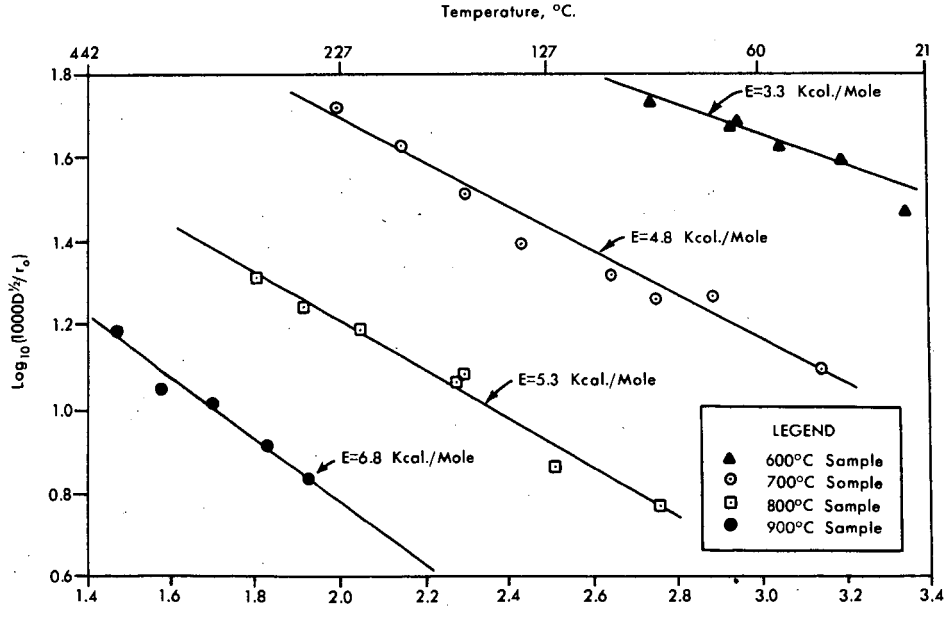

FIGURE 6

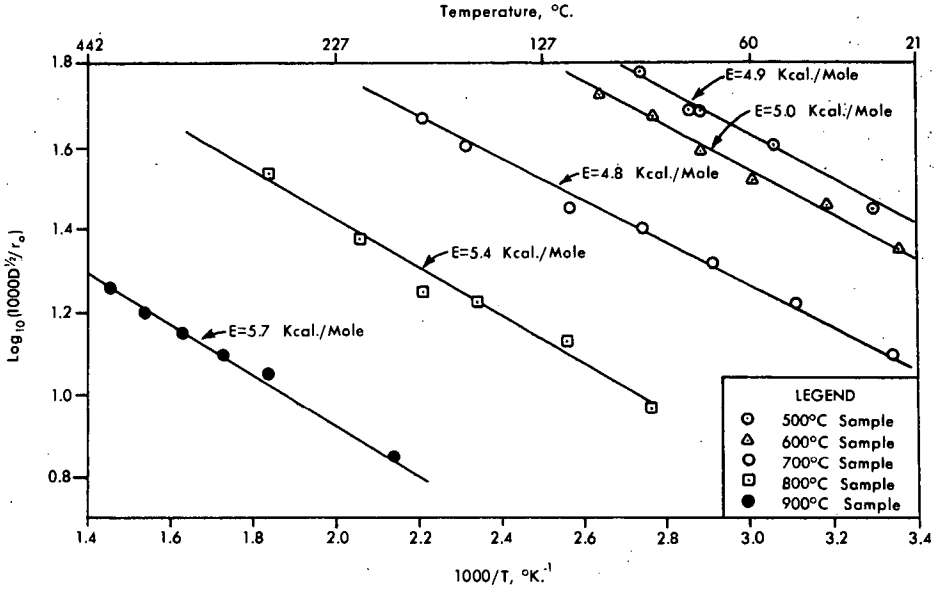
Temperature, °C.
442
227
127
60
21
1.8
1.6
1.4
1.2
1.0
0.8
E=4.9 Kcal./Mole
E=5.0 Kcal./Mole
E=4.8 Kcal./Mole
E=5.4 Kcal./Mole
E=5.7 Kcal./Mole
LEGEND
500°C Sample
600°C Sample
700°C Sample
800°C Sample
900°C Sample
1.4
1.6
1.8
2.0
2.2
2.4
2.6
2.8
3.0
3.2
3.4
1000/T, °K.-1
Log10 (1000D½/r0²)

FIGURE 7

Presented Before the Division of Fuel Chemistry
American Chemical Society
Chicago, Ill., August 30 - September 4, 1964

"PYROLYSIS OF COAL AND COAL TAR PRODUCTS"

ROBERT T. JOSEPH
CONSULTANT*

INTRODUCTION

The history of organic chemistry is intimately tied to the history of the production and refining of coal tars. From the heyday of the period when the prime source of organic chemicals (the dye stuffs, the medicinals, the preservatives, the disinfectants) was black coal tar, to the present (when almost any organic chemical whose structure can be conceived, may be synthesis almost directly from carbon, hydrogen, oxygen and nitrogen), the tar by-product from coal pyrolysis has been processed for the 10% low boiling products to supply the fine organic chemicals market. The 90% residue remaining after refining has been channeled to wherever it would fit, from creosote oils for wood preservation to bituminous products for construction and road building, or to fuel for boilers and open hearths whenever the general economy drove the price of the residues into the fuel range.

The work reported herein was done in an attempt to:

1. Upgrade the residue products from coal tar refining.

2. Seek a method of increasing the yield of highly aromatic tar from coal by direct pyrolysis under equilibrium conditions as opposed to pyrolysis under a dynamic temperature situation as found in the slot type coke oven.

To accomplish these aims, certain assumptions had to be made in order to circumvent the prejudice that had persisted for almost a century as to the nature of tar formation in coal processing. These assumptions can be listed as:

1. The products to be derived from coal by pyrolysis are not indigenous to the coal, but are controlled by the process conditions imposed during such pyrolysis.

2. The tar and light oils recovered from carbon-hydrogen-oxygen-nitrogen fragments, of free radical type, along the path of distilling pyrolysis products as these products pushed through the bed of coal maintained at temperatures in the region of 1800° F.

* Present Address: FMC Corporation
P. O. Box 8
Princeton, N.J.

3. The evidence for 2 lay in the fact that while the material collected as tar and oil left the pyrolytic chamber in the vapor phase with a coke residue in the chamber, these tars and oils can not be redistilled under any conditions without leaving a substantial residue of coke similar in nature to the coke left in the pyrolytic chamber wherein the tar and oil had their genesis as a vapor.

EXPERIMENTAL - General Attitudes

Unlike research on fine, purified organic chemicals, the field of coal and coal products exploration is characterized by the need of a combined chemist and engineer approach. On one hand, the reactions which occur are obviously governed by the known laws of rates and energy utilization. On the other hand, so little is known of the composition of the starting materials that inference, assumptions as to the specific reactions occurring, thermo-chemical calculations, or model structures, while extremely useful, can lead to serious oversight if taken as gospel over experimental observations, because the large number of components to be dealt with necessitates quantities of materials for test tube operation normally considered as pilot plant studies in the fine chemical field. Furthermore, in order to achieve the extremely short residence times and steady-state operation, a continuous flow system is required.

Accordingly, a rather elaborate description of the ground rules, feedstock identification, apparatus, and operating procedure, is given. The methods of analysis which are not unique are described by reference.

EXPERIMENTAL - Ground Rules

With these assumptions in mind, it was decided to attempt to reproduce and apply the pyrolytic conditions found in the slot type coke oven in such a fashion that:

1. The temperature of pyrolysis would remain constant.

2. The heat rate applied to the feedstock would be at a rate approaching 2000°F per second.

3. The pyrolytical action on the feedstock would be imposed for that period necessary to raise the temperature of the feedstock to 1400 to 1800°F.

4. The pyrolytical products would be quenched to ambient temperatures at the same or faster rate as the feedstock was raised to pyrolysis conditions.

EXPERIMENTAL - Feedstock Identification

In order to demonstrate the general applicability of the system, it was decided to use the following materials as feedstock:

1. The liquid oil fractions from coke oven tar refining left after the removal of tar acids, tar base, naphthalene, resin and solvents from that fraction of coke oven tar that boils up to 270°C termed by the industry - carbolic oil.

2. The high boiling residues from the distillation refining of the crude quinoline fraction (230 to 250°C) extracted from coke oven tar carbolic oil.

3. A coal tar from low temperature pyrolysis of an Appalachian coal via the "Disco" process.

4. A coal tar from the low temperature pyrolysis of Texas lignite (Rockdale) in the Parry fluid bed process.

5. A bituminous coal of Eastern origin.

EXPERIMENTAL - Apparatus Description

The apparatus used is diagrammed as flow sheet and in detail on Figures 1, 2, 3, and 4. Figure 1 represents the apparatus in flow sheet. Figure 2 represents the heating chamber and reforming column for effecting the heating and reforming operations in connection with the pyrolysis of liquid feedstocks. Figure 3 is a horizontal section of the heating chamber taken on the line 3 - 3 of Figure 2. Figure 4 represents the cooled nozzle for spraying liquid feedstocks into the heating chamber.

Referring to Figure 1 of the drawing, the numerals 1 and 1A represent storage tanks for the feedstock, which are suitably provided with the heating jackets to maintain their contents in fluid form, and which are adapted to be alternately connected to the feed line 3 by suitable valved connections 2. The line 3 is connected to the inlet of a pump 4 for the feedstock, which in turn is connected by a suitable conduit 5 to the inlet 6 of the jacketed spray nozzle 7 which is mounted with its spray tip 8 within a heating chamber 9.

The heating chamber 9 is adapted to be heated to temperatures above 600°C by external heat such as hot flue gases, gas flame, or the like, contacting the outer walls 10 of the chamber within a suitable furnace 11. The heating chamber is formed of suitable material to withstand the temperature, such as 310 steel, the inner surface of which is lined with a thin lining of refractory material such as alumina or an alumina-silica fire clay, which functions as cracking catalyst.

Heating chamber 9 is also supplied with an inlet for superheated steam 15 which is supplied through conduit 16 from a steam superheater 17 adapted to superheat by indirect contact steam supplied to the superheater by a conduit 18 from a steam generator 19. Water for generation of the steam is supplied from a suitable reservoir 22 thru valved connection 23 by a pump 24 and a conduit 25.

The heating chamber 9 communicates directly with an elongated reforming column 30 which is suitably heated to temperatures above 600°C by indirect heat, within a heating jacket 31. The chamber 30 is formed of suitable material capable of withstanding the elevated temperatures, such as 310 stainless steel.

The outlet 32 of column 30 is connected to the inlet 33 of a condenser 34 adapted to be cooled by a suitable fluid flowing through a jacket 35. The outlet 36 of the condenser is connected to a primary liquid product receiver 37 which leads to a reflux condenser 38. The vapor outlet 39 of the reflux condenser is connected by a conduit 40 to a condenser 41, the outlet 42 of which is connected by a dip pipe 43 which leads into oil scrubber 44 which is partially filled with mineral oil adapted to scrub the gases and vapors passing through it. The outlet 45 of the scrubber is connected by a conduit 46 to an empty overflow chamber 47 which, in turn, is connected by conduit 48 with a dip pipe 49 which leads into a scrubber 50 partially filled with a suitable mineral acid adapted to remove ammonia and organic bases present in the gas and vapor mixture passing through it. The outlet 51 of the scrubber 50 is connected by a conduit 52 with an overflow chamber 53 which, in turn, is connected through conduit 54 with a dip pipe 55 which leads into a scrubber 56 partially filled with 20% aqueous sodium hydroxide for removal of H_2S. The outlet 57 of the caustic scrubber 56 is connected by a conduit 58 to an overflow chamber 59 which, in turn, is connected in series with two vessels 60 and 61 which are surrounded by a dry-ice-acetone mixture jackets 62 and 63 to reduce the temperature. The outlet 66 of the chamber 61 is connected by a conduit 67 with a gas sampler 68 which, in turn, is connected by a conduit 69 to a wet test meter 70, the outlet of which is connected to a flare 75 by a conduit 74.

Referring to Figures 2 and 3 of the drawing, the heating chamber 9 consists of a shell 80 formed of 310 stainless steel, mounted in spaced relation within a furnace 81 and surrounded by flues 82, 83, 84 and 85 carrying burner gases from gas burners 87. The exits from the flues are connected to a stack (not shown). The inner surface of the heater 9 is coated with a thin layer of alumina-silica fire clay 79. The heater 9 is provided with a jacketed spray nozzle 7 which is mounted centrally of one wall of the chamber 9 so as to project a fine dispersion of the liquid fed into the chamber onto the hot inner walls of the chamber.

As shown in Figure 4, the jacketed spray nozzle 7 consists of a tube 100 surrounded by two progressively larger tubes 101 and 102 mounted in spaced relation to provide a narrow passage 105 between them and between tubes 100 and 101 for the flow of temperature-regulating fluid, such as water, steam, oil, etc., depending on the temperature to be maintained. Tubes 101 and 102 are provided with couplings 103 and 104 for the entrance and exit of the temperature-regulating fluid. The inner end of the tube 100 is provided with a spray tip 8 which is of the type normally employed for dispersing oil in the form of a cone into an oil burner of the conventional type. Such nozzles are rated according to the number of gallons per hour of No. 2 fuel oil which they are adapted to deliver as spray under a head of 100 p. s. i. g.

The heater 9 is also provided with an inlet 15 for superheated steam which is mounted within the heater on the opposite wall from the spray nozzle 7 so as to deliver superheated steam into the interior of the chamber 9 in intimate contact with the spray of feedstock from nozzle 7.

The reforming column 30 is mounted on the heating chamber 9 in direct communication with the interior thereof, and is surrounded by heating jacket 31. It is provided with a screen 110, 16 mesh stainless steel screen, mounted near the bottom thereof and adapted to retain a column of reforming catalyst 29 within the column 30.

The apparatus is provided with suitable temperature-recording mechanism connected to thermocouples at the following points: 115 within the interior of the heater 9; 116 in the interior of the heating column 30; 117 in the interior of the heating column 30 near the top thereof; 118 in the outlet 32 of the column 30; 119 at the outer wall of the column 30; 120 in the interior of the jacketed nozzle 7; and 121 in the interior of the steam inlet 15.

The apparatus is further provided with means for recording pressures (not shown) at suitable points within the apparatus, such as the interior of the heating chamber 9, the top of the column 30, the steam superheater 17, and the conduit 5 of the spray nozzle inlet 6. Suitable heating jackets (not shown) are also provided for the lines and other parts carrying fluids at temperatures above atmospheric temperature.

EXPERIMENTAL - Operating Procedure

In the operation of the apparatus referred to above, with oil feedstocks, the heating chamber 9 and reforming column 30 are first brought to temperature by suitable passage of burner gases through the furnace 11 and heating jacket 31. Water is then introduced into the steam generator 19 and heat is supplied to the steam superheater 17, and superheated steam is pumped into the heating chamber 9. If coke is employed in the reforming column 30, which constitutes the preferred practice, some water-gas is formed in the reforming column and passes through the system and is burned at the flare 75. Operation is continued until the system is cleared of air by the passage of steam, evidenced by condensation of water in the condenser 34 and primary liquid product receiver 37.

Pump 4, supplying the particular liquid feed to be pyrolyzed, is then placed in operation and the temperature-regulating fluid is passed through the tubes 101 and 102 to regulate the temperature of the feed and maintain it at the desired temperature. To prevent the starting material from undergoing undesirable preliminary decomposition, with resultant plugging of the spray nozzle, the feed to the pyrolyzer is preferably maintained at a temperature below 150°C, and usually at a temperature merely sufficient to insure adequate fluidity for spraying through the spray nozzle. Ordinarily the feed is adequately fluid at temperatures lower than 110°C.

Adequate pressure is exerted by pump 4 to secure a fine dispersion of the feed within the heating chamber 9, depending upon the rate of feed desired and the size of the spray tip 8. The rate of feed of superheated steam through inlet 15 is then adjusted to the desired ratio with respect to the feed of stock through the spray tip 8.

Operation is then continued with adjustment of the heat supplied to the heating chamber 9 and reforming column jacket 31; since with continued operation the supply of heat required to maintain operating temperature decreases, presumably by reason of the fact that exothermic as well as endothermic reactions occur in the heating chamber and reforming column.

Tars produced by the process are condensed and collected in the receiver 37 together with unreacted steam which condenses as water. Light oil fractions are absorbed and removed in the mineral oil scrubber 44. Organic bases and ammonia are removed in the acid scrubber 50. Hydrogen sulfide is removed in the alkaline scrubber 56.

The tars do not always form completely in receiver 37, but sometimes tars also are formed farther along in the recovery system. Thus tar has been found to collect in the oil scrubber 44, and in some cases a crystalline material was formed in vessels 60 and 61 which, when warmed to room temperature, formed a tar.

With pulverized coal, the oil feed mechanism was replaced by a screw feeder and the coal was blown into the chamber by superheated steam as it left the water cooled screw within the chamber. The operation of this type of mechanism proved extremely difficult, and in most cases, impossible. This was in 1953.

EXPERIMENTAL - Material Balances and Yields

Interpretation of the data demanded accurate account of the distribution of the intake materials. Accordingly, all feedstock, water, sweep gases were measured by weight or volume and subsequently converted to weight. The weight of all samples taken was accounted for and such weight prorated to the proper part of the flow sheet. Wherever possible, quantities were obtained by direct weight before, during, and after each experimental run.

An accurate log of each run was maintained which permitted logical distribution of losses in the calculation of the yields. Yields could then be based on the hydrocarbon feedstock, the steam feed, or a combination. In this fashion, some assessment of the origin of the products could be made.

EXPERIMENTAL - Analytical

Composition of the gases was determined by mass spectral analysis (Consolidated Electrodynamics) on samples taken continuously throughout the run.

Composition of the tars and light oils was determined by analysis of component fractions cut from the tar by fractional distillation, using a 1 inch by 36 inch Stedman packed column operated at maximum efficiency. One percent readings were taken for the drawing of boiling curves and fractions were cut to correspond to standard cuts used in the coal tar refining industry - pre-benzene, benzene toluene, solvent naphtha, high flash solvents, naphthalene, crude quinoline, creosote oils and pitches. Analysis of these fractions were by methods standard to the industry and published in the ASTM Specifications, the British* Methods of Testing Coal Tar Products and publications of tar refiners in the United States.

RESULTS AND DISCUSSION OF THE RESULTS

Results, along with conditions that produced such results, are given in Tables I thru V. In Tables III and IV, the format is so arranged as to facilitate comparison between individual feedstocks and products derived therefrom. The data presented, of necessity, are selected. In making the selection, considerable effort was made to include representative results where such results were relatively representative. However, wherever observation indicated that an apparent variation could not be assessed against known difficulties in experimental technique, these are recorded and so annotated.

While not shown in all cases where the cracking temperature was below 700°C very little reaction took place other than the formation of coke in the chamber by distillation of the light ends. As indicated in Table I, in all cases the water fed to the reaction reacted to some small percentage. And while there is some indication of straight water gas reaction, there is also evidence that the water may have decomposed and added to the carbon-hydrogen fragments as tar. One thing was noted throughout the experiments - the use of steam drastically inhibited carbon lay-down and coke formation.

In all cases, the most drastic change in composition of the feedstock occurred by gasification. Gas yields varied from 4% for the tar base residues to 41% for the lignite tars. Both low temperature tars produced high gas yields.

The light oils, oils with densities lower than water at room temperature, were produced in about the same quantities regardless of feedstock, and for the most part, were a crude BTX fraction.

Considering Table II, the obvious points of departure are the production of unsaturated gases as opposed to more stable hydrocarbons. Acetylene seems to be the function of the cracking temperature varying from a trace to 2.0% over a temperature range of 750°C to 925°C. However, about 150% more acetylene was derived from coal at 825°C than from lignite tar at

* Tar Products Test Committee, Gomersal

925°C. No data were collected to differentiate between the reaction temperature and the feedstock as the cause of this difference. However, since at 800°C high temperature coke oven tar yields about .3% acetylene, it seems logical to assess this increase in this product against the feedstock.

A second observation deals with the ease with which primary aromatics are produced. Benzene, while not shown specifically in Table II as such, is the predominant component of the solvents to 200°C. This situation also holds for the tar acids and bases. Pyridine and quinoline form almost 80% of their corresponding fraction while substituents in these genera are absent or present only in minor quantities.

Naphthalene, a most valuable constituent in coal tar, volumewise, forms readily at all temperatures employed. The compound, almost completely absent from tars produced by carbonizing coal in 500°C range, is obtained in yields upward to 14% of the feedstocks. Not shown because of doubtful reliability are yields of naphthalene as high as 28% of the feedstocks charged - using either carbolic oil residues or the lignite tar from the Parry process.

The resulting pitches are peculiar in that for comparable softening points the quinoline insoluble component is low. As they stand, these products are easily employed in saturation operations. No molecular weight distributions were obtained on these materials, but the high benzene insoluble, coupled with the low quinoline value, would indicate a product of low molecular weight in narrow distribution - a product of high uniform quality.

With respect to the effect of this type of treatment on high boiling tar bases, Table II indicates that pyridine, quinoline, and a high nitrogen content pitch can be formed from this heterogeneous low value crude. This type of pitch may well have seeding advantage in the electrode formation process because of the nitrogen backbone in its polymer structure.

Concerning the work with Pond Creek coal, the results should not be taken in any sense other than the indicative. Extreme difficulty was encountered with the feed mechanism and a really reliable set of data could not be obtained. Insufficient tar was recovered for accurate evaluation, but by ordinary smell, the tar would be classified as produced at high, rather than low temperature carbonization.

Table IV lists the proximate analysis of the coal use. No other information, other than the name, was available. The coal appeared dried and aged. However, if it were aged, the aging was insufficient to destroy coking properties.

Since there has been much argument as to the paraffin nature of low temperature tars, a paraffin distribution study was run on the feedstock to Run No. 3. The producer of this tar indicated that yields of 20 to 25% tar might be expected from the coal used. And while this sample contained approximately 40% uncarbonized or partially carbonized coal, he said production would yield

tars of 1 to 5% solids content. This pyrolytic study and the resultant paraffin distribution analysis were run on tar that had been cleaned by filtration.

Table III lists the results of this study. While there is no major paraffin component in this low temperature tar, those that are there appear to be evenly distributed. On pyrolysis, these are cracked to low boilers and fragments which appear to cyclize to aromatics.

Table V attempts a comparison between the pyrolysis products as they are formed on contact with the hot chamber and the flared gases after tar removal by condensation and scrubbing. These samples were taken and quenched immediately in a bath of dry ice and acetone and kept at that temperature until admission to the mass spectrometer.

It can be seen that the hydrogen, methane and acetylene that appear on pyrolysis are rapidly transformed to tar and oil products in the period of time necessary to traverse the apparatus - about 2 seconds. Another observation was noted in this same work. The material withdrawn from the cracking chamber crystallized out as a fine white crystal on the walls of the trap. When allowed to come to room temperature in not less than five minutes, the white crystals first turned to a pale yellow, then a bright brown-red, then a brown. At those stages, melting began and the brown crystals coalesced to form droplets of black tar.

This work is a summary of a much more complete study that covers some 5 years of effort and explored in replication, a wide variety of feedstocks.

Nevertheless, regardless of the source of the feed, the data so obtained fits the general pattern of the results reported here.

TABLE I

OPERATING CONDITIONS, MATERIAL BALANCES, YIELDS

1. Source of Feedstock	Neutral Oils H. T. Co. Tar		Tar Base Residues H. T. Co. Tar		Appalachian Coal Tar-Low Temp. Carb.		Texas Lignite Tar Low Temp. Carb.		Pond Creek Coal	
2. Run No.	grams[1]	wt%	grams[2]	wt%	grams[3]	wt%	grams[4]	wt%	grams[5]	wt%
3. Pyrolysis Temperature	900°C		800°C		750°C		925°C		825°C	
4. Weight of Feedstock Charged	10,000	50%	20,000	50%	7,920	54%	22,000	50%	309	46%
5. Weight of Water Charged	10,000	50%	20,000	50%	6,800	46%	22,000	50%	475	54%
6. Total Input	20,000	100%	40,000	100%	14,720	100%	44,000	100%	784	100%
7. Weight of Products Recovered	8,730	43.5	19,534	48.7	7,640	52.0	22,510	51.5	319	39.5%
8. Weight of Water Recovered	8,900	44.5	19,000	47.5	6,600	44.7	20,500	46.5	300	39.5%
9. Total Output	17,630	88.5	38,534	96.2	14,240	96.7	43,010	98.0	619	79.0%
10. Material Balance (Line 9/Line 5)		88.5		96.2		96.7		98.0		79.0%
DISTRIBUTION OF PRODUCTS										
11. Tar Recovered	5,783	66.4	17,074	87.3	3,450	45.0	10,700	47.4	35	10.7
12. Light Oil Recovered	680	7.8	900	4.6	455	6.0	800	3.6	4	1.2
13. Trapped Oils	340	3.9	260	1.4	150	2.0	390	1.7	10	3.1
14. Flared Gases	1,052	11.9	780	4.0	2,015	26.4	9,200	41.0	270	85.0
15. Carbon	875	10.0	520	2.7	1,570	20.6	1,420	6.3	---	---
16. Total	8,730	100.0	19,534	100.0	7,640	100.0	22,510	100.0	319	100.0

TABLE II

ANALYSIS OF PRODUCTS

Source of Feedstock	Neutral Oils H. T. Co. Tar		Tar Base Residues - H. T. Co. Tar		Appalachian Coal Tar-Low Temp. Carb.		Texas Lignite Tar Low Temp. Carb.		Pond Creek Coal	
Run Number	1		2		3		4		5	
Material	Feed stock	Product	Feed stock	Product	Feed stock	Product	Feed stock	Product	Feed uct	Product
Flared Gases(Below 75°C)	0.00	12.3%	0.00	3.98	0.00	26.61	0.00	40.10		85.0
Hydrogen	No gaseous components STP	2.88	No gaseous components STP	0.57	No gaseous components STP	0.82	No gaseous components STP	1.65		47.3
Methane		3.98		1.00		9.25		9.79		15.7
Nitrogen		1.77		0.51		0.43		10.42		0.0
Carbon Monoxide		1.74		1.11		8.00		0.00		17.0
Acetylene		1.00		0.27		Trace		1.40		2.1
Ethylene		0.07		0.01		5.25		8.73		0.6
Ethane		0.05		Trace		0.90		1.16		0.4
Oxygen		0.00		0.16		0.55		0.00		0.0
Carbon Dioxide		0.81		0.14		1.10		4.23		1.99
Propylene		0.00		0.00		0.31		2.70		0.0
n-Butane		0.00		0.00		0.00		0.00		0.0
Total from 75 to 200°C	1.30	7.80	0.00	6.33	7.00	14.70	10.00	11.10	No volatile components below 400°C	Apparently normal HT COT
Solvents	0.66	4.67		1.36	1.51	10.54	8.11	9.51		
Tar Acids	0.34	0.66		0.00	5.49	4.16	1.50	0.75		
Tar Bases	0.30	2.47		4.97	0.00	0.00	0.39	0.90		
Total from 200 to 250	19.50	22.70	96.00	46.55	22.60	6.30	16.29	9.00		
Solvents & Oils	13.86	6.32	5.43	6.58	4.30	3.85	12.12	1.00		
Naphthalene	0.15	13.91	0.00	0.00	0.00	1.44	0.00	7.00		
Tar Acids	2.22	1.00	0.25	0.05	14.10	1.39	3.17	0.32		
Crude Quinoline	3.27	1.47	90.32	39.92	0.00	0.00	1.00	0.68		

TABLE II (Contd)

Source of Feedstock	Neutral Oils H. T. Co. Tar		Tar Base Residues - H. T. Co. Tar		Appalachian Coal Tar - Low Temp. Carb.		Texas Lignite Tar Low Temp. Carb.		Pond Creek Coal
Run Number	1		2		3		4		5
Total from 250 to 300°C	76.00	10.90	3.00	10.62	---	---	16.90	0.10	
Solvent & Oils	66.83	8.73	0.30	9.90	---	---	8.91	0.10	
Tar Acids	3.62	1.01	0.00	0.05	---	---	4.67	---	
Tar Bases	5.55	1.16	2.70	8.47	---	---	3.42	---	
Total from 300 to 330°C	0.00	6.40	0.00	6.01	---	---	25.00	4.10	
Solvents & Oils	0.00	4.88		0.72	---	---	17.13	3.27	
Tar Acids	0.00	1.09		0.00	---	---	4.46	0.70	
Tar Bases	0.00	0.43		5.28	---	---	3.41	0.13	
Total above 330°C	3.00	16.60	1.00	10.98	68.30	31.40	31.80	35.20	
Carbon Produced	0.00	10.60	0.00	2.66	2.10*	20.70	0.00	0.00	

*Distillation loss - Not carbon

TABLE III

ANALYSIS OF THE PITCHES

Softening Point(R&B)	Fluid	98°C	No Pitch	153°C	135°C	46°C	Tar & Coke	188°C
Pitch Carbon Insoluble in CS_2	0.1%	13.9%		56.0%	37.7%	8.1%		54.8%
Pitch Carbon Insoluble in Quinoline	0.1%	0.6%		50.0%	0.5	0.4%		5.0%
Pitch N_2 Content	0.4%	0.4%		4.0%	0.9	0.7%		1.0%
Pitch Ash Content	0.0%	0.0%		0.0	0.2	1.0%		0.2%

TABLE III

COMPARISON OF PARAFFIN CONTENT OF FRACTIONS

Low Temperature Tar (Run #3) Vs. Reformed Low Temperature Tar

	Feedstock		Product	
Fraction by Boiling Point	% of Feedstock	% of Fraction	% Product	% of Fraction
75 to 90°C	0.00	0.00	0.00	0.00
90 to 125°C	1.17	17.00	1.42	71.00
125 to 150°C	0.10	17.80	0.00	70.00
150 to 200°C	1.01	18.60	0.01	0.10
200 to 230°C	2.84	18.50	0.04	0.10
230 to 250°C	1.69	22.20	0.00	0.00

TABLE IV

ANALYSIS OF COAL USED

Name	
Volatile Matter	17.0%
Fixed Carbon	79.0%
Ash	6.0%
Moisture	0.0%

TABLE V

COMPARISON OF GAS COMPOSITION (Run No. 5)

Cracking Chamber Vs. Flared Gas

Component	Cracking Chamber (wt %)	Flared Gas
Hydrogen	70.4	55.8
Methane	22.1	18.5
Water	0.2	0.2
Carbon Monoxide	0.0	20.0
Nitrogen	0.0*	0.0
Acetylene	4.2	2.4
Ethylene	0.3	0.7
Ethane	0.3	0.5
Oxygen	0.7	0.0
Argon	0.0	0.0
Carbon Dioxide	1.5	2.2
Benzene	0.2	0.0

* Not representative since gas was analyzed on a nitrogen-free basis

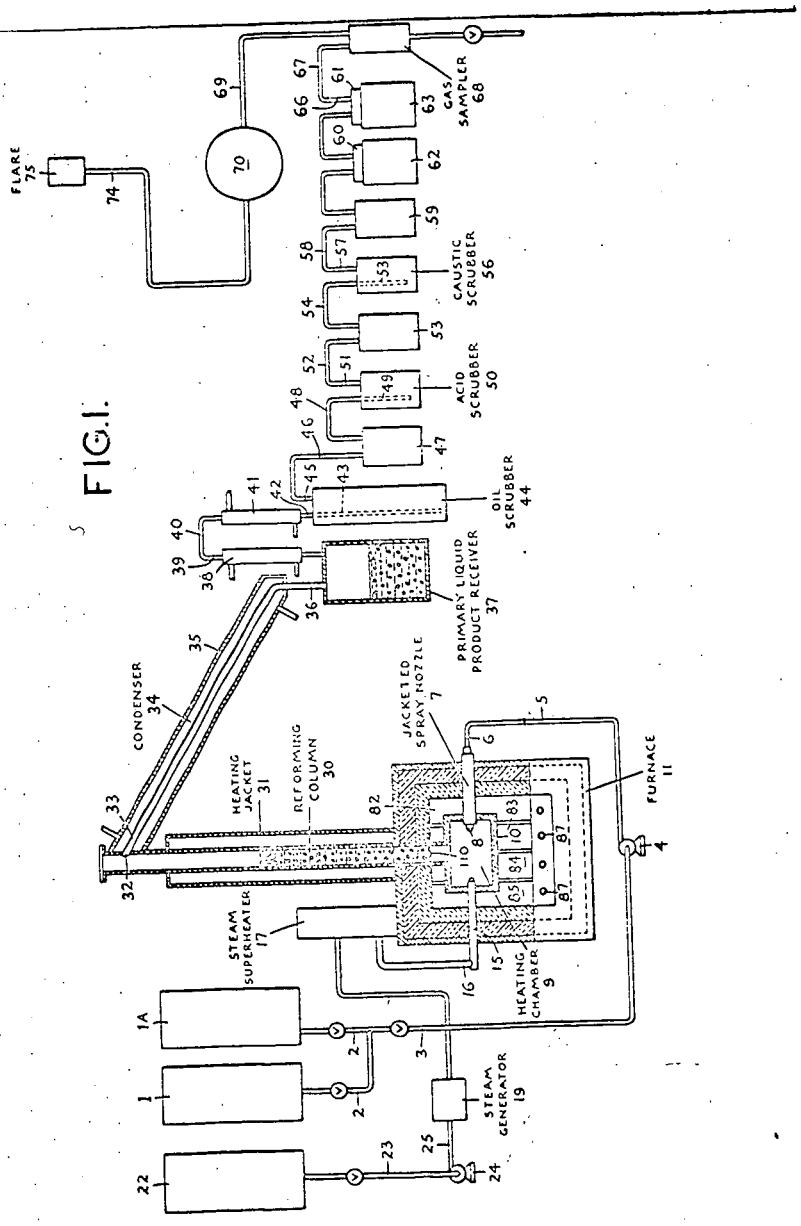
FLARE
75
74
70
69
66 67
61
63
GAS SAMPLER
68
60
62
59
58
57
53
CAUSTIC SCRUBBER
56
54
53
52
51
49
ACID SCRUBBER
50
48
46
47
45
43
41
42
OIL SCRUBBER
44
39 40
38
36
PRIMARY LIQUID PRODUCT RECEIVER
37
35
CONDENSER
34
33
32
HEATING JACKET
31
REFORMING COLUMN
30
82
JACKETED SPRAY NOZZLE
7
6
5
FURNACE
11
4
STEAM SUPERHEATER
17
16
15
HEATING CHAMBER
9
110
8
83
81
85
87
87
1A
1
22
2
2
3
23
25
1
24
STEAM GENERATOR
19

FIG.1.

FIG.4.

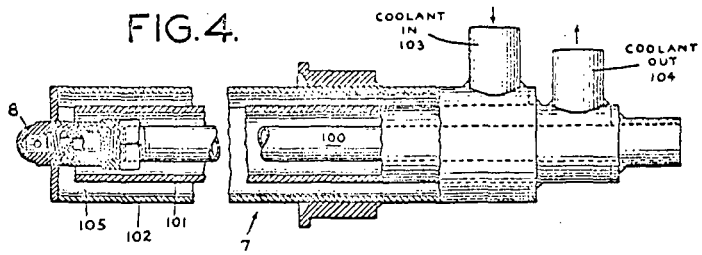

FIG.2.

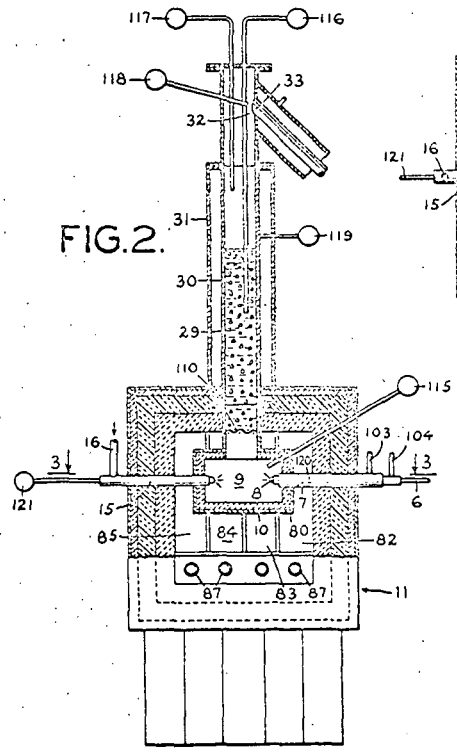

FIG.3

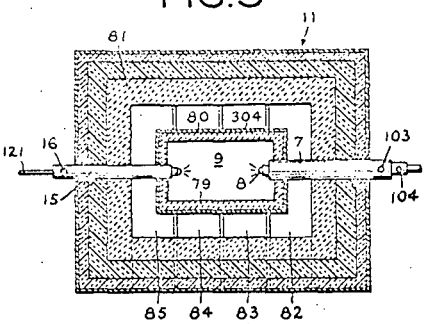

Presented Before the Division of Fuel Chemistry
American Chemical Society
Chicago, Ill., August 30 - September 4, 1964

DEVOLATILIZATION OF COAL IN A TRANSPORT REACTOR

L. D. Friedman, E. Rau, R. T. Eddinger

FMC Corp., Chemical Research and Development Center, Princeton, N. J.

INTRODUCTION

The objective of the Char Oil Energy Development (COED) project, sponsored by the Office of Coal Research, is to develop a process for conversion of coal to a pumpable mixture of char and oil. The work reported herein is part of the Project COED investigation. One approach to developing such a process involves the pyrolysis of coal using very high heating rates and very short residence times. Aside from reducing equipment costs, rapid pyrolysis is also desirable because volatile yields from coal are increased. In fact, under selected conditions, the quantity of material volatilized exceeds the ASTM volatile-matter content of the coal.

Systems most commonly employed to achieve the extremely rapid heating rates needed for maximum devolatilization--shock tubes, flash-heating apparatus and hot-strip microscopes--use such small samples that analysis and characterization of the products is difficult or uncertain. This drawback can be largely overcome by using a dispersed-phase transport reactor. With this system, larger quantities of coal can be heated for short periods at rates of more than 2500°C. per second.

EXPERIMENTAL AND RESULTS

The transport reactor, shown in Figure 1, is an externally heated tube through which coal is transported by means of an inert gas. Coal is charged from a hopper by means of a Syntron vibrator or a screw feeder. The coal is transported through the reactor by the carrier gas. The reactor is heated by a Globar-heated combustion furnace. On leaving the reactor, the bulk of the char is collected in a cyclone; the balance, in a settling vessel along with some tar. Tar mist and ultrafine particles are collected on glass-wool filters. (These were found to be more effective than an electrostatic precipitator followed by dry ice-acetone and/or liquid nitrogen cold traps.) A cold trap after the filters collects moisture entrained in the gas, and the gas is metered and sampled for mass-spectrographic analysis.

Char collected after the cyclone is washed with acetone to remove condensed tar. The washed char is dried at 110°C. and is analyzed along with char from the cyclone. Acetone is evaporated from the acetone-solution of tar, and the weight of acetone-soluble tar determined. The respective amounts of solids and tars on the filters is determined by quinoline solubility.

Elkol coal, a sub-bituminous B coal from Wyoming was used in these studies. The analysis of this coal is shown in Table I.

TABLE I

Analysis of Elkol Coal
Elkol Mine
The Kemmerer Coal Company

Proximate Analysis, wt. %	As-Received	Dry Basis
Moisture	12.8	-
Volatile Matter	35.5	40.8
Fixed Carbon	47.6	54.5
Ash	4.1	4.7
Ultimate Analysis, wt. %		
Carbon		70.7
Hydrogen		5.4
Nitrogen		1.2
Sulfur		1.0
Oxygen		17.1
Ash		4.7

One of the objectives of this study was to volatilize a maximum amount of coal. From these studies, it was found that the two most important factors in the volatilization of coal were the carrier gas velocity and the furnace temperature.

The quantity of residual volatile matter in the product chars decreases as the carrier gas velocity, calculated at 22°C. and 1 atmosphere, is decreased from 20 to 4 feet per second. This decrease in gas velocity, shown in Figure 2, increases the calculated average residence time of coal in the 8-inch hot zone of the combustion furnace from about 8 to 40 milliseconds. All of these runs were made with the same coal feed rate and with a furnace temperature of 1100°C. The lowest volatile-matter content shown in this figure is about 6 times greater than that obtained when the same coal is heated in a fluidized bed at 1100°C. for 15 minutes. It is not known whether the relatively low devolatilization obtained in the transport reactor at 1100°C. results from insufficient time for devolatilization to be completed or from the char being quenched before it reaches the furnace temperature. Because of the difficulty in determining true char temperatures during devolatilization, all temperatures given herein are furnace temperatures.

Higher furnace temperatures cause increased devolatilization of coal, as shown in Figure 3. This is true for all carrier gas velocities shown in the figure. On the other hand, reducing the carrier gas velocity below 4 feet per second does not increase the amount of coal devolatilized. Because of heating limitations, temperatures above 1500°C. could not be attained with this system. It should be noted that char prepared at 1500°C. with a linear helium velocity of 4.0 feet per second still contains 2.7 percent of volatile components, as determined by the ASTM volatile-matter test.

The foregoing indicates that complete devolatilization of the coal cannot be obtained in the transport reactor when using cold helium as the carrier gas. In an attempt to add additional heat to the system, helium preheated to 550°C. was used as the carrier gas. A comparison of results obtained when using heated and unheated helium as carrier gases is shown in Figure 4. At 1100°C., the product char obtained with heated helium carrier gas contains about four percent less volatile material than that obtained with the cold helium, but the difference decreases at higher temperatures and virtually disappears at 1400°C. With heated helium also, no difference can be found in the amount of coal devolatilized when the linear helium velocity is reduced from 4.0 to 2.5 feet per second.

When steam is used in place of helium as a carrier gas, about 10 to 15 percent less devolatilization is observed. This is attributed to the higher specific heat and lower thermal conductivity of steam, as compared to helium.

Typical product yields obtained with glazed porcelain tubes at 1100 and 1300°C. are shown in Table II. Although more coal is devolatilized at 1300°C. than at 1100°C., as shown in Figure 3 and, in the volatile-matter and ash contents of the chars shown in Table II, more solids are produced at the higher temperature. The gas produced at 1300°C. contains less hydrocarbons than the gas formed at 1100°C. This suggests that volatile hydrocarbons are cracked at the higher temperature to form solids. Confirmation of the cracking reactions was obtained by isolation of vapor-cracked carbon from practically all of the runs made at 1300°C. and higher temperatures. This carbon accumulates in the coarse and fine fractions of the product chars on sieving, or it may be elutriated from the char in a fluidized bed.

Photos of vapor-cracked carbon are shown in Figures 5 and 6.

The quantity of vapor-cracked carbon formed in miscellaneous runs at 1300°C. is shown in Table III. After repeated use, porcelain tubes cause more cracking, as evidenced by the vapor-cracked carbon contents of Runs 89 and 93. The low vapor-cracked carbon content of the solids from Run 95 is attributed to the use of undried coal. Apparently coal moisture delays the temperature rise of coal particles. The high yield of carbon in Run 96 may be partly due to cracking of the hydrocarbons in the carrier medium which simulated a recycle gas.

TABLE II

Product Yields Obtained in Glazed Porcelain Reactors
100-x200-mesh Elkol Coal
Helium Carrier Gas Velocity, 4.0 ft./sec.

Run No.	88	97
Furnace Temperature, °C.	1100	1300
Feed Rate, gm./hr.	132	124
Coal Charged, gm.	111	62.2
Coal Converted, %, dry basis		
Char	50.1	55.3
Tar	3.6	1.8
Moisture	2.7	2.1
Gas	43.6	40.8
Make-Gas Analysis, mol %		
H_2	22.5	49.0
CH_4	18.2	7.7
C_2H_2	4.3	7.2
C_2	10.5	1.1
CO	35.4	28.6
CO_2	7.5	6.0
C_3+	0.7	0.3
Char Analysis, %, dry basis		
Volatile matter	15.6	5.6
Ash	4.6	6.4

TABLE III

Formation of Vapor-Cracked Carbon at 1300°C.
(Basis: Ash Balance)

Run No.	Solids Recovered, wt. %	Percent Vapor-Cracked Carbon	Corrected Char Yield, wt. %
89	46.0	4.8	41.2
93	52.0	14.6	37.4
95[1]	50.5	6.9	43.6
96[2]	57.9	16.2	41.7

[1] Undried Elkol coal used.
[2] Recycle gas used as carrier.

The most significant aspect of Table III, however, is that, if the solids recovery is corrected for the calculated carbon content, the corrected char yield is about 41 percent. This figure is considerably lower than the char yield obtained at 1100°C. Thus, it appears that on raising the furnace temperature from 1100°C. to 1300°C. the amount of coal volatilized is increased, but the effect is masked by the simultaneous production of vapor-cracked carbon.

If the true char yield of 1300°C. is 41 weight percent of the dried coal, then 59 percent of this coal must have been volatilized. This is far above the 41 percent indicated by the ASTM volatile-matter determination. Moreover, the char still contains about 6 percent volatile matter which can be removed. Thus, about 60 to 65 weight percent of this coal can probably be volatilized by rapid pyrolysis.

In order to reduce the secondary cracking reactions, the heating zone of the combustion furnace was shortened from 8 to 4 inches by changing the Globars. To get a temperature of 1100°C. with the shorter heating zone, it was necessary to preheat the carrier gas to about 450°C. Results obtained with the 4-inch Globars are presented in Table IV.

The total amount of volatile products produced at 1100°C. in these runs is about one-fourth lower than in Run 88, Table II, but the distribution is different. Thus, tar production is increased substantially and the yield of gas is decreased. The gas has a higher concentration of hydrocarbons and less hydrogen, indicating that less cracking occurs in the shorter hot zone. Also, the yield and volatile content of the chars are higher than from Run 88 shown in Table II, indicating less devolatilization of coal in the shorter heating period.

DISCUSSION OF RESULTS

The high yield of volatile material from the devolatilization of coal in the transport reactor is believed due to the extremely fast heating rates and the short residence times used. When coal is pyrolyzed, devolatilization and polymerization reactions occur simultaneously. The velocity of the polymerization reactions is slower than that of the devolatilization reactions; and in the short residence times employed in this dilute-phase reactor system, reaction products are quenched and recovered before extensive polymerization of reactive species can occur.

TABLE IV

Devolatilization with 4-inch Globar Heaters
100-x200-mesh Elkol Coal
Helium Carrier Gas Velocity, 4.0 ft./sec.

Run No.	80	81
Furnace Temperature, °C.	1100	1100
Feed Rate, gm./hr.	120	127.5
Total Coal Charged, gm.	50.1	53.3
Coal Conversion, wt. %, dry basis		
Char	57.1	60.0
Tar	10.6	9.3
Water	6.3	7.0
Gases	26.0	23.5
Make-Gas Analysis, mol %		
H_2	15.9	17.4
CH_4	17.9	17.5
C_2H_2	1.2	0.6
C_2	13.9	15.7
CO	37.8	33.6
CO_2	9.9	12.4
C_6H_6	0.4	0.3
C_3	3.0	2.5
Char Analysis, wt. %, dry basis		
Volatile matter	20.5	21.9
Ash	4.2	4.8

TABLE V

Products Residence Times in Transport and Fluidized-Bed Reactors

Residence Time, seconds	Transport Reactor	Fluidized-Bed Reactor
Gas	0.01-0.04	1-2
Solids	0.01-0.04	900

In Figure 2 it was shown that coal particles do not reach the indicated furnace temperatures, even at the lowest carrier gas velocities (or longest residence times) used. In order to estimate the temperature to which gases and solids were heated in the transport reactor, the char and gas analyses were compared with similar analyses obtained by devolatilizing this same coal in a 3-inch fluidized-bed reactor. This method of determining temperature is less rigid than might be desired, and the residence times of char in the two reactors is very different, as shown in Table V. Based on the analyses of products from the two reactors, the temperatures of the gas and char in the transport reactor were estimated to be about 300 and 500°C., respectively, below that of the furnace. These results are summarized in Table VI.

TABLE VI

Estimated Temperatures Inside Transport Reactor
Carrier Gas Velocity, 4.0 ft./sec.

Furnace Temperature, °C.	1100	1300
Estimated Temperature, °C.		
From hydrogen content of gas	775	980
From hydrocarbon content of gas	790	980
From VM of char	625	760

The lower char temperature probably results from ablation effects in which the rapid evolution of gases and tars lowers the temperature of the char particle. Similar, though less striking, results are reported by W. Peters[1] in devolatilization studies made with longer char residence times.

In summary, the transport reactor is effective for studying devolatilization of coal. Coal devolatilization reactions proceed very rapidly. With extremely short residence times, the amount of coal that can be volatilized is appreciably greater than that determined by the ASTM volatile-matter determination. Above 1100°C., formation of vapor-cracked carbon becomes extensive, probably due to cracking of tars and gases. Lastly, by varying the residence times within a hot zone, the distribution of products may be altered considerably.

ACKNOWLEDGMENTS

The authors wish to thank the Office of Coal Research and FMC Corp. for permission to present this paper. They also wish to acknowledge the help of other members of the project staff. Analyses were made by members of the FMC Analytical Department.

[1] Peters, W., Chemie-Ing-Techn. 32 (3) 178 (1960).

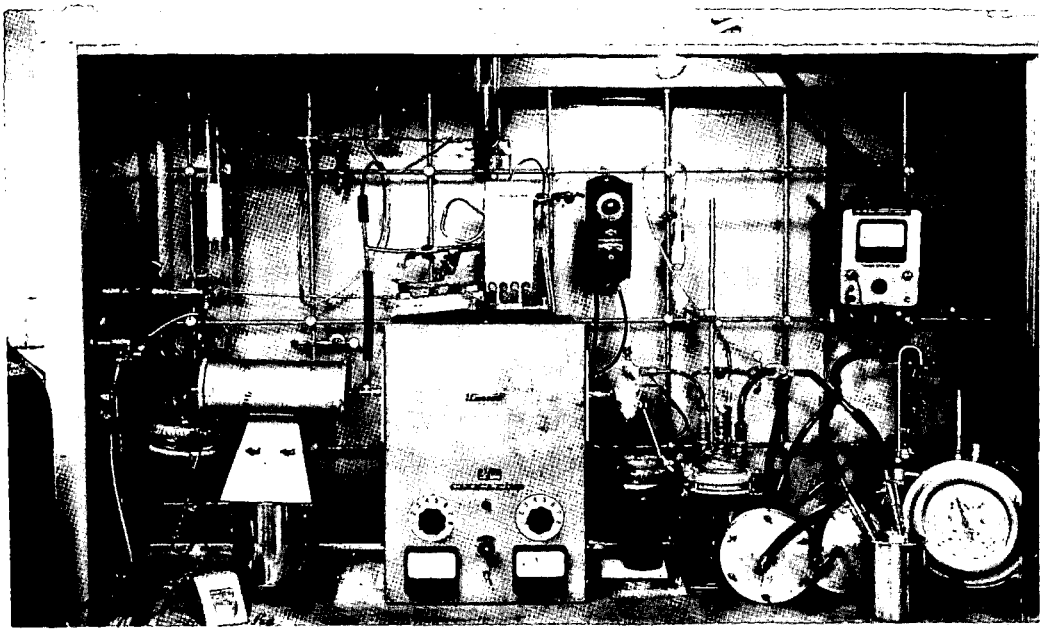

FIGURE 1
Transport Reactor Assembly

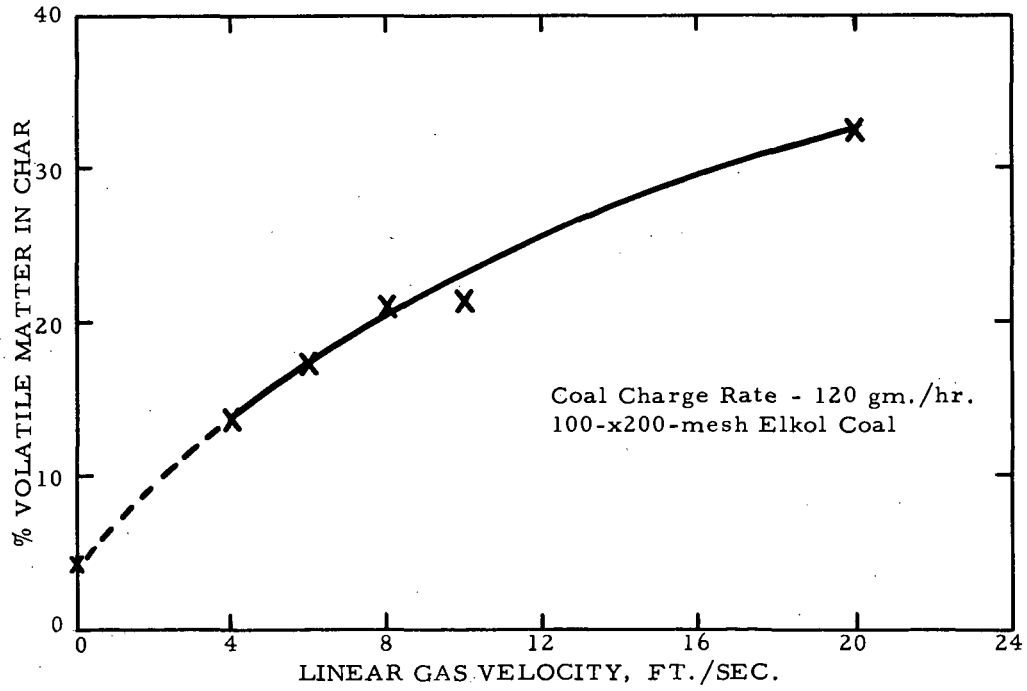

FIGURE 2
Effect of Carrier Gas Velocity on Coal Devolatilization
Furnace Temperature 1100°C.

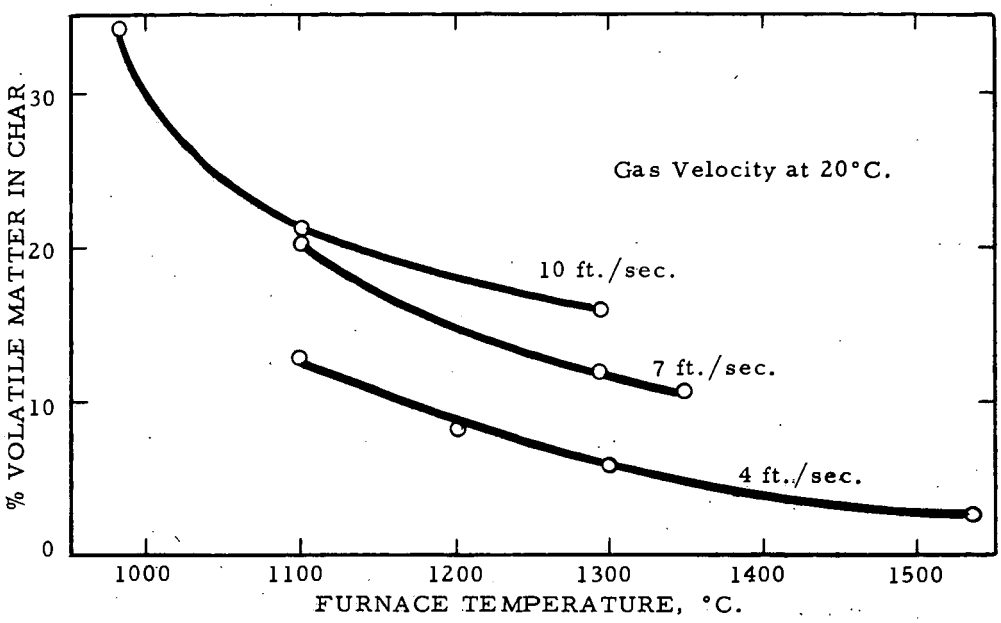

FIGURE 3
Effect of Furnace Temperature on Coal Devolatilization
Coal Charge Rate - 120 gm./hr.

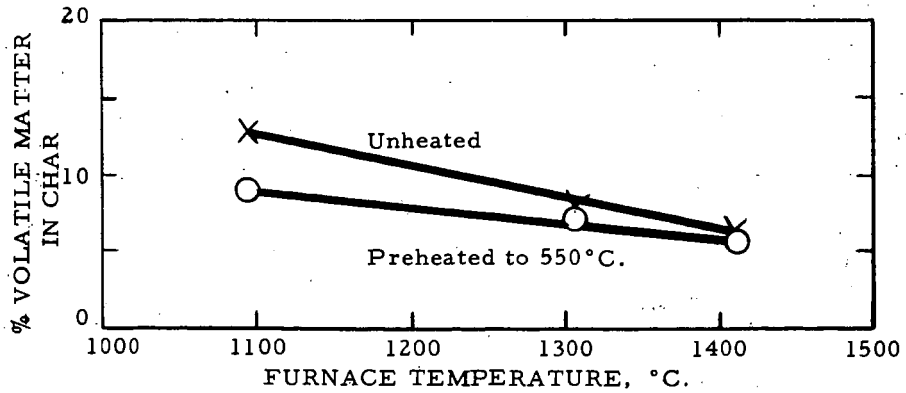

FIGURE 4
Effect of Carrier Gas Temperature on Devolatilization

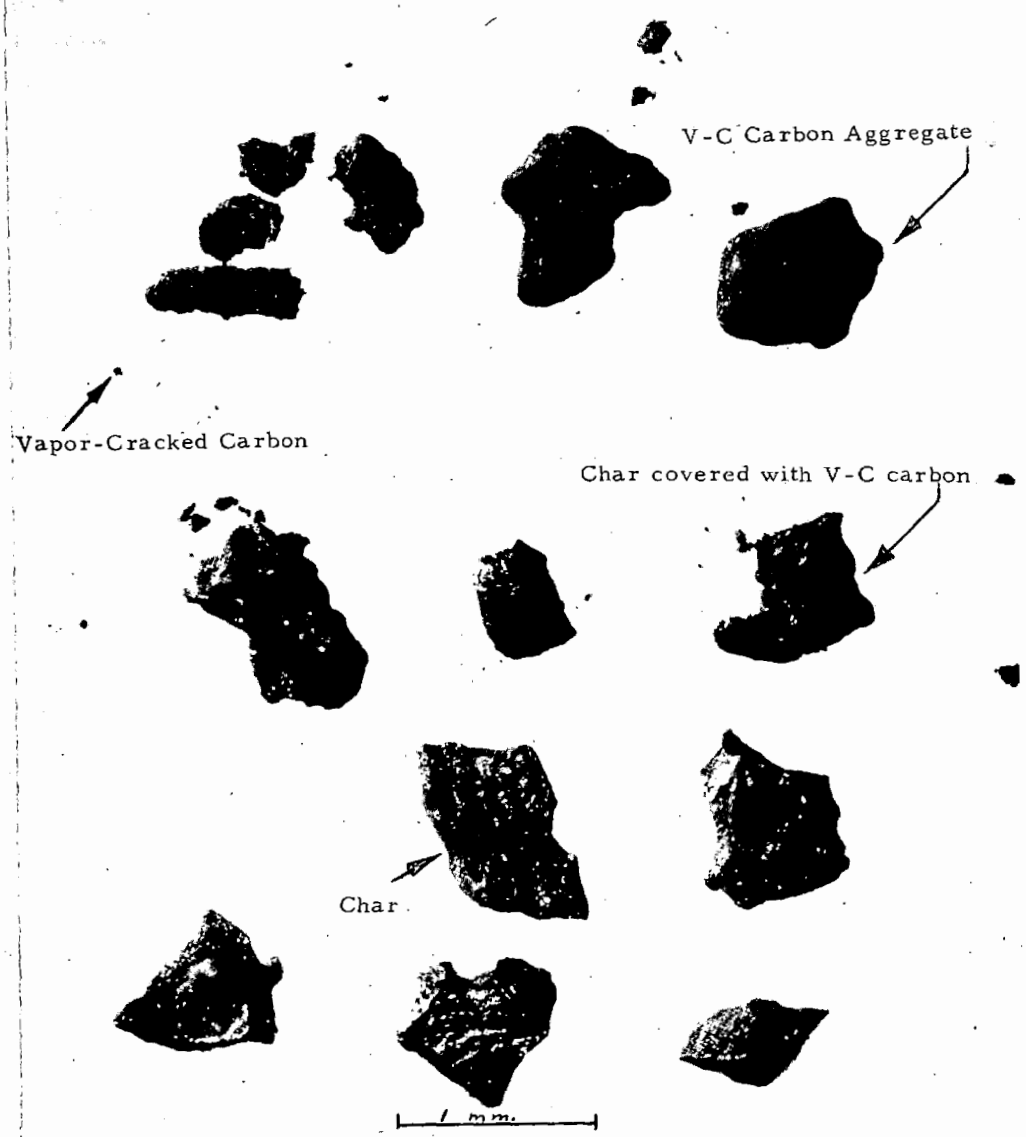

Magnification 33 1/2 X
28-x48-mesh fraction collected in recovery section
Run conditions: 2400°F. Furnace Temperature
14-x60-mesh Elkol coal
4 ft./sec. He carrier gas

FIGURE 5

Vapor-Cracked Carbon in Coarse Fraction of Char

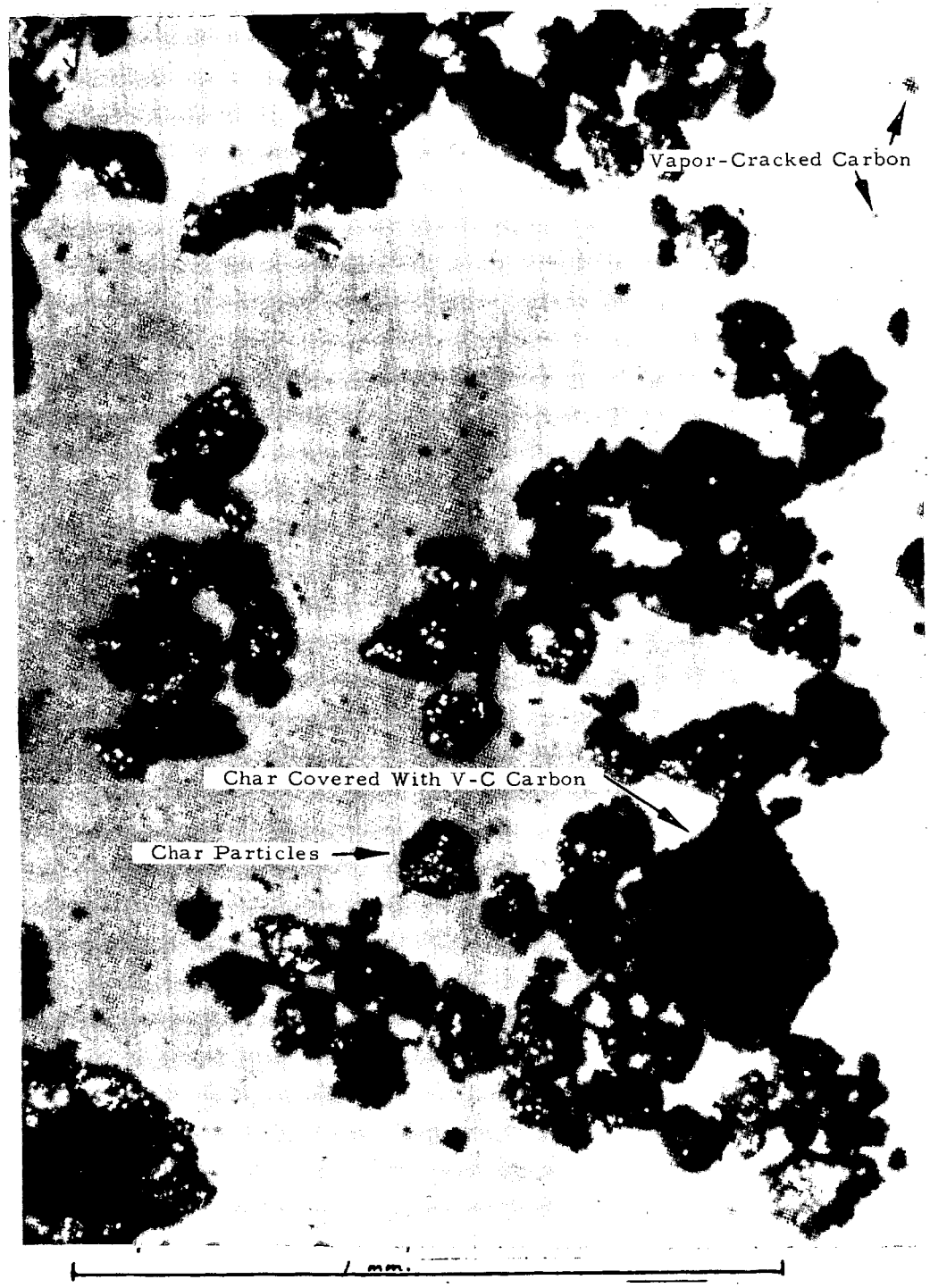

Magnification 130 X

FIGURE 6

Vapor-Cracked Carbon in Elutriated Material

Presented Before the Division of Fuel Chemistry
American Chemical Society
Chicago, Ill., August 30 - September 4, 1964

Kinetics of the Rapid Degasification of Coals

by W. Peters and H. Bertling

Bergbau-Forschung G.m.b.H., Essen-Kray

1. Introduction

In form of the socalled "LR-Process", developed in team-work by "Lurgi Gesellschaft für Wärmetechnik mbH" in Frankfurt and "Ruhrgas AG" in Essen, the rapid degasification of coal has obtained technical importance.

The basic phenomena of the rapid degasification of coal has been investigated in the laboratory-scale in essential with an equipment shown in figure 1. The most important part of this equipment is the degasification mixing chamber (b). After heating up, the fine-grained heat carriers (coke or sand) are placed into the reactor (b). Immediately behind the inlet of heat carriers, coal of the same granulation is fed into the mixing chamber. Due to the high mixing ratio of heat carriers to coal (about 30 to 6 : 1), each individual coal grain is very rapidly heated and degasified. As the gas development takes place spontaneously and as the mixing chamber is fairly small, the period of sojourn is less than 0.5 sec. After discharge, the products are immediately chilled and partly condensated (f to h). The char coke is transported from the second degasification reactor (d) into the collection reactor (a), from which it is fed, a little overheated, as a heat carrier again to the mixing chamber (b).

The rapid heating and cooling of the products causes a much higher yield of tar. This socalled "rapid degasification effect" is of great interest for the research of coal. It will be the object of this paper to describe the physical-chemical phenomena of this effect. Studying these phenomena, it will be possible not only to describe the reaction kinetics of the rapid degasification, but to draw also some conclusions therefrom on the structure of the substance of coal.

2.1. Heating-up speed of the coal

With the high mixing ratio of heat-carrier:coal, the coal grain, immediately after its entry into the degasification mixing chamber, is surrounded after intensive mixing by hot heat carriers. At the same time it is heated-up presumably very quickly. As it is very difficult to measure the heating-up speed directly, one must fall back on calculations.

The second figure shows the calculated curves at the surface and in the centre of a 1.2 mm Ø coal grain with two different heat transmission ratio related to the temperature of the heat carriers. The heat transmission ratio, of course, is of decisive importance. With a slow heat transmission, the difference between the temperature at the surface and in the centre of the coal grain is relatively small but with a rapid heat transmission it is quite high. This fact will play an important part.

Which of the curves plotted on the figure will most approximate the

true state of affairs, can be decided more easily, when the temporal yield of the degasification products is known, as the thermal diffusivity and the heat transmission ratio cannot be measured directly.

Of these investigations, a mixing chamber with a continuous feeding of coal appeared to be unsuitable. Therefore, a pilotequipment (figure 3) was built which corresponded sufficiently exactly to the conditions in the technical degasification mixing chamber.

A cylindrical tube of 80 mm inside diametre constantly heated from the outside is equipped with a stirring rod with pins. Half of the chamber is filled with fine chips of corundum as a heat carrier. For the test, a sample of coal is blown with nitrogen into the chamber and the time is precisely recorded. An ignitor directly at the free outlet of the gas brings the degasification products leaving the chamber to combustion. The size of the flame is an approximate measure for the quantity of the gases and tar fumes. The flames are photographed together with a watch showing the time in short intervals. Figure 4 shows a series of pictures taken of coking coal grains of the size 1 to 1.5 mm, the temperature of the heat carriers amounting to about 1000 °C. The seconds recorded underneath the photos are counted as from the impact of the coal grains to the corundum thips onwards.

After 0.37 seconds in phase two, a high flame can be seen which, however, is falsified by the nitrogen which still flows out. After that, the cone of the flame is much reduced. Comparing this observation with the calculated temperatures of the coal in fig. 2, much more can now be said about the heating-up process. When coal is heated, the first combustible degasification products develop at a temperature of about 350 °C. Real degasification becoming visible in phase 2, however, occurs at a temperature of 400 °C at the earliest. That means that, after 0.37 seconds, the coal must have temperatures of above 400 °C at its surface. According to fig. 4, a temperature of 400 °C at the surface, i.e. the value $\vartheta = 0.4$, is reached with a heat transmission coefficient of $\alpha = 100$ kcal/m^2 h °C, in 5 seconds only. In practice, the heat transmission coefficient must be much higher. With $\alpha = 1000$ kcal/h m^2, 400 °C at the surface will be reached in 0.28 seconds. It can be assumed, however, that degasification started much earlier so that heat transmission coefficients of at least $\alpha = 1000$ can be reckoned with. The further development of the heating-up curves agrees with the series of pictures, too. This leads to important consequences. With such a high heat transmission coefficient, a steep temperature gradient must be given in the inside of the grain. The reactions of degasification begin at the outside of the grain, when there are still nearly initial temperatures (30 °C) in the inside. The temperature of beginning decomposition in the centre is attained only, when after-coking temperatures have been reached at the surface of the grain already and when the gas yield is already strongly decreasing, as fig. 4 shows.

These rather qualitative statements show clearly that the reactions of degasification and the heating-up are much interdependent. This becomes evident also when lower temperatures of the heat carriers are applied, thus decelerating degasification with the result that more details show up from the diagramm. This test can be seen from fig. 5. The phases 2 to 4 give reason to assume, that, during the main phase of degasification, the yield of products is nearly constant. This, however, would again indicate the particular importance of the heat transmission.

2.2. Speed of degasification

The extremely rapid heating of the coal with this process promised interesting results with regard to the structure of the substance of coal. The equipment shown in fig. 3 proved to be suitable for such tests, too. However, different devices for the quantitative recording of the temporal yield of the products of degasifichation had to be connected to the gas outlet. A difference was made between the products condensated at room temperature and gaseous products which were measured, for experimental reasons, separately in parallel tests. The diagrams in the two following figures show the yield of products as a function of the time of sojourn of the coal in the degasification chamber. For instance, figure 6 shows the tar yield of three different coals and figure 7 the gas yield at different temperatures.

The curves of the gaseous products and the condensate products are added, at last, to the degasification curves plotted in fig. 8 for different temperatures.

All these curves show one and the same characteristic development: a linear start until 60 to 70 % of the products have been released, then a bend and, finally, an asymptotic development into the horizontal. After the main yield of products, relatively more gas is increasingly released than tar and, in the development of the curve behind the bend, practically gases with a low molecular weight only are released. Summing up, it can be stated:
With rapid heating, the socalled "rapid degasification" is a reaction of zero order which ends in a different process of second degasification. This statement may be surprising as the coal pyrolysis is composed of decompostition reactions of first order. That we had to do with quite a different process, is proved by the energy of activitation found to amount to 2.5 kcal/Mol (1) which is by 10 to 20 times smaller than the values known so far. This low energy of activitation is an argument against the assumption that the reactions of decomposition determine the speed.

Presumably, a mutual dependence of transporting processes is decisive for the rapid degasification. A transmission of heat from the heat carriers to the coal and the endothermal degasification process are joined with eachother by the flow-off of the degasification products which hinder the inlet of heat. These two processes give an equilibrium as long as still efficient substance for degasification is available in the coal grain.

As for the dependence of the speed of degasification on the temperature of degasification and the grain size, the following equation for the yield of products M is obtained, considering the fact that we have to do with the reaction of zero order:

$$M = 0{,}03\ (T_a - 330)\ d^{-0{,}26}\ t$$

in which M means the yield of products in % (by weight), T_a the temperature of degasification in °C, d the grain size in mm and t the time of reaction in seconds (1).

The interpretation of the equation is rendered easier by the fact that the drying of coke represents a similar process. Therefore, processes for the drying of coke were carried out in a modified

degasification mixing chamber. Figure 9 shows clearly, how much the two processes are related to eachother. In both cases, there is again the initial straight characterising a stationary process of evaporation, a bend in the curve and, at the end, an asymptotic turn into the horizontal.

The yield of water vapour from the drying of coke was calculated in the same way as the yield of gas and tar from the rapid degasification of coal. This led to the formula (1)

$$M = 0.029\ (T - 83)\ d^{-0.65}\ t.$$

Again, there is an analogy which gives reason to assume that the two processes are still much more similar than can be recognized directly:

Thus, the rapid degasification of coal represents a process of evaporation the same as a drying process.

The above expositions lead to the following summarizing picture of the degasification processes:

Figure 10 shows the development of the degasification curve in time as well as the calculated temperatures of the coal grain. At first, a fresh coal grain is very rapidly heated up under the influence of the hot heat carriers. After about 0.2 seconds, the surface of the grain reaches a temperature of about 350 °C. The primary bitumen which is then formed, begins to evaporate from the surface. With further heating, more primary bitumen is brought to the surface of the coal grains and evaporates there. The released distillation products now hinder the transmission of heat, and there is an equilibrium of the two processes opposed to eachother: with a constant boiling temperature the same quantity of heat per time unit thus flows to the surface from which the bitumen evaporates in constant quantities. During this period, temperature does not increase any more as the amount of new heat covers just the demand for evaporation heat, except the negligible amount flowing-off into the inside of the grain for heating up. A balance of temperature in the grain is established only after a good second.

When not enough primary bitumen flows to the surface of the coal grain any more, the front of evaporation is shifted concentrically to the inside of the grain. This does not yet mean a disturbance of the equilibrium, as the good heat conductivity of the coke affords a good transmission of heat. Besides, the coarse pores of the coke do not offer much flow resistance to the vaporous product. When the front of evaporation shifted far enough to the inside, the equilibrium is disturbed and the curve begins to bend, until the yield of products decreases much in the last course of the curve. In the final phase, the outside zones of the grain heat up essentially. During this process, semi-coke is forming, with the release of gaseous products. Finally, the temperature adapts itself everywhere to the temperature of the heat carriers.

3. Yields of degasification

The evaporating substance, called "primary bitumen" in this paper, must not exist necessarily in the coal in the same way. We try to clarify this question by investigation of the degasification products, especially of the tar. In doing so, it was not so much the intention

to identify as many individual substances as possible but rather to obtain a good review of larger complexes of substances.

For the purpose of comparison with products obtained under normal conditions of the pyrolysis of coal, tars were analysed which had been made in the Fischer-retort from the same coal. This was thus a tar which had been formed at a much slower heating-up speed (12 °C/min) and a much longer time of sojourn in the reaction room.

The two tars were made at a temperature of 600 °C as we obtained at this temperature the highest yield of tar as reported elsewhere (2). Investigations about secondary reactions led us to assume that the decompositions occurring during these reactions at this temperature are much suppressed. But this question, too, can be explained in the following.

The pronounced differences between both methods of degasification become visible already in the next table (fig. 11). Particularly striking is the high yield of tar with the rapid degasification. With the gasification according to Fischer, however, the yield of gas and coke is higher as the longer influence of heat caused, in this case, a cracking and coking of the tar. Very different fractions are obtained from the vacuum distillation of both tars. By virtue of the cracking, the tar according to the Fischer degasification possesses a high fraction of light oil, whereas the tar from the rapid degasification process has the highest yield of pitch. The last column of the table shows the quotient of the different yields from both methods of pyrolysis. According to these figures, the tar products from the rapid degasification process have a much higher molecular weight. This could be determinded, however, so far only with regard to the total yield of tar.

3.1. Composition of tar

The tars obtained were not to be treated with the usual methods. Therefore, methods of analysis had to be developed which separated the tar products under most mild and gentle conditions, as the tar, already from its origination, is most sensitive against thermal and chemical influences. It is thus very difficult to elaborate suitable methods.

A scheme for the entire preparation of tar in fig. 12 shows, how many steps were required to obtain fractions which could be assumed for the gas chromatographic analysis (4). It proved to be impossible to separate further the undistillable residues of pitch. Therefore, we carried out, after a further extraction, a structural analysis according to van Krevelen (6).

Surely, it would lead too far to mention all results of tar investigations in this paper. It is hoped, however, that the following data of analysis will contribute to elucidate the problem. It is sufficiently known that the pyrolysis of coal is composed of several part reactions which take place partly parallel to eachother and partly subsequent to eachother. The primary products represent large molecular units which are decomposed in the secondary process into fragments of different sizes. In the end, larger units can develop again by polymerisation and condensation. The composition of the final products depends decisively on the pre-set conditions for the secondary reactions. Especially temperature and the time of reaction are of great importance.

Kröger (3) showed in a paper about the structure of coal macerales that the substance of coal is made up of at least three main complexes of groups of material. These are at first the group of waxes and resins, secondly the group of oxyhuminic components and, finally, the group of dehydrohuminic substances.

Kröger presumes that the coal represents a structure of solid material built up of many cells, into which bituminous coal components are embedded. He proved this by microscopical photos of a vitrinite before and after cauterization with dimethylformamid. A solvent shows clearly the structure of the cells of the otherwise structureless vitrinite after cauterization. During this process, the material inside the cells (waxes, resins, oxyhumines) - which are probably connected to the skeleton of the cells not without any bonding but also through functional groups - , are released.

If such a structure of cells is slowly heated, gaseous products are formed in the individual cells leading to excess pressure and diffusing to the outside through fissures and pore passages. How far there will be secondary reactions, depends on several parameters such as the structure of the cells and of the pore system as well as type and manner of thermal treatment. Due to such factors of influence, there will always be a different compostition of the products of degasification,

With a very rapid heating of the coal, the pressure inside a cell increases very quickly. Then, the walls of the cells are torn up at weak points and the contents of the cells are so rapidly distilled that a cracking and reaction of the material is hardly still possible. On the other hand, it can be observed, that certain groups of substances are decomposed into smaller fragments at the prevailing relatively high temperatures already at extremely short times of sojourn. According to this idea of the process of pyrolysis, it can now be concluded from comparison between the yields of tar obtained from the rapid degasification process and of tar obtained from the Fischer process how these two processes act on the composition of such tars.

As the individual chemical compounds are very different indeed, it is preferable to evaluate them separately, viz. in the condition how they were obtained from the primary separation. In doing so, it is practical to limit this evaluation to the neutral components, moreover as this fraction is the largest. Then, the main two groups are obtained within this fraction: the aliphatic and the aromatic components. The values found by the urea method are partly very significant. Figure 13 shows the yield of aliphates. With hydrocarbons with 14 and 20 C-numbers, there are clearly two maxima which are a little higher for the tar obtained by the Fischer analysis. With high C-numbers, the curve of the tar obtained by the rapid degasification process, however, lies essentially above that for the tar obtained by the Fischer analysis. As products would be proved only up to the C-number of 31, it can hardly be assumed that there will be much longer chains in the substance of coal. There must be mainly hydrocarbons with C-numbers of 20 to 25 in the coal assumed for the tests. The maxima at a C-number of 14 indicate reactions of decomposition of the long chains into 2 halves. This does not mean, of course, that the lower hydrocarbons are formed only by reactions of separation. On the contrary, it must be assumed that these aliphates exist already in the substance of coal in form of waxes of vegetable origin.

By thermal treatment, the paraffins are distilled and diffused from the structure of the cells to the outside. With a "slow heating", they distill successively when reaching their boiling temperatures. With "rapid heating", however, the substances are at once exposed to high temperatures, at which they split up. Only the long-chain hydrocarbons, the boiling points of which lie at higher temperatures, are hardly decomposed. With the Fischer analysis, the longer time of sojourn leads to a cracking into smaller fragments. Therefore, the yields of these hydrocarbons with the slower degasification are lower.

It was much more difficult to determine the aromatic components as shown by a gas chromatogram of a fraction (fig. 14). Both tars contained nearly the same substances, of course, with different concentrations. A clear representation of the percentages of substances is given in the following picture (15), where the percentages of the individual ring systems of both tars have been plotted. Under the conditions of the "rapid degasification", the 3-ring-system arises preferably, whereas mostly 4 rings occur with the "slow" degasification. Besides, the percentage of substituted components of more than 50 % with the rapid degasification process is much higher than the percentage of only about 27 % with compounds obtained from the Fischer analysis.

It has been proved elsewhere (4) that these substances come from the resin in the coal. During the thermal treatment, this component is subject to reactions of decomposition and condensation. As mainly 3- and 4-ring-system could be found in these reactions which can be assigned to the base molecules of resins, the effects of secondary reactions can be small only. Due to the longer time of sojourn in the hot reaction chamber, the reactions of condensation of the tar obtained from the Fischer analysis are more progressed than for the tar obtained from the rapid degasification process. Therefore, the maximum of the ring distribution is with the 4-ring-system. Apart from the reaction of condensation, the low yield of alkylated aromates gives reason to assume stronger reactions of decompostion.

In order to investigate also the high amount of pitch in the tar obtained from the rapid degasification process, a structural analysis of the fractions obtained according to van Krevelen (6) was carried out. The median ring size calculated by this method has been plotted in fig. 16 in percentages. The maximum at the 10-ring-system shows that this is a much higher condensated system. This is indicated also by the median molecular weights between 140 and 554 found by experiment.

As such high molecular units, surely, are not released unchanged from the substance of coal, it can be assumed that the composition of the pitch is much more determined by secondary reactions than the compostition of the liquid tar. This is due, above all, to the above mentioned reactions of condensation which, at a sufficiently long time of sojourn, progress to an exent that macromolecules develop which can no more be distilled and coked in the course of the degasification process even if temperature would be further increased. This can be easily derived from the following table (fig. 17). According to this table, 122.9 g of the pitch formed by the rapid degasification of 1 kg coal, has been changed with the degasification according to Fischer secondarily into 98.9 g of coke and 24 g of gaseous products.

The longer period of heat influence with the degasification process according to Fischer thus led to an intensified condensation and decomposition. The macromolecules developed during this process were coked. During the rapid degasification process, however, the reactions of condensation could be interrupted at an early stage by a quick discharge of the degasification products.

These results of investigation are in accordance with the assumption that tar is principally formed by the wax-resin-component of the coal. According to a calculation described by Kröger (5), it could be shown that this complex of substances is being obtained, with the rapid degasification process, nearly entirely in the form of tar, whereas the yield of products obtained by the Fischer analysis is far below the calculated values.

Thus, it is possible by means of the rapid degasification process to obtain this basic complex of the coal completely in the form of tar. It is true, that the degasification products are not portions of the original substances of coal but represent the primary bitumen developed during the primary decomposition of the coal. The primary bitumen is only a little changed by secondary reactions as they are tied up at an early stage by the quick discharge of the degasification products.

4. Summary

By virtue of these results of investigation, the reactions during the rapid degasification of coal can be explained as follows:

Under the conditions of rapid degasification, notably the heating speed at the coal grain and the quick discharge of degasification products, primary bitumen is obtained which developed from the coal during the primary decomposition. During this process, the same regularities prevail as with any process of evaporation.

The substance, most of which are to be assigned to the wax-resin-component of the coal, can be completely evaporated by this process. To which exent the primary bitumen is being changed by secondary reactions, depends especially on the pre-set temperature of the heat carriers. The tests showed that the maximum of the tar yield is obtained at a temperature of about 600 °C.

After numerous analyses of the degasification products evaporated at this temperatures, it can be stated that the substances obtained are hardly decomposed by secondary reactions.

BIBLIOGRAPHY

1) Thesis to obtain the "venia legendi"
by W. Peters, Technische Hochschule Aachen 1963

2) W. Peters, "Gas- und Wasserfach" 41 (1958)

3) C. Kröger, paper read at the International Coal Scientific Congress in Cheltenham, 1963

4) Dissertation by H. Bertling
Technische Hochschule Aachen 1964

5) C. Kröger and H. Hortig, unpublished

6) D.W. van Krevelen
"Brennstoff-Chemie" 34 S. 167 (1953)

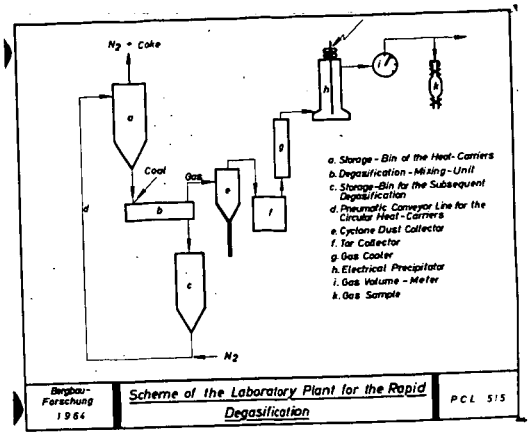

Figure 1

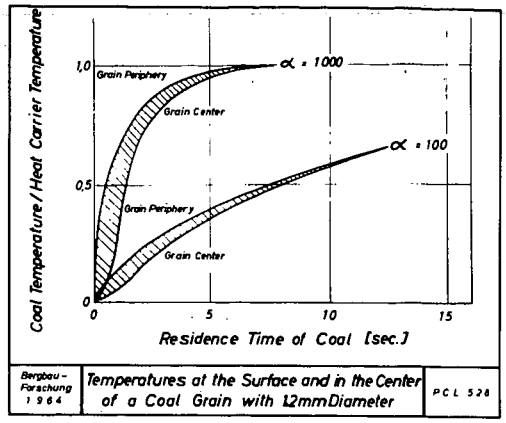

Figure 2

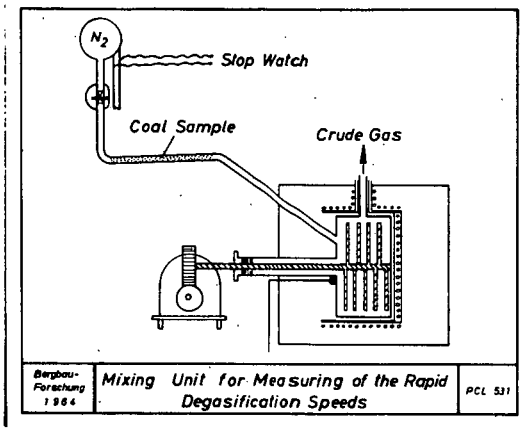

Figure 3

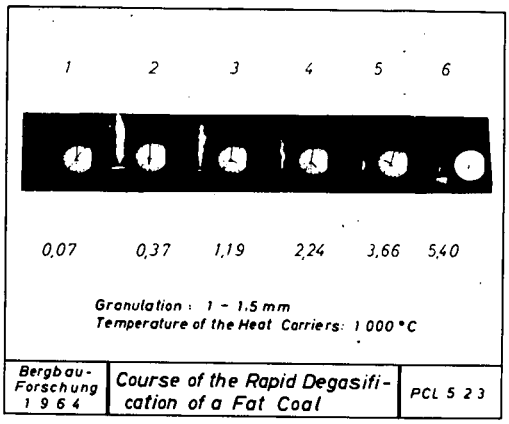

Figure 4

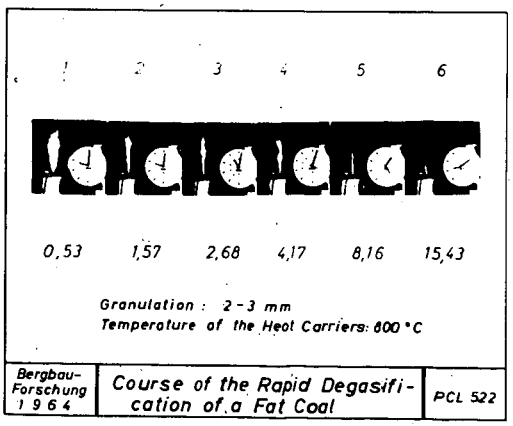

Figure 5

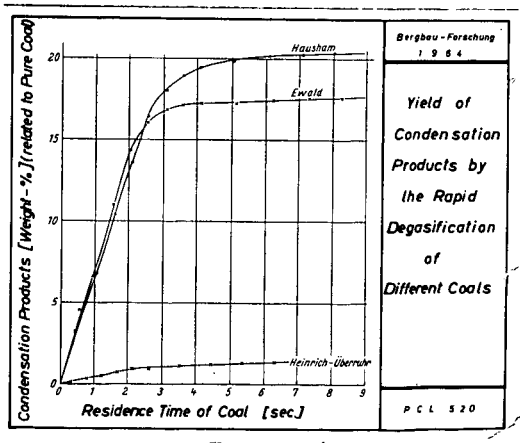

Figure 6

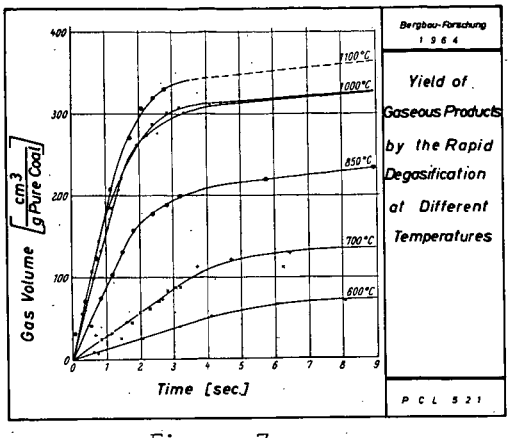

Figure 7

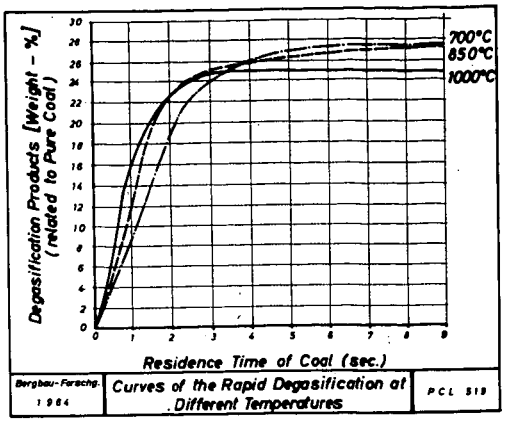

Figure 8

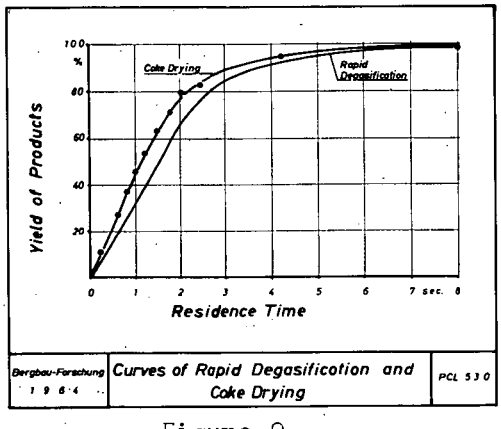

Figure 9

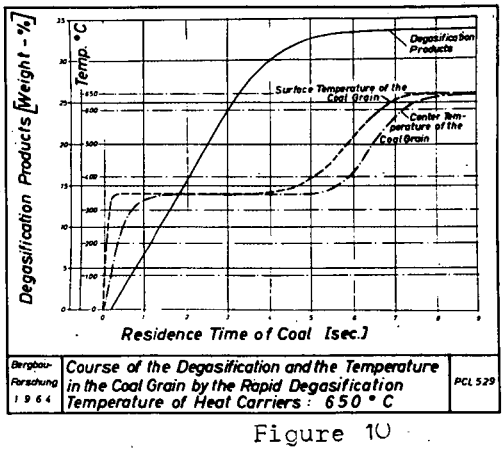

Figure 10

Product	Rapid Degasification	Carbonisation by Fischer	Ratio rapid:slow
Gas	7,25	8,44	0,86
Carbonisation Water	4,10	4,60	0,89
Tar + Carbonisation Benzine	26,40	14,82	1,78
Fraction I up to 140°C/1mmHg	6,50	8,02	0,81
Fraction II up to 140°C/1mmHg	2,87	2,71	1,06
Pitch	17,05	4,11	4,15
Carbonisation Coke	62,25	72,14	0,86

Values are given in Weight-Percent of the Pure Coal

Bergbau-Forschung 1964 — **Yields of the Carbonisation Products** — PCL 518

Figure 11

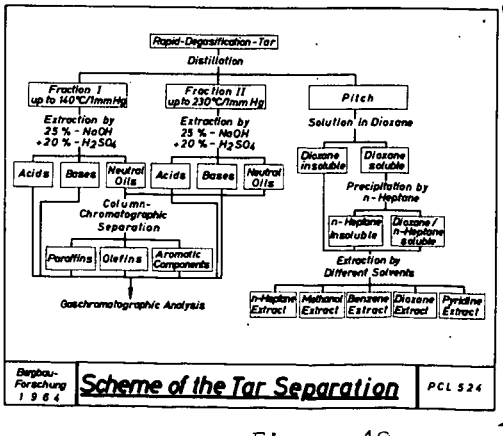

Figure 12

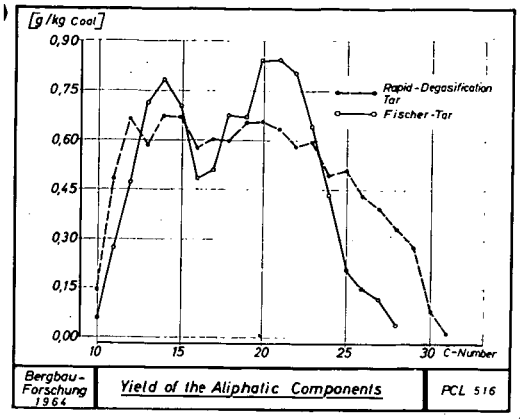

Figure 13

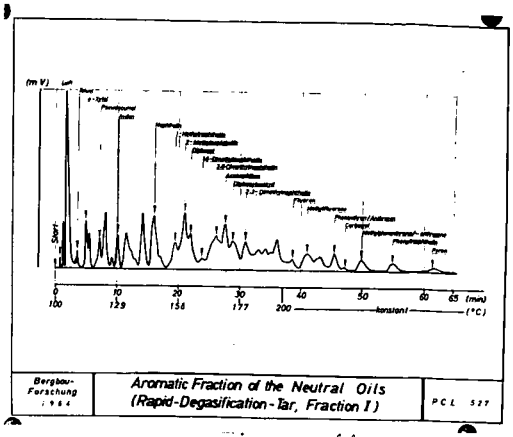

Figure 14

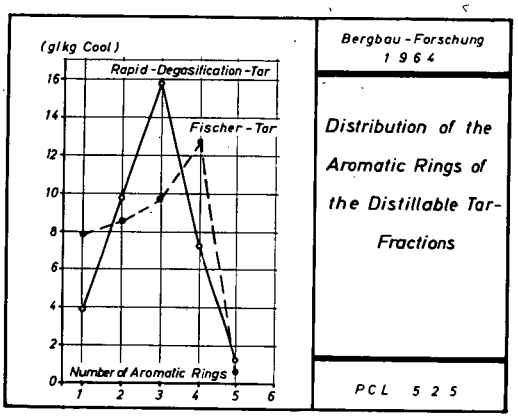

Figure 15

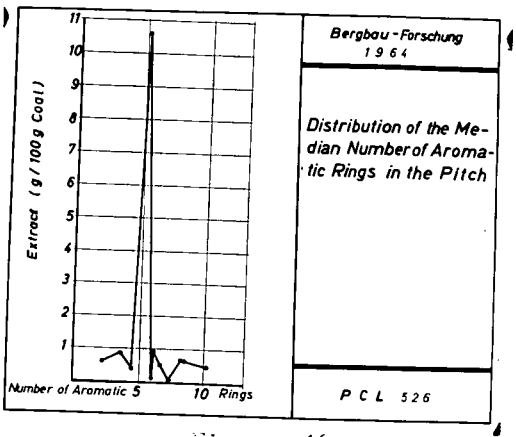

Figure 16

	Pitch		Coke		Sum
Rapid-Degasification-Tar	164,0	+	622,5	=	788,5 g/kg Coal
Fischer-Tar	41,1	+	721,4	=	762,5 g/kg Coal
Difference	122,9		98,9		24,0 g/kg Coal

Bergbau-Forschung 1964 — Yields of Pitch and Coke — PCL 517

Figure 17

Pyrolysis Kinetics of a Western High Volatile Coal

by Norbert Kertamus and George Richard Hill
Fuels Engineering Department, University of Utah

Although a number of time studies have been made on coal devolatilization, three principal models have been developed to explain the weight loss curves (1).

This study is an attempt to evaluate the mechanism of pyrolysis of a Western U. S. high volatile coal. The weight loss-time curves are interpreted according to the three classical models and as a simple unimolecular reaction. A new mechanism, more in accord with all the data, is proposed.

Several typical pyrolysis curves are plotted in Figure 1. In each instance the weighed coal sample was placed on a quartz spring, thermogravimetric furnace and the weight loss determined as a function of time. In the figure the ordinate is the fractional weight loss $\Delta W/W_o$. In the equations that follow, the following definitions apply. W_o = initial sample weight on an ash free basis. $x = [W/W_o]$. $a = [W/W_o]_{max}$. (at infinite time). $Z = x/a$. $\Delta H^{\ddagger}$ = heat of activation. $\Delta S^{\ddagger}$ = entropy of activation. E = activation energy (Arrhenius). R· is a reactive intermediate similar to van Krevelen's metaplast. B_i is the initial concentration of the i th species in Pitt's pyrolysis mechanism.

The general differential equation defining an n th order reaction is $dx/dt = k\ (a-x)^n$ when k is the reaction rate constant. In a graph of log (dx/dt) vs log (a-x), the slope of the line gives the value of n. In Figure 2, it is noted that the apparent order of the reaction varies from an initial 4.5 to unity. Obviously the decomposition is not by a simple unimolecular mechanism.

Earlier writers on coal pyrolysis kinetics (2-9) have assumed the basic reaction to be at least one unimolecular decomposition followed by other slower steps which become rate determining. Intuitively (10) bond breaking reactions of organic molecules would be unimolecular and the reaction rate proportional to the remaining undecomposed volatile producing material (a-x). To determine whether a region of "first order" kinetics exists the log (1-x/a) can be plotted versus time as in Figure 4. All of the curves are linear for the first 10-15 minutes and for times in excess of 200 minutes. If it is assumed that one or the other linear portion of the curve represents true first order rate dependence the slope of the line k_i (initial) or k_f (final) would be the rate constant.

The validity of the assumption can be checked by determining the magnitude of the heat and entropy of activation from Arrhenius or Eyring Absolute Reaction Rate plots of the log of the rate versus 1/T. Figure 5 is an Arrhenius plot of k_f (fit by least squares). The activation energy is 2.4 kcal/mole. This value is considerably less than Pitzer's (11) value of 80 kcal for C-C bond decomposition. The entropy of activation which should be almost zero, is -50 e.u.

Arbitrarily selected times of 150 and 500 minutes were chosen to determine rate constants in Figure 6. The values of "a" determined by extrapolation to infinite time were less than the experimental values in all cases.

Arrhenius plots of the rate constants (Fig. 7) and Eyring plots, fit by the method of least squares give E = 10.6 kcal/mole and $\Delta H^{\ddagger}$ = 9 kcal/mole respectively.

To a large extent the volatile matter is released from the coal during the first 10 to 30 minutes. The initial rate constants should be the most significant. The least square Arrhenius plot (Fig. 8) gives activation energy of 26.6 kcal/mole. The $\Delta H^{\ddagger}$ is 24.8 kcal/mole and the entropy of activation is -10.1 e.u.

It has been suggested by Reed (12) that the intercept at infinite temperature of an activation energy plot may be a more reliable test of a unimolecular mechanism than the activation energy. Daniels (13) states that for most unimolecular bond breaking reactions the entropy of activation in an Eyring plot is almost zero since the activated complex is so much like the original reactants. This means that the frequency factor from an Arrhenius plot should be $\sim 10^{13}$. In each region of coal decomposition, initial, intermediate, or final it is seen that energy considerations rule out simple unimolecular decomposition as being rate determining.

Since a simple unimolecular kinetic model does not explain the weight loss curve, or even parts of it rigorously, three extensions have been advanced. The first of these might be roughly defined as the unimolecular approach. This assumes that the weight loss-time curve can be defined by a number of independent unimolecular decompositions. Various writers (2-5) have considered from one to five, although Pitt (6) derives the general case where a great many decompositions take part in the weight loss curve.

The second model was proposed by N. Berkowitz (7). In his representation, he assumes as coal is placed in a hot environment, that a rapid pyrolytic reaction occurs. This reaction produces a large volume of volatile material that is stuffed into the inter-porous space of the coal particle. He postulates a slow diffusion of volatile matter from the inter-porous volume as giving rise to the kinetics. He considers the initial decomposition as unimolecular and estimates appropriate rate constants to fit the slow diffusion controlled process.

The third approach is that defined by van Krevelen and co-workers (8, 9). They postulate a mathematical scheme to define not only the pyrolytic weight loss curves, but other coal pyrolytic phenomenon. This approach assumes that the decomposition of a bituminous coal can be distinguished into three successive reactions; formation of an unstable intermediate phase (metaplast) which is (partly) responsible for the plastification and transformation of this intermediate into semi-coke and finally into coke with three individual rate constants.

In addition to the assumption of one unimolecular decomposition the following assumptions are made in the three models. Case I, Berkowitz; (1) an undefinable equation of state of the product gases in the pore structures, (2) a diffusionally controlled rate loss which can not be treated rigorously, and (3) an assumed time of completion of pyrolysis which determines the activation energy. Case II, Pitt; (1) a value for the frequency factor "a", (2) the initial concentration of all volatile species is the same, (3) a large number of independent unimolecular decompositions of different activation energies. Case III, van Krevelen; (1) an initial depolymerization to unstable intermediate (metaplast) which decomposes to give gas, (2) equality of rate constants for formation and decomposition of metaplast and (3) the occurrence of a second (semi-coke) decomposition which produces additional gas.

Berkowitz found that significant differences existed between the weight loss-time curves for a -10 to +28 mesh coal and a -60 mesh coal. In our laboratory representative samples of -40 to +60 and -200 to +250 mesh coals were pyrolyzed. The weight loss time curves were identical. It is possible that heat distribution and thermal conductivity may be important with larger particle sizes.

In Pitt's model (Case II) it is assumed that the independently decomposing coal molecules have a distribution of activation energies for decomposition between E and E+dE. The number of undecomposed molecules remaining after some time t is given by the equation:

$$n_t = n_o \quad f(E)e^{AT}\, e^{-E/RT}\, dE$$

Mathematically assuming an energy distribution from zero to infinity and plotting a range of activation energies, the data give a broad maximum in the distribution curve in the energy range 50 to 55 kcal/mole.

An alternate treatment using Pitt's model gives the equation:

$$x = \sum_{i=1}^{j} B_i - \sum_{i=1}^{j} B_i e^{-kiT}$$

where j decompositions occur. Using Pitt's assumptions of equal initial concentration of volatile matter a curve analogous to Figure 4 can be constructed. From k_1 for our run 17/R (682°K), an activation energy of 51.6 kcal/mole is obtained. From k_f the activation energy is 55.2 kcal/mole. For run 24/R (770°K), the respective values are 55.2 and 61.4 kcal/mole. The one disadvantage of Pitt's model is the assumption of equal initial concentration of all the volatile species. If the species pyrolyzed were large a more tenable assumption is equal k_i's (equal activation energies). If so, the above equation reduces to simple first order kinetics and the initial concentration of B_i is unimportant.

In van Krevelen's model (Case III), the assumption that the rate constants k_1 and k_2 are equal and that one half of the gas evolved is from each of two steps does not result in a good fit of the experimental curve, according to Pitt (6). The problem can be solved by modifying

slightly the van Krevelen model to permit an estimation of the gas produced in each step. Mathematically the final expression is the same as the integrated form for a consecutive reaction except that the fraction of gas produced is defined by a ratio of rate constants. The modified model consists of the following steps:

Coal $\xrightarrow{k_d}$ R· R· $\xrightarrow{k}$ Gas and R· $\xrightarrow{k_1}$ M M $\xrightarrow{k_o}$ Gas and M $\xrightarrow{k_2}$ Coke, where R· is a reactive intermediate similar to van Krevelen's metaplast and M is equivalent to semi-coke; a steady state is assumed for R·. By making certain simple approximations k_d can be determined from Figure 4. From the points of an Arrhenius plot, the variation in k_d with temperature gives the least square equation of $\log_e (k_d) = -11.1/T + 12.7$ which gives an activation energy of 22.1 kcal/mole and a frequency factor of 3.3×10^5. If $k_o \cong k_2$, then $k_o + k_2$ corresponds roughly to k_3 of the van Krevelen model or k_f discussed previously. This means that the activation energy for the second step is very small ($\sim$2.4 kcal/mole). Pyrolysis could not account for the second step.

A new model which fits the experimental data involves the following two assumptions. The decomposition follows a simple first order rate law; the decomposition exhibits first order dependence upon the number of surface sites (S:) available at any time.

This model is based upon the earlier worker's observations and data cited and upon additional experimental data. In the pyrolyses conducted in this laboratory, the calculated residence time of volatile products is 9.3 seconds. Analyses of the nitrogen carrier gas stream utilizing an F and M model 720 Chromatograph and a Consolidated Electrodynamics Model 21-620 Mass Spectrometer showed no detectable low molecular weight hydrocarbons. The usual distillate was a tar mist. The product gases were frozen out in a liquid nitrogen cooled trap and analyzed. The total hydrocarbon and carbon dioxide concentration was determined to be 1.8% with CH_4, C_2H_6, C_3H_8, C_4-C_6 and higher hydrocarbons being present in the ratio 80:60:62:129. The gas analysis indicates that in addition to the CO_2 and H_2O produced, the principle primary decomposition products were of high molecular weight. The light gases found may be due to secondary reactions. These analytical data strongly suggest that large molecules in the coal are fragmented to produce the primary products, probably in a single bond breaking, unimolecular reaction.

The second postulate involves a first order dependence upon surface sites; the pyrolysis reaction would be written S: + (1-Z) $\xrightarrow{k_o}$ Z + S:. The differential equation defining the rate is: $dZ/dT = k_o (1-Z)(S:)$. The second postulate requires that $d(S:)/dZ = -b(S:)$ which on integration gives $(S:) = e^{-bZ}$. Substituting one obtains $dZ/dT = k_o(1-Z)e^{-bZ}$. From Eyring's rate theory (14) the rate constant $k_o' = \frac{kT_e}{h} e^{-\Delta F^{\ddagger}/RT}$ where k is Boltzmann's constant and h is Planck's constant. If the free energy of activation varies in a linear manner with the amount pyrolyzed, $\Delta F^{\ddagger} = \Delta F_o^{\ddagger} + qZ$. If q is a function of the entropy of activation only, i.e. of the relative complexity of the activated complex to the undecomposed

reactant, the temperature dependence of entropy cancels when this equation is substituted into Eyring's equation. If this is substituted into a unimolecular rate equation, the equation $dZ/dT = k_o (1-Z)e^{-bZ}$ results where b is an entropy dependent term or $dZ/dT = (kT/h)e^{-\Delta F^{\ddagger}/RT}(1-Z)e^{-bZ}$. A plot of log $\frac{dZ/dT}{T(1-Z)}$ versus Z should give a straight line of slope b/2.3.

If the model is correct the slope should not be temperature dependent. In Figure 9 the appropriate plots are represented from 0 to 75% completion. As can be seen, excellent point linearity and slope agreement at different temperatures, are found, especially for the lower temperature curves.

At the lower temperatures linearity is observed for 90% of the pyrolysis. At higher temperatures a departure from linearity occurs at 75% completion. This might indicate a break down of the coal surface at higher temperature (6) or an increase in secondary reactions.

From the intercepts of Figure 9, Figure 10 was constructed. The heat of activation was found to be 55.8 kcal/mole. The intercept is 13.51. This corresponds to a very small positive entropy of activation or to a frequency factor of about 10^{14}, a value to be expected from theoretical considerations. The activation energy is of the right magnitude for bond breaking reactions.

Van Krevelen's observation is most germain: "Any kinetic interpretation is much too simple to provide a complete description of the complicated decomposition process; therefore, it is more correct to regard it as a mathematical model which does not pretend to be more than an aid for obtaining a semi-quantitative description of the experimental results.

Appreciation is expressed to the Office of Coal Research which, with the State of Utah co-sponsors this research. We are grateful also for the advice and counsel given by Dr. R. I. Reed and Dr. Larry L. Anderson in the interpretation of the data.

BIBLIOGRAPHY

1. W. I. Jones, J. Inst. Fuel, 37, 3 (1964), Abstr. in "Fuel Abst. and Curr. Titles" 139 (1964) pp 136.

2. W. Fuchs, and A. G. Sandhoff, "Ind. Eng. Chem.", 34, 567 (1942).

3. E. A. Shapatina, V. V. Kalyuzhny, and Z. F. Chukhanov, "Dokl. Akad. Nauk. S. S. S. R.", 72, 869 (1950).

4. H. N. Stone, J. D. Batchelor, and H. F. Johnstone, "Ind. Eng. Chem." 46, 274 (1954).

5. S. F. Tschuchanow, "Brennst. Chemie.", 37, 234 (1956).

6. G. J. Pitt, "Fuel", London, 41, 237 (1962).

7. N. Berkowitz, "Fuel", London, 39, 47 (1960).

8. H. A. G. Chermin, and D. W. van Krevelen, "Fuel", London 36, 85 (1957).

9. D. W. van Krevelen, "Coal", Elsevier, New York (1961), pp 287.

10. Ibid. pp 289.

11. Pitzer, "Quantum Chem.", Prentice-Hall, New York (1953) pp 170.

12. Suggestion from Dr. R. I. Reed, Univer. Glasgow.

13. F. Daniels, and A. Alberty, "Physical Chemistry", John Wiley and Sons, Inc., New York, (1955) pp 353.

14. H. Eyring, "Theory of Rate Processes", McGraw-Hill, New York (1941), pp 14.

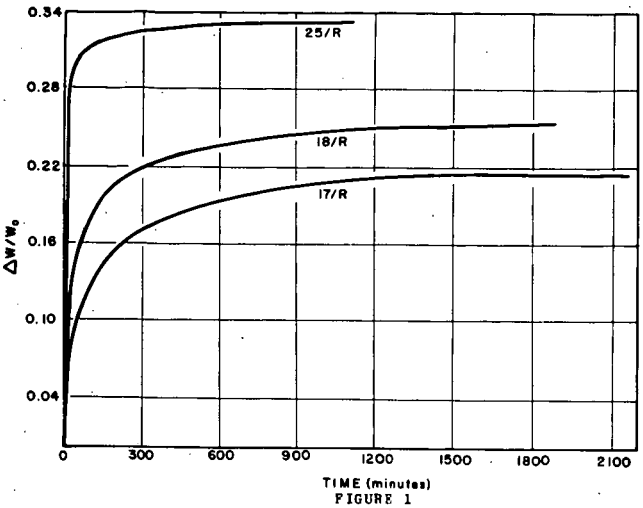

FIGURE 1

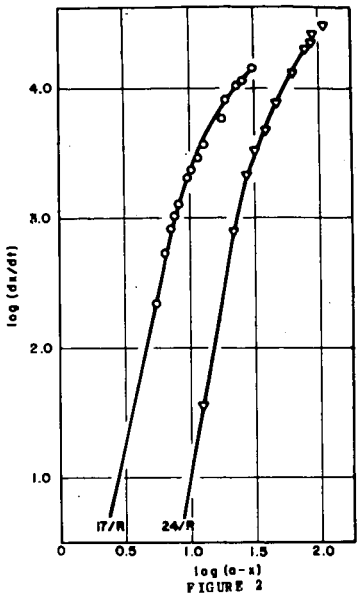

FIGURE 2

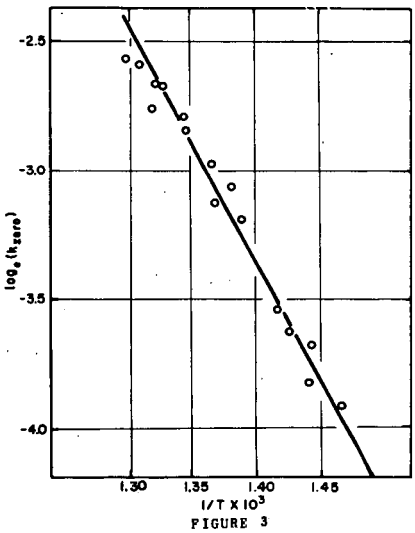

FIGURE 3

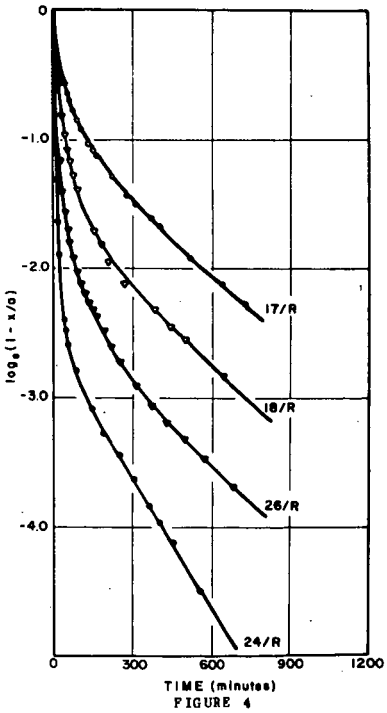

FIGURE 4

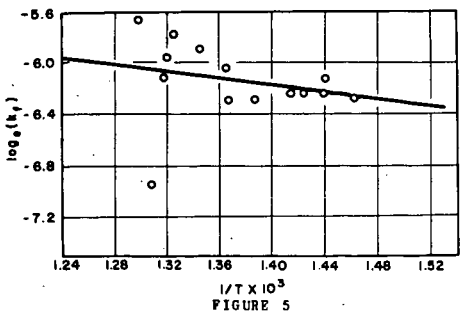

FIGURE 5

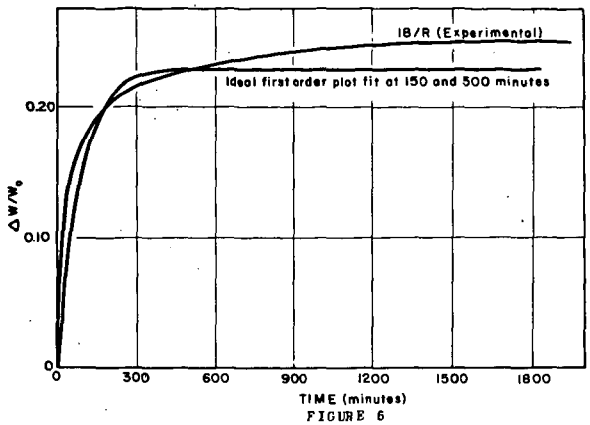

FIGURE 6

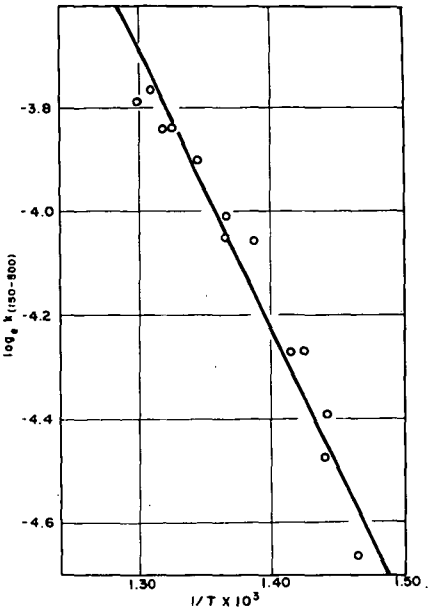

FIGURE 7

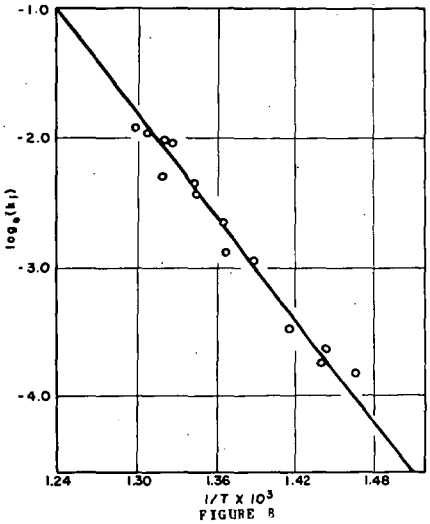

FIGURE 8

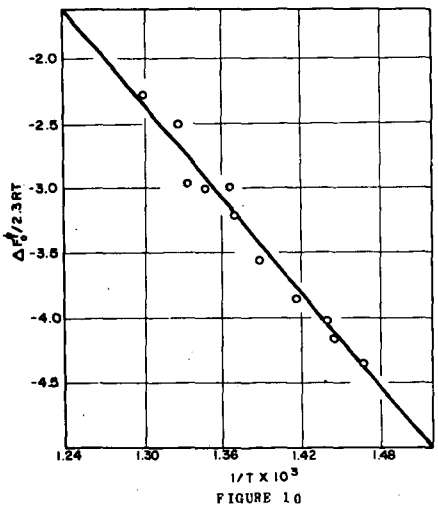

FIGURE 10

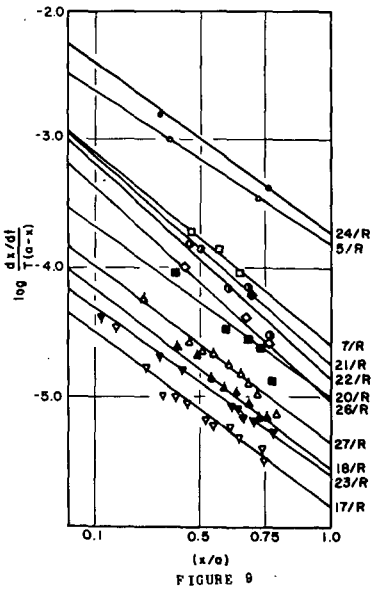

FIGURE 9

Presented Before the Division of Fuel Chemistry
American Chemical Society
Chicago, Ill., August 30 - September 4, 1964

BOND RUPTURE PROCESSES IN COAL PYROLYSIS

H.M. Brown and N. Berkowitz
Research Council of Alberta
Edmonton, Canada

The purpose of this paper is to report some preliminary findings of a study which, while primarily concerned with the kinetics of carbon crystallite growth at T > 650°C, is also beginning to delineate a major route by which unpaired electrons (i.e. socalled "free radicals") form in coal chars. The results are of particular interest inasmuch as they demonstrate that skeletal C-O and C-C bond rupture processes are not - as is commonly thought - confined to the temperature region between 400° and 650°C (in which tar forms by elimination of naphthenic structures).

Experimental

Experimentally, the investigations here under discussion centre on (i) heat treatment of a coal sample in vacuo at a series of pre-selected temperatures; (ii) rapid quenching after such heat treatment; and (iii) measurement of the magnetic mass susceptibility and pure diamagnetic susceptibility of the quenched residue.

For the experiments so far completed, cleaned (-65 +200 mesh) samples of a low volatile bituminous coal (ash <0.5%; Ref.1) were chosen. These were vacuum-carbonized at $<10^{-5}$ mm Hg and 6°C/min., held at the selected final temperatures for periods varying between <5 seconds and 0.5 hr., and then rapidly cooled by external air jets. Figure 1 exemplifies a typical heating and quenching program. When the carbonized residues had attained room temperature, the furnace assembly was flooded with purified nitrogen, and the residues removed and transferred to a continuously evacuated desiccator.

Immediately prior to their use in the magnetic balance (cf. below), and always within less then 24 hrs. after preparation, samples were rapidly filled into the upper chamber of a compensated specimen holder (cf. Detail B, Figure 2) and the loaded holder re-evacuated in order to allow proper settling of the char. After 30 minutes' pumping, the holder was again flooded with purified nitrogen, removed, weighed and inserted into the vacuum chamber of the specially constructed Gouy-type balance. Sample weights were usually of the order of 1.0 gm.

The assembly in which magnetic susceptibilities were measured is diagrammatically shown in Figure 2. It consists of (i) a custom-made quartz fibre balance* (Detail A, Figure 2) suspended in a shielded vacuum chamber V; (ii) a specimen tube suspension S extending from V into an evacuated tube fitted with the necessary temperature control and measuring equipment; and (iii) a Cambridge electromagnet capable of creating fields of up to 16,000 gauss across a one-inch gap between conical pole pieces. Balance readings were taken with a cathetometer M after major weight changes had been compensated by adjusting the current to a carefully calibrated solenoid coil C. Calibration of the balance and magnet at current densities from ca. 2 to 15 amp. was carried out with pure specimens of rhombic sulphur for which $\chi = -0.490 \times 10^{-6}$ cgs units per gm. over the temperature range from 25° to -196°C.

Measurements of χ with coal chars were made at 25°C, while χ_{dia} was obtained from plots of χ vs. 1/T, i.e. by assuming Curie's Law to be operative and extrapolating χ vs. 1/T to zero. To permit construction of the necessary graphs, determinations of χ were also made at -78.5°C (the sublimation temperature of CO_2) and at -196°C (the boiling point of nitrogen)**. The linearity of the resultant χ vs. 1/T plots, and the accuracy with which it proved possible to estimate χ_{dia} from these plots, can be gauged from Figure 3.

Individual values of χ cited below represent averages of 5 determinations which were, in turn, each replicated by measurements at several different field strengths in the range 6000 - 14000 gauss. Maximum deviation within any one set of 5 determinations was always less than 0.005×10^{-6} cgs gm^{-1}.

Experimental data so far available are summarized in Figures 4 and 5. Figure 4 shows the variation of χ and χ_{dia} with heat treatment time t_H at 500°, 600° and 750°C, while Figure 5 shows the corresponding variation of $\Delta\chi$, i.e. of $\chi_{dia} - \chi_{25°}$. On the assumption that the entire paramagnetic component of χ is associated with unpaired electrons on carbon atoms, i.e. that residual mineral matter makes no significant contribution to χ, $\Delta\chi$ affords a direct measure of the "free radical" concentration.

Comments on Procedure

The temperatures at which coal samples were pyrolyzed in the present series of experiments were selected to correspond to particular points in the behaviour pattern of equilibriated specimens, i.e. of specimens which were, in each case,

---

* Manufactured by Worden Laboratories, Houston. The instrument used by us had a total capacity of better than 10 gms. and a sensitivity of 5 micrograms at full load.

** These temperatures were checked with a calibrated chromel/p-alumel thermocouple.

held at the final temperature for 2 hr (1). The 500°C point thus corresponds to the onset of active thermal decomposition (as evidenced by a sharp downward turn of the χ/T plot, by increasing rates of weight loss, and by an increasing d-spacing and decreasing $\bar{c}$-dimension of the crystallite). The 600°C point corresponds to the near-end of active decomposition. And at 750°C, marked growth of the carbon lamellae (as evidenced by large increases in their $\bar{a}$-dimension) is in progress.

This dependence of behaviour on temperature - and the fact that heat treatment temperatures in the present series of experiments were approached gradually - imposes an important limitation on the data shown in Figure 4. Since transient processes at temperatures below the final heat treatment temperature will take place while the coal sample approaches this final temperature, both the form and location of individual χ vs. t_H graphs within the coordinate system must be seen as extensions of changes which commence at "negative" times (i.e. to the left of the χ-coordinate in Figure 4) and at correspondingly higher χ values than the nominal initial values shown in the diagram at $t_H = 0$.

This recognition, which accounts for the inverse relationship between the "initial" susceptibility and heat treatment temperature and which also explains the fact that the χ vs t_H curve at 750°C passes through so much shallower a minimum than the 600°C curve, necessarily complicates a kinetic interpretation of the data*. But it is pertinent to note here that the problem is essentially unavoidable - that it arises from the nature of coal per se. Theoretically, the best alternative to the heating schedule chosen in this study would be shock-heating, i.e. an approach to the final temperature in minimum time. However, with diffusion control over disengagement of volatile pyrolytic products (2, 3), such a course - followed by short heat treatment periods - would produce chars containing an indeterminate residue of undischarged pyrolytic matter making an indeterminate contribution to χ. The measured value of χ would here, in other words, be meaningless.

Discussion

So far as we are aware, only H. Honda (4) has published data on the variation of χ with t_H. He does not, however, seem to have concerned himself with the detailed form of this variation - Figure 4 of his paper (4) shows results for t_H = 15, 30, 60 and 120 minutes only - and while the text of the paper refers to "diamagnetic mass susceptibility", it is clear that the reported values refer to the uncorrected mass susceptibility, i.e. to χ rather than χ_{dia}. For these reasons (and also because of the uncertainty attaching to the conditions under which Honda pyrolyzed his samples), the results summarized in Figures 4 and 5 cannot be viewed against an established background. But subject to the recognition that they represent initial data (and bearing in mind the limitations referred to above), they nevertheless allow of some important tentative conclusions.

---

*Efforts to develop graphical methods by which the necessary corrections can be interpolated seem to be meeting with some success. They will be reported in due course.

In principle, a fall in χ may be associated with either (a) the formation of unpaired electrons by any mechanism, or (b) a decrease in the size of the average aromatic area of the statistical structure unit (or lamella). (b) itself may or may not be accompanied by formation of unpaired electrons and would, if not so accompanied, cause a fall in χ by reducing the socalled London contribution to the observed mass susceptibility. Conversely, a rise in χ can be attributed to either a removal of unpaired electrons from the system (by $\sigma - \sigma$ or $\sigma - \pi$ coupling) or simple growth of aromatic lamellae. The fact that variations of χ and χ_{dia} with t_H follow virtually parallel courses (which are only displaced with respect to each other along the χ - coordinate), i.e. the relative insensitivity of $\Delta\chi$ to changes in t_H (cf. Figure 5), is in these circumstances highly significant. Bearing in mind transient processes at "negative" time values (cf. above) and noting that $\Delta\chi$ itself increases with the heat treatment temperature, it implies that, for short heat treatment periods at least, a modified (b) operates, i.e. that χ and χ_{dia} fall as a result of lamellar size reductions and simultaneous formation of unpaired electrons, but that unpaired electrons are subsequently "frozen" into the structure without actually being eliminated by pairing. In view of Figure 5, the rise in χ and χ_{dia} must clearly be ascribed to lamellar growth only.

The corollary of this conclusion is, of course, that unpaired electrons are created by rupture of σ - bonds, i.e. by rupture of C-C and/or C-O lattice bonds.

It might usefully be observed that such an identification is in general harmony with certain other findings. It is, for example, qualitatively supported by Mrozowski and Andrew's observation (5) that the "free radical" concentrations in polycrystalline graphitized carbons can be greatly increased by prolonged grinding in inert atmospheres (or in vacuo). And it also lends support to the suggestion (6) that ultimate elimination of unpaired electrons by extended heating at $T > 650°C$ can be associated with a change in the semiconductor mechanism at 650°-700°C - from excess electron to excess "hole" conduction (7) - by pastulating a progressive $\sigma - \pi$ electron interaction.

But more immediate interest attaches to the fact that conclusions derived from the data contained in Figures 4 and 5 bear directly on descriptions of the overall coal pyrolysis process.

The gross features of this process are conventionally described in terms of a 3-stage sequence which, successively, involves (i) elimination of peripheral functional groups at $T < 400°C$; (ii) skeletal breakdown and reorganization between ~400° and 650°C; and (iii) progressive growth and ordering of aromatic lamellae at $T > 650°C$. It is, in other words, supposed that only the second stage involves more than peripheral reactions*.

---

*A recent study concerned with the kinetics of hydrogen formation at temperatures in the range 600°-800°C has led to the conclusion (9) that rates of H-elimination are controlled by lamellar mobility and that abstraction of hydrogen from positions at the peripheries of the lamellae is the immediate precursor of crystallite growth.

In the light of evidence now available, this view requires some revision. In particular, it must now be concluded that skeletal reorganization can extend well into the third stage and that it is here connected with the elimination of residual oxygen from coal chars.

Investigations into the kinetics of water formation at temperatures in the range 650°-850°C (8) have shown that all (or almost all) oxygen lost in this range ultimately appears as water; that the reactions leading to formation of water (which must itself be regarded as a secondary or tertiary product) are all relatively fast; and that kinetic control over water formation is exerted by bond rupture processes (which, insofar as they involve non-quinoid oxygen, must partially disrupt lamellae and result in a fall in χ even if no unpaired electrons are formed in the process). If it is now borne in mind that elemental hydrogen (deriving from peripheral H-atom abstraction) and water (at least partly deriving from carbonization of ether-structures and heterocyclic O-bearing aromatics) are the only products actually formed by decomposition of coal at T >650°C* , association of reductions in χ (and χ_{dia}) with oxygen-breakout at these temperatures is virtually inescapable. The fact that oxygen-breakout is, as already noted, fairly fast (and generally 90% complete within 10 minutes from the start of reaction; Ref. 8) and that χ and χ_{dia} undergo rapid changes at correspondingly low values of t_H, may be seen as additional support for such a view.

It is, however, in this connection of interest to observe that measurements of rates of water formation between 650° and 850°C indicate sequential oxygen removal by at least two reactions. If the association between oxygen elimination and changes in χ here suggested is accepted, plots of χ vs. t_H would therefore be expected to pass through at least two corresponding minima - with the second tentatively placed at $t_H \approx$ 7-8 minutes. This point is currently being checked.

References

1. P.A. Cavell and N. Berkowitz; Fuel, 39 (1960), 401.
2. N. Berkowitz; Fuel, 39 (1960), 47.
3. H. Luther and S. Traustel; Brennstoff Chemie, 44 (1963), 65.
4. H. Honda; Proc. 3rd Conf. on Carbon (Pergamon Press, 1957), 159.
5. S. Mrozowski and J.F. Andrew; Proc. 4th Conf. on Carbon (Pergamon Press, 1960), 207.
6. N. Berkowitz, P.A. Cavell and R.M. Elofson; Fuel, 40 (1961), 279.
7. E.A. Kmetko; Phys. Rev., 82 (1951), 456.
8. Lynne F. Neufeld and N. Berkowitz; Fuel, 43 (1964), May.
9. N. Berkowitz and W. den Hertog; Fuel, 41 (1962), 507.

*The (relatively small) quantities of methane and oxides of carbon disengaged from coal chars at these temperatures appear to be formed by autohydrogenation and steam gasification of the chars (8) and therefore to be basically unrelated to the decomposition of coal per se.

Figure 1. A Typical Heating and Quenching Program.

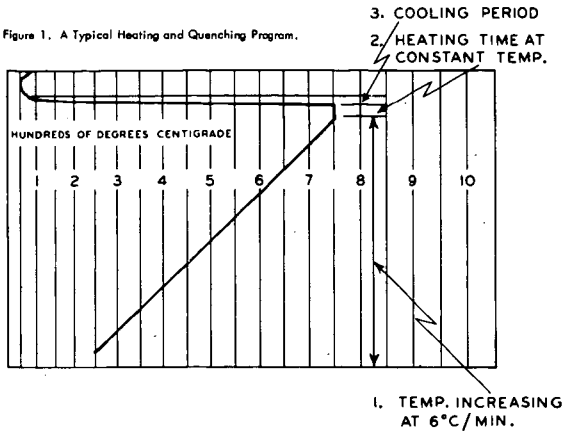

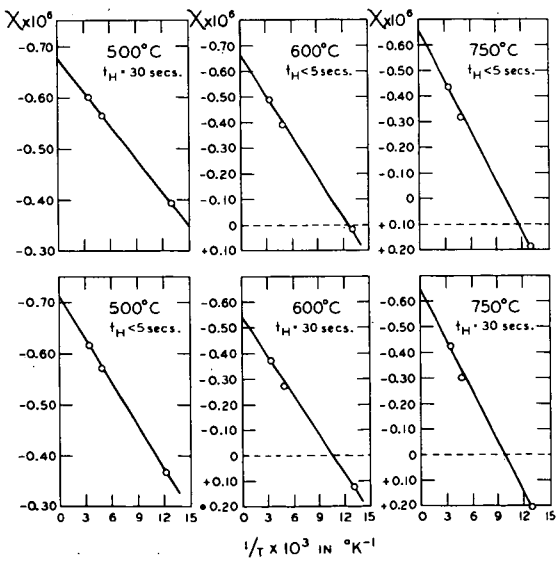

Figure 3. Some Typical Plots of χ vs. 1/T. (χ_{dia} = χ when 1/T = 0.)

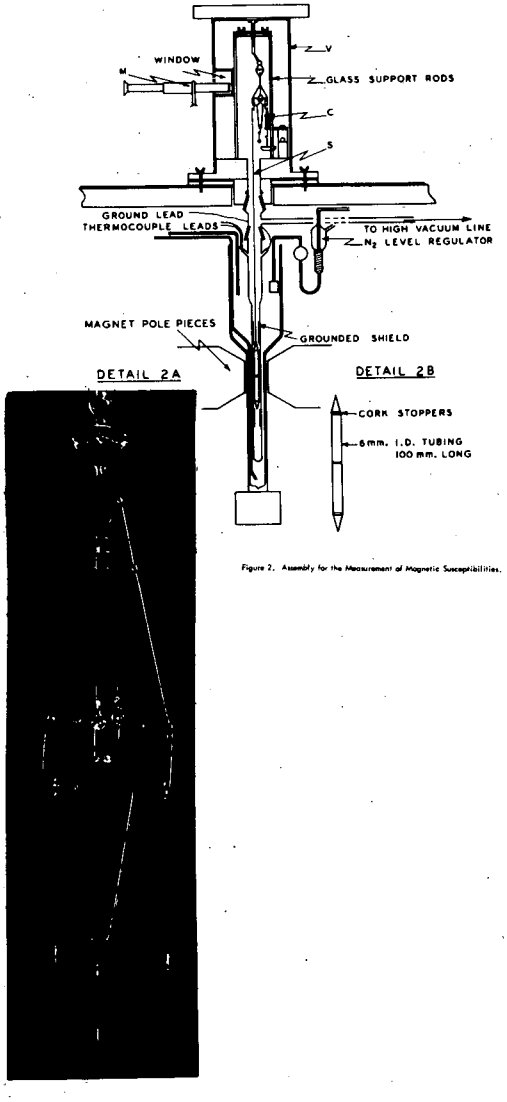

Figure 2. Assembly for the Measurement of Magnetic Susceptibilities.

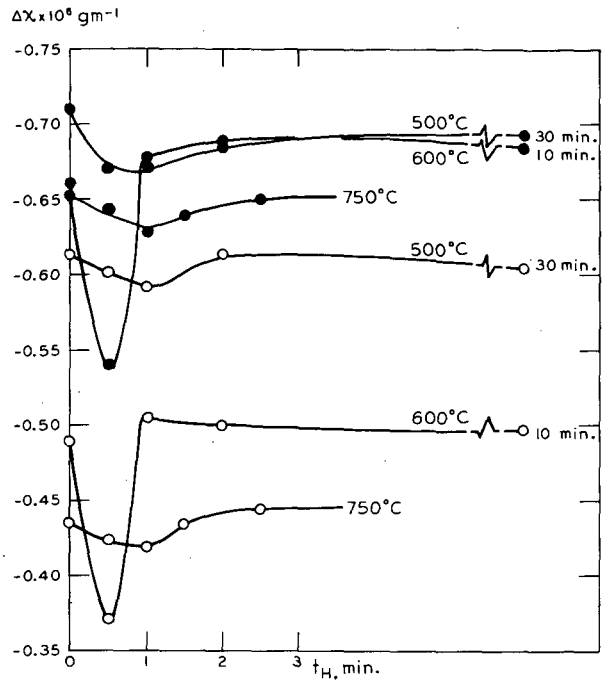

Figure 4. The Variation of Magnetic Susceptibility with Heat Treatment Time t_H. (Full circles denote χ_{dia}; empty circles χ_s.

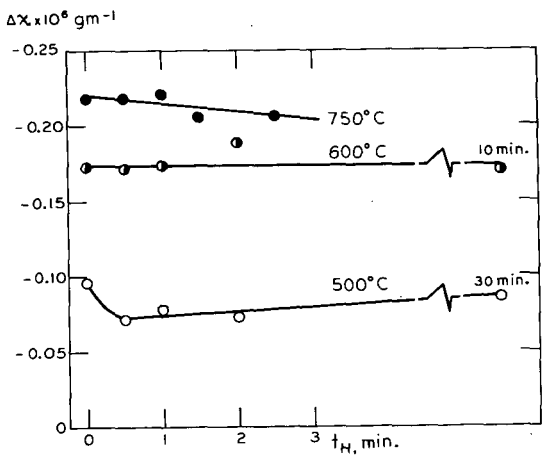

Figure 5. The Variation of $\Delta\chi_s$ with t_H.

Presented Before the Division of Fuel Chemistry
American Chemical Society
Chicago, Ill., August 30 - September 4, 1964

THE USE OF THE MICROSAMPLE STRIP FURNACE IN COAL RESEARCH

E. Rau and J. A. Robertson

FMC Corp., Chemical Research and Development Center, Princeton, N. J.

INTRODUCTION

The pyrolysis and carbonization behavior of coal has been studied intensively since the industrial revolution. Many techniques have been developed, but most require relatively large quantities of material; they are time-consuming and expensive to perform. The Microsample Strip Furnace described in this paper uses only a few milligrams of material and evaluations can be carried out in a matter of minutes. Techniques have been developed to study coking behavior on heating, weight loss on heating, the nature of the product evolved during the heating sequence, and ash distribution and properties.

These techniques generally yield qualitative information. The observations assist in the interpretation of the phenomena involved, and serve as a guide in setting up more quantitatively precise experiments. Qualitative differences in pyrolysis behavior can readily be observed and problems such as sample heterogeneity readily detected.

APPARATUS

The Microsample Strip Furnace (or often called simply a hot-stage microscope) has been described in previous publications[1]. The model available at Princeton (Figure 1) is similar except that manual temperature controls are employed. Essentially, the unit consists of an enclosed microstrip furnace and swing-out, stereoscopic, variable power microscope. The microscope is fitted with a vertical illuminator, so that an optical pyrometer can be used to

---

[1]A. R. Conroy and J. A. Robertson, "Controlled Atmosphere Hot Stage for Microscopic Observations of Glass Melting Phenomena. Part I," The Glass Industry, 44, 76-9, 139-43 (1963).

measure the temperature of the hot strip. The furnace consists of a strip of platinum, molybdenum or other refractory metal held between two water-cooled electrodes. Power for resistance heating is supplied by a 4-volt, 100 ampere step-down transformer. The temperature can be raised slowly by manually adjusting the autotransformers or quickly by presetting the autotransformers and then snapping the switch on. The furnace assembly is covered with an envelope consisting of a piece of three-inch Pyrex pipe to the top of which is sealed a plane piece of optical quartz. The sample is viewed through the quartz plate, and since a long working distance objective is used at 7-30 X total magnification, cooling of the microscope is not required. The enclosed area can be flushed with any gas desired. This gas is introduced so as to sweep across the quartz window and thus prevent fogging by condensibles.

The temperatures that can be reached depend mainly on the resistivity and thickness of the strip material. We used 3-5 mil thick, 8 mm wide platinum or molybdenum in this study. The maximum temperature obtainable is limited by the melting point of the material, 3190°F for platinum and 4750°F for molybdenum.

PRELIMINARY OBSERVATIONS

Microscopically, coal is a heterogeneous composite of macerals. It is desirable to make a preliminary microscopic observation to determine the minimum particle size which is representative of the material under study. If the heterogeneity is large with respect to the size of the particle preferred for microscopic study, then the various components can be separated and studied individually. The final conclusions are then weighted accordingly. Or, a composite of fine particles can be studied as representative of the total composition. If the heterogeneity is of fine structure, so that individual particles of the desired size are representative, the sample can be considered as homogeneous for the tests described. The latter was the case in the coals used in this study.

The individual behavior of the various macerals on heating can be observed, if desired, by heating a thin section, in which the macerals have been identified, in direct contact with the strip. The thin section must be carefully cleaned to remove the cement used in its preparation. Also, the cement-solvent system chosen must not modify the section.

Slow oxidation of the coal particle in air often brings out the structural discontinuities which are difficult to see in the untreated particle. This oxidation can be carried all the way to the final ash skeleton, showing the distribution of ash-forming minerals.

A few minutes spent in this preliminary examination will permit the selection of more meaningful samples for subsequent studies, and will provide a better understanding of the phenomena to be observed later.

CARBONIZATION OF COAL

Different ranks of coal show great differences in behavior under fixed heating conditions, and coals of the same rank show different behaviors if heating rates or atmospheres are varied. For example, it can be readily seen that a lignite which undergoes excessive particulate shrinkage, through loss of gas only, can be processed in equipment that would be completely unable to handle a coking coal. Observations of this nature before designing of laboratory or pilot set-ups reduce later problems. The time required for such observations is minimal.

Observations made before designing laboratory equipment should be followed by periodic examination of intermediates and products prepared in laboratory, pilot and shake-down plant runs. Often a product characteristic not apparent, except by microscopic study, can indicate needed process changes. The anomaly can often be duplicated under the microscope and the remedy checked for effectiveness before being applied on a larger scale.

Experiments in which heating rate was varied have been especially informative. The hot stage offers a much wider range of available heating rates than most pyrolysis equipment and so allows one to determine what might happen beyond the limits of the larger equipment. This is illustrated in experiments involving shock heating of various coals.

A small piece of coal, about 1-2 mg, was placed on the strip and shock heated to about 1000°C by snapping the switch with the transformers preset for 1000°C. Coking coal, such as Federal melts, exudes tars and vapors which condense on the glass vessel, and forms a coke button. A non-coking subituminous coal such as Elkol does not melt, but puffs out into a porous structure with the loss of light vapors (Figure 2). A simple test for coking is to heat two particles of coal in contact with each other. Coking coals will fuse while non-coking coals will not. The strength of the bond after cooling can be easily estimated by probing with a needle while observing through the microscope.

WEIGHT LOSS

It had been thought that the observed volume changes could be used to estimate the percentage of coal volatilized. However, because of density and porosity changes in the char, this was not

possible. It was therefore decided to attempt a semi-quantitative approach by weighing a coal particle before and after exposure on the hot stage. It was found that, with care, particles of coal weighing one to three milligrams could be handled. Weighing was performed on a microbalance sensitive to ±0.000001 gm (1 microgram).

Considerable technique development was necessary to reduce the experimental scatter found initially. Direct handling of coal particles with forceps proved impractical as the chars tended to be too friable. Microcrucibles about 2 mm on the edge were folded from platinum foil or gauze. The tared crucibles were then used to contain the coal. Besides increasing reproducibility, this system allowed the evaluation of fine-grind particles on the hot stage. However, the metal of the crucible did not make perfect contact with the metal strip, even though the strip was bent to the shape of the crucible and the latter was held as by a spring. Also, the total weight of metal that had to be heated was about doubled. As a result, the maximum temperature obtainable was reduced from 3200°F to 2200°F.

Heat transfer to the sample was from the heated strip only. Thus, heat flow was essentially unidirectional, with the bottom heated first. This phenomenon could be clearly observed in coking coals, where liquefaction and coking occurred in waves starting from the heat source.

The time to reach set temperature was estimated from the current pulse observed on an ammeter. When the switch was closed, the current rose quickly to a high value. As the metal strip heated, its resistance increased, decreasing the current. It was presumed that, when the current had decreased from the peak value to a steady state, the strip had reached temperature equilibrium. The effect of crucible and coal on time to steady state could be observed. It was estimated that it took 1.5 to 2.5 seconds to reach a temperature of 1830°F.

Weight-loss curves for several coals are presented in Figures 3-7. All curves reflect increased volatilization with increasing temperature. Further, the amount volatilized is often greater than that obtained in theASTM volatile-matter test. The amounts volatilized at 1742°F are compared in Table I. In Figure 4 the number beside each point represents the number of experiments averaged to obtain it.

These findings are similar to those of Loison and Chauvin[2].

---

[2]R. Loison and R. Chauvin, "Rapid Pyrolysis of Coal," Cerchar, Cheltenham International Coal Science Conference, 1963.

Since volatilizations by shock heating are for the most part greater than those obtained by the ASTM technique, the heating rate must be responsible for the increase. At the time the results were obtained, the possibility that error inherent in the technique was responsible for all the variation was considered. Now this can be discounted because of other data obtained in Project COED which supports the conclusion concerning the dependence of volatilization on the heating rate[3]. However, the data obtained here gave us the confidence that increased volatilization could be obtained, and therefore guided the experiments which quantitatively proved this finding.

TAR AND LIQUOR YIELD

In order to estimate more quantitatively the amount of tar and liquor formed, a measured amount of coal was placed in a melting-point capillary tube. The hot strip was bent into a loop to hold the coal-containing end of the capillary. On shock heating, it was found that the vapors exuded and condensed in the upper regions of the capillary with the heavier material condensing nearer the coal. The nature of the exudate, whether tar, liquid, or gas, could be easily observed through the microscope and its condensation behavior followed. As shown in Figure 8, coking coal such as Federal tended to have more heavy tar, while the product from non-coking coals such as subbituminous Elkolare lighter and more mobile. A semi-quantitative comparison of yield can be made by measuring the lengths of capillary containing the various fractions.

The capillary tube technique has been found to be particularly useful in the rapid screening of unknown coals. By using a standard fill (0.5 cm) of a sized coal (40-60 mesh), an unknown coal can be compared with known standards with regard to water content, melting (coking) behavior, volume change on heating, tar evolution, tar character (light or heavy) and sometimes gas evolution (made visible by entrained tar). The entire observation takes about five minutes and requires only a few milligrams of sample.

ASH DISTRIBUTION AND PROPERTIES

Considerable information can be gained by observing the burning of a single particle of coal under the microscope. If desired, the oxidation can be carried out slowly, avoiding visible flames thus making possible the observation of the slow removal of carbon from the ash skeleton; or the combustion can be forced to determine its

---

[3] J. F. Jones, M. R. Schmid, R. T. Eddinger, Chem. Eng. Prog. 10, No. 6, 1964.

influence. By regulating the oxygen content of the atmosphere, the rate of oxidation can be controlled and the influence of temperature isolated.

When a coal particle is slowly oxidized, the ash-producing minerals are left at their original sites and a skeleton structure is retained. The original minerals may be converted to oxidized forms, e.g., pyrite converted to hematite, but in the absence of liquifaction, the converted minerals remain distributed in space about the same as their predecessors. This allows the observer to decide if beneficiation techniques would be useful in upgrading the coal and to what degree of size reduction the coal must be ground before separation could be expected.

After the ash structure has been studied, the temperature can be raised and the ash melting characteristics observed. The ash melting point or melting range can be easily measured and the reaction or fluxing of ash components noted. The behavior of the ash on heating gives clues as to problems that might be encountered in commercial use of the coal, such as clinker formation, fluxing of fire brick, or fly-ash control.

CONCLUSIONS

The techniques just described show that the hot-stage microscope can be a very useful tool in coal research. It can be used for qualitative observation of coal-structure carbonization behavior, and ash characteristics. Semi-quantitative results can be obtained, providing reasonable guide lines for scale-up work.

ACKNOWLEDGEMENT

The authors thank FMC Corporation for permission to publish this paper. Part of this work was supported by the Office of Coal Research through the United States Government Contract 14-01-0001-235 (Project COED).

ER:hvh
6/3/64

TABLE I

Comparison of Volatilization at 1742°F (950°C), Dry Basis

	ASTM Procedure	Hot Stage	Percentage Increase
Elkol[1]	40.7	48	17
Federal[2]	37.7	49	30
Kopperston No. 2[2]	31.6	36	14
Colver[2]	25.3	19	neg. -25
Orient No. 3[2]	44	41	neg. -7

[1]Kemmerer Coal Company, Frontier, Wyoming

[2]Eastern Associated Coal Corp., Pittsburgh, Pa.

[3]Freeman Coal Mining Corp., Chicago, Illinois

Figure 1

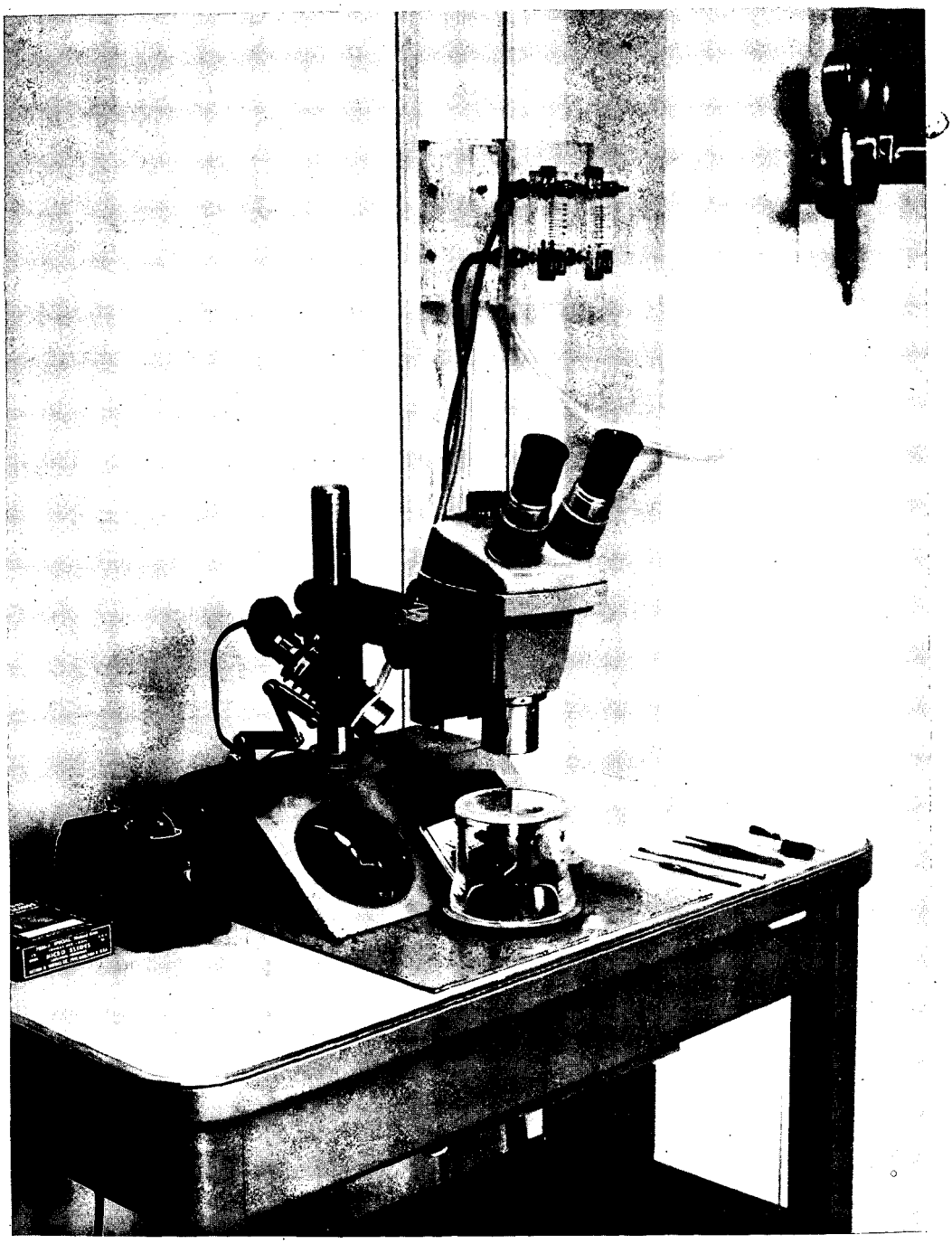

Microsample Strip Furnace with Microscope
Note glass envelope covering the electrode posts.

Figure 2

A. Federal Coal before shock heating

B. Federal Coal after shock heating. Residue formed from a tarry liquid which solidified.

C. Elkol Coal after shock heating. Material cracked open to release gases.

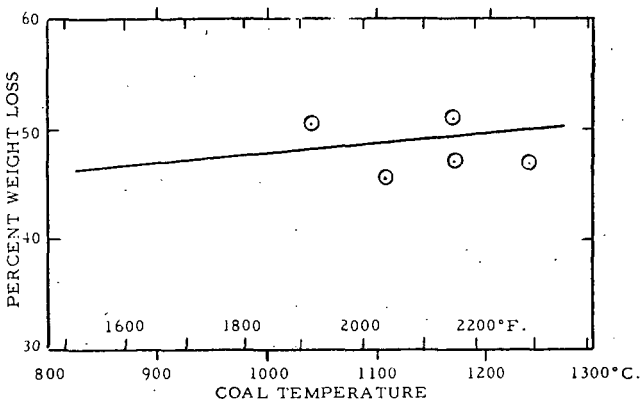

FIGURE 3

Weight Loss of Elkol Coal on Hot Stage

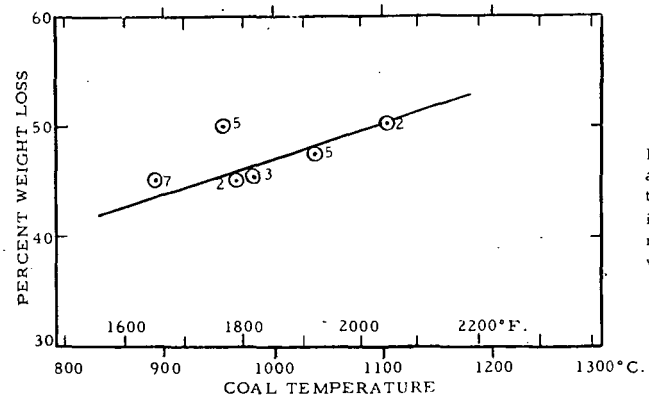

Points are average of tests, (number indicates how many tests were made).

FIGURE 4

Weight Loss of Federal Coal on Hot Stage

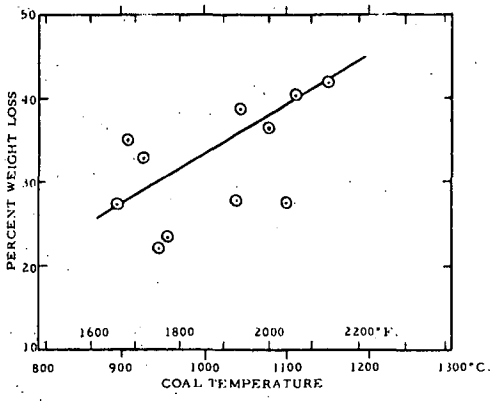

FIGURE 5

Weight Loss of Kopperston No. 2 Coal on Hot Stage

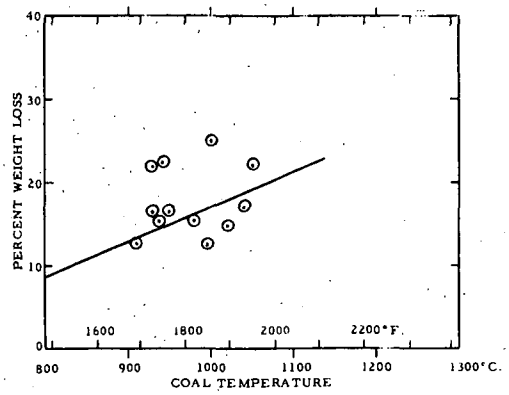

FIGURE 6

Weight Loss of Colver Coal on Hot Stage

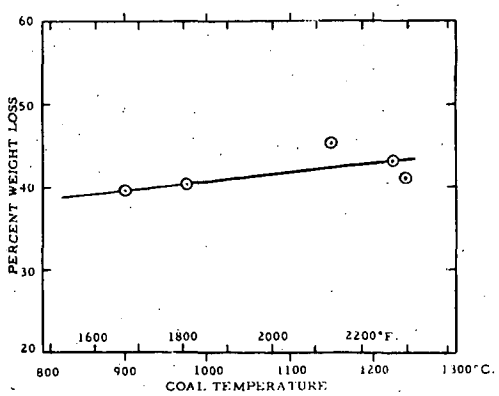

FIGURE 7

Weight Loss of Orient No. 3 Coal on Hot Stage

Figure 8

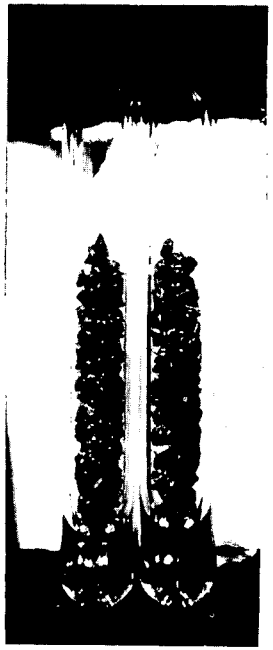

A. Before shock heating. Federal on right, Elkol on left.

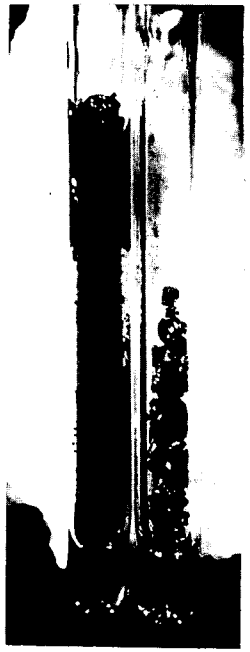

B. After shock heating. Federal has given more of a heavier tar than Elkol.

Figure 9

Elkol coal after mild oxidation. Ash is uniformly distributed throughout particle.

Presented Before the Division of Fuel Chemistry
American Chemical Society
Chicago, Ill., August 30 - September 4, 1964

Reactions of Coal in a Plasma Jet

R. D. Graves, W. Kawa, and P. S. Lewis

U.S. Bureau of Mines, 4800 Forbes Avenue
Pittsburgh 13, Pennsylvania

INTRODUCTION

The Bureau of Mines has made an exploratory study of the reaction of coal in a plasma jet in which plasma temperatures up to about 15,000° C can be attained. The objective was to obtain new knowledge of coal chemistry which may lead to new methods of producing chemicals from coal. Plasma consists of more or less ionized gases or vapors, and is present in any electrical discharge. Temperatures generated in electrical discharges are high enough for molecular bonds to be broken and for the resultant atoms to dissociate into ions and electrons. The complex mixture of ions, electrons, neutral atoms, and excited molecules produced is called a plasma and is referred to as the fourth state of matter. It conducts electricity, is a good heat conductor, and is luminous. The highly excited species that exist in plasmas can react to produce compounds whose formation is thermodynamically unfavorable at conventional conditions.

A plasma jet is formed when plasma generated from a fluid flowing through an electrical arc confined within a chamber is made to flow out of the chamber through a nozzle or orifice. Various plasma jet devices have been used in recent years to study high-temperature chemical syntheses. Leutner and Stokes[1], using a consumable graphite anode, produced acetylene by reacting the graphite with hydrogen in an argon-hydrogen plasma. About 34 percent of the carbon consumed was converted to acetylene. Adding graphite in powdered form did not increase the yield of acetylene. These same investigators also reacted methane in argon plasmas and converted 80 percent of the carbon in the methane to acetylene. Acetylene synthesis has also been reported by Freeman and Skrivan[2], who reacted methane in argon and argon-hydrogen plasmas, and by Baddour and Iwasyk[3], who reacted hydrogen with carbon vapor obtained from a consumable graphite electrode.

The plasma-jet device used in the present study was a commercial plasma gun designed for spray-coating applications. Experiments were made with high-volatile A bituminous (hvab) coal using argon as the working gas and also as a carrier gas in which coal was entrained and fed into the plasma gun. The effects of coal rate, coal particle size, and plasma temperature on yields and product composition were determined.

EXPERIMENTAL PROCEDURE

Apparatus

The plasma-jet unit consists of a plasma gun, product recovery system, coal feeder, power supply, cooling water facilities, and a control console. Direct current used to operate the plasma gun is supplied by two 3-phase alternating current transformers and selenium rectifiers. This system is rated at 28 kw and

is capable of delivering 700 amp at 40 volts or 350 amp at 80 volts. It also contains a high-frequency oscillator used to start an arc. The electrical potential required to sustain an argon plasma was about 20 volts.

The plasma gun, shown schematically in figure 1, has a 3/16-inch thoriated tungsten cathode and a 1/4-inch id cylindrical water-cooled copper anode. The working gas enters the gun radially near the cathode and flows downward into the anode. The gas is converted to a plasma as it flows through the electrical discharge between electrodes. Coal entrained in the carrier gas enters the plasma through an inlet in the side of the anode. The reaction mixture leaves the bottom of the anode as a luminous jet and flows down through the water-jacketed cooler which consists of a 3-inch copper tube about 12 inches long. The residence time of coal in the plasma is less than a millisecond. Reaction products leave the cooler at several hundred degrees C and enter the solids receiver via a dip tube. The receiver is 6 inches in diameter and 12 inches long and contains about 3 inches of water. Most of the solids collect in the bottom of the receiver, while the gases and finer solid particles at near room temperature bubble up through the water and a tubular baffle. Gases flow through a cloth filter, which collects additional fines, and are sampled, metered, and vented.

Operating Procedure

The system is assembled, purged with argon, and pressure tested. Flows of cooling water and working gas are established, and then the electrical discharge between electrodes is started. The flow of carrier gas is established, and the coal feeder is started. Coal is fed into the plasma gun for 10 minutes unless a coal feed stoppage or other system failure causes a premature termination of an experiment. Initially, the system is at a pressure of about 3 to 4 psig but gradually increases several psi as solids accumulate on the filter. Temperatures of cooling water entering and leaving the plasma gun are measured. Product gases are sampled after steady state conditions are reached. At the conclusion of an experiment, solid products are washed from the cooling system, receiver, filter, trap, and interconnecting lines with water. The washings are combined, and then the solids are filtered and dried in air at 70° C for 20 hours.

Calculations

Total power input is determined from electrical current and voltage measurements at the gun, whereas net power input to the plasma is calculated as the difference between total power input and the power loss to the cooling water. The enthalpy of the primary gas and the average plasma temperature are determined from the net power input into the plasma, the working gas flow rates, and a plot of specific enthalpy as a function of temperature. This calculation assumes no energy loss other than that to the cooling water.

Yields of solids are determined from weighings of coal fed and solids recovered. Yields of gaseous products are calculated from analyses of product gas and the known coal and argon feed rates. This calculation assumes constant coal feed rate and steady state conditions at the time the gases were sampled.

RESULTS AND DISCUSSION

Reactions of 70 x 100 Mesh Coal

Experiments with 70 x 100 mesh coal (U.S. sieve) were made using feed rates of about 3.1 and 1.1 pounds per hour. Argon rates were constant at 1.17 scfm as the primary gas and 0.26 scfm as the carrier gas. The power input at each coal rate was varied to give average plasma temperatures ranging from 3,400° to 7,700° C

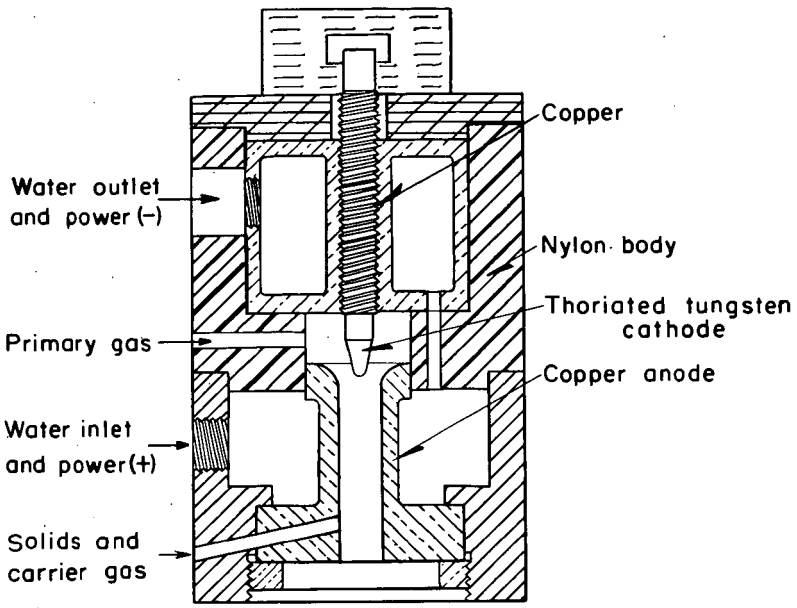

Figure 1.– Schematic diagram of the plasma generator.

at about 3.1 pounds per hour and from 3,900° to 8,600° C at about 1.1 pounds per hour. Reaction products were a solid residue and a gas containing hydrogen, methane, acetylene, diacetylene, and carbon monoxide.

Operating conditions, yield data, and analyses of the coal feed and residues produced are shown in table 1. Yields are expressed as weight-percent of moisture- and ash-free (maf) coal. At a coal rate of 3.1 pounds per hour, increasing the power input (or average plasma temperature) had only a slight effect on the extent of coal decomposition. Yields of solid residue decreased from 92.2 percent at 3,400° C to 89 percent at 7,700° C. Yields of hydrogen and acetylene increased almost linearly from 0.4 to 1.1 percent and from 2.6 to 4.5 percent respectively. The yield of methane was constant at about 0.2 percent, while the yields of diacetylene showed no significant trend. With a coal rate of about 1.1 pounds per hour, the effect of increasing the plasma temperature on yields was similar. Yields of residue decreased while yields of hydrogen increased from 0.4 to 1.7 percent, yields of acetylene increased from 2.2 to 6.0 percent, and yields of diacetylene increased from 0.1 to 0.6 percent with increasing temperature. The amount of methane produced was again constant at about 0.2 percent. At both coal rates, yields of carbon monoxide increased with increasing temperature.

The effect of decreasing the coal feed rate from 3.1 to 1.1 pounds per hour can be seen by comparing the results from experiment 9 with experiment 18 and experiment 10 with experiment 14. Estimated plasma temperatures in each pair of experiments were comparable. At the lower coal rate, higher coal heating rates, higher average coal temperatures, and, hence, more extensive coal decomposition would be expected because there was more heat available per unit weight of coal. However, there was no significant effect of coal rate on yields of gaseous products in these experiments. Although the yields of solid residue were about 5 percent lower at the lower coal rate, this is not necessarily an indication of more coal decomposition. Carbon recoveries were also lower by about the same amount, and it is possible that losses of solid products were higher at the lower coal rate.

Analyses of the solid residues showed that extensive thermal decomposition did not occur in any of the experiments because the coal was not heated sufficiently. Ultimate analyses of the coal and residues did not differ appreciably, and the residues contained only 3 to 6 percent less volatile matter. It is possible that most of the coal particles, because of poor mixing, remained in the periphery of the plasma where temperatures are much lower than along the axis.

The distance between the coal entry port of the anode and the discharge port is 1/4 inch. This may be considered as the coal-plasma mixing zone. To improve the mixing of coal and plasma, an anode was modified to give a threefold increase in the length of the mixing zone. Experiments were then performed at conditions similar to those in experiments 14, 16, and 18 (1.1 pounds of coal per hour). However, as yields and ultimate compositions of the residues produced in the two sets of experiments were similar at comparable conditions, this change was ineffective. Assuming that better mixing was achieved with the extended nozzle, it appeared that heat transfer rate rather than the degree of mixing limited the temperature rise and extent of coal decomposition.

Reaction of -325 Mesh Coal

To reach higher coal temperatures, the particle size of the coal feed was decreased to -325 mesh. Experiments were made with power input as a variable, and average plasma temperatures of 4,800°, 7,300°, and 8,800° C were obtained. Argon rates were constant at 1.17 scfm as working gas and 0.26 scfm as carrier gas. Average coal rates were 1.03, 0.84, and 0.74 pounds per hour although intended to be 1.0 pound per hour. Product distributions and the analyses of the coal feed and

TABLE 1.- Reactions of 70 x 100 mesh hvab coal in argon plasmas
Effects of power input and coal feed
rate on yields and residue compositions
(1.17 scfm argon as primary gas, 0.26 scfm argon as carrier gas)

Experiment number		9	10	4	18	14	16
Average coal rate, lb/hr		3.11	3.06	3.14	1.20	0.99	1.11
Average plasma temp., ° C		3,400	6,300	7,700	3,900	6,600	8,600
Total power input, kw		3.8	7.3	9.4	4.1	7.5	12.6
Net power input, kw		1.7	3.2	3.9	2.0	3.3	4.7
Products, wt pct maf coal							
Solid residue, maf		92.2	89.2	89.0	87.7	84.0	78.3
Hydrogen		0.4	0.8	1.1	0.4	1.0	1.7
Methane		.2	.2	0.3	.2	0.1	0.2
Acetylene		2.6	3.5	4.5	2.2	4.3	6.0
Diacetylene		0.3	0.3	-	0.1	0.4	0.6
Carbon monoxide		4.1	5.3	5.6	3.8	5.6	11.0
Total		99.8	99.3	100.5	94.4	95.4	97.8
Carbon recovery, pct		96.8	96.8	97.1	91.3	92.3	92.8
Hydrogen recovery, pct		96.4	98.0	105.4	94.2	100.3	104.1
Analyses, wt pct							
Material	Coal	----------	----------	Solid residue	----------	----------	----------
Moisture	0.8	0.8	1.3	0.4	0.1	0.6	0.6
Ash	3.8	4.4	5.4	5.1	4.7	4.2	4.6
Ultimate composition, maf basis							
H	5.6	5.2	5.1	5.0	5.3	5.2	4.6
C	84.3	83.3	87.5	87.0	83.4	87.4	86.0
N	1.7	1.7	1.6	1.5	1.6	1.6	1.5
S	0.9	0.9	0.9	1.0	0.8	0.8	0.9
O (by difference)	7.5	8.9	4.9	5.5	8.9	5.0	7.0
Volatile matter, maf basis	37.6	34.8	31.2	32.6	34.4	33.9	31.1

solid residues produced are shown in table 2. As power input was increased, yields of solid residue decreased from about 74 to 45 percent and yields of hydrogen and acetylene increased. No trends were observed in the yields of methane and carbon monoxide. Trace quantities of diacetylene were formed in each experiment.

There was considerably more decomposition in all experiments with -325 mesh coal than in experiments with 70 x 100 mesh coal. The -325 mesh coal evidently reached higher temperatures. Volatile matter contents of the residues from -325 mesh coal were much lower, and yields of gaseous products were much higher. In experiments with 70 x 100 mesh coal in argon plasmas, the highest yield of acetylene obtained was 6 percent. The solid residue produced from this experiment contained 31 weight-percent volatile matter on a maf basis. As shown in table 2, acetylene yields obtained from -325 mesh coal were about 10, 12, and 15 percent, and the residues contained about 17, 10, and 12 percent volatile matter. These results clearly show that particle size had a pronounced effect on the extent of coal decomposition. However, the -325 mesh coal was still not completely devolatilized although it is estimated that coal temperatures of about 2,900° to 6,300° C would have been reached if thermal equilibrium had been attained. Complete devolatilization would be expected at a temperature somewhat above 1,000° C.

Total yields and carbon and ash recoveries were low in experiments 40 and 41 (table 2), possibly because of losses of extremely fine solid residue that filtered through the recovery system. In all three experiments, the recoveries of hydrogen and oxygen were high, and in experiments 38 and 40, the yields of carbon monoxide obtained would not be possible even if all the oxygen in the coal had been converted to carbon monoxide. It is likely that some leakage of cooling water into the plasma had occurred. The reaction of this water with coal or coal decomposition products would account for the high hydrogen recoveries and the high yields of carbon monoxide.

CONCLUSIONS

Acetylene was the principal hydrocarbon gas produced when hvab coal was injected into argon plasmas and was obtained in yields as high as 15 weight-percent of maf coal. However, the coal was not heated to temperatures high enough for complete devolatilization to occur. To obtain higher coal temperature and yields of gaseous products, changes in plasma generator design and/or operating techniques that will result in more efficient utilization of the heat available in plasmas will be required.

REFERENCES

1. Leutner, H. W. and C. S. Stokes. Producing Acetylene in a Plasma Jet. Ind. and Eng. Chem., v. 53, No. 5, May 1961, pp. 341-342.

2. Freeman, M. P. and J. F. Skrivan. Plasma Jet....New Chemical Processing Tool. Hydrocarbon Processing and Petroleum Refiner, v. 41, No. 8, August 1962, pp. 124-128.

3. Baddour, R. F. and J. M. Iwasyk. Reactions Between Elemental Carbon and Hydrogen at Temperatures Above 2,800° K. Ind. and Eng. Chem. Process Design and Development, v. 1, No. 3, July 1962, pp. 169-176.

TABLE 2.- Reactions of -325 mesh hvab coal in argon plasmas
Effect of power input on yields and residue compositions
(1.17 scfm argon as working gas, 0.26 scfm argon as carrier gas)

Experiment number		38	41	40
Average coal rate, lb/hr		1.03	0.84	0.74
Average plasma temp., ° C		4,800	7,300	8,800
Total power input, kw		4.8	7.5	10.2
Net power input, kw		2.4	3.7	4.9
Products, wt pct maf coal				
Solid residue, maf		73.6	62.9	45.3
Hydrogen		2.4	3.0	3.9
Methane		2.7	0.5	0.6
Acetylene		9.5	12.3	15.4
Diacetylene		trace	trace	trace
Carbon monoxide		18.1	11.4	24.3
Carbon dioxide		1.4	0.0	0.0
Total		107.7	90.1	89.5
Carbon recovery, pct		103.2	89.4	80.9
Hydrogen recovery, pct		126.6	115.8	130.5
Analyses, wt pct				
Material	Coal	----Solid residue----		
Moisture	1.1	0.7	0.5	0.6
Ash	8.3	11.2	11.4	11.9
Ultimate composition, maf basis				
H	4.9	3.2	2.5	2.5
C	81.9	89.2	90.0	90.9
N	1.5	1.5	1.1	1.0
S	1.5	1.1	1.1	1.1
O (by difference)	10.2	5.0	5.3	4.5
Volatile matter, maf basis	37.2	17.4	10.2	12.3

Presented Before the Division of Fuel Chemistry
American Chemical Society
Chicago, Ill., August 30 - September 4, 1964

Evaluation of the Moisture Content of a Coking Coal for the Heat Consumption During Carbonization

by Dr. rer. nat. K. G. Beck,
Dr. rer. nat. R. Beckmann
and Dr. Ing. W. Weskamp

of Steinkohlenbergbauverein,
Essen, Germany

On an invitation by the American Institute of Mining, Metallurgical, and Petroleum Engineers three years ago, we had the opportunity to present to the Blast Furnace, Coke Oven, and Raw Materials Conference in Philadelphia a report on carbonization tests, which specifically dealt with the more essential coke characteristics and how they are affected by carbonization conditions[1]. The results of these tests had been obtained in a semi-industrial scale coke oven with a charging volume of 11.1 cu.ft.. Such test ovens are used with good success both in Europe and the USA for the determination of coke characteristics[2]. However, it is not possible to carry out thermo-technological investigations with such ovens, because the considerable surface and waste gas losses prevent an exact evaluation of the underfiring heat, which can be related to practical operation. Such thermo-technological investigations, however, are of particular significance for the West-German coke oven plants, since the expenses for underfiring constitute by far the largest factor of all costs which can be influenced by the mode of operation. Steinkohlenbergbauverein, thus, decided to build a test plant to be erected on a large coke oven plant in commercial operation. The test plant consists of an oven block with five industrial-scale semi-divided flow controlled coke ovens of underjet design. A bricked-up bulkhead of 59.1 in. width connects the test ovens (Fig. 1) with the adjoining oven group. On the other side there is a buttress of the usual type, with bricked cooling duct and concrete end. The dimensions of the ovens in cold condition and the hot dimensions determined during operation are shown in the following table (Fig. 2). In order to be able to heat all oven walls uniformly, "quantometers" and needle valves have been incorporated in each set of heating flues on the coke and ram side. The heat for underfiring the central oven can be measured individually. This separate gas feeder and measuring system proved necessary, because a comparison of the heat consumption ascertained

1) Size Distribution, Strength and Reactivity of Coke and how they are affected by the Coking Process
H. Echterhoff, K. G. Beck and W. Peters, 1961

2) Doherty, J.D., R.J. Hodder, L.N. Anthony
Some Effects of Moisture in Coking Coal,
Blast Furnace and Steel Plant 1962, pages 3/16

from the five test ovens with the heat consumption of newly constructed larger oven groups revealed great differences. This is in agreement with the results obtained by the British Coke Research Association at their test plant at Wingerworth. From the report by D.A. Hall, W.J. Pater, and F.K. Warford[3] on "The effect of drying coal charge and filter cake on coke oven performance and the yield and properties of the products" it can be seen that even an industrial-scale coke oven of 10 t capacity, which is operated separately from a coke oven battery, has a thermal efficiency of only 50%, as compared with the usual 70-80% efficiency of coke ovens arranged in batteries.

The coke is classified in a special screening plant (Fig. 3) and tested for its strength. A condensation plant (Fig. 4) serves to determine the amount and composition of the raw gas. This plant is designed in such a way that both the gas evolved from the five ovens, and the yield of by-products can be followed over the carbonization time of one oven. All measured data are centrally registered in a control station to monitor the operation.

From among the various serial tests so far carried out to ascertain the effects of heating flue temperature and moisture in the coking coal, the influence of the moisture content of the coal on high-temperature carbonization will be illustrated in the following.

Similarly to the method adopted by Brisse and Price[4], who used a wooden chamber, the distribution of the bulk densities as dependent on the moisture content of the coal was investigated in a test chamber of steel, prior to the commencement of carbonization tests (Fig. 5). Altogether 37 sampling points were arranged at three different levels. The coal used had a volatile content of 25.3% (free of water and ash), a size consists of 72% under 0.08 in. and 34% under 0.02 in., its ash content was 7.1% (free of water). Fig. 6 shows the distribution of bulk densities at moisture contents of 10%, 8%, and 6% at the three measuring levels. Due to the effect of dropping, the bulk density below the charging holes is always substantially above the bulk density between the charging holes. Naturally, this difference is reduced with the height of dropping. In the upper section of the

[3] Hall, D.A., W.J. Pater, F.K. Warford
Journal of the Inst. of Fuel (1963), pages 3/11

[4] Brisse, A.H., J.G. Price
Explorations in coke making research with a full scale coke oven model
Blast Furnace and Steel Plant 1959, pages 1285/90

Hock, H., M. Paschke
Archiv Eisenhütten 3 (1929), pages 99/102

Koppers, H., A. Jenkner
Glückauf 66 (1930), pages 834/38

Eisenberg, G.A.,
Glückauf 68 (1932), pages 445/61

Ejdelman, A.B., F.Z. Elenkij, G.D. Butuzov
Coke and Chemistry (USSR) 1961, pages 3/6

chamber there is also a more uniform distribution due to levelling. The following Fig. 7 shows the distribution of bulk densities under charging hole 1 and between charging holes 1 and 2. The hatched area is a measure of the inequality of the bulk densities. It illustrates the difficulty of heating an oven chamber with coal of high moisture content in such a way that the same carbonization rate is attained throughout the chamber. The results show how important it is for coke oven plants to lower the moisture content of the coking coal and, thus, to bring about an equalization of the bulk densities in the oven chamber in order to warrant a uniform carbonization of the chamber contents resulting in coke of homogeneous structure and strength.

After charging, the bulk density of the coke does not at all remain constant, but it changes during carbonization. Immediately after charging the coal, it starts shrinking. This shrinking phenomenon continues for 2 hours. It is caused by an intrinsic oiling effect inherent with coal. During the distillation, part of the gas evolves through uncarbonized coal. This gas, let us call it internal gas, carries with it about 122 gr./cu.ft. compounds from the plastic zone which are solid or liquid under normal conditions. They are partially precipitated as an oily film on the surface of the coals. To initiate the first shrinkage it only requires a stimulus which is created by the gases and vapours passing through the coal.

The second shrinkage does not begin until after the formation of the first semi-coke. It should be due to the relaxation of tensions in the structure of the coke, and subsidence of the coke, caused by cracks.

Fig. 8 shows the duplication of the shrinkage effect between 10 and 6% moisture, its reduction at 4% to a value lower than at 10%, and the almost complete disappearance of shrinkage at 2% moisture content. If the bulk density is calculated after the initial shrinkage, it turns out to be the same between 10% and 4% moisture content. Thus, the first shrinkage is effective until the same bulk density (wf) is reached. In the case of coals with swelling properties a reduction in the moisture content will not have any influence on the mode of operating the ovens. At 2% moisture content, the bulk density (wf) of the coal is so high that the coal grains cannot, of their own weight, become more compacted. The second shrinkage of the coal tested was not large enough to regain the initial coal volume. The coal struck to the wall, and pushing the coke was difficult.

There are generally two possibilities of investigating the effect of the moisture content of the coal on heat consumption. Either the heating flue temperature is kept constant for all tests and the influence of differences in the moisture content is balanced by modifying the carbonization time, or the tests are made at equal carbonization times, while a change in the heating flue temperature will compensate for differences in the moisture content.

The first mode of operation was chosen for our investigations, i.e. at a heating flue temperature of 2280°F. the carbonization time according to the respective moisture content of the coal was determined in preliminary tests. The serial tests comprised 6 tests in which the water content of the coal was changed in steps of 2% between 2 and 12%. A new test with modified moisture content was not commenced until the battery was surely at an equilibrium. The duration of the test, at each moisture content, was at least 5 times 24 hours.

The coking coal, in a thermal drier, was adjusted to the desired moisture content. No larger deviations than 0.1% from the desired moisture content of the coal were determined in the larry car.

Fig. 9 illustrates the bulk densities, carbonization times and throughputs in their dependency of the moisture content. The bulk density (moist) has a minimum at 4 to 6% moisture content of the coal. This minimum, in the curve of the bulk density (wf) is shifted towards the higher moisture content. The curve of the carbonization time has about the same tendency as the curve of the bulk density (moist). The negligible differences can be accounted for by modifications in the carbonization conditions owing to the influence of the moisture content of the coal. In this case, it is particularly the great dependency of the heat conductivity on the water content which makes itself felt. The dependency of bulk density and carbonization time on the moisture content of the coal are also reflected in the throughput. The hatched area between the curves for moist and water-free throughput is a measure for the amount of water which must be processed as a ballast during carbonization. Referred to the coke yielded wf/wf an increase in the throughput of 18% will result, when the moisture content of the coal is reduced from 12 to 2%.

In discussions about the heat consumption for carbonization, as dependent on the moisture content of the coal, the question is always raised how much energy is required for expelling the moisture of the coal in the oven and if under certain circumstances it may be more economical to reduce the moisture content of the coal in a special drying process[5]. The heat consumption figures measured in our test ovens with the coal described above have been illustrated in Fig. 10. They change from 832 Btu/lb. at 2% moisture content of the coal (moist) by 70 Btu/lb. to 902 Btu/lb. at 12% moisture content of the coal (moist). As the illustration further reveals, the differences in the heat consumption figures are by no means equal for each 2% change in the moisture content. At higher moisture contents they are essentially larger than at lower ones, although the changes in the amounts of moisture and coal at 0.02 lb. are the same.

Before following up the reasons for the non-linearity of the course of the heat consumption curve, the calculated heat consumption figures likewise illustrated in Fig. 10 should be mentioned which result from operating the ovens at equal carbonization time and at a heating flue temperature as modified in correspondence with the moisture content of the coal. The data necessary for the re-calculation have been taken from an earlier investigation into the effect of the heating flue temperature on high temperature carbonization[6]. The carbonization time of 20 hours which results from coking a coal with 10% moisture at a heating flue temperature of 2280°F. has

[5] Wollenweber, W., Glückauf 57 (1921), pages 987/92
Koppers, H., Koppers-Mitteilungen 14 (1932), pages 3/8
Baum, K., Glückauf 68 (1932), pages 1/8, 40/45
Litterscheid, W., Brennstoff-Chemie 13 (1932), pages 386/91
Hofmeister, B., Glückauf 88 (1952), pages 367/70

[6] Weskamp, W., W. Dressler, E. Schierholz, Glückauf 98 (1962), pages 567/77

been taken as the basis. The heat consumption differences for any 2% change in the moisture content are larger than they are at constant heating flue temperature. Table 2 (Fig. 11) compares the results of the two modes of operation. When reducing the moisture content of the coal from 12 to 6% a saving averaging 14.4 Btu is attainable for each 1% reduction in the moisture content at constant carbonization time, while an average of only 9.0 Btu could be determined at constant heating flue temperature.

On the other hand, when operating at constant heating flue temperature, a larger increase in the throughput of the coke ovens can be achieved by changing the carbonization time.

The question about the real heat requirement for the evaporation of the moisture led us to further investigations and observations regarding the heat economy of a coke oven and how it is influenced by differences in the moisture content. In carrying out these further investigations it appeared expedient to extensively break up the individual thermo-technological mechanisms in a coke oven. By means of a section through a coke oven (Fig. 12), an explanation of the individual items should be given initially. The underfiring heat Q_1 fed through the heating flue is only partially utilized for carbonization. Items Q_2 and Q_3 represent the total losses. Item Q_2 collects the waste gas and surface losses of the lower part of the oven up to the coal line. Item Q_3 includes the surface losses above the coal line. The heat amount Q_1 minus Q_2 is largely transferred to the chamber charge (Q_{10}). Only a negligible portion, through heat transfer, flows into the area above the coal line Q_4. This heat, depending on the temperature condition prevailing in the gas collecting space, can be transferred to the gas or is lost as surface loss. During carbonization, together with external Q_6 and internal Q_7 gas, a substantial amount of heat reaches the gas collecting space and leaves it again with the developed mixed gas Q_5. Item Q_8 is constituted of the evaporation heat of the water, the tar and the light oil at 32°F. and the gas formation energy (Gasarbeit) of the gaseous distillation products at 32°F. At the time of pushing, the coke possesses the sensible heat, item Q_9. The chemical processes occurring during the carbonization have an overall heat inherence which is considered under Item Q_{11}. A sensible heat Q_{12} is brought into the coke oven by the feed coal, the underfiring gas and the combustion air.

During the tests, all temperatures for the calculation of the sensible heats have been measured excepting the temperature of the external gas and internal gas when entering into the gas collecting space. For these measurements special suction pyrometers had to be designed because it is very important not to disturb the flow conditions prevailing in the measured range during measurements. The suction pyrometer to measure the temperature of the external gas was equipped with a narrow hood which on the one hand keeps off the radiation of the wall and on the other offers a screen against the internal gas. The hot must at least have the width of one piece of coke in order to be independent of the geometry of the coke lumps. Suction must be so dimensioned that the same velocity will prevail inside and outside the hood. When the suction is too strong, the temperature will drop immediately which indicates that gas from other sources is simultaneously sucked in which can only be colder in any case.

A similar procedure was adopted for measuring the temperature of the internal gas. In a pipe with a diameter of 3.94 in. a second pipe with a diameter of 1.97 in. is inserted to screen off the heat influx from the gas collecting space. The space in between the two pipes is filled with asbestos and a gas inlet is created by a conical shell. The distance of the thermocouple from the coal surface can be changed at random by using an adjusting screw.

Since the internal gas will surely have a temperature exceeding a 212°F., the system was heated above 212°F. to avoid condensation of steam. Approximately 1 minute after the commencement of measuring, a temperature of approximately 392°F. was reached; 6 to 8 minutes later, the temperature continues to raise further. By this time, the asbestos, heated up by the gas from the gas collecting space has attained a temperature higher than 392°F. and superheats the internal gas.

Further measurements revealed that the internal gas has a temperature of 212°F. immediately after charging. After one hour, the temperature has risen to 302°F., to remain constant at 392°F. from the 2nd to the 7th hour of carbonization. With these temperatures, all variables required for the establishment of a detailed heat balance are known.

At a temperature of 59°F. of the coal input, 1210 Btu/lb. water is required for heating up, evaporation and superheating to 392°F. At an efficiency of the underfiring system of 80%, 1510 Btu will be required in terms of underfiring heat per lb. moisture. The further heating up of the steam is effected almost exclusively by heat exchange with the hotter external gas.

This value of 1510 Btu/lb. water now serves to calculate the heat consumption for dry coal. This turns out to be approximately 810 Btu/lb. for the coal used, at a constant heating flue temperature of 2280°F. At a moisture content of 6% it is lowest and raises by 12.6 Btu towards coals with 2% and 12% moisture content.

If an attempt is made at calculating the heat consumption at a change in the moisture content by 2%, it must be taken into consideration that in case of moist coal as used in practical operation, a change in the moisture content is automatically connected with a modification in the amount of coal, for the carbonization of which additional heat is required. The savings in terms of underfiring heat for the reduced moisture of 0.02 lb. can be calculated at 30.2 Btu if the above two pyrometers are taken into consideration. On the other hand, an additional heat consumption of 16.2 Btu is required for the additional 0.02 lb. dry coal. From the difference of these 2 values of 30.2 - 16.2 results a constant reduction in consumption of 14 Btu/lb. for each 2% reduction in the moisture content.

If this calculated value of 14 Btu is compared with the measured differences in heat consumption illustrated in Fig. 10 it can be shown that the calculated and the measured differences agree when reducing the moisture content from 8 to 6%. Below 6%, the measured difference is smaller, below 8% larger than 14 Btu. Now, what are the reasons for these deviations from the calculated figures?

A quantitative treatment of these phenomena would become too complex at this point. Therefore, our report will be confined to an explanation of the results. In a balance in which all items stated in Fig. 12 have been considered it can be shown that the curve of the sensible heat of the total gas is responsible for the tendency of the underfiring curve. This heat results from the sensible heat of the external and internal gas and from a portion absorbed by heat exchange from the vault of the gas collecting space. The curve of the sensible heat of the total gas runs through a minimum at 6% moisture content of the coal. Its rise towards higher, and lower moisture contents has different reasons.

At 6% moisture content of the coal the sum of the sensible heat of the external and internal gases is equal to the sensible heat of the total gas. Thus, in the wall, there flows only such heat as is lost as a surface loss. Since in this range there is no heat exchange in the vault of the gas collecting space, the heat consumption difference calculated from changes in the amounts of moisture and coal is equal to the measured difference.

At higher moisture contents, the mean wall temperature in the area of the charge drops, and with it the sensible heat of the external gas. As the amount of steam in the internal gas, moreover, has a rising tendency, the temperature of the total gas decreases. By convection and radiation, heat from the vault of the gas collecting space is transferred to the total gas, which, through heat conduction in the wall is transferred from the area of the charge into the area of the gas collecting space and must, therefore, be fed as underfiring heat.

Below 6% moisture content of the coal, the reasons for the rise of the sensible heat of the total gas are of different nature. With the reduction in the moisture content there is an increase in the average chamber wall temperature and, thus, in the sensible heat of the external gas. However, since the internal gas, owing to the decreasing amount of moisture, demands less heat for superheating, a high temperature of the total gas is attained. The lower the moisture content the earlier the time when the total gas has a higher temperature than the vault of the gas collecting space, and thus yields heat. The temperature gradient between the wall in the area of the charge and above the charge is now very much smaller and hence less heat flows as item Q_4 into the area of the gas collecting space. The heat determined as surface loss below 6% moisture content of the coal is, thus, partially supplied by external gas. This heat need no longer be fed via Q_4 through underfiring, and so the measured heat consumption difference becomes smaller than the calculated one.

Let us briefly survey the results of these investigations:

The steam evolved from the moisture of the coal reaches the gas collecting space at a temperature of 392°F. This required 1510 Btu underfiring heat per lb. water at a thermal efficiency of the coke oven of 80%. The heat for further superheating of the steam is supplied by the hotter external gas. With the aid of this value, a detailed heat balance of the coke oven can be established permitting to critically observe the measured heat consumption and to scrutinize the correctness of the chosen carbonization time at constant heating flue temperature. Besides, the non-linear course of the heat consumption curve has been interpreted.

The economic significance of reducing the moisture content will be different according to the conditions of coke oven operation and can only be seen within the total economy of a mining company. If potential savings by reducing the moisture content of the coal are not referred to coal with a coal ready to be charged but to a dry coal amount of 0.9 lb. which corresponds to a coking coal with 10% moisture and which constitutes the figure used in economic calculations by German coke oven operators, savings in the heat consumption averaging 17 Btu, for each 1% reduction in the moisture content of the coal are revealed in the range of 10 to 6% moisture content which is the range of primary technical interest. For expelling 1 lb. moisture, in the range of 10 to 6% moisture content at an efficiency of 80%, an average of 1530 Btu or, at an efficiency of 70%, an average of 1840 Btu will have to be expended. For a modern drier one likewise calculates with a heat expenditure of 1710 Btu/lb. moisture, if a flotation concentrate is for instance dried from 22% moisture content to 6% moisture content. The savings in heat consumption are thus absorbed or even surpassed by the expenses for previous drying. However, the reduction of the water content brings about other advantages which are apt to exert a favourable influence on the economy of a coke oven plant. The question of drying can gain vital significance if the basis of raw materials can thus be extended considerably, as it happed in the case of the Lorraine coking plants after the process using dried coal had been successfully developed at the Marienau test plant and proved in practical operation at the Hagendingen coke oven plant[7]. An effect which cannot be underestimated will be the influence of a lower moisture content of the coal on the life of a battery. An essential advantage is a possible increase in the throughput which permits savings in the capital service and a reduction in other overheads.

There is a substantial difference between the conditions prevailing in USA and in Germany which must be considered in judging the importance of the moisture content of the coking coal for the economy of coke oven plant operation.

In the Federal Republic of Germany more than 80% of the total coke outputs is produced at coking plants located in the immediate vicinity of collieries supplying coking coal. Our investigations confirmed that in terms of thermal economy there is no advantage in reducing the moisture content of a coking coal in a thermal drying unit prior to its carbonization. Accordingly, the average moisture content of the feed coal used in German coking plants located at collieries is at 9 to 10%. However, if the coking coal has to be transported to the coking plant over long distances, as it happens in many cases in the USA, there will be freight savings which can be significantly higher than the expenditure for thermal drying[8]. Thus, it is understandable that, as a rule, American coking coals have a lower moisture content.

7) Loison, R., P. Foch
Revue de l'industrie minerale (1961), pages 593/618

8) Doherty, I.D., J. Griffen
Blast Furnace, Coke Oven, and Raw Materials
Conference, 1960, pages 117/37

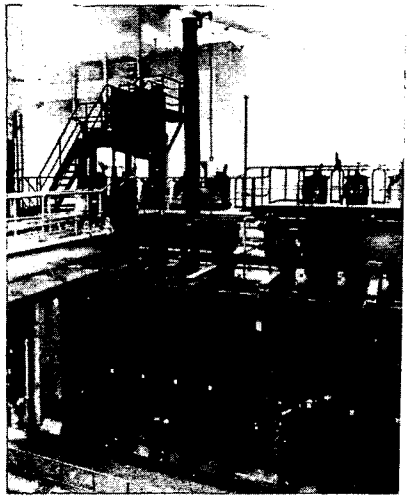

Fig. 1

	Cold Dimensions In.	Hot Dimensions In.
Length between buckstays	500	509
Length between door plugs	468	477
Height of chamber	164	167
Charging height (Coal line)	152	-
Width of chamber (Machine side)	16.5	16.2
Width of chamber (Coke side)	18.9	18.5
Mean chamber width	17.7	17.3
Thickness of oven roof	39.4	-
Pitch	45.3	-
Capacity of oven Cu.ft.	729	

BWV 1964	Oven Dimensions	VK 150

Fig. 2

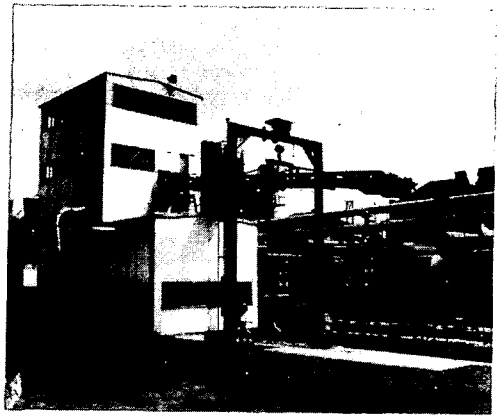

Fig. 3

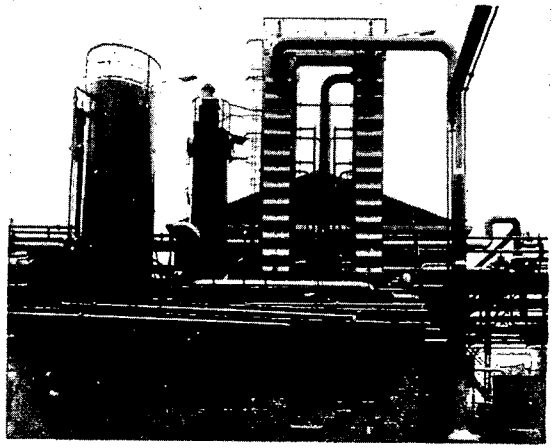

Fig. 4

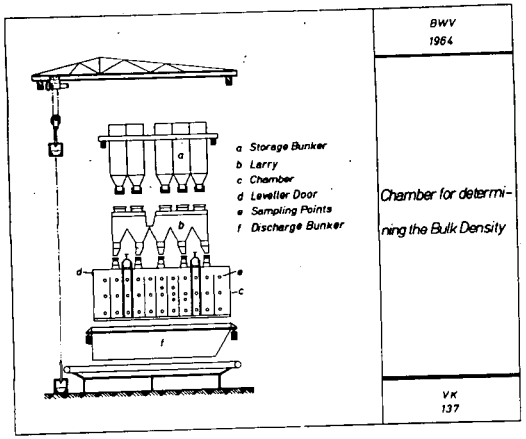

Fig. 5

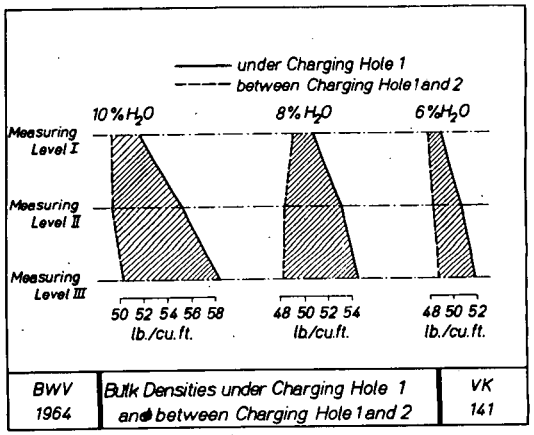

Fig. 7

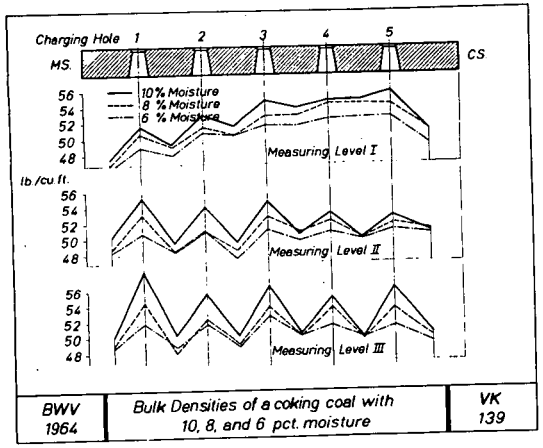

Fig. 6

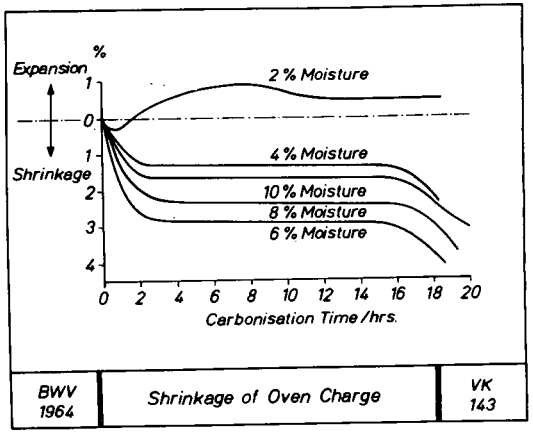

Fig. 8

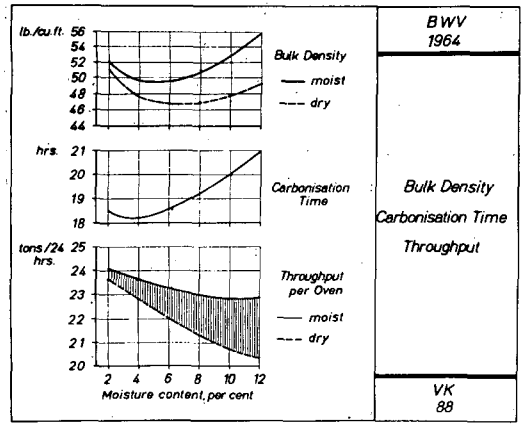

Fig. 9

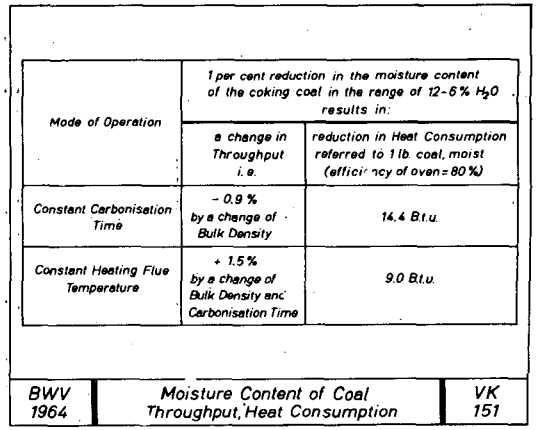

Mode of Operation	1 per cent reduction in the moisture content of the coking coal in the range of 12-6 % H_2O results in:	
	a change in Throughput i. e.	reduction in Heat Consumption referred to 1 lb. coal, moist (efficiency of oven = 80 %)
Constant Carbonisation Time	- 0.9 % by a change of Bulk Density	14.4 B.t.u.
Constant Heating Flue Temperature	+ 1.5 % by a change of Bulk Density and Carbonisation Time	9.0 B.t.u.

BWV 1964 | Moisture Content of Coal Throughput, Heat Consumption | VK 151

Fig. 11

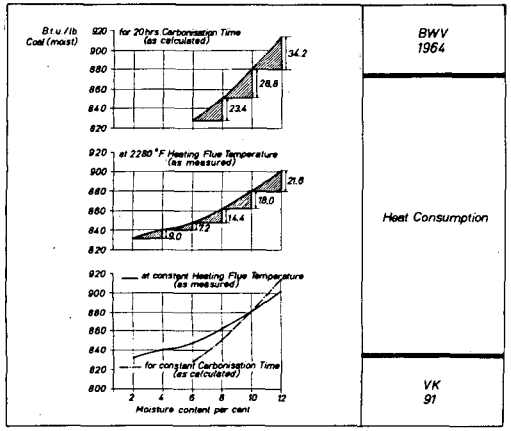

Fig. 10

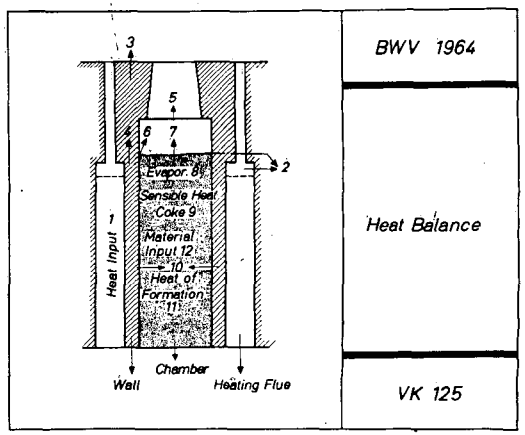

Fig. 12

Presented Before the Division of Fuel Chemistry
American Chemical Society
Chicago, Ill., August 30 - September 4, 1964

Devolatilization Studies on Coal Vitrinoids By Use of a Thermobalance

R. W. Shoenberger and E. F. Strickler

United States Steel Corporation
Applied Research Laboratory
Monroeville, Pennsylvania

The petrographic entities, which originate from the vegetation making up coal, help to establish the properties of coal that influence its mining, preparation, and use. Consequently, the properties of these entities should be known if the potential use of petrographic techniques and of the coal itself is to be made. Various physical and chemical properties of coals have been determined with significant contributions to the basic knowledge of coal and with practical application in industry, particularly in the carbonization of coal. To further exploit these entities, a study was initiated to determine their pyrolytic and plastic properties. In the initial phase, the vitrinoids of different rank coals were chosen for this study since vitrinoids are the most abundant and easiest entity to obtain from coal.

The thermal-decomposition behavior of entities has been visually examined in the hot-stage microscope. These observations are mostly qualitative. To obtain more quantitative results, the authors used a thermogravimetric balance (thermobalance) to determine the pyrolytic properties of the vitrinoids. The thermobalance, which has been used satisfactorily by numerous investigators,[1,2,3,4]* was selected because it continuously records the weight and temperature of the sample in respect to time as the sample is heated automatically.

When coal is heated, it not only devolatilized but also becomes fluid. Consequently, the plastic properties of coal have been associated with its pyrolytic properties. By using the rate of devolatilization and plastic properties, Soth and Russell[5] explained the coking pressure developed by coal blends. Van Krevelin,[3,6] Berkowitz,[7] and Brown[8] used the pyrolytic and plastic properties to present concepts of coal structure and the mechanism of carbonization. The relative plastic properties of the vitrinoids were obtained when possible, to determine the relationships that exist with their pyrolytic properties.

This paper presents the results of the thermogravimetric study on vitrinoids of various rank coals and the relationships of these results to the rank and plastic properties of the vitrinoids.

Materials and Experimental Work

The samples, high in vitrinoids, were selected from coking coals representing different ranks of coal. Because vitrinoids can be distinguished from the other coal entities by their bright luster in banded coals, these bright bands were removed with a table saw. The samples were then selected from these specimens with a dissecting needle under a magnifying glass. These samples, listed in Table I,

* See References

were then pulverized to 100 percent minus 60 mesh. The volatile-matter content of these samples, determined by standard procedures (ASTM Test Designation D 271-58), are included in Table I. The petrographic analyses conducted by the procedures used at the U. S. Steel Corporation's Applied Research Laboratory (ARL)[9] are shown in Table II. These analyses indicate that the samples contained high concentrations of vitrinoids. Only Wellington and Donegan coal samples contained less than 90 percent vitrinoids, but even they contained more than 83 percent. The average reflectances were also determined on these samples, Table I.

The devolatilization measured by the weight loss was determined on a Stanton thermogravimetric balance, Model TR-1. This thermobalance continuously records the temperature and the weight of the samples that were automatically heated at a rate of 6 degress C per minute. The 0.5-gram sample was contained in a silica crucible supported by a silica weighing mechanism attached to the balance and heated by a tube furnace. The balance is sensitive to 1 milligram.

The plastic properties were determined in the Gieseler Plastometer by the standard procedures used in ASTM Test Designation D 1812-60T. The results of these tests are listed in Table III. The amount of sample was limited and, therefore, only single tests were made. Furthermore, the stirrer broke loose on some of the low-rank coals and no values could be obtained.

Results and Discussion

The data obtained from the thermobalance show the cumulative weight losses at corresponding temperatures. These "S"-type curves are presented in Figure 1. The initial level of weight loss reflects the total moisture content and amount of occluded gas in each sample, the low-rank coals containing high percentages of inherent moisture. In all samples the weight loss increased slightly for a short time after the first devolatilization; the temperature of the initial devolatilization increased with the rank of vitrinoids. Very rapid devolatilization then occurred for a considerable time (about 100 minutes) until the weight loss gradually decreased. Most of the volatile matter was driven off by the time the temperature reached 900 C.

To obtain additional information, the differential pyrolysis curves were then determined from these data. The graphs that show the rate of devolatilization with respect to temperature are shown in Figure 2. The maximum rates of devolatilization for the low-volatile coals are lower than those for the high-volatile coals. A summary of the maximum rate of devolatilization and the temperature of this maximum rate is listed in Table IV. The relationship between the maximum rate of devolatilization and volatile matter is shown in Figure 3. This relationship appears to substantiate published results which show that maximum devolatilization rates are obtained with coal containing about 35 percent volatile-matter content.[3] High-rank coals have much less volatile matter and, therefore, would be expected to have low rates of maximum devolatilization. However, since the low-rank high-volatile coals decompose at the lower temperatures because of their aliphatic structure, the devolatilization is distributed over a longer initial time or temperature range; therefore, the maximum rate would decrease after a certain rank coal was reached.

The results also indicate that the temperature of maximum rate of devolatilization increased as the rank of the coal increased. A good correlation is shown in Figure 4 where average reflectance is used as a rank parameter. A similar correlation is shown in Figure 5 where volatile matter is used.

Because plastic properties are related to rank, the temperature of maximum fluidity was related to the temperature of maximum rate of devolatilization. This relationship, shown in Figure 6, indicated a difference of about 50 degrees C between

these values. Published work on whole coals indicates that these values should be about the same.[3,6,7] However, the data reported by van Krevelen[3] show that the difference of 3 degrees per minute in the heating rate would account for about 20 degrees in the temperature of the maximum rate, since the faster the heating rate the higher the temperature.

The plastic properties and thermogravimetric analyses indicate that the vitrinoids start to decompose before they soften. However, the rapid devolatilization occurs at temperatures higher than the softening point for coal. In these vitrinoid samples, the maximum fluidity as measured in the Gieseler Plastometer occurred before the maximum rate of devolatilization. The relationships found in this study indicate that the thermal-decomposition characteristics can be estimated from the rank and plastic properties of the coal.

Summary

The results of this study indicated that the vitrinoids started to decompose before they became fluid. The initial temperature of devolatilization increased as the rank of the sample increased. Rapid devolatilization then occurred after the coal softened. From the differential pyrolysis curves, a good correlation was obtained between the temperature of maximum rate of devolatilization and the rank of coal. The maximum rate appears to be greatest for coals containing volatile matter (dry basis) of about 35 percent. The maximum fluidity of the vitrinoids was reached shortly before the temperature of maximum-rate devolatilization, and a good relationship was found between the temperature of maximum fluidity and the temperature of maximum rate of devolatilization.

The relationships obtained in this study indicate that the pyrolytic properties of coal can be estimated from its rank and plastic properties. This information should be useful to show what changes occur to coal when heated in the various processes used in industry.

References

1. H. C. Howard, "Pyrolytic Reactions of Coal," Chemistry of Coal Utilization, H. H. Lowry, Ed., Supplementary Volume, John Wiley & Sons, Inc., New York, pp. 363-394 (1963).
2. P. L. Waters, "Recording Differential Balances for Thermogravimetric Analysis," Coke and Gas, July 1958, pp. 289-291, and August 1958, pp. 341-343.
3. D. W. van Krevelen, F. J. Huntjens, and H. H. M. Dormans, "Chemical Structure and Properties of Coal XVI — Plastic Behaviour on Heating," Fuel, 35, 1956, pp. 462-475.
4. H. Luther and B. Bussmann, "Die Theomische Zersetyung von Steinkohlen in Abhangigkeit van de Korngrosse 1. Mikroskopishe und Thermogravemetrishe Untersuchungen," Brennstoff-Chemie, Vol. 43, No. 12, December 1962, pp. 353-361.
5. G. C. Soth and C. C. Russell, "Sources of Pressure Occurring during Carbonization of Coal," Transactions, AIME, Vol. 1957 (1944), Coal Division, pp. 281-305.
6. D. W. van Krevelen, "The Behaviour of Coal on Heating," Coal Science, Elsevier Publishing Company, New York, 1957, pp. 286-311.
7. N. Berkowitz, "On the Nature of Coking Coals and the Mechanism of Coke Formation," Blast Furnace, Coke Oven, and Raw Materials Proceedings, Vol. 9, AIME, 1960, pp. 95-111.
8. H. R. Brown, "The Decomposition of Coal in Relation to the Plastic Layer," Coke and Gas, October 1956, pp. 390-393.
9. N. Schapiro and R. J. Gray, "Petrographic Classification Applicable to Coals of All Ranks," Proceedings of the Illinois Mining Institute, 68th Year, 1960.

Table I

Identification and Rank of Vitrinoids

Rank of Original Coal	Seam	County	State	Concentration of Vitrinoids, %	Rank	
					Volatile Matter, % (dry basis)	Average Reflectance, R_o
High-Volatile B	Illinois No. 6	Vermilion	Illinois	97.3	43.7	0.50
High-Volatile C	Herrin No. 6	Saline	Illinois	95.3	38.3	0.51
High-Volatile B	Sunnyside	Carbon	Utah - Colorado	86.2	37.4	0.71
High-Volatile B	Herrin No. 6	Saline	Illinois	94.6	34.1	0.77
High-Volatile A	High Splint	Harlan	Kentucky	91.2	33.6	0.93
Medium-Volatile	Sewell	Nicolas	West Virginia	83.8	29.4	1.15
Medium-Volatile	"A"	Pitkin	Colorado	94.8	22.6	1.39
Low-Volatile	Pocahontas No. 3	McDowell	West Virginia	90.4	21.5	1.39
Low-Volatile	"A"	Pitkin	Colorado	97.0	16.5	1.42

Table II

Petrographic Entity Composition of Indicated Samples,* Volume Percent**

Coal	Reactive														
	V4	V5	V6	V7	V8	V9	V10	V11	V12	V13	V14	V15	E	R	SF	Total
Illinois No. 6	49.6	45.7	2.0										0.9	-	0.1	98.3
Herrin No. 6 "C"	40.0	55.3											0.5	-	0.2	96.0
Sunnyside			35.3	50.0	0.9								1.0	8.8	0.2	96.2
Herrin No. 6 "B"			6.6	60.6	27.4								1.6	-	0.2	96.4
High-Splint				2.7	21.0	62.9	4.6						1.2	0.5	0.2	93.1
Sewell						2.5	12.6	46.1	20.9	1.7			3.5	0.2	0.6	88.1
Colorado Medium										61.6	33.2		-	-	0.3	95.1
Pocahontas No. 3										62.4	28.0		-	-	0.2	90.6
Colorado Low										34.0	61.1	1.9	-	-	0.1	97.1

Coal	SF	M	F	Total
Illinois No. 6	0.2	1.2	0.3	1.7
Herrin No. 6 "C"	0.5	3.0	0.5	4.0
Sunnyside	0.5	1.7	1.6	3.8
Herrin No. 6 "B"	0.4	2.5	0.7	3.6
High-Splint	0.4	5.7	0.8	6.9
Sewell	1.2	7.8	2.9	11.9
Colorado Medium	1.0	2.8	1.1	4.9
Pocahontas No. 3	0.9	7.2	1.3	9.4
Colorado Low	0.6	1.4	0.9	2.9

*Abbreviations for entities:
V4 = vitrinoid type 4, etc.
E = exinoids
R = resinoids
SF = semifusinoids
M = micrinoids
F = fusinoids

**Pure-coal basis (excluding mineral matter).

Table III

Plastic Properties of Vitrinoids*

Sample	Maximum Fluidity ddpm** at	C	Temperature Range, C Softening	Solidification
Sunnyside	1.3	412	373	451
High-Splint	100	433	355	472
Sewell	16,300	443	385	485
Colorado Medium-Volatile	330	459	390	498
Pocahontas No. 3	432	466	397	499
Colorado Low-Volatile	80	467	401	503

*Stirrer broke loose on all Illinois coals.
**Dial divisions per minute.

Table IV

Summary of Thermogravimetric Analyses

Sample	Maximum Weight Rate Loss, % per minute	Temperature of Maximum Weight Rate Loss, C
Illinois No. 6	0.54	463
Herrin No. 6 "C"	0.47	480
Sunnyside	0.67	475
Herrin No. 6 "B"	0.48	490
High-Splint	0.60	483
Sewell	0.64	510
Colorado Medium-Volatile	0.40	520
Pocahontas No. 3	0.40	520
Colorado Low-Volatile	0.37	530

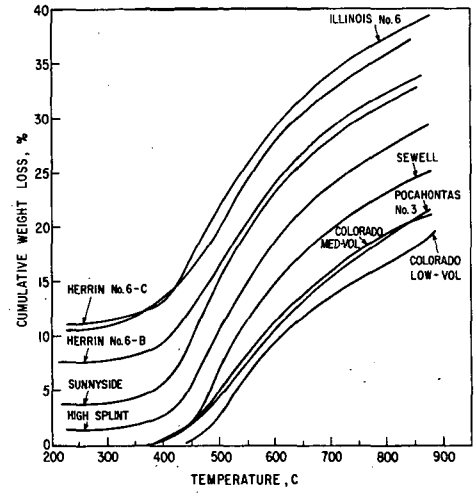

Figure 1

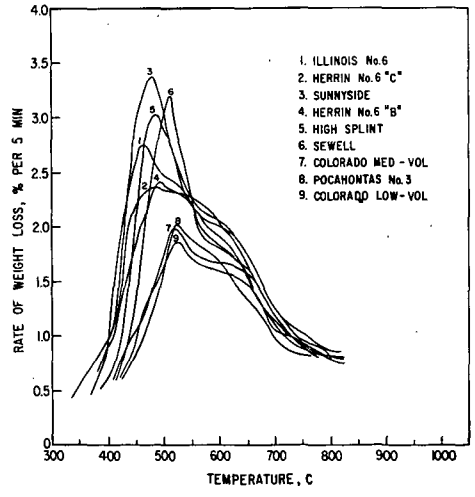

Figure 2

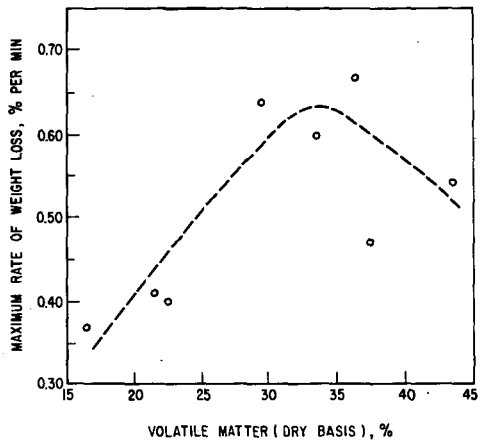

RELATIONSHIP OF VOLATILE MATTER AND MAXIMUM RATE OF DEVOLATILIZATION

Figure 3

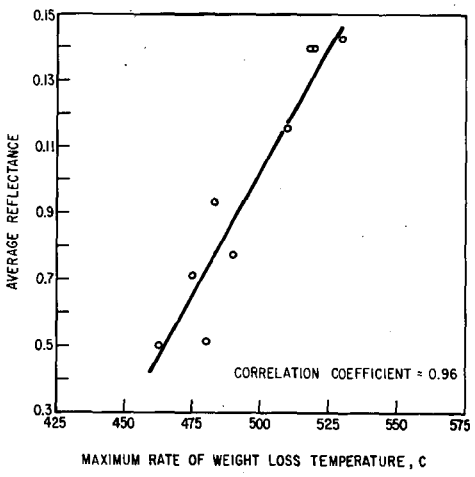

RELATIONSHIP OF THE TEMPERATURE OF MAXIMUM RATE OF DEVOLATILIZATION AND RANK

Figure 4

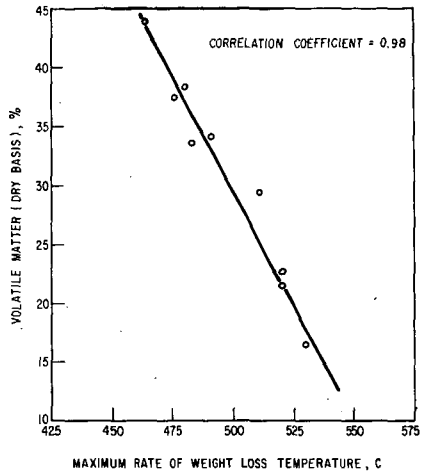

RELATIONSHIP OF THE TEMPERATURE OF MAXIMUM RATE OF DEVOLATILIZATION AND RANK

Figure 5

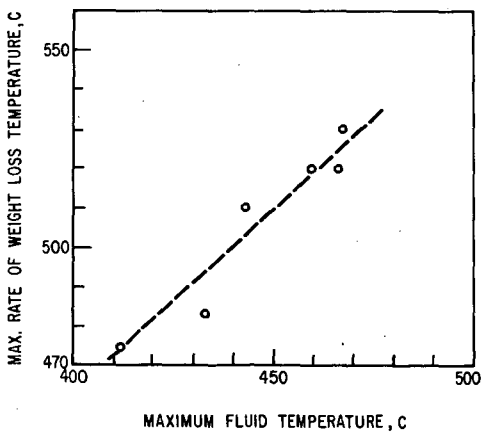

RELATIONSHIP OF MAXIMUM FLUIDITY AND MAXIMUM RATE LOSS TEMPERATURES

Figure 6

Presented Before the Division of Fuel Chemistry
American Chemical Society
Chicago, Ill., August 30 - September 4, 1964

OXIDATION OF A LOW-TEMPERATURE LIGNITE TAR PITCH

John S. Berber and Richard L. Rice

U.S. Department of the Interior, Bureau of Mines
Morgantown Coal Research Center, Morgantown, W. Va.

INTRODUCTION

As part of a broad program of coal research, Bureau of Mines scientists are conducting research on the characterization and upgrading of low-temperature tar. An important part of this work is the study of pitch from low-temperature lignite tar.

In the processing of tar obtained by low-temperature carbonization of coal, a residue or pitch is obtained that distills above 350° C and has physical characteristics intermediate between those of coke oven (high-temperature) tar pitch and those of petroleum bitumens. Low-temperature pitches are complex resinous masses of polymerized and polycondensed compounds. They are amorphous, solid or semisolid plastic materials, and consist predominantly of carbon with several percent by weight of hydrogen, somewhat less oxygen, nitrogen, and sulfur, and small amounts of inorganic materials. They are chemically similar to the tars from which they are prepared, being mainly mixtures of the higher homologs of the compounds contained in the distillable fractions of the tar. The pitch fraction from low-temperature tar usually is 30 percent by weight or more of the tar, depending upon the source of the tar and processing conditions. There has been little demand for the material because it is hard and brittle. The Bureau of Mines is attempting to modify this pitch to convert it into a more marketable product.

One method that has worked with high-temperature pitches is to blow air through the pitch mass while the mass is being heated. Other methods include solvent refining, the use of additives, the use of catalysts, and thermal treatment in an inert atmosphere. This paper discusses the results of air-blowing tests designed to convert pitch into a material useful as electrode binder.

ELECTRODE BINDER PITCH

Pitch is used as a binder in the manufacture of four major classifications of electrodes: baked-in-place (cathodes), Soderberg, preformed baked, and graphitized high density. To make each of these types, the aggregate is mixed with the solid or melted pitch in a special mixer until the aggregate is completely coated. The mixture is then rammed in place, extruded or molded into the desired shape, then baked (2).*

* Underlined numbers in parentheses refer to items in the list of references at the end of this report.

Soderberg electrodes are produced by mixing pitch binder with a graded aggregate of calcined petroleum coke, pitch coke, anthracite coal, bituminous coal coke, or mixtures of these. In the aluminum industry, only calcined petroleum or pitch coke is used to make electrodes to keep the impurities at a minimum.

So little is known about the structure or exact chemical composition of pitches that it is not possible to establish specifications other than by reference to arbitrary tests. Generally, the main properties involved in specifications for electrode binder, besides the softening point and carbon-to-hydrogen ratio, include specific gravity, coking value, ash content, distillation test, the amounts insoluble in benzene and soluble in quinoline, and the concentration of iron, silica, sulfur, and boron.

Softening point is particularly important in the production of electrode binder because the binder must be soft enough to properly mix with the electrode carbon and still contain enough resins to impart the desired compressive strength to the finished electrode. For electrode binder, the softening point should be about 95° to 110° C for Soderberg electrodes and 105° to 115° C for prebaked electrodes.

Electrode binder pitch must contain at least 20 percent of so-called "beta-resin," which is that portion soluble in quinoline, but insoluble in benzene (3). Concentrations of tar acids, tar bases, paraffins, saturated cyclic compounds, olefins, and alkyl groups attached to aromatic nuclei must be minimal because an excess of these adversely affect the properties of the pitch (1).

Carbon-hydrogen ratio is another property that pitch users consider of importance as it is an indication of plasticity, ductility, and elasticity of the binder. Most high-temperature pitches have a carbon-hydrogen ratio of about 1.8. The low-temperature pitch from lignite used in the tests in this report, however, had a carbon-hydrogen ratio of only about 0.84, and a low-temperature pitch from a bituminous coal had a C-H ratio of about 1.0. It can be readily seen that the C-H ratio of the low-temperature tar pitch must be increased if the material is to more nearly resemble commercial pitches.

The pitch used in these tests was obtained by batch distillation, under vacuum, of a low-temperature tar produced by the Texas Power and Light Company from Sandow lignite. Properties of the pitch are given in Table 1.

AIR-BLOWING OF PITCH

Since the binder characteristics of low-temperature tar pitch differ from those of high-temperature tar pitches, the pitch must be modified or upgraded if it is to be used for that purpose. As indicated, blowing with air (or oxygen) has been used to convert certain high-temperature bituminous pitches into material meeting specifications. It is a means of increasing the binder resin content of the pitch. The oxygen in the air acts as a condensation and dehydrogenating agent. The formation of water indicates that dehydrogenation has taken place, and the presence of carbon monoxide and carbon dioxide in the exit gases shows carbon has been lost. Little combined oxygen is found in the oxidized pitch.

As mentioned previously, a high carbon-to-hydrogen ratio appears a requisite for an acceptable electrode binder. Softening point and carbon-to-hydrogen ratio were taken as criteria of the effectiveness of the air-blowing treatment of these experiments to produce an electrode binder.

RESULTS

In the tests, the pitch was placed in a reactor (Figure 1), heated to the desired temperature, air or oxygen admitted at 2 to 4 scfh per pound, and agitation started at about 925 rpm. Runs ranged from 1 to 5 hours in length. Results are tabulated in Table 2.

It was found that the softening point generally increased in proportion to the length of time the air was blown through the pitch. The data plotted in Figure 2 illustrate the trend for air rates of 2.7 to 3 scfh per pound. Figure 2 also shows that for fixed run lengths, the softening point went up with increase in temperature of the heated mass.

Figure 3, a plot of reaction temperature versus softening point, better illustrates the effect of temperature. Blowing with oxygen raised the softening point temperature more than blowing with air.

Air rate also affected the softening point (Figure 4). It is apparent that air-blowing gave a very wide range of softening points, depending upon the reaction conditions. These conditions must be controlled very closely to give reproducible results.

A limited number of tests were made to determine the effect of sulfur addition on the softening point. Table 3 gives these results. In general, no definite pattern is apparent to indicate a material advantage for this treatment.

Blending was investigated to a limited extent. Industrial pitches are produced by distillation from high-temperature coke oven tars selected and blended to give the properties desired in the finished product, which vary in the different uses (4). It appeared that blending of different pitches, as shown in Table 4, would give a product having predictable characteristics. These blends, evaluated by the United States Steel Corporation electrode binder testing laboratory, indicate that the blends do not compare favorably with the pitch from coke oven tar in such properties as apparent density, crushing strength, electrical resistivity, and CO_2 reactivity. Table 5 gives the properties of the test electrodes.

CONCLUSIONS

This study on the air-blowing of pitch from low-temperature lignite tar was undertaken to prepare an effective electrode binder possessing properties of a bituminous pitch. Except for softening temperature, none of these properties were attained. The carbon-hydrogen ratio was increased slightly, but not significantly, and was below that of the blends made with high-temperature bituminous coal pitch which did not produce acceptable electrodes. Addition of sulfur does not significantly increase the carbon-hydrogen ratio. Either the blowing procedure was inadequate or air oxidation is not an effective means of upgrading low-temperature lignite tar pitch.

REFERENCES

1. Greenhow, E. J., and J. W. Smith. The Structure of Coal Tar Pitch. Australian J. Appl. Sci., v. II, No. 1, 1960, pp. 169-179.
2. Jones, H. L., Jr., A. W. Simon, and M. H. Wilt. A Laboratory Evaluation of Pitch Binders Using Compressive Strength of Test Electrodes. J. Chem. and Eng. Data, v. 5, No. 1, January 1960, pp. 84-87.
3. Lang, E. W., and J. C. Lacey, Jr. Low-Temperature Carbonization of America Seam Coal. Ind. and Eng. Chem., v. 52, No. 2, February 1960, pp. 137-140.
4. Thomas, B. E. A. Electrode Pitch. Gas World, v. 151, No. 3946, April 2, 1960, (Coking Supp., v. 56, No. 564), pp. 51-66.

TABLE 1. - Typical composition and properties of pitch before air-blowing compared with the desired properties

Properties	Typical	Desired
Softening point, °C	90[1]	95-110
Analysis, weight-percent		
Moisture	0.00	0.00
Carbon	83.78	92-93
Hydrogen	8.27	4-4.5
Sulfur	1.04	< 1.00
Nitrogen	1.06	1.00
Oxygen[2]	5.71	1-2
Ash	0.14	< 0.3
C-H ratio, atomic	0.84	1.8
Solubility, weight-percent		
Benzene	87.1	60
Petroleum ether	31.9	10

[1] Ring-and-ball softening point.
[2] Oxygen obtained by difference.

TABLE 2. - Air-blowing of pitch from low-temperature lignite tar

Run no.	Length of run, hours	Temp., °F	Air rate, scfh/lb	Softening point at start, °C	Softening point at end, °C	Carbon, wt-pct	Hydrogen, wt-pct	C-H atomic ratio
110	3	300	2	92	111	83.50	7.59	0.92
14	2	428	2	--	121	84.08	7.67	0.91
15	2.5	428	2	--	123	83.10	7.68	0.90
16	3	428	2	--	132	83.54	7.71	0.90
27	3.5	482	2	--	207	84.15	7.30	0.96
115	1	300	2.7	90	93	85.42	7.47	0.95
116	2	300	2.7	90	96	85.23	7.61	0.93
114	1	350	2.7	90	94	85.30	7.58	0.94
112	2	350	2.7	90	109	84.92	7.64	0.93
113	2	350	2.7	90	109	84.48	7.65	0.92
117	3	350	2.7	90	118	85.16	7.73	0.92
118	3.5	350	2.7	90	119	85.08	7.77	0.91
18	4	428	2.7	--	150	83.85	7.59	0.92
19	2	455	2.7	--	146	83.94	7.44	0.94
23	4	455	2.7	--	168	83.41	7.33	0.95
24	2	482	2.7	--	154	84.55	7.55	0.93
107	2.5	300	3	92	101	84.00	7.68	0.91
109	3	300	3	92	111	83.90	7.45	0.94
78	5	334	3	--	159	83.80	7.47	0.93
7	1	400	3	--	108	83.72	7.97	0.88
6	1	455	3	--	129	83.00	7.90	0.88
26	3	482	3	--	185	84.04	7.22	0.97
2	1	500	3	--	166	83.59	7.68	0.91
1	2	500	3	--	202	84.58	7.54	0.93
95	1	300	4	76	95	84.00	7.43	0.94
46	2	482	4	--	175	84.00	7.29	0.96

TABLE 3. - Pitch blown with oxygen, nitrogen, and air, with sulfur added

Run no.	Length of run, hours	Temp., °F	Rate, scfh/lb	Carbon, wt-pct	Hydrogen, wt-pct	C-H atomic ratio	Softening point, °C	Softening point before treating, °C	Sulfur, pct
				Oxygen					
41	2	428	0.3	83.25	7.61	0.91	123		
42	3.5	527	0.4	86.79	6.74	1.07	>250		
44	4	500	0.3	83.20	7.20	0.96	>250		
49	3	482	0.27	85.49	7.13	0.99	>250		
121	1	275	0.57	84.98	7.68	0.92	108	105	
122	1	275	0.57	85.19	7.74	0.92	117	105	
123	2	300	0.57	85.35	7.68	0.93	121	105	
124	1	275	0.57	84.69	7.78	0.91	113	105	
54	5	400	0.27	84.17	7.33	0.96	>250		5
57	2	400	0.27	83.28	7.76	0.89	130		3
58	2	428	0.27	83.30	7.78	0.89	141		3
59	2	455	0.27	84.10	7.48	0.94	172		3
				Nitrogen					
60	2	400	2.7	83.47	7.85	0.89	136		3
61	4	400	2.7	83.44	7.75	0.90	123		3
62	4	455	2.7	83.50	7.65	0.91	121		3
63	4	500	2.7	83.72	7.68	0.91	129		3
66	2	482	2.7	83.78	7.76	0.90	118		3
67	2	482	2.7	83.76	7.80	0.89	121		3
68	4	482	2.7	83.58	7.70	0.90	121		3
69	23.65	482	2.5	84.09	7.17	0.98	178		3
71	31.25	482	2.7	84.15	7.18	0.98	>250		5
				Air					
55	5	400	2.7	83.39	7.21	0.96	>250		5
56	3	400	2.7	83.40	7.44	0.93	177		3
132	1	282	2.7	81.60	7.57	0.90	105	90	5
135	1	240	3	84.76	7.55	0.94	111	93	5
136	1	350	3	84.79	7.52	0.94	112	93	5
137	1	420	3	84.86	7.56	0.94	124	93	5
138	1	470	3	85.30	7.44	0.96	132	93	5
139	1	440	3	85.18	7.47	0.95	128	93	5
140	1	410	3	85.00	7.52	0.94	116	93	2.5

TABLE 4. - Data on samples evaluated by U.S. Steel for electrode binders

Properties	Pitch blends No. 1[1]	No. 2[2]
Carbon	86.05	85.73
Hydrogen	6.40	6.39
C-H ratio	1.12	1.12
Softening point, °C	106	105
Penetration	0	0
Benzene insolubles	30	24

[1] 60 Percent low-temperature tar with softening point of 110° to 112°C and 40 percent high-temperature tar with softening point of 104° to 108° C.

[2] 60 Percent low-temperature tar with softening point of 97° to 101°C and 40 percent high-temperature tar with softening point of 110° to 121°C.

TABLE 5. - Properties of electrodes prepared with Bureau of Mines binders

Properties	Bureau of Mines pitch blends No. 1	No. 2	U.S. Steel coke oven pitch
Optimum binder content, wt-pct[1]	34	31	34
Apparent density, g/cm^3	1.32	1.38	1.46
Electrical resistivity, ohm-cm x 10^{-4}	79.3	72.0	59.2
Crushing strength, kg/cm^2	302	388	642
CO_2 reactivity, mg/g/hr	79.5	74.5	74.3
Dust, wt-pct	10.4	6.4	3.1

[1] Standard commercial aggregate, mix temperature 155° C.

CONTINUOUS DETERMINATION OF MOISTURE IN COAL BY NEUTRON THERMALIZATION

Robert F. Stewart and Arthur W. Hall

U. S. Department of the Interior, Morgantown Coal Research Center
Bureau of Mines, Morgantown, W. Va.

An automatic and continuous method of measuring the moisture content of coal is needed by the coal industry. Automatic control of the coal quality would reduce the cost of coal preparation, improve the product and thus indirectly increase the use of coal.

Moisture in coal can be determined by several methods, but the time required to obtain samples and analyze them by existing methods make it difficult, if not impossible, to control the quality of the product. Both producers and consumers need a method for continuous and instantaneous measurement of moisture content without sampling in order to regulate process equipment and keep the moisture content of coal within specifications.

At the Morgantown (W. Va.) Coal Research Center we are developing a nuclear method for continuous measurement of moisture in coal. This method is based on the thermalization of fast neutrons by hydrogen in the water and organic matter of coal. Neutrons from a small radioisotope source penetrate the coal, are scattered by hydrogen and measured by a thermal neutron detector. The number of thermal neutrons counted can be directly correlated with the moisture content of coal. Design of a moisture meter based on neutron thermalization depends on many variables, any or all of which can affect the sensitivity of the meter. These factors include those related to the nuclear aspect--type and size of neutron flux and source, type of detecting device, and background count--and those related to the coal being tested--rank, particle size, and ash content. A survey was initiated to eliminate the relatively insignificant factors and to ascertain the magnitude of the major effects. Such information was necessary to fully evaluate the technique and to establish design criteria.

Coal contains a relatively large amount of hydrogen in the organic coal substance and the water of hydration of the shaly material as well as in the moisture.

To apply this concept of moisture measurement to coal requires that the organic substance in coal from any one seam of a particular mine be uniform in hydrogen content. The difference in total hydrogen content of wet and dry coal is relatively small, so that a moisture measurement based on this concept requires a measurement between two large numbers to a high degree of precision. Thus, it was necessary to develop a highly precise instrumentation system for continuous measurement and to obtain a physical arrangement permitting measurement of moving coal with a minimum effect from density variations.

Experiments with Trays of Coal. Tests were conducted with metal trays containing 50 to 100 pounds of coal to develop an instrument system of high precision. A scaling system with a maximum instrument error of 0.2 percent was used to test different types of thermal neutron detectors. The most stable type of detector was a boron-10-lined proportional counter tube. While this type of detector showed satisfactory stability, extensive testing disclosed a long-term count reduction probably due to some type of deterioration in the detector. However, development of an electronic system using dual detectors eliminated this deterioration as a serious problem.

Table 1 shows typical results with a one curie plutonium-beryllium neutron source and a thermal neutron detector beneath a tray of coal and illustrates the

TABLE 1. Repetitive measurements of moisture in trays of coal

Consecutive tests,	Tests on same tray at 1-day intervals		Different trays of same coal,	
counts/10 min.	counts/10 min.	% H_2O, calculated	counts/10 min.	% H_2O, calculated
322406	525229	1.299	525490	1.300
320855	525376	1.299	513720	1:270
322452	525677	1.300	513240	1.269
321174	527906	1.305	514080	1.271
321348	524378	1.297	514360	1:272
320757	528416	1.307		
320381	524832	1.298		
320954	524362	1.296		
320226				
321099	516850*	1.300		
320073	514260*	1.297		
320062	517890*	1.300		
	522530*	1.312		
avg 320980				
% s.d.=0.25				

*Various parts of same tray, same day.

TABLE 2. Moisture measurements of hvab Pittsburgh-seam coals of different moisture contents

Lump Coal

% H_2O, ASTM analysis	B-10 detector		BF_3 detector	
	counts/10 min.	% H_2O	counts/10 min.	% H_2O
2.6	575176	2.61	1036164	2.60
	574084	2.61	1038184	2.60
	571850	2.60	1042280	2.60
1.9	533320	1.7	967950	1.9
1.8	541500	1.8	-	-
.3-1.3*	525770	.2	-	-
.3	526810	.2	724550	.4
0	520230	.1	646090	0
	Pulverized coal, variable density			
1.2	581420	1.1	839460	1.16
dried	528690	-	697160	-
.78	568810	.8	753760	.6
dried	522620	-	658120	-

*Variable due to loss of moisture during storage.

precision of measurement. Consecutive measurements of thermal neutrons at various times and positions beneath the same or different trays show a precision equivalent to ± 0.1% H_2O. With the successful development of a precise measuring system, several nuclear problems could be investigated. Figure 1 shows a typical distribution of thermal neutrons in a tray of bituminous coal obtained with a small thermal neutron detector buried in the coal. The contour lines indicate the relative flux distribution expressed as counts per minute per unit volume of detector (about two cubic inches). It can be seen that the count rate decreased with distance from the source, about 7 inches of coal being required to decrease the count rate to half that measured at a two inch distance. The contours are peaked in the forward direction, indicating the initial preferential scatter at small angles.

The thermal neutron count decreased when the detector was moved away from the source (points A, B, C) and the effective volume of coal measured was altered. A different calibration curve relating count rate and percent moisture, obtained from each of the locations A, B, and C, was found to vary in shape from concave through linear to convex with increase in distance between source and detector. At a certain distance between source and detector, a point was found at which density changes in the coal had practically no effect on the count rate. At this point the volume of coal measured by the detector compensates for changes in density of the coal. This effect may be pictured as a reduction in source size (the volume of measured coal) with increasing density that compensates for the shorter distance of measurement with increasing density. The net effect of this arrangement is that to a large extent the moisture content can be measured independent of fairly large changes in density or particle size of the coal.

Sensitivity of Measurement. Several tests were made with different coals using experimentally determined calibration curves. The coals were air and oven dried to constant moisture content and carefully mixed. Typical results, shown in table 2, illustrates the sensitivity of the method with coals having small differences in moisture content. Neutron measurements of lump coal agreed with analysis by ASTM methods within 0.2 percent moisture. The neutron measurements of pulverized coal were consistent, but the results cannot be compared directly with results from the lump coal because a physical arrangement compensating for density was not used in these tests. The results indicate that the nuclear measurement of moisture content can be empirically related with actual moisture content as determined by standard methods of sampling and analysis within an accuracy of 0.2 percent moisture. For a more detailed investigation of variations in the effects of particle size ash content, rank of coal, etc., improved methods of blending, mixing and sampling were necessary. Automatic mixing and sampling could best be done in a dynamic system of moisture measurement using pilot-plant scale equipment.

Pilot-Plant Testing. A pilot-scale system was designed and installed to test the operation of a neutron moisture meter in a system of moving coal. Figures 2 and 3 show the equipment used.

In this system, coal is recycled by a Zipper-type conveyor through an automatic sampler and blending duct into the moisture meter test section. This moisture test section holds 600 to 1,000 pounds of coal in a 30-inch square duct. Centered in this 4-foot depth of coal is a 6-inch port containing the neutron source and thermal neutron detector. Moisture content of a spherical volume of coal is measured as the coal moving through the duct passes the measuring port. Because of the shielding effect of coal, radiation levels outside the 30-inch duct are near background levels. The thermal neutron detector is connected by co-axial cables to a separate instrument system which records the increase in count rate of wet coal above a preset value for dry coal.

Pilot-Plant Results. In tests to determine the accuracy of the nuclear method, the pilot-scale unit operated satisfactorily in runs lasting up to 50 hours. Coal samples were collected periodically with the automatic sampler for moisture a-

nalysis and compared with the experimental values. In one test, the system was filled with 859 pounds of 3/4-inch by 3/8-inch hvab Pittsburgh seam coal of 1.6% H_2O. The neutron moisture meter recorded a value of 1.5% moisture for several hours dropping slowly as the coal lost moisture during recycling, finally becoming constant at 1.3%. At this constant moisture value, the meter recorded an average value of 1.3% for the next 24 hours, varying only 0.3%. At irregular intervals, usually about 8 hours, the meter had to be reset because of instrument drift. Except for this instrument drift, the results from the meter were within 0.5% of the chemical analysis at settings giving rapid response, and within 0.3% H_2O for slow-response settings.

Response time and precision of measurement were calculated by adding 100-pound lots of wet coal to the 800 pound charge of dry coal and recording the time between peaks as coal passed the measuring port. For example, when a lot of coal containing 4% H_2O was added, the moisture recorded increased from 1.2% to 3.5% the first cycle, then returned to 1.2 percent moisture. On the second pass of this lot of wet coal, the reading increased to 2.5% then returned to 1.2%. The third pass showed a slight increase, with a final reading leveling out at 1.5 percent moisture. Tests of this type were used to relate response time to precision of measurement.

Precision of Measurement. The precision of measuring moisture content is related to response time--the longer the response time the better the precision. A precision of $\pm$ 0.5 H_2O was obtained in a 20-second interval; $\pm$ 0.3% H_2O with a 2-minute response time; and $\pm$0.2% H_2O after 10 minutes of measurement. To increase the response time a neutron source considerably larger than 1 curie of plutonium-beryllium would be needed. A compromise between response time and precision of measurement depends on the specific application.

Discussion. The neutron meter for continuous moisture measurement in coal recorded the moisture content of coal moving at 1 to 20 tons per hour within 1/2 percent. We expect to increase the precision of the method by improving the electronic system. There are several ways this system might be used in industrial applications. For example, it could be used at the end of a conveyor to continuously measure moisture in coal moving at tonnage flow rates--50 to 100 tons per hour. It also could be applied in a by-pass system measuring coal at 10 tons per hour from an automatic sample cutter. We plan to obtain a more rugged electronic instrument system and test a prototype neutron moisture meter in a commercial plant. This should provide a sound evaluation of the practicability of the method for industrial use.

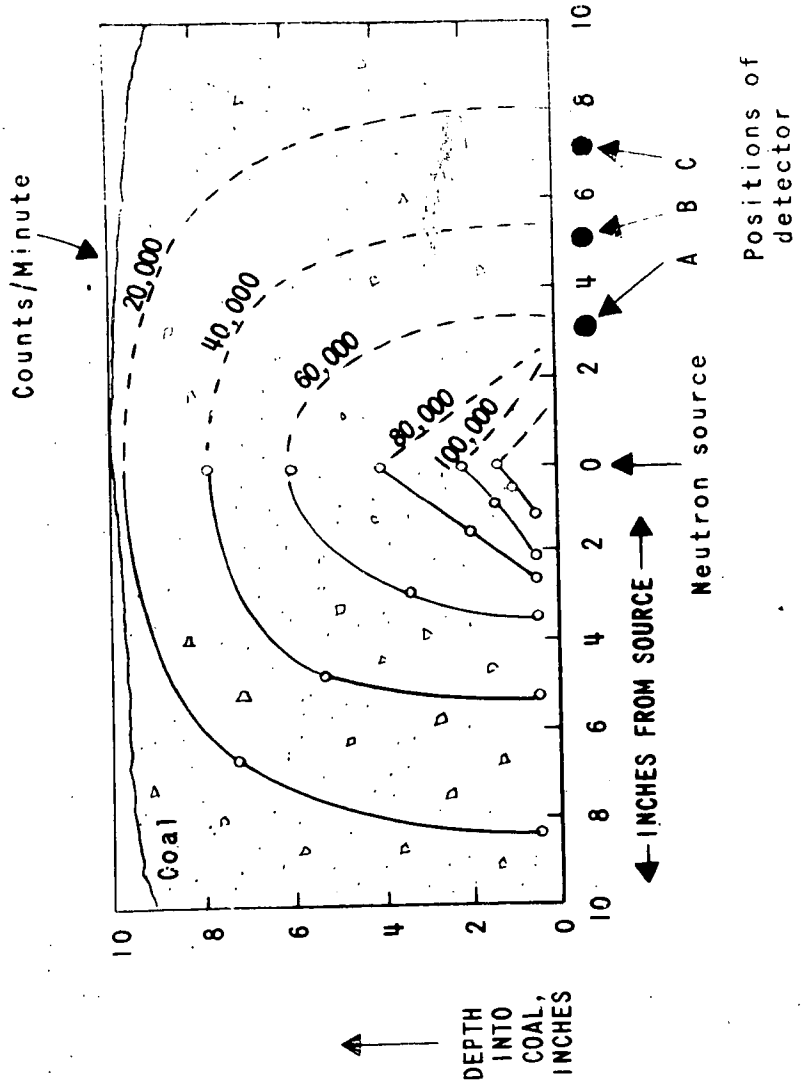

FIGURE 1 Cross Section of Tray of Coal Showing Distribution of Thermal Neutrons

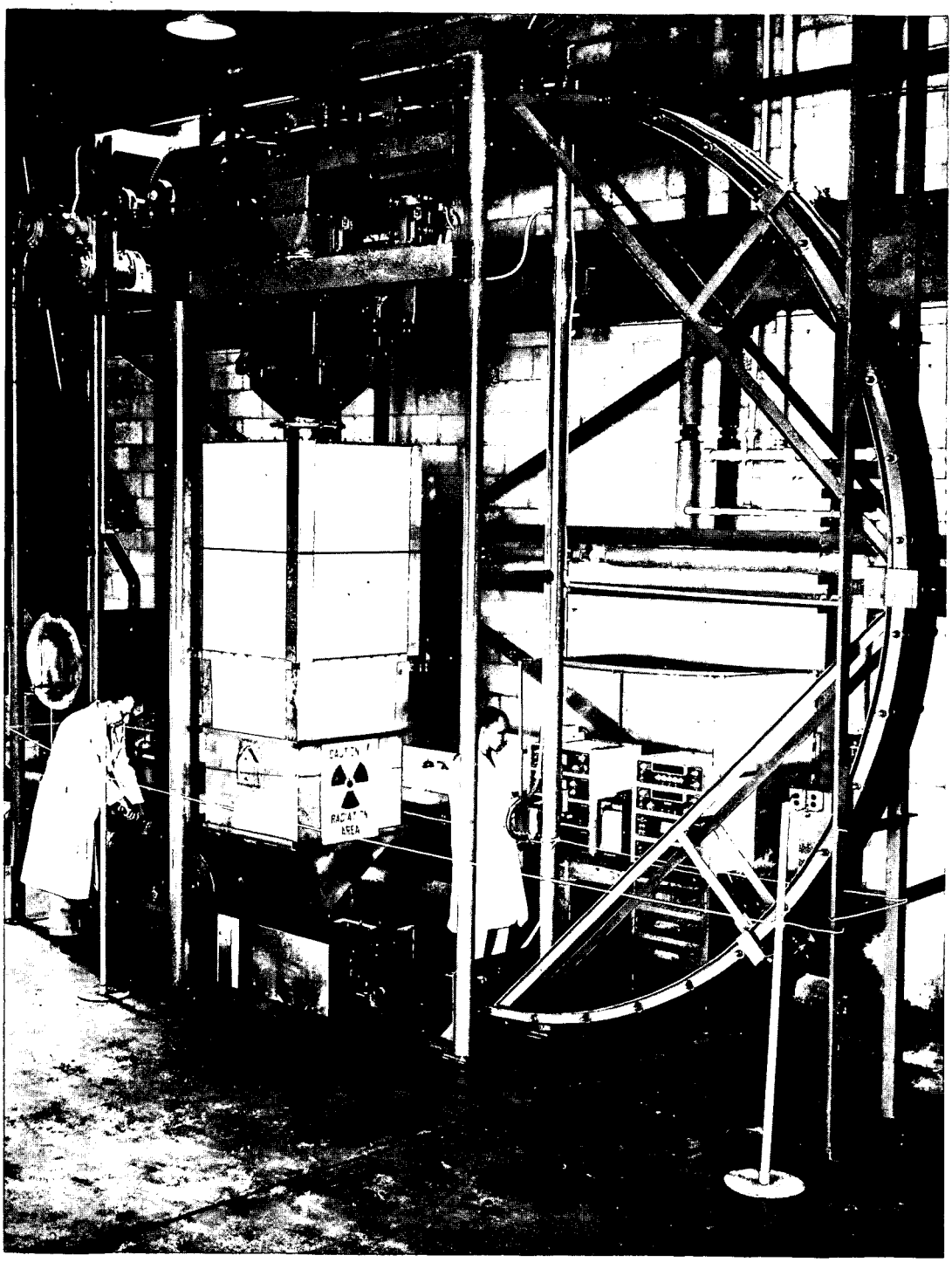

FIGURE 2-Pilot-Scale Equipment for Testing Continuous Moisture Meter for Coal

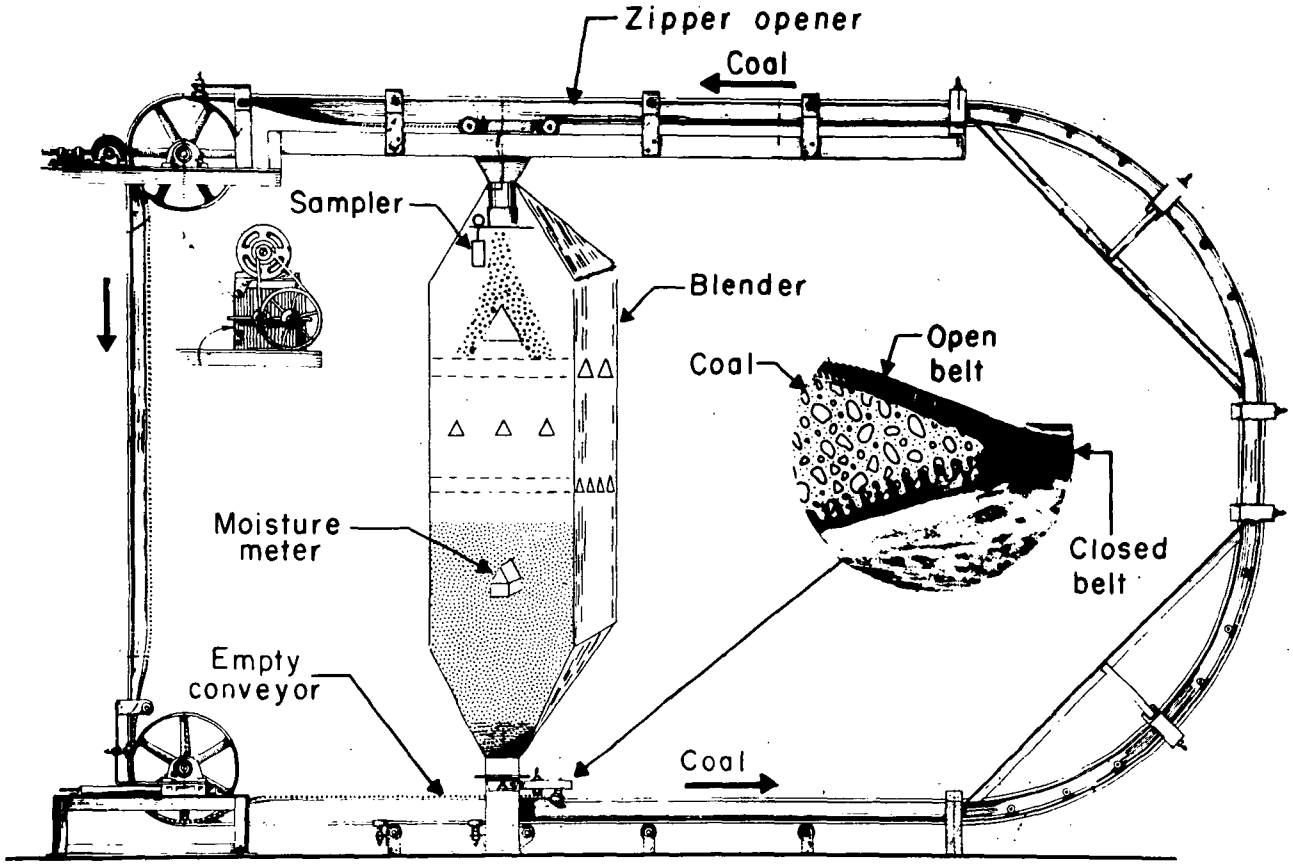

Fig. 3 - Zipper Conveyor - Elevator for Use With Moisture Meter

OCCURRENCE OF SULFUR IN ILLINOIS COALS

Harold J. Gluskoter and Jack A. Simon

Illinois State Geological Survey
Urbana, Illinois

Introduction

Sulfur in its several forms is prominent among the species of mineral matter known to occur in coal. Not only is its presence widespread but its effects may be very detrimental, particularly in specialized uses. The many problems associated with the presence of sulfur in coal include those involving air pollution, restrictions on amount of sulfur allowed in metallurgical coke, boiler corrosion and deposits, difficulties in mining, acid drainage from mines and spoil piles, and spontaneous combustion of coal.

Because of the recognition of the importance of sulfur in the utilization of coal, investigations concerning sulfur in coal have been pursued at the Illinois State Geological Survey since founding more than 50 years ago. This paper attempts to summarize the pertinent data concerning the occurrence of sulfur in Illinois Coals from this long term study. These data have been acquired by many members of the Survey staff.

Except when specifically stated to the contrary, all data discussed in this paper were obtained from analyses of face channel samples of coal. These samples were taken in the mines by Survey personnel following recommended United States Bureau of Mines methods of sampling, which provide for exclusion of mineral bands over 3/8 inch in thickness (Holmes, 1911).

Distribution of Sulfur Within Illinois Coals

It has long been recognized that sulfur occurs in coal in both inorganic and organic forms. It occurs inorganically as sulfides and sulfates, but the exact mode of occurrence of the organic sulfur is not known. Given and Wyss (1961) state that it is usually assumed that sulfur is in one of the following four forms:

1. mercapitan or thiol, RSH
2. sulfide or thio-ether, RSR'
3. disulfide, RSSR'
4. aromatic systems containing the thiophene ring,

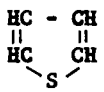

Free sulfur or native sulfur has been reported in coal (Yurovski, 1959; Berteloot, 1947). However, its occurrence is rare, and small enough an amount to be disregarded for most purposes. It has not been reported from Illinois coals.

Sulfate Sulfur. Sulfate sulfur is present in minor amounts in nearly all of the samples analysed. The sulfate sulfur values range from a high of 0.57 percent to a low of 0.00 percent. The mean, calculated from sulfate sulfur analyses of 300 face channel samples of Illinois coals is 0.071 percent and the mode, although not calculated, would be lower than the mean.

Organic Sulfur. Organic sulfur values ranged from a low of 0.27 percent to a high of 2.98 percent in Illinois coals sampled to date. The distribution of organic sulfur for all face channel sample analyses of No. 2 Coal, No. 5 Coal, No. 6 Coal and No. 7 Coal are given in the histograms on figure 1. None of the histograms have the shape of a normal distribution. The organic sulfur values of No. 2 Coal and No. 5 Coal are rather evenly distributed and are between 0.4 percent and 2.4 percent. It is probable that these diagrams would show a normal distribution if additional data were included. Too few analyses of samples from No. 7 Coal are available to draw any conclusions from the histogram. Organic sulfur from No. 6 Coal shows a distinct bimodal distribution with one peak between 0.2 and 0.8 percent and the second peak between 1.6 and 2.2 percent.

Pyritic Sulfur. The range in values of pyritic sulfur in face channel samples is even greater than the range in organic sulfur. The range is from a low value of 0.10 percent to normally high values of 4.5 percent to 5.0 percent with a few extreme values approaching 9.0 percent. Histogram depicting the distribution of the pyritic sulfur values for each of four coals are given in figure 2. The histogram of pyritic sulfur values in No. 5 Coal shows the most nearly normal distribution and that for No. 6 Coal shows a bimodal distribution. Again it must be emphasized that these data are obtained from face channel samples and any mineral bands in the coal, including iron sulfides, over 3/8 inch thick were excluded from the sample.

Total Sulfur and Relationship Between Pyritic and Organic Sulfur. Total sulfur in face channel samples ranges from low values of less than 0.5 percent to high values of 5.5 percent with a few extreme cases of nearly 10 percent. Sulfur in these few very-high-sulfur channel samples is predominantly pyritic.

Four graphs showing the relationships between organic and pyritic sulfur for four Illinois coals are given in figure 3. Each point on graphs 3a and 3b (No. 2 Coal and No. 7 Coal) represents sulfur values from a single face channel sample analysis, whereas each point on graphs 3c and 3d (No. 5 Coal and No. 6 Coal) represent average sulfur values for a single mine. Using mine averages rather than individual analyses does not alter the overall picture but does facilitate handling of the data.

Correlation coefficients for the four graphs vary considerably. The correlation is poor for Coal No. 5 (correlation coefficient .24) and non-existent for Coal No. 7 (correlation coefficient -.09). However, coals No. 2 and No. 6 do show a fairly good correlation between pyritic and organic sulfur (.76 for No. 6 Coal and .75 for No. 2 Coal). Both of these latter values demonstrate a high degree of significance, well over the 99.9 percent level. The rate of increase of pyritic sulfur with an increase in organic sulfur is much greater for No. 6 Coal than for No. 2 Coal. The one graph showing negative correlation (No. 7 Coal) is not statistically significant because of the small number of analyses.

Differing conclusions have been drawn by various workers as to the relation of pyritic to organic sulfur in coals. A number of researchers have reported such a correlation (Rose and Glenn, 1959; Leighton and Tomlinson, 1960; Wandless, 1959) whereas others have not observed the correlation in their studies (Yancy and Fraser, 1921; Brooks, 1956).

Discounting No. 7 Coal because of lack of sufficient data, the Illinois coals do show a positive correlation between organic and pyritic sulfur. This correlation is much better for No. 2 Coal and No. 6 Coal than for No. 5 Coal.

The fact that a correlation does exist, suggests that in a coal-forming-swamp environment which was relatively high in sulfur, the sulfur contribution to the plants would be high and that sulfur in the environment also would be available for the formation of pyrite during the early stages of peat formation. The correlation exists even though much secondary inorganic pyritic sulfur has been added to the coal as veins and deposits along fractures which occurred subsequent to the peat formation and possibly very late in the history of the coal bed. It is also conceivalbe that much of the late secondary pyrite may represent a reorganization of the sulfur that was introduced into the environment at a very early stage of coal formation.

The bimodal distribution of both pyritic sulfur and organic sulfur shown in figures 1 and 2 also might suggest a close correlation between the two forms. However, the low sulfur coals in Illinois have been mined extensively and therefore have also been of much interest to the Survey and have been sampled heavily. The low sulfur peaks in the bimodal distribution may simply represent preferential sampling.

Mineralogical Occurrence of Sulfur

Sulfate Sulfur. The small amount of sulfate sulfur that occurs in nearly every face channel sample of Illinois coal is contained primarily within the mineral gypsum ($CaSO_4 \cdot 2H_2O$) which occurs as a secondary vein and cleat filling.

The amount of sulfate sulfur increases rapidly upon weathering of the coal as the oxidation of pyrite (FeS_2) gives rise to ferrous and ferric sulfates. The following minerals have been identified from samples collected in deep mines from old mined-out areas and from samples of coal which have weathered from exposure at the surface either in outcrop, mine dumps, or in the laboratory:

Rozenite	$FeSO_4 \cdot 4H_2O$
Melanterite	$FeSO_4 \cdot 7H_2O$
Coquimbite	$Fe_2(SO_4)_3 \cdot 9H_2O$
Roemerite	$FeSO_4 \cdot Fe_2(SO_4)_3 \cdot 12H_2O$
Jarosite	possibly the hydronium jarosite (carphosiderite) $3Fe_2O_3 \cdot 4SO_4 \cdot 7H_2O$

More than one of these phases often occur in a single sample. It is also difficult to know exactly which phases occur in the mines since melanterite ($FeSO_4 \cdot 7H_2O$) dehydrates to rozenite ($FeSO_4 \cdot 4H_2O$) and then to szomolnokite ($FeSO_4 \cdot H_2O$) in the

laboratory. The dehydration is very rapid; occurring in a few minutes time in the case of melanterite ⟶ rozenite.

Pyritic Sulfur. Iron disulfide can occur as either pyrite which forms in the isometric crystal system or as marcasite which is orthorhombic. Pyrite is the most commonly reported dimorph although marcasite is often mentioned as occurring in lesser ammounts. Marcasite has only rarely been reported in Illinois coals and pyrite is apparently the dominant sulfide.

The macroscopic forms of pyrite in coal were systematically described by Yancy and Fraser (1921). A summary of their description follows: 1) fine pyrite, as small disseminated particles or thin film-like coating on joint planes (cleat) or along the bedding; 2) lenses, from 1 to 2 inches long and a fraction of an inch thick to those 3 or 4 feet thick and hundreds of feet long; 3) nodules, roughly spherical in shape, may also be either inches or several feet in diameter; 4) beds or continuous bands of pyrite, often may include coal or bony coal and/or may be intimately associated with argillaceous sediments.

The finely disseminated pyrite grades downward in size to the microscopic forms of the mineral. Microscopic pyrite is very widespread in coal and has been observed in all coal macerals except massive micrinite. A complete range from euhedral crystals to irregular anhedral aggregates may be observed microscopically in Illinois coals (J. A. Harrison, personal communication). Observations similar to those preceeding were made for the Pittsburgh coal by Gray, Schapiro and Coe (1963).

Sulfur in the Banded Ingredients of Coal

A study was made by Survey personnel into the distribution of the forms of sulfur in the megascopically distinguishable banded ingredients (Cady, 1935a). The banded ingredients sampled were vitrain, clarain and fusain. Durain or dull splint coal is very rare in Illinois coals and none was sampled. Figure 5 summarizes the sulfur analyses of approximately 100 samples of banded ingredients.

In general the pyritic sulfur content is greater in the fusain than in the other bands, although it does show a wide range in the different fusain samples. This is due to the degree to which the cavities in the fusain are filled with pyrite. Vitrain and clarain have a higher organic to pyritic ratio with ratios generally greater than one. The organic sulfur content of vitrain is usually lower than of clarain from the same coal. The preceeding generalizations not withstanding, Cady (1935a) concluded that the variations in organic sulfur content of Illinois coals cannot be ascribed only to variation in relative amounts of banded ingredients.

Occurrence of Low-Sulfur Coal in Illinois

There are three known areas in the state where there has been significant production of low-sulfur coal, most of which contain less than 1.5 percent sulfur. These areas, outlined in figure 6, are highly generalized and are subject to appreciable modification.

The largest of the three low-sulfur areas, and the most important on the basis of tonnage of coal produced, is in No. 6 Coal in Franklin County and

adjacent portions of Jefferson County to the north and Williamson County to the south and is similar to the area reported by Cady (1919). The delineation of the low sulfur area has been based on the following information:

1) Data from the files of the Illinois State Geological Survey on face channel samples of mines, most of which have been published by Cady (1935b, 1948).
2) Evaluation of a few miscellaneous coal samples from mines in the general area and from diamond drill core analyses.
3) Interpretation of drill logs based on character of overlying strata.

Utilization of the data in 1) and 2) above is self-explanatory, but 3) should be more fully explained. The interpretation of drill logs is based on the observation that in this general area where No. 6 Coal has a thick gray shale overlying the coal, the sulfur content is relatively low. Conversely, where the black "slaty" shale and marine limestone lie close to the top of the coal, the sulfur content is substantially higher. This association of high sulfur coal and overlying marine beds has also been reported for Russian and British coals (Yurovski, Mangubi, and Zyman, 1940; Wandless, 1959; Williams and Cawley, 1963).

The low sulfur area in Franklin, Williamson and Jefferson Counties is outlined primarily by analyses of mine samples. However, details of the configuration of the "low-sulfur" line are based on interpretations of drill hole logs of variable quality including electric logs of oil test holes. The presence of more than 20 feet of gray shale immediately above the coal has been used as indicating low sulfur content and less than 10 feet between the coal and the overlying black shale and limestone as indicating higher sulfur area. Intermediate thicknesses of gray shale have been variously interpreted depending in large measure on the geographic relationship of such datum points.

All of the low sulfur lines on the map indicate areas in which the sulfur content is believed to average 2 percent or less. The analytical data within the Franklin-Williamson-Jefferson Counties area indicate that most of the area outlined contains coal with less than 1.5 percent sulfur (as received basis, face channel sample), and a substantial part of the area has included coal, now largely mined, which averaged less than 1 percent sulfur.

In the western part of this low-sulfur area there is a portion mapped as containing "split coal." The split consists of beds of shale and siltstone interbedded between coal benches. It is believed that most of the coal in the "split-coal" area is probably of low-sulfur content. As shown on the map (fig. 6), the low sulfur area extends locally a relatively short distance west of the "split coal" area.

A second important area of low-sulfur coal occurs in the Harrisburg (No. 5) Coal in Saline County. Coal with less than 1 percent sulfur has been mined in this area and there is a substantial area in which the coal probably averages less than 2.5 percent sulfur as shown in Figure 7. This area is much less well defined than the previously described low-sulfur area of No. 6 Coal because much less data concerning it are available.

A third substantial area of low-sulfur No. 6 Coal lies in parts of Madison and St. Clair Counties in the vicinity of Troy, Illinois, and is shown

in figure 6. Although less is known of this area than the areas described previously, there is perhaps up to 70 square miles of coal with a sulfur content less than 1.5 percent. Analyses of face channel samples from one mine which operated in this low-sulfur area, reported by Cady (1948), showed the coal to average less than 1 percent sulfur.

Vertical and Lateral Distribution of Varieties of Sulfur

The variations in both pyritic and organic sulfur in the individual coal seams are very large when considering the state as a whole, as can be seen from figures 1 and 2. There have been, however, differences of opinion as to the amount of local variation which exists in the organic sulfur content. There are no such differences of opinion concerning the pyritic sulfur distribution inasmuch as extremely localized concentrations of secondary pyrite are common.

Cady (1935a, p. 30, 31) observed, "Local variation in organic sulfur is rarely more than 1 percent..." "...and generally not more than 0.5 percent irrespective of the locality.", and "...the organic sulfur is the best index of the sulfur content and the organic sulfur content is regionally consistent for each coal bed." Yancy and Fraser (1921) studied extensively the variations in varieties of sulfur both vertically and laterally within a single mine in southern Illinois. Concerning the lateral variation in organic sulfur they concluded that uniformity in organic sulfur distribution is confined to very limited areas in the coal seam (Yancy and Fraser, 1921). They found this variation to be large within a single mine, although not as large as variations in pyritic sulfur. Within the mine studied, the organic sulfur in the face channel samples (No. 6 Coal) ranged from .69 to 1.90 percent and the pyritic sulfur from .66 to 3.17 percent. It has been suggested (Cady, 1935a, p. 31) that the wide range in organic sulfur observed by Yancy and Fraser (1921) may be attributable in some way to the location of the sampled mine on the margin of the area of low sulfur coal in Franklin County.

Yancy and Fraser (1921) also analyzed individual benches of face channel samples for varieties of sulfur. They took 12 face channel samples from a mine in southern Illinois, six samples from a mine in west Kentucky in No. 7 Coal, and two samples from a mine in Kentucky No. 8 Coal. The organic sulfur content was relatively uniform between benches of the individual face channel samples. The greatest variation in any single section was a minimum of 0.57 percent and a maximum of 1.25 percent. Most of the benches in a single face channel had an organic sulfur content within 25 percent of each other.

The vertical variation in pyritic sulfur was found to be very large between different benches in the same face channel sample, ranging, in two instances, from 0.81 percent to 5.54 percent and from 0.02 percent to 2.09 percent. Yancy and Fraser (1921) reported that in nearly every section (face channel sample) the pyritic sulfur, and thereby also the total sulfur, were much higher in uppermost and lowermost benches. This conclusion was found to be true for their samples of Illinois No. 6 Coal and for the Kentucky No. 7 Coal. The two samples of the Kentucky No. 8 Coal had the highest pyritic sulfur in the lowest benches but the uppermost benches were relatively low in sulfur. Wandless (1959) in a general discussion of the occurrence of sulfur in British coals reached conclusions which support Yancy and Fraser in recognizing the concentration of pyrite at the top

and bottom of the coal and also in the rather uniform organic sulfur composition in a single section. However, Wandless' (1959) observation that organic sulfur is uniform over a wide area in a single seam is in better agreement with the similar observation for Illinois coals by Cady (1935a).

Further studies on the varieties of sulfur and their vertical and lateral variation are in progress. Preliminary results suggest that a concentration of pyritic sulfur at the top and bottom of the coal tends to occur in No. 6 Coal samples obtained from southern Illinois, and that the vertical distribution of organic sulfur within these coals is relatively uniform. Further data will allow more definite conclusions to be drawn concerning the local variation laterally in organic sulfur.

Wandless (1959) in a review article on sulfur in British coals stated an admonition with which we heartily concur. Concerning conclusions drawn from chemical analyses of sulfur in coal he wrote, (Wandless, 1959, p. 259) "Unfortunately the number of exceptions to these generalizations is sufficient to render them non-specific in individual cases. Here, as elsewhere, the examination of very large numbers of samples provides a graveyard for promising generalizations; nevertheless, the trends noted are interesting and can, with proper caution, prove useful on occasion."

REFERENCES

Berteloot, J., 1947, Presence of native sulfur in coal. Variations in the sulfur content from top to bottom of a coal seam: Ann. Soc. Geol. Nord., v. 67, p. 195-206; Chem. Abstr. v. 44, 818.

Brooks, J. D., 1956, Organic sulfur in coal: Jour. Inst. Fuel, v. 29, p. 82-85.

Cady, G. H., 1919, Mines producing low-sulfur coal in the central district: Illinois State Geol. Survey, Illinois Mining Investigations Bull. 23, 14 p.

Cady, G. H., 1935a, Distribution of sulfur in Illinois coals and its geological implications: Illinois Geol. Survey Report of Investigations 35, p. 25-41.

Cady, G. H., 1935b, Classification and selection of Illinois coals: Illinois Geol. Survey Bull. 62, 354 p.

Cady, G. H., 1948, Analysis of Illinois coals: Illinois Geol. Survey, Supplement to Bull. 62, 77 p.

Given, P. H., and Wyss, W. F., 1961, The chemistry of sulphur in coal: British Coal Util. Res. Assoc. Monthly Bull., v. 25, p. 165-179.

Gray, R. J., Schapiro, N., and Coe, G. Dale, 1963, Distribution and forms of sulfur in a high volatile Pittsburgh seam coal: Transactions, Soc. Mining Engnrs., American Inst. Mining Engnrs., v. 226, p. 113-121.

Holmes, J. A., 1911, The sampling of coal in the mine: United States Bur. Mines Tech. Pap. No. 1, 22 p.

Leighton, L. H., and Tomlinson, R. C., 1960, Estimation of the volatile matter of pure coal substance: Fuel, v. 39, p. 133-140.

Rose, H. J., and Glenn, R. A., 1959, Coal cleaning in relation to sulfur reduction in steam coals: Mech. Engng. v. 81, No. 2, p. 104 (abstract).

Wandless, A. M., 1959, The occurrence of sulfur in British coals: Jour. Inst. Fuel, v. 32, p. 258-266.

Williams, F. A., and Cawley, C. M., 1963, Impurities in coal and petroleum: in Johnson, H. R., and Littler, D. J., The Mechanism of corrosion by fuel impurities: London, Butterworths, 660 p.

Yancy, H. F., and Fraser, T., 1921, The distribution of the forms of sulfur in the coal bed: Univ. of Illinois Eng. Exp. Station Bull. No. 125, 94 p.

Yurovski, A. Z., 1959, Basis of the theory of the origin of sulfur in coal: Proc. Symp. on Nature of Coal, Central Fuel Res. Inst. Jealgora, India, p. 51-55.

Yurovski, A. Z., Mangubi, B. V., and Zyman, S. N., 1940, The origin of gray pyrite in coal: Coke and Chem. (USSR), No. 4-5, p. 7-9. Chem. Abstr. v. 37, 1107.

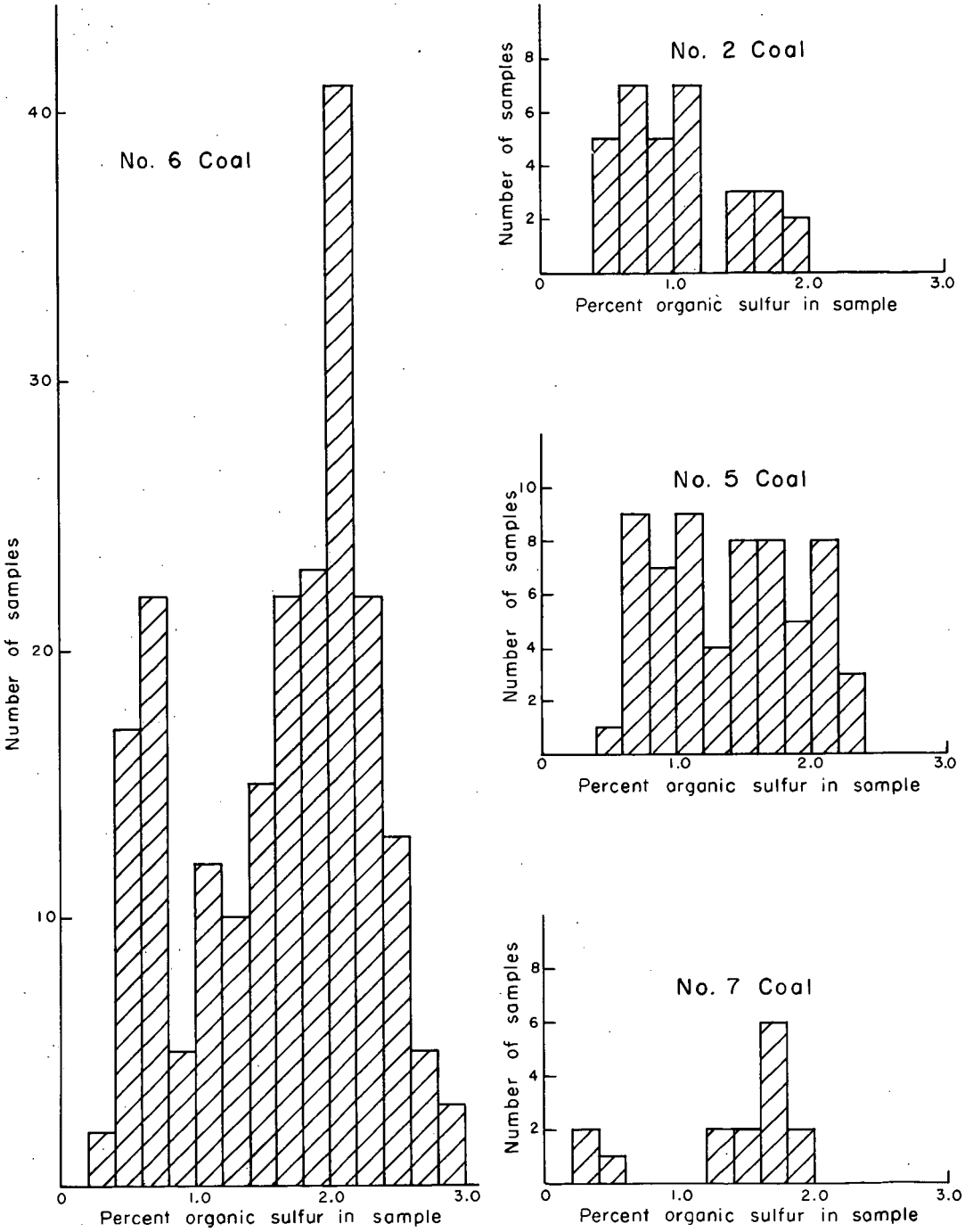

Fig. 1 - Organic Sulfur - Distribution in Illinois Coals

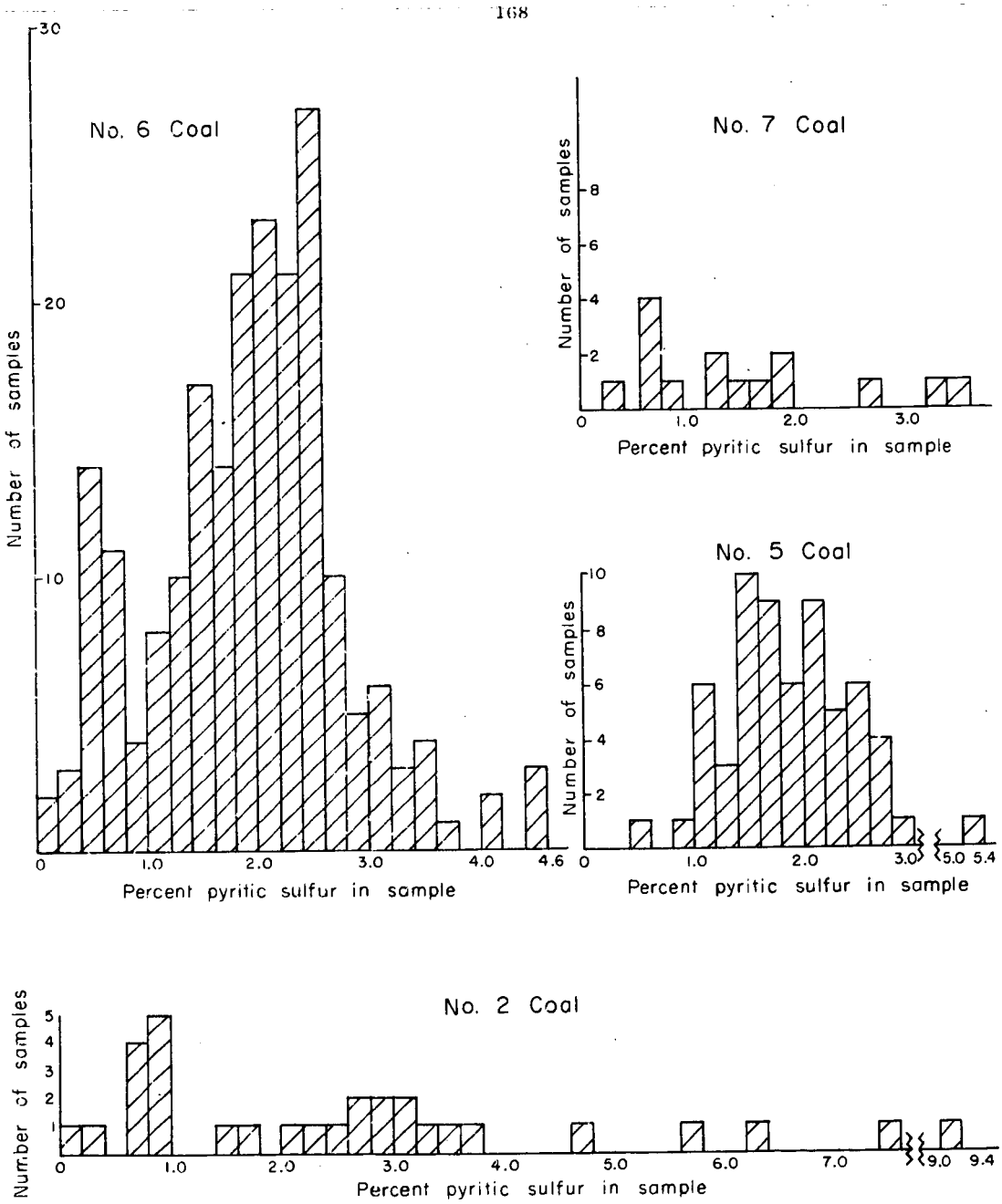

Fig. 2 - Pyritic Sulfur - Distribution in Illinois Coals

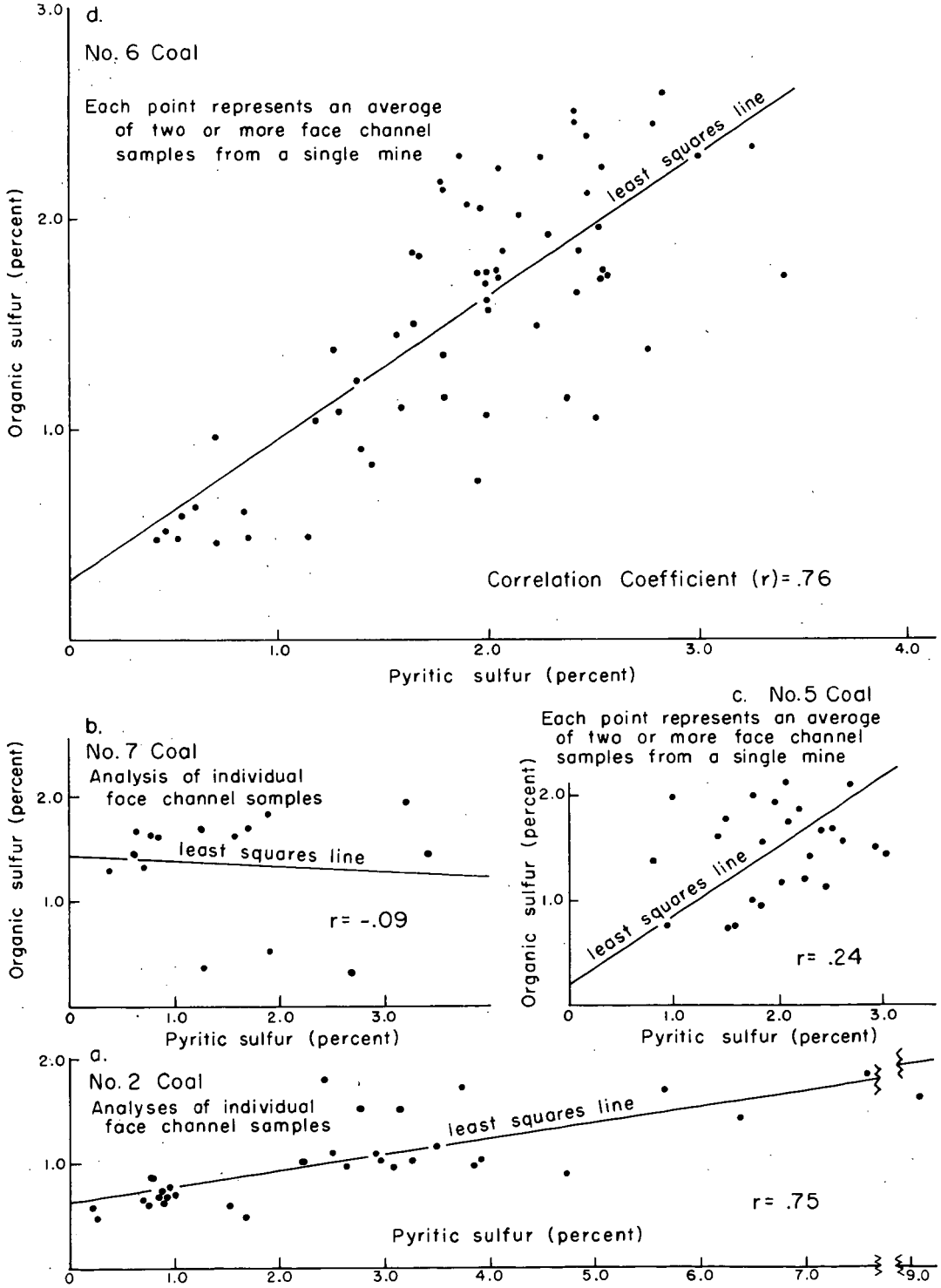

Fig. 3- Pyritic Sulfur-Organic Sulfur Relationships in Face Channel Samples of Illinois Coals

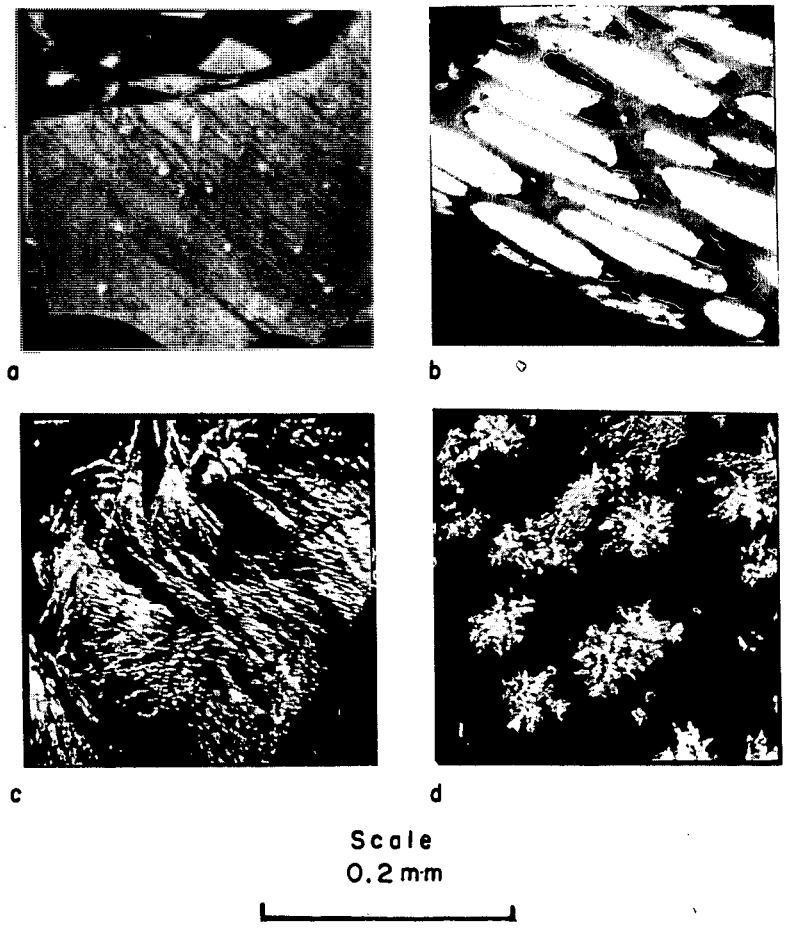

Figure 4. Microscopic pyrite in coal. All photomicrographs are of samples of No. 6 Coal taken in reflected light.

a. Discrete grains in vitrinite
b. Cavity fillings in fusinite
c. Crystalline "fiber-bundles" in vitrinite
d. Crystalline aggregates in vitrinite

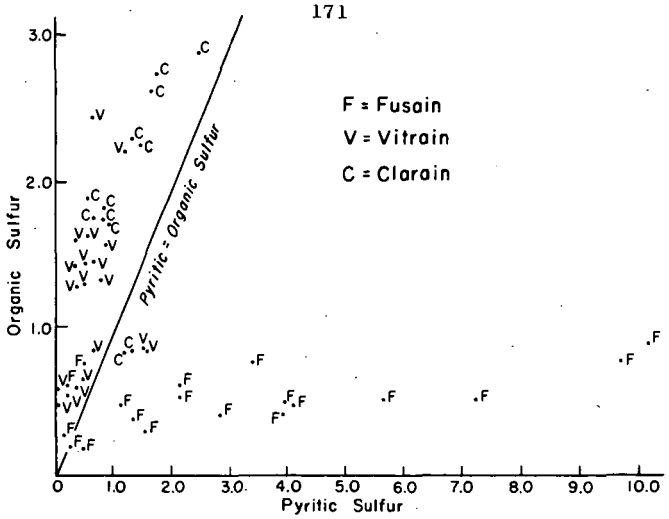

Figure 5 — Pyritic and Organic Sulfur content of Banded Ingredients modified from Cady (1935a, p. 34)

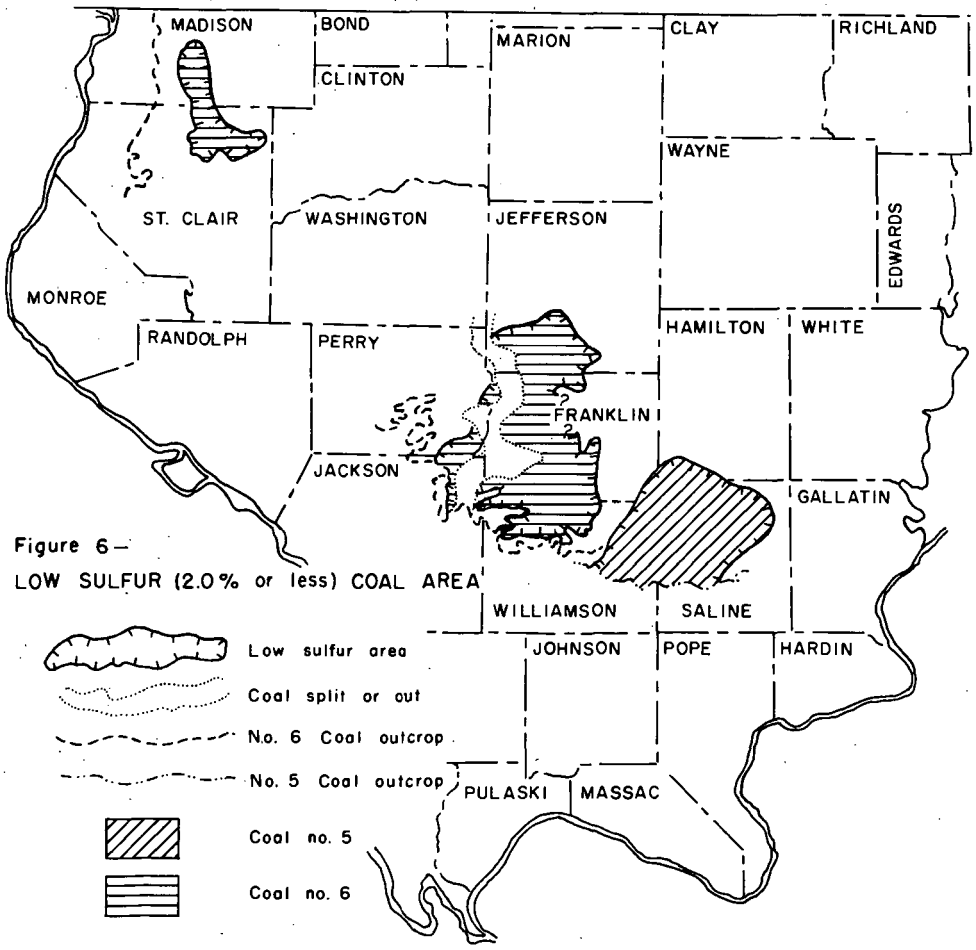

Figure 6 —
LOW SULFUR (2.0% or less) COAL AREA

SCANDIUM IN AUSTRALIAN COALS AND RELATED MATERIALS

D.J. Swaine

Division of Coal Research
Commonwealth Scientific and Industrial Research Organization
P.O. Box 175, Chatswood, New South Wales, Australia

INTRODUCTION

There is a continued interest in the general chemistry of scandium and in special properties of the metal and its compounds. For example, ferrites containing a small amount of scandium have been used as solid state devices in electronics, and the properties of alloy systems of scandium are being investigated in various laboratories. The metal has a high melting point and a low density. The atomic radius of Sc^{3+} is smaller than that of yttrium and the lanthanide ions, which means that it is not commonly associated with the lanthanide elements, but rather with elements such as iron (as Fe^{2+}). Scandium forms complexes readily.

Despite its widespread occurrence in rocks and minerals, only two definite minerals of scandium have been reported, namely thortveitite $(Sc,Y)_2.2SiO_2$ and sterrettite $ScPO_4.2H_2O$. The scarcity of these and other minerals containing more than 0.1-0.5% Sc has led to interest in sources of scandium, amongst which coal ash, with its wide variety of inorganic constituents, often enriched relative to common rocks and sediments, would seem to be a possibility. The first determinations of scandium in coal were probably those carried out by Goldschmidt and Peters (1), who found 3-300 p.p.m. Sc in 14 samples of ash from bituminous and brown coals (0.1-8 p.p.m. on a coal basis). Deul and Annell (2) found <1 to 100-1000 p.p.m. Sc, with most values between 10 and 100 p.p.m., in 319 samples of low-rank coals from the U.S.A. As part of a general survey of diverse possible sources of scandium in the U.S.A., Ross and Rosenbaum (3) analysed 13 coal-ash samples; these contained 10-30 p.p.m. Sc. The present paper gives the results of an extensive survey of Australian coals and related materials for scandium.

SCANDIUM IN COALS AND VITRAINS

General information on the coal samples is given in Table 1, and the geographical locations of the coalfields are shown in Fig. 1. Details of the emission spectrographic method of analysis are given in the Appendix. It is clear from the results for coals from the Sydney Basin (Table 1) that the overall assessment of the scandium status given by clean-coal composites differs little from that given by whole-seam composites or subsection samples. Hence, later determinations were usually carried out on clean-coal composites. These results showed that there was a fairly constant concentration (mean 2-4 p.p.m.) in the N.S.W. and Queensland Permian coals. However, slightly higher values were found for the Rosewood-Walloon coals (mean 7 p.p.m.) and the highest values were found for the West Moreton coals (mean 15 p.p.m.). These trends were also apparent in the vitrains (Table 2) which had been separated by flotation, usually at a specific gravity of about 1.3, from samples of most of the seams referred to in Table 1.

Most of the coal ashes had scandium contents close to the clarke (i.e. the mean abundance of scandium in the earth's crust), which has recently been reassessed (4) as 30 p.p.m. Sc, the main exceptions being some of the Queensland coals. However, apart from the Latrobe Valley brown coals, in which scandium was not detected, the concentrations in most of the coal ashes exceeded the mean content of 10 p.p.m. Sc in sedimentary

rocks (5) and that of 8 p.p.m. Sc for subsoils (6). Shale bands associated with coals in the Sydney Basin had < 3-16, with a mean of 7 p.p.m. Sc. The ashes of the vitrains generally showed distinct enrichment relative to the earth's crust or sedimentary rocks, and the enrichment factors for the former (i.e. the ratio of mean content to the clarke) varied from about 1.5 to 10. The maximum content of 600 p.p.m. Sc (i.e. 0.09% Sc_2O_3), which was found in samples from three seams in the West Moreton coalfield, exceeded the highest reported value in coal ash of 300 p.p.m. Sc (1).

MODE OF OCCURRENCE OF SCANDIUM

The fact that there is a fairly high concentration of scandium in the vitrains, which contain only traces of clay and other minerals present in the bulk coal, suggests that part of the scandium in the coal is organically bound. Experiments were carried out on six samples of coals from the Sydney Basin in order to ascertain the extent and variability of this association with the coal substance. Each sample was demineralized by treatment with acids to reduce the ash yield to about 1% or less (7). Scandium was determined in the coal before and after demineralization and calculations showed that between 40 and 95% of the scandium in the original coal was organically bound to the coal substance.

As there was also some scandium associated with the mineral matter in the coals, it was decided to ascertain the scandium content of minerals or mineral-rich materials which had been separated from certain coal seams. As will be seen from Table 3, scandium was detected in some siderites, kaolinites and calcites, albeit in low concentrations. On the basis of its atomic radius (0.8Å) scandium may be expected to be able to replace several cations - for example, Fe^{2+}, Mg^{2+}, Mn^{2+}, Zr^{4+}, Sn^{4+}. The most common host minerals for Sc^{3+} are those high in Fe^{2+} - for example, pyroxenes and biotite - although it is not clear how the substitution is effected, depending as it does on a secondary replacement or rearrangement to balance the otherwise excess positive charge. The presence of scandium in some of the siderites may be the result of a Sc^{3+}-Fe^{2+} replacement. The association of scandium with a limestone, possibly replacing Ca^{2+} (8), may be relevant to the detection of scandium in some of the calcites, where a similar replacement may have occurred. As scandium is unlikely to be substituted in lattice positions or interstitially in kaolinite, its presence in the latter is probably due to adsorption. So far, it has not been possible to separate an apatite from Australian coals, but a subsection sample of a Burrum coal, known to be high in phosphorus present as fluorapatite, contained a lower concentration of scandium than the clean-coal composite of which it was a part. Hence in this case there was no enrichment of scandium as phosphate.

SCANDIUM IN COKE, BOILER DEPOSITS AND FLY-ASH

The results in Table 4 show that scandium, unlike several other trace elements in Australian coals, is not enriched in boiler deposits (9). The concentrations in coke and fly-ash are much the same as in coal ash. As expected, the Queensland cokes had higher scandium contents than those made from N.S.W. coals.

DISCUSSION

The results for scandium in Australian coals indicated a trend from the Latrobe Valley brown coals, in which this element was not detected (i.e. < 0.5 p.p.m.), to the West Moreton bituminous coals with a mean content of 15 p.p.m. Although the latter coals are Triassic, so is Callide coal, which is low in scandium, and, if the one vitrain sample is a guide, then Leigh Creek coals, which are also Triassic, will have similar scandium contents to the N.S.W. and Queensland Permian coals (mean 2-4 p.p.m.). Hence, age is probably not the factor relevant to increase in scandium concentration. It is more likely that the high scandium contents in the West Moreton coals were brought about by adsorption from solutions emanating from source rocks, especially those of

igneous origin, which were able to supply a higher concentration of scandium than was available in other areas. The trivalent scandium ion is readily adsorbed and its small radius and high charge should favour the formation of stable organic complexes, effecting the removal of Sc^{3+} from percolating solutions and its fixation in the coal substance. Although the relative amounts of organically bound scandium vary, there are no minerals associated with Australian coals that are greatly enriched. Some siderites, kaolinites and, to a lesser extent, calcites, showed low scandium contents, and these are the constituents of the mineral matter in coal which contribute scandium. As in the earth's crust, scandium is ubiquitous in Australian coals.

Results for a range of boiler deposits formed during the burning of bituminous and hard brown coals either by grate or pulverized-fuel firing, showed that no enrichment of scandium had occurred. From the point of view of possible use as a source of scandium, the ash from certain coals and vitrains from the West Moreton coalfield merits some consideration. It is difficult to ascertain the present price of scandium, but in 1962 it was quoted as $2700 per pound of 99% pure Sc_2O_3 (3). However, the desirability of further production of scandium, either from a low-grade, by-product source by solvent extraction (10) or from a higher-grade material, rests on the value assigned to its compounds and alloys in modern technology.

REFERENCES

(1) Goldschmidt, V.M. and Peters, Cl. Nachr. Ges. Wiss. Göttingen, Math.-phys. Kl., Fach. 4, No.40, 371 (1933).

(2) Deul, M. and Annell, C.S. Bull. U.S. Geol. Surv., No.1036-H (1956).

(3) Ross, J.R. and Rosenbaum, J.B. Rept. Invest. U.S. Bur. Mines, No.6064 (1962).

(4) Fryklund, V.C.Jr. and Fleischer, M. Geochim. et Cosmoch. Acta, 27, 643 (1963).

(5) Vinogradov, A.P. Geochemistry (English Translation) No.7, 641 (1962).

(6) Swaine, D.J. Tech. Commun. Bur. Soil Sci., Harpenden, No.48 (1955).

(7) Brown, H.R., Durie, R.A. and Schafer, H.N.S. Fuel, Lond., 38, 295 (1959).

(8) Clark, Marie, C. and Swaine, D.J. Geochim. et Cosmoch. Acta, 27. 1139 (1963).

(9) Brown, H.R. and Swaine, D.J. J. Inst. Fuel, (in press).

(10) Canning, R.G. Aust. Inst. Min. Met., Proc. No.198, 113 (1961).

APPENDIX. METHOD OF ANALYSIS

Gravimetric and spectrophotometric methods, often after separation of a scandium-rich fraction by solvent extraction, cation exchange or paper chromatography, have been reported frequently in the recent literature from the U.S.A., Japan and Russia. However, since satisfactory chemical methods for scandium are usually long and involved, more direct methods, such as neutron activation, X-ray spectrography and emission spectrography, are preferable. For a survey of diverse materials varying widely in scandium content, emission spectrography is well suited, and was used in this investigation.

Samples which were mainly carbonaceous, for example coals and vitrains, were ashed at 800°C prior to analysis, while low-carbon materials, such as boiler deposits and fly-ash, were not ashed. Samples should be about 100 B.S. mesh or less. Two spectrographic techniques were used, brief details of each being as follows:

(i) When sufficient sample was available, 20 mg, for example, of coal ash was mixed with 20 mg of graphite powder in a small vibratory ball mill, and the mixture was filled into a graphite electrode of the type undercut below the cup to increase the temperature

and thereby assist volatilization. Anode excitation was used in a 9-amp. d.c. arc, with a 4.5-mm arc gap and an exposure time of 2.5-3 min (total burn). A Hilger Automatic Large Quartz (E492) spectrograph was used and the spectra were photographed on Ilford N.50 (Thin Film Half Tone) plates. The final semi-quantitative estimations were made by visual comparison with standard spectrograms. Standards were prepared in a synthetic matrix of similar major-element composition to the samples. The analysis lines used were the ion line at 2552.36Å and the atom line at 3269.90Å. The former line is singularly free from interference, apart from platinum which is rarely found, and the latter line can be used in the presence of up to 20% iron and/or 1% zirconium without interference. Each of these lines had a detectability of 10 p.p.m. Sc. The synthetic standards were checked by using them to determine scandium in the synthetic rock sample W-1 (U.S. Geological Survey). The value of 40 p.p.m. Sc obtained is close to most of the values reported; of the 20 values listed by Fryklund and Fleischer (4), 17 were in the range 25-70, with a mean of 40 p.p.m. Sc.

(ii) When only 1-3 mg of sample was available - for example, in the case of some minerals removed from coals - a microspectrographic method was used. The sample was mixed with lithium tetraborate plus graphite powder (usually 2+3+5 mg respectively), and filled into a small graphite electrode. The arcing procedure was the same as before. New standards were prepared, and the detectability was 20 p.p.m. for Sc 2552 and 40 p.p.m. for Sc 3269.

For the determination of scandium in minerals separated from coal (for example, pyrite, siderite and calcite) separate tests were carried out to ascertain the suitability or otherwise of the standards, and corrections were made, if necessary. The standard Sulphide Ore-1 (Canadian Association of Applied Spectroscopy) was found to contain ~20 p.p.m. Sc compared with the recommended value of 25 p.p.m.

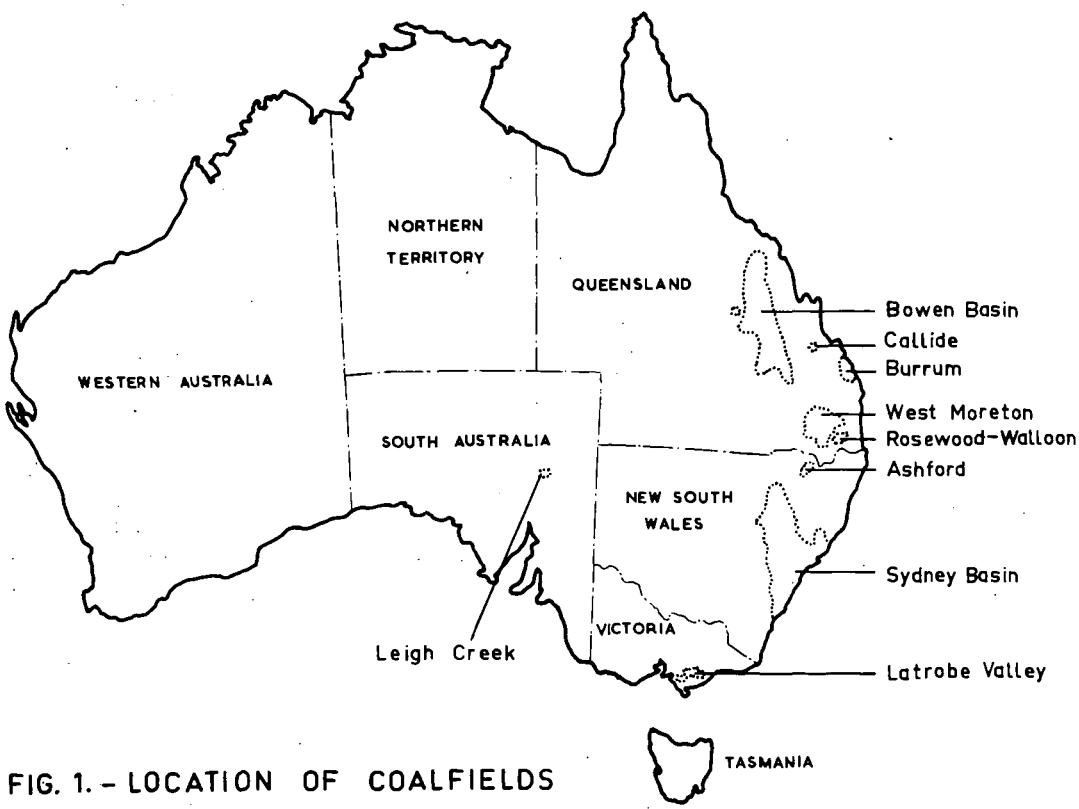

FIG. 1. - LOCATION OF COALFIELDS

TABLE 1. CONTENT OF SCANDIUM IN AUSTRALIAN COALS

Coalfield	Geological Age	No. of Seams Sampled	No. of Samples	p.p.m. Sc			
				On Ash Basis		On Air-dried Basis	
				Range of Values	Mean	Range of Values	Mean
QUEENSLAND (bituminous)							
Callide	Triassic	1	1	-	30	-	4
West Moreton	Triassic	12	24	30-150	60	7-30	15
Rosewood-Walloon	Jurassic	2	7	25-40	35	5-8	7
Burrum	Cretaceous	1	1	-	30	-	3
Bowen Basin	Permian	10	12	10-50	30	1.5-6	3
NEW SOUTH WALES (bituminous)							
Ashford	Permian	1	1	-	20	-	2
Sydney Basin	Permian	20	88	<10-40	20	<0.4-6	2.5
(coal subsection samples)		20	282	<10-100	20	<0.3-10	2.5
(whole-seam composites)		20	26	≤10-40	20	≤1-6	2.5
VICTORIA (soft brown)							
Latrobe Valley (low ash, i.e.< 5%)	Tertiary	2	22	-	<10	-	<0.5
SOUTH AUSTRALIA (hard brown)							
Leigh Creek	Triassic	3	37	*	-	-	-

Note. The above results refer to clean-coal composites, except where otherwise stated.

* Detected in 36 samples, but standards were not available for semi-quantitative estimation.

TABLE 2. CONTENT OF SCANDIUM IN VITRAINS

Coalfield	No. of Samples	p.p.m. Sc			
		On Ash Basis		On Air-dried Basis	
		Range of Values	Mean	Range of Values	Mean
QUEENSLAND					
Callide	1	-	150	-	2.5
West Moreton	27	100-600	350	4-20	10
Rosewood-Walloon	11	60-300	150	2-10	6
Bowen Basin	6	100-150	120	1.5-3	2
NEW SOUTH WALES					
Sydney Basin	20	30-250	100	0.9-7	2.5
SOUTH AUSTRALIA					
Leigh Creek	1	-	40	-	4

TABLE 3. SCANDIUM IN MINERALS OR MINERAL-RICH SAMPLES SEPARATED FROM COALS

Main Constituent	No. of Samples	Brief Details of Samples	p.p.m. Sc
Pyrite	6	4 from Queensland and N.S.W. coals; 2 from Leigh Creek coal	< 20
Siderite	1	From a Sydney Basin coal - 'nodular'	30
Siderite	1	From a West Moreton coal - 'nodular'	40
Siderite	1	From a West Moreton coal - 'massive'	< 15
Siderite	1	From Leigh Creek coal - 'nodular'	< 15
Calcite	3	From Sydney Basin coals	< 10, 10?, ≤10
Secondary carbonate (high in Ca)	1	Cleat filling from a West Moreton coal	40
Gypsum	1	From Leigh Creek coal	< 10
Mudstone	1	From a dirt band in a Sydney Basin coal	10
Bentonite	1	From the roof measures of a Rosewood-Walloon coal	< 10
Kaolinite	1	From a Rosewood-Walloon coal	15
Kaolinite	1	From a Sydney Basin coal	25

TABLE 4. CONTENT OF SCANDIUM IN COKE, BOILER DEPOSITS AND FLY-ASH

(Values are in p.p.m. Sc)

Description of Samples	No. of Samples	Range of Values	Mean	Scandium in Ash of Coal Used
Cokes made from N.S.W. coals	14	25-40	30	-
Cokes made from Queensland coals	3	60-100	80	-
Fused material and deposits from walls of carburettor in water-gas plant	8	-	15	20
Deposits from various parts of a spreader-stoker-fired boiler, burning bituminous coal	32	20-30	25	20
Deposits on super heater tubes of chain-grate stoker fired boiler, burning bituminous coal				
Inner deposits	4	10-20	10	30
Outer deposits	1	-	30	
Deposits from screen tubes and superheaters of boiler, burning Leigh Creek coal under p.f. conditions	10	<10-20	10	-
Fly-ash from a N.S.W. bituminous coal	21	25-30	30	30
Fly-ash from Leigh Creek coal	2	20,30	25	-

The Effect of Molten Caustic on Pyritic Sulfur in Bituminous Coal

P. X. Masciantonio

Applied Research Laboratory, U. S. Steel Corporation, Monroeville, Pa.

Introduction

In a study related to the improvement of basic raw materials in the steel industry, the Applied Research Laboratory of the United States Steel Corporation has been investigating the behavior of chemical reagents on mineral matter in coal. The effect of various chemical reagents on pyrite in coal has been investigated as a part of this study.

It is well known that some mineral matter can be removed from coal by physical separation techniques; however, the effectiveness of such methods is limited by the degree of pulverization that is practical and the quantity of finely dispersed mineral matter that is present. Physical methods do not appear to be capable of removing either organic sulfur from the coal or finely dispersed pyritic sulfur that is embedded in the coal matrix. For example, after removal of pyrite by mechanical means, the sulfur content of Robena coal decreases from 2.5 percent to about 1.7 percent.

Chemical methods for removing mineral matter from coal have been reported to be quite successful. Chemical methods reported[1)]* include leaching with aqueous solutions of nitric acid, chlorine, hydrofluoric acid, and caustic, as well as extraction with various organic solvents to remove the coal from the residual mineral matter. The effect of microorganisms on pyritic sulfur in coal has been reported by the U. S. Bureau of Mines.[2)] The effect of molten-caustic solutions on the mineral matter in coal has not been reported previously.

Molten-caustic solutions have been used with success previously for heat-transfer media, heat treating, metal-finishing baths, and electrolytic refining processes. The addition of various basic compounds such as sodium carbonate during graphitization or carbonization has also been reported. The investigation reported in this paper describes the effect of molten-caustic solutions on the pyritic sulfur in bituminous coal.

Experimental Work

Robena coal was the principal coal studied in this investigation. Samples of Illinois coal and Wyoming coal were also examined to extend the scope of the study. Properties of the coals can be seen in Table I. Ordinary reagent-grade pellets of sodium hydroxide and potassium hydroxide were used to prepare the molten-caustic media. The experiments were conducted in a 1500-milliliter stainless steel vessel with an outlet valve at its base for removal of molten materials.

The procedure employed for the treatment consists of preparing a molten-caustic solution by melting together equal parts of sodium hydroxide and potassium hydroxide. The caustic is heated to the desired temperature, stirred vigorously, and the coal is added slowly as a powder to avoid foaming and overheating. About 4 parts of caustic to 1 part of coal are used to obtain a readily handled melt. The treatment is exothermic and some gases are evolved, especially during the coal addition. After the treatment is completed at the desired temperature and for the appropriate length of time, stirring is stopped, and about five minutes are allowed for separation of the coal from the molten caustic. The molten caustic is removed through the bottom outlet valve, and the coal layer is then cooled quickly in a

* See References.

water bath and subsequently slurried in 40 to 50 percent aqueous caustic to disperse the coal and remove residual inorganic materials. The coal is filtered off and washed with water to remove residual caustic. The samples are then dried under vacuum at 70 to 80 C and stored in sealed containers.

The coals were analyzed for sulfur content, ash, volatile matter, carbon, and hydrogen. Data were also obtained on free-swelling index and Gieseler plasticity.

Results and Discussion

Laboratory studies demonstrated that the pyritic sulfur in bituminous coal can be completely eliminated by molten-caustic treatment. Although a number of highly alkaline materials such as sodium acetate, sodium hydroxide, potassium hydroxide, and calcium hydroxide were investigated, a 1-to-1 melt of sodium hydroxide and potassium hydroxide appears to be the most suitable medium because of its thermal stability and low melting point.

The effect of temperature on the extent of desulfurization is quite pronounced, Table II and Figure 1. At temperatures between 150 C and 225 C only pyritic sulfur is removed from the coal, and below 150 C no observable pyrite removal occurs. A part of the organic sulfur of coal also appears to be removed as the temperature is increased above 225 C. Pyrite removal by molten caustic is a very fast process at either 250 C or 400 C, Figure 2, and appears to be complete after about five minutes at either temperature. The sulfur content of the coal increases with a long treating time at 400 C because of the formation of stable sulfur compounds by reaction of the coal with sulfides in the molten caustic.

The effect of coal size on the molten-caustic treatment appears to be important only below 300 C. Table III shows that plus 1/4-inch coal can be treated effectively at 400 C and that pyrite removal is poor at temperatures below 300 C unless minus 40-mesh coal is employed. Robena coal appears to become "plastic" at about 325 C and interaction between the caustic and pyritic sulfur is thereby enhanced. A high degree of pulverization is necessary to obtain good results at low temperatures since only sulfur at the surface of solid particles can be contacted by the caustic when the coal is not plastic.

The properties of coals treated with molten caustic appear to be somewhat different from those of the original coal. A comparison of proximate analysis, free-swelling index, Gieseler plasticity, and other properties can be seen in Table IV. Coals treated at 400 C and higher exhibit the most significant change in properties.

Although Robena and Illinois coal can be treated readily by this technique, low-rank coals such as Wyoming coal are seriously decomposed by molten caustic. Data on molten-caustic treatment of Wyoming coal and Illinois coal are shown in Table V.

The molten-caustic treatment may be suitable for preparing carbonaceous materials for special applications where low-sulfur and low-ash contents are of importance. This technique may also be useful as an analytical method for determining pyritic sulfur in coal.

Summary

An experimental investigation of the effect of molten caustic on pyritic sulfur in coals of various rank has been conducted. Laboratory tests showed that all pyritic sulfur can be removed from Robena coal by treatment with molten caustic. Robena coal and Illinois coal appear to perform similarly in molten caustic; however, Wyoming coal is severely decomposed during treatment.

This technique may be useful in preparing low-sulfur, low-ash carbonaceous materials for special applications. Molten-caustic treatment of coal might also serve as an analytical method for determination of pyritic sulfur.

Acknowledgements

The assistance of Mrs. Genevieve Dudgeon, Max Katz, and J. D. Clendenin of the Applied Research Laboratory is appreciated. Mrs. Dudgeon and Mr. Katz provided analyses of the various samples of coals and coke, and Mr. Clendenin supplied the coal samples and evaluation of coking properties for this investigation.

References

1. H. H. Lowry, Chemistry of Coal Utilization, Vol. 1, John Wiley and Sons, Inc., New York City (1945).

2. M. H. Rogoff, M. P. Silverman, and I. Wender, "The Elimination of Sulfur from Coal by Microbial Action." Presented before the Division of Gas and Fuel Chemistry, American Chemical Society, New York Meeting, September 11 to 16, 1960.

Table I

Coal Samples Used in Molten-Caustic Studies

Coal Sample	Screen Size	Total Sulfur, percent	Pyritic Sulfur, percent	Organic Sulfur,* percent
Robena 354	-40 mesh	1.64	0.58	1.06
Robena R415	1/4 by 0 in.	1.85	--	--
Illinois, Orient	1/4 by 0 in.	3.03	0.80	2.23
Wyoming, Elkol	-40 mesh	0.72	negligible	0.72

* Calculated difference between total sulfur and pyritic sulfur.

Table II

Molten-Caustic Treatment at Various Temperatures
(Minus 40-Mesh Robena Coal)

Temperature, C	Time, minutes	Sulfur in Coal, %	Coal Yield, %
150	30	1.56	93
200	30	1.14	92
250	30	1.04	94
300	30	0.99	89
350	30	0.80	92
400	30	0.51	93
450	30	0.56	--

Table III

Comparison of Molten-Caustic Treatment of Various-Sized Robena Coal

Coal Size	Treatment Temperature, C	Treatment Time, minutes	Sulfur in Coal, %
1/4 by 0 in.	250	10	1.40
-40 mesh	300	30	0.99
1/4 by 0 in.	300	30	0.96
1/2 by 1/8 in.	350	10	0.91
-40 mesh	400	5	0.90
1/4 by 0 in.	400	5	0.99
1/4 by 0 in.	400	30	0.36
1/2 by 1/4 in.	400	15	1.13

Table IV

Comparison of Properties of Untreated and Molten-Caustic-Treated Robena Coals

Treatment	Sulfur, %	Ash, %	Volatile Matter, %	Fixed Carbon, %	H_2O, %	Free-Swelling Index	Gieseler Maximum Fluidity
Robena coal	1.64	7.31	36.1	55.6	1.05	6-1/2	34,000
Robena coal extracted with tap water	1.64	6.93	36.4	56.4	0.25	7-1/2	17,300
Robena coal							
1/2 hr at 150 C	1.56	6.16	35.2	57.9	0.74	5-1/2	--
1/2 hr at 250 C	1.04	5.86	39.3	60.8	0.97	5	4,380
1/2 hr at 300 C	0.99	5.35	33.7	59.9	1.07	3-1/2	--
1/2 hr at 350 C	0.80	6.06	32.2	60.0	1.80	3	1.0
1 hr at 350 C	0.92	5.75	--	--	0.13	2-1/2	0.5
1/4 hr at 350 C	0.91	5.22	33.0	61.1	0.68	3-1/2	7.7
5 min at 400 C	0.90	6.22	32.5	61.2	0.00	3	0.3
1/2 hr at 400 C	0.51	4.9	23.6	63.1	8.1	0	-

Table V

Data on Molten-Caustic Treatment of Illinois and Wyoming Coal

Coal	Temperature, C	Time, minutes	Sulfur in Treated Coal, %	Yield, %	H_2O, %	Volatile Matter, %	Fixed Carbon, %	Ash, %	Free-Swelling Index	Carbon, %	Hydrogen, %
Wyoming	(Not treated)		0.72	-	19.8	35.0	42.2	2.96	1-1/2	60.26	5.57
Wyoming	200	30	0.50	52	9.4	41.9	47.7	0.96	1-1/2	68.56	5.78
Illinois	(Not treated)		3.03	-	5.7	34.8	50.0	9.49	2	69.03	5.17
Illinois	300	30	2.19	91	3.9	31.9	54.3	9.13	0	70.30	5.15
Illinois	400	30	0.97	76	2.1	29.5	61.7	6.67	0	76.31	4.14

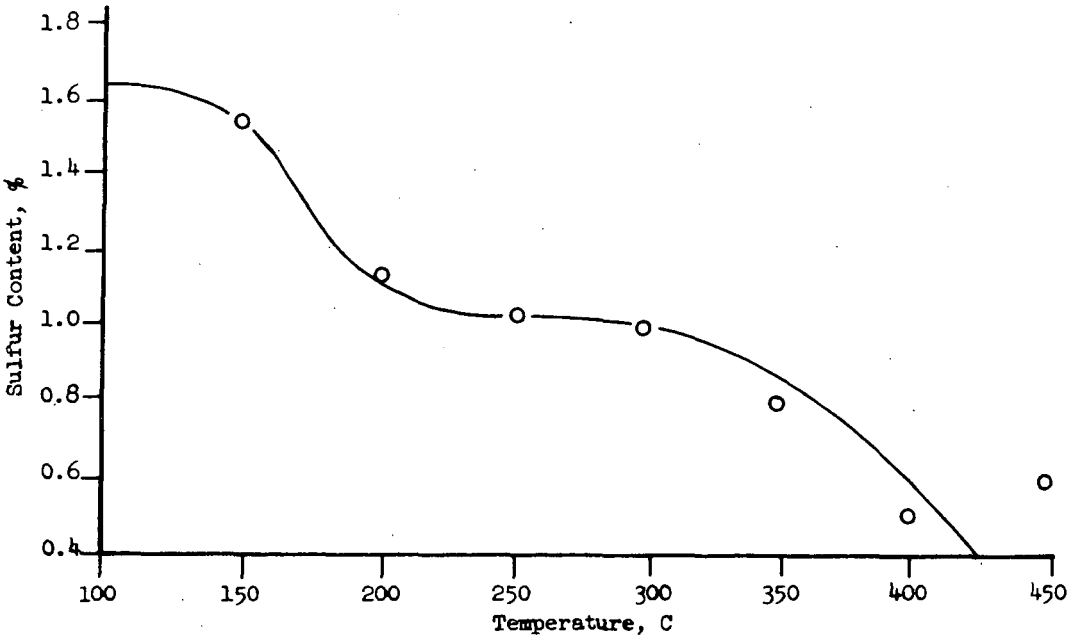

MOLTEN-CAUSTIC TREATMENT OF -40 MESH ROBENA COAL AT VARIOUS TEMPERATURES

Figure 1

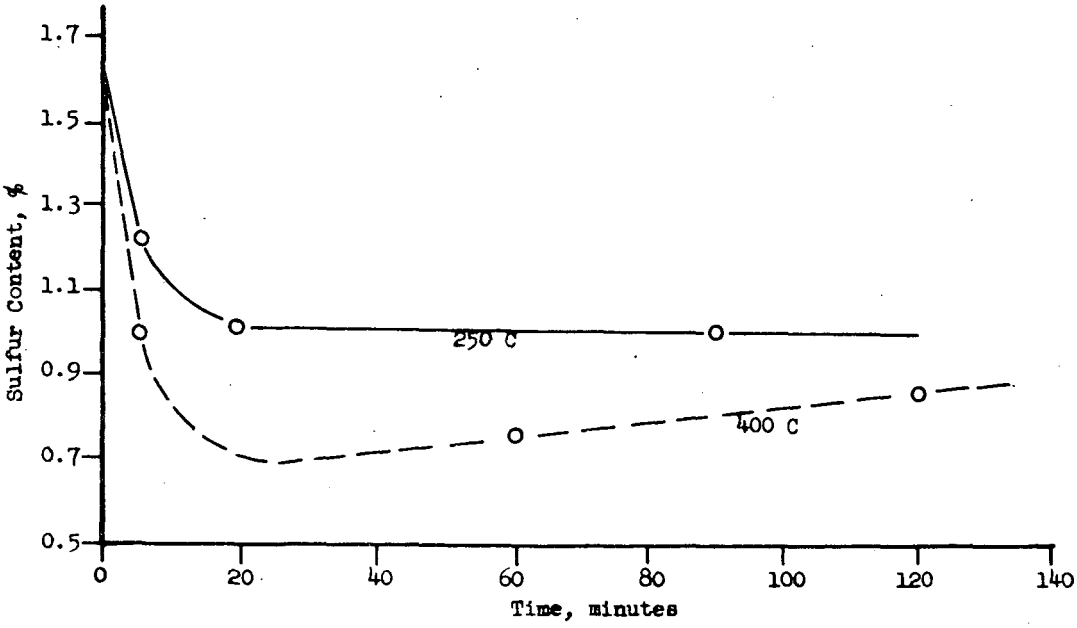

MOLTEN-CAUSTIC TREATMENT OF ROBENA COAL AT 250 C AND 400 C

Figure 2

Attempted Removal of Sulfur from Coal and Coke

P. H. Given and J. R. Jones*

Department of Fuel Technology, The Pennsylvania State University,

University Park, Pa.

The purpose of this paper is to report briefly on some experiments designed to remove inorganic sulfur from coal or to prevent its retention in coke, by chemical means. It may be said at once that although some success was achieved, no method with promise of industrial practicability was found.

A substantial proportion of the sulfur in coals occurs as ferrous disulfide, $Fe^{+2}S_2^{-2}$, usually in the mineral form known as pyrite. It is well known that pyrite dissociates to ferrous sulfide and sulfur, the dissociation pressure becoming appreciable at 450-500°. Ferrous sulfide is stable and undergoes little change before 1300-1400°. Various lines of work show that the sulfur released by the pyrite in coal during carbonization becomes fixed in the carbonaceous matter of the coke. Thus Cernic carbonized a series of coals in the presence of finely dispersed synthetic pyrite labelled with S^{35}; she found that in all cases a more substantial proportion of the radioactivity was retained in the coke than could be accounted for by the ferrous sulfide.

Mazumdar, Lahiri and their co-workers[2] investigated the reaction of sulfur with coal at 250-350°. Much hydrogen sulfide was released, which they attributed to dehydrogenation of hydroaromatic structures in the organic matrix; others have suggested that in addition dehydrogenation and cross-linking of aromatic nuclei takes place[3]. If the coal is heated with sulfur at 300-350° and then carbonized, the yield of volatile matter is drastically reduced and the coke has an increased sulfur content[2]. Some known sulfur compounds decompose at 500-600° with formation of hydrogen sulfide or mercaptans[4]; the latter substances, released during coal carbonization, could react elsewhere on the coal surface to give some firmly bound type of sulfur-carbon complex, their sulfur thus remaining in the coke.

It is evident therefore that a number of reactions involving sulfur can take place during coal carbonization, in which both inorganic and organic components play a part. Some of these reactions result in the formation of very stable organically bound sulfur complexes. Hence one possible way to reduce the sulfur content of coke would be to interfere with these reactions at temperatures below 600°, preferably in such a way that relatively stable volatile sulfur compounds are formed. The above ideas guided one of the series of experiments described in this paper: a coal was carbonized at 600° in the presence of various additives, and the sulfur content of the char compared with that of a standard char prepared in the absence of additive.

The other series of experiments was based on the reported solution chemistry of pyrite[5,6]. Various reagent mixtures are stated to dissolve

*Research Chemist, Research and Development Centre, Armstrong Cork Company, Lancaster, Pennsylvania.

pyrite at temperatures of 20-100°, and it was hoped that one could be found that would remove the disulfide from coal without serious oxidation or other change of the organic substance. It is not clear from the literature what reactions occur in bringing the pyrite into solution. The presumed interpretations of the reactions tested with pyrite in coal are:

1. Boiling potassium nitrate or chlorate with oxalic acid[7]; the ferrous iron in the presence of the mild oxidizing agent probably gives the very stable ferric oxalate complex, while the sulfur forms potassium sulfite or sulfate.

2. Stannous chloride and hydrochloric acid[8]: the pyrite may be reduced so that ferrous chloride and hydrogen sulfide result.

3. Calcium hypochlorite[9]: the pyrite must be oxidized to ferric sulfate. This reagent has also been used for "sweetening" gasoline, since it removes sulfur from many organic sulfur compounds, including thiophene if the pH is adjusted to weakly alkaline.[9]

4. Aqueous potassium cyanide[10]: it is stated[10] that pyrite does not dissolve on treatment with boiling saturated potassium cyanide for 6 hours. However, the following argument[4] suggests that under the conditions dissolution might take place.

The solubility of pyrite in water is said[11] to be 4×10^{-5} gm mol./l., so that the solubility product would be 1.6×10^{-9} and the concentration of Fe^{++} in equilibrium with the solid 4×10^{-5} gm. ion/l. However, recent unpublished work[12] suggests that the figures are considerably too high, but that in view of the instability of the S_2^{-2} ion its concentration could be suppressed and that of Fe^{++} materially increased by removing oxygen from the system. Now if a suitable ligand were added to the suspension, such that Fe^{++} is strongly complexed and its concentration in equilibrium with the complex reduced below that calculated from the solubility product of pyrite, the pyrite should in principle go into solution. One of the most stable complexes formed by Fe^{++} is the ferrocyanide:

$$Fe^{++} + 6CN^- \rightleftarrows Fe(CN)_6^{-4}$$

for which the stability constant at 25° is 10^{24}. Simple calculation shows that if pyrite dissolved in 5N cyanide solution until the ferrocyanide concentration became 0.1 N, the equilibrium concentration of Fe^{++} would be 6×10^{-30} gm. ion/l. Even if the solubility product of pyrite is considerably less than 1.6×10^{-9}, it should still dissolve in cyanide solution. Equilibria should be more favorable at room temperature than 100°. Some experiments on the treatment of coal with cyanide solution have been made.

Results

The coal used in this study was a high-volatile A bituminous coal from Champion Mine of the Pittsburgh seam. Relevant analytical data are given below:

Proximate Analysis:	Volatile matter	35.85%	Ash	11.35%
	Fixed carbon	52.8%	Moisture	1.19%

Ultimate Analysis (d.m.m.f., Parr's basis) 83.4%C, 5.7%H, 1.6%N, 0.6%S, 8.6% O (by diff.)

Sulfur Distribution:

total 2.46%,	pyritic 1.95%,	organic 0.49%,	sulfatic 0.02%
% of total sulfur:	79%	20%	1%

A. Change in Sulfur Distribution on Carbonization

A 30 gm. sample of coal (65 x 150 mesh) was placed in a sample holder and lowered into a furnace already preheated to the desired temperature; a flow of nitrogen (1 litre/min.) passed upwards through the furnace. The sample was left in the furnace for one hour after it reached temperature equilibrium, and then cooled in nitrogen. The char was then analysed for the total sulfur and the various inorganic forms of sulfur by standard A.S.T.M. procedures;[13] the organic sulfur is determined by difference. Data were obtained for a series of temperatures from 200-700°. The results are plotted in Figs. 1 and 2, where the sulfur distribution is shown as percentages of the total sulfur in the char and as percentages of the total sulfur in the raw coal respectively; the latter curve includes the proportion of sulfur lost in volatile products (obtained by difference).

It should be noticed that even by 200-300° there appears to be some gain of organic sulfur and loss of pyrite even though no ferrous sulfide could be detected. Possibly the organic material reduces pyrite, forming unstable sulfur-containing groups which subsequently are lost as volatile matter. The points for organic sulfur could be made to lie on a curve having a maximum at 200-250° and a minimum at about 400°, which would support the above suggestion, but the number of points available hardly justifies the drawing of more complex curves than those shown in the figures.

It is clear that by 600-700° most of the pyrite has decomposed, that the sulfur lost by the pyrite is much more than equivalent to the amount of sulfide formed, and that the proportion of organic sulfur in the char has considerably increased.

B. Carbonization in the Presence of Additives

For these experiments, the same apparatus and methods were used as above. For each experiment, 27 gms. of coal and 3 gms. additive were mixed by hand for 30-60 minutes; the mix was apparently dry even when the additive was liquid, owing to adsorption. Two rates of heating were used, 5.5-5.8°/min., and 80-90°/min.; conditions during carbonization were static, that is, no nitrogen flow was used. In the first case the sample was held at the maximum temperature (600°) for 15 minutes, and in the second for 60 minutes. The product, after cooling in nitrogen, was finely ground and analysed for total sulfur by the Eschka method.

Twenty seven substances were tested as additives, of which all but three were organic. They included various alcohols and sugars, which would give water and possibly olefins on pyrolysis; several high polymers, which should give on pyrolysis monomers capable of picking up sulfur; and some aromatic and aliphatic oxygen compounds that might take up sulfur to give a stable but volatile heterocyclic compound. Carbonization in the presence of most of these substances gave a char containing less sulfur than if no additive had been used, but the effect was small. It was appreciable for the four substances listed in Table I. It has been reported[14] that powdered pyrite is slowly decomposed by ammonium chloride, a sublimate of ammonium sulfide being formed; at 335°, 7% sulfur is lost in 25 minutes.

TABLE I

Carbonization of Pittsburgh Seam Coal at 600° in the Presence of Additives (10% concentration)

Additive	Heating rate °/min.	% loss in wt. at 600°	% S in Char	$\frac{\text{S in coke}}{\text{S in coal}} \times 100$
None	92.2	28.5	2.11	61.3
	5.6	23.8	2.22	68.8
Benzene-1,2,4,5-tetra-carboxylic dianhydride	80.0	21.5	1.60	51.0
	5.6	16.2	1.42	48.4
p. diphenyl-benzene (Santowax P)	77.5	29.7	2.03	58.0
	5.4	23.6	1.57	48.8
Sodium borohydride, $NaBH_4$	72.5	10.0	1.64	60.0
	5.63	6.72	1.47	55.7
Ammonium chloride	72.5	23.0	1.68	52.3
	5.6	21.4	1.32	42.2

It will be noticed that sulfur removal was more effective at the lower rate of heating. With the diphenylbenzene and the borohydride, hard cokes were obtained. Ammonium chloride yielded a very soft coke. The dianhydride gave a soft granular product, and the plastic zone appeared to have been destroyed or greatly reduced. At 5% concentration of additive the use of ammonium chloride showed some reduction of sulfur (1.87 and 1.93% S in the char at 70.5 and 65.6°/min. heating rate respectively); the other substances had little effect.

C. Treatment with Aqueous Solutions

1. Potassium Cyanide. 200 ML of 10% cyanide solution (approx. 1.5N) were allowed to percolate through 30 gm. coal in a column. The coal was (a) 65 x 150 mesh, and (b) -200 mesh, and percolation took 105 minutes and 36 hours respectively. No attempt was made to remove oxygen from the system. The product was washed with 200 ml. water, dried at 110° and carbonized as before. The total sulfur contents of the char were (a) 2.44, (b) 2.00%.

2. Potassium Cyanide and Potassium Nitrate. 15 Gm. coal (65 x 150 mesh) was refluxed gently for 6 hours in a solution of 0.15 mole each of cyanide and nitrate in 250 ml. water. The filtered, washed and dried coal contained 1.90% S (compared with 2.46% in the untreated coal).

3. Potassium Nitrate and Oxalic Acid. A suspension of 15 gm. coal in 250 ml. of a solution of 0.01 mole oxalic acid and 0.02 mole nitrate was left at room temperature for 24 hours, and then refluxed for 8 hours. The sulfur content of the product was 1.94%.

4. Stannous Chloride and Hydrochloric Acid. The treatment was as in #3 (0.01 mole each $SnCl_2$ and HCl). The sulfur content of the product was 2.35%.

5. Calcium Hypochlorite. A solution of 10 gm. hypochlorite in 190 ml. of water, adjusted to pH8 by addition of acetic acid, was allowed to percolate through 30 gm. 65 x 150 mesh coal (this took 3 hours). The ash content of the product was 13.3% (untreated coal, 11.35%) and the sulfur content 2.13%

D. Discussion and Conclusions

The preliminary experiments on sulfur distribution confirmed that

sulfur from pyrite becomes fixed in the organic matter of the char on carbonization, and that any interference with this process must take place at 350-500° if it is to reduce the sulfur content of the char. Carbonization in the presence of certain additives did cause a marked removal of sulfur, though probably not as much as would be desirable in industrial practice. Under the conditions used, the amount of additive needed was relatively large and would be costly in practice; in two cases weak cokes were obtained. In addition, the use of ammonium chloride would give rise to serious corrosion problems. However, the principle that sulfur fixation can be interfered with and reduced in extent is confirmed. For effective action it is no doubt necessary that the additive should volatilize and penetrate the coal particles (if the latter are as big as 65 x 150 mesh) or diffuse readily through the fused mass. If very finely divided coal could be charred in a fluidized bed up to 500-600° as a pretreatment in a fluidizing gas containing a fair partial pressure of ammonia, hydrogen, or possibly moist carbon dioxide, it is likely that the sulfur content of the char could be greatly reduced.

None of the treatment with aqueous solutions was particularly effective. However, it is striking that the cyanide treatment had no effect on 65 x 150 mesh coal with a contact time of 1 3/4 hours, but an appreciable one on -200 mesh coal in 36 hours. Of the other treatments, potassium nitrate/cyanide and potassium nitrate/oxalic acid had an appreciable effect even on the coarser coal size.

There seems little doubt that the primary difficulty in all the sulfur removal processes tested is in getting adequate contact between the reagent and the finely dispersed pyrite grains. It seems probable that with a more sophisticated appreciation pf pyrite chemistry much of the pyrite could be removed from a coal with an aqueous solution of a suitable complexing agent, provided finely pulverized coal can be used.

Acknowledgement

This work was supported by a contract from the Coal Research Board of the Commonwealth of Pennsylvania.

References

1. (Mrs.) S. Cernic, paper presented to 4th International Conference on Coal Science, Le Touquet, France, 1961.
2. B. K. Mazumdar, S. K. Chakrabartty and A. Lahiri, Fuel, 38, 15 (1959).
3. D. W. Van Krevelen, M. L. Goedkoep and P. H. G. Palmen, Fuel, 38, 256 (1959); see, also M. S. Iyengar, S. N. Dutta, D. D. Banerjee, D. K. Banerjee and S. K. Rai, Fuel, 39, 191 (1960).
4. P. H. Given and W. F. Wyss, Monthly Bull. of British Coal Utilisation Research Assoc., 25, 165 (1961).
5. J. W. Mellor, Comprehensive Treatise on Inorganic and Theoretical Chemistry, Longmans Green and Co., London and New York, Vol. 14, 1935, pp. 221-232.
6. H. L. Barnes and G. Kullerud, Econ. Geol. 56, 648 (1961).
7. H. C. Bolton, Ann. New York Acad., 1, 18 (1877), 2, 9 (1882); Proc. Amer. Assoc. Science, 31, 271 (1882); Chem. News, 37, 99, (1878); 47, 252 (1883); Berichte, 13, 728 (1880).

8. V. Rodt, Mitt. Materialprufungsamt, 32, 432 (1914).
9. National Benzole Co., Memorandum No. R452, 1945 (out of print) See also ref. 4, p. 171.
10. T. G. Pearson and P. L. Robinson, J. Chem. Soc., 821 (1928).
11. O. Weigel, Sitzber, Ges. Naturw. Markung, 2 (1921); Zeit. phys. Chem., 58, 294 (1907).
12. H. L. Barnes, Dept. of Geology and Geophysics, Pennsylvania State University, personal communication.
13. American Society for Testing Materials, Standards on Coal and Coke (1954).
14. A. P. Brown, Proc. Amer. Phil. Socl., 33, 225 (1894); Chem. News, 71, 120, 130, 144, 155, 171, 179 (1895).

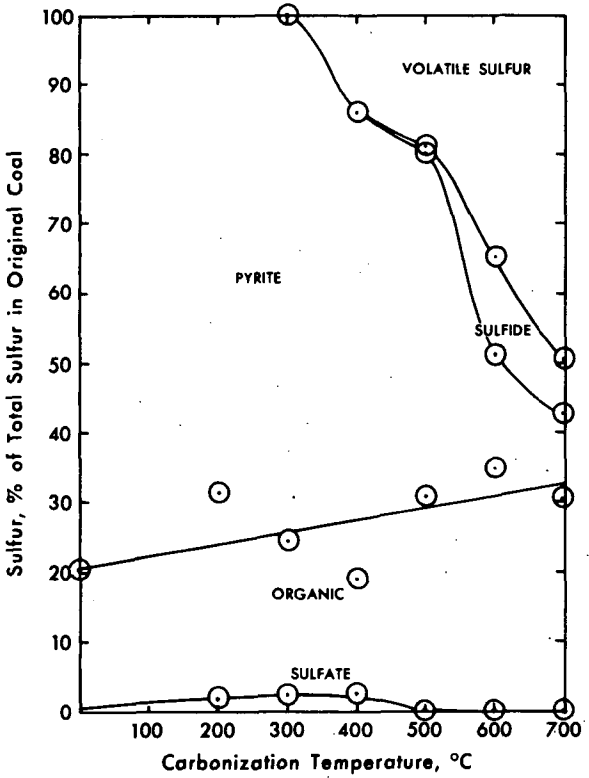

DISTRIBUTION OF FORMS OF SULFUR IN PITTSBURGH SEAM COAL AND CHARS, BASED ON TOTAL SULFUR IN UNHEATED COAL

Figure 1

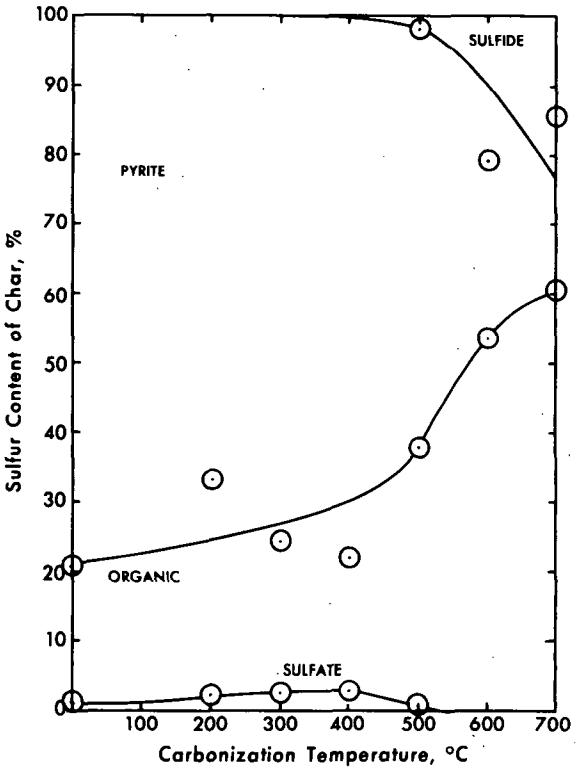

DISTRIBUTION OF FORMS OF SULFUR IN PITTSBURGH SEAM COAL AND CHARS, EXPRESSED AS FRACTIONS OF TOTAL SULFUR IN SAMPLE ANALYSED

Figure 2

FEASIBILITY OF CONTINUOUS ASH MEASUREMENT OF COAL

Robert F. Stewart and William L. Farrior, Jr.

U. S. Department of the Interior, Morgantown Coal Research Center
Bureau of Mines, Morgantown, W. Va.

An automatic and continuous method of measuring the ash content of coal is needed by the coal industry. Automatic control of coal quality would reduce preparation costs, improve the product, and thus indirectly increase markets for coal. Existing methods of ash analysis involve a laborous process of sampling, sample preparation and chemical analysis, and the results may not be available for several hours--perhaps long after the coal has been shipped. For bulk products like coal, sampling costs can easily become a significant proportion of production costs. The industry needs a continuous method of analysis that will permit immediate control of quality.

One possible method involves a process in which some type of nuclear radiation penetrates a considerable depth into the coal, undergoes a nuclear reaction with the chemical elements, and produces characteristic radiation that emerges from the coal and is measured. For this method, only neutrons and gamma rays will provide the required depth of penetration. When large samples of coal are bombarded by energetic neutrons, three nuclear processes can occur: (1) elastic scattering; (2) inelastic scattering; and (3) capture and subsequent decay. If the energetic neutrons are in the Mev-energy range, the usual sequence of events is for each neutron to make a number of elastic and inelastic collisions, losing energy with each collision, every inelastic collision leaving the bombarded nucleus in an excited state. When the excited nucleus returns to ground state, prompt gamma rays of characteristic energy, called inelastic gammas, are emitted. Eventually, after a large number of elastic and inelastic collisions, the neutron reaches thermal energies (about 0.025 ev) and neutron capture takes place. If the capture process excites the nuclide, prompt gammas are emitted by mechanisms similar to that of the inelastic scattering. These characteristic gamma rays are known as radiative capture gammas. Later, usually after relatively long periods depending on the half-lives of the radioisotopes, the nuclide may decay and emit a beta particle, a gamma ray, or both. These latter gamma rays are known as activation gammas. Both types of gamma rays have energies characteristic of the nucleus of the element from which they were produced, hence the number of such gamma rays can be counted and related to the concentration of elements in the coal.

Measurement and evaluation of gamma rays of different energies involves measurement by a scintillation detector and analysis by a pulse-height analyzer that produces an energy spectrum. Gamma ray spectra from coal show broad base-lines due to various interference effects and peaks that are characteristic and proportional to the individual elements in the material. This method offers the possibility of analyzing large volumes of material--say hundreds of pounds of coal--and since these processes are relatively instantaneous they would be applicable to continuous analysis of tonnage quantities of moving coal.

The mineral matter content of coal, commonly referred to as ash, includes many compounds. Alumina, silica, iron oxide, lime and magnesia generally comprise over 95 percent of coal ash.1/ If each of the elements in these compounds, Si, Al, Fe, Ca, and Mg, could be measured by the nuclear method described above, a summation of these measurements should give the ash content. To explore this possibility, basic measurements were made in a physical arrangement that could be adapted to tonnage flow of coal.

1/ Ode, W. H. Coal Analysis and Mineral Matter. Ch. 5 in Chem. of Coal Utilization (Supp. Vol.), ed. by H. H. Lowry. John Wiley and Sons, Inc., New York-London, 1963, pp. 202-231.

Experimental Equipment and Procedure. Apparatus used in this work is shown in figure 1. It consisted of a neutron source, a heavy metal attenuator, and a scintillation crystal detector surrounded by a cylinder of coal. The neutron sources were mixtures of plutonium and beryllium or of americium and beryllium which produce a broad spectrum of neutron energies ranging from 1 to 10 Mev by the reaction of alpha particles with the beryllium target. Radioisotope sources were chosen as neutron sources because they are relatively inexpensive and because they provide long-term unattended operation at constant flux. Commonly, 50-million neutrons per second are produced by a few curies of americium in a 1-inch-diameter steel capsule. The neutron source may be shielded by an inch of lead to reduce the gamma flux without adversely affecting the neutron output. The scintillation crystal detector is shielded from the beam of neutrons by placing it in the shadow of a cone-shaped tungsten attenuator, 8 to 12 inches in length. The detector, consisting of a 3- by 3-inch sodium iodide crystal and photomultiplier tube, is shielded from thermal neutrons by a boron shield surrounding the crystal.

About 50 pounds of coal is placed around the detector in the direct path of the neutrons. Fast neutrons from the source penetrate the coal producing inelastic and capture gamma rays, some of which interact with the detector crystal. Electrical pulses produced by the detector are proportional to the energy of the incident gamma photon. The latter are then measured by the multichannel analyzer and sorted by amplitude to represent the gamma ray spectrum.

Results. Gamma ray spectra were obtained that showed small peaks from the elements in the coal, plus a large amount of interference from unwanted radiation measured by the detector. Figure 2 shows the various interference components together with an unresolved spectrum from high-ash coal. The unresolved spectrum, or upper curve, includes background interference and is that part of the total spectrum between 0.6 and 2.5 Mev. It was obtained after coal, neutron source, and detector were kept in place for 90 minutes to approach equilibrium with respect to neutron activation. Curve A shows several small peaks and two prominent peaks corresponding to the silicon, aluminum, and hydrogen in the coal. Most of the spectrum is due to three major interference components which were estimated by several procedures and are indicated by curves A, B, and C. Curve A shows interference from neutrons transmitted through the attenuator directly into the crystal, curve B represents activation of the crystal detector by transmitted and scattered neutrons, while curve C is only the crystal activation from transmitted neutrons.

Although several improvements were made subsequently, including alteration of the composition and shape of the attenuator, better detector shielding, and different configuration of the coal samples--interrelated interference effects--it was found difficult to remove all of the interference and still retain a physical configuration adaptable to tonnage flows of coal. Improvements in one part of the spectrum often decreased the sensitivity of measurement in another part. Ultimately, however, interference effects were identified and reduced until a spectra was obtained having characteristic peaks that were reasonably sharp and consistent.

Typical results are shown in figure 3, a 50-minute measurement of 40 pounds of bituminous coal containing 9.4 percent combined silicon, aluminum, and iron. Prominent gamma peaks in the spectrum are from carbon, hydrogen, and the major ash constituents--silicon, aluminum, and iron. The 4.43 Mev carbon peak and its two pair peaks being at relatively high energy required special instrument adjustment to obtain good resolution, as shown by the insert to figure 3. The 2.22 Mev hydrogen peak contains some contribution from sulfur at 2.24 Mev, which is difficult to separate; the 1.78 Mev peak of silicon contains some contribution of the 1.77 Mev aluminum peak; and the 1.01 Mev peak of aluminum includes a few counts of the 1.04 Mev silicon peak. Iron appears prominently at 0.84 Mev and adds a small peak at 1.24 Mev, where aluminum

and silicon also contribute small peaks. A small and inconsistent peak appears at about 0.77 Mev, probably from calcium. There should be a fairly sharp peak from magnesium at 1.37 Mev but this particular coal sample did not contain enough magnesium to show it. This spectrum actually is only a part of the total spectrum which extends to 10 Mev. Some indication of an oxygen triple peak was found at 5.12, 5.63, and 6.14 Mev, and amplification gave several other peaks representing unidentified elements.

Sensitivity of Measurement. To estimate the sensitivity of measurement, tests were made on 15-pound samples of Pittsburgh-seam coal containing 3.3-percent and 21-percent ash. The 21-percent ash sample contained 5.8-percent Si, 2.3-percent Al, and 1.3-percent Fe--oxides of these elements comprising 90.4 percent of the ash in this sample. The 3.3-percent-ash sample contained 0.6-percent silica, 0.5-percent Al, and 0.39-percent Fe--oxides of these elements accounting for 90.2 percent of the ash.

Spectra of these two coals are shown in figure 4 at two amplifications. The difference between the 1.78 Mev silicon-aluminum peaks in the two spectra is readily apparent. There are 160,800 total counts under this peak for the low-ash coal and 177,300 total corresponding counts for the 21-percent ash coal, a difference of 16,500 counts. Coals containing 8.1- and 1.19-percent silicon plus aluminum respectively, gave a difference of 16,500 $\pm$ 581 counts, a sensitivity of 0.02 percent. Thus a change of 0.02 percent in silicon and aluminum theoretically was detected, although this was not entirely true because silicon and aluminum were assumed to contribute equally on a weight basis to the 1.78-Mev peak. With normal coal samples this estimate probably would not be off by more than a factor of two, so it is reasonable to expect that a change of 0.1 percent in silicon or aluminum content of the coal could be detected.

Subsequently, the actual sensitivity of this method was determined in static tests with coal. Samples of anthracite containing 6.2-, 7.0-, and 7.3-percent ash, respectively, were used in these tests. The small differences in the percentage of ash in these samples approximate the combined errors of sampling and analysis. Spectra obtained from the three samples, using 50-minute counting periods for each, are shown in figure 5. The shift in the 2.22-Mev hydrogen peak indicates a channel drift from instrument instability, so the peaks are blunter than under ideal conditions. A small but definite difference is apparent between the 7.3- and 7.0-percent-ash samples. Iron, aluminum, and silica peaks for the 6.2-percent-ash coal, however, are virtually identical to the coal containing 7-percent ash. (The slight differences are indicated by the dotted line.) The reason for this was shown subsequently to be due to a slight difference in degree of activation of the crystal detector and thus the amount of interference. Although the results cannot yet be considered as completely reliable, they indicate that differences can be obtained between coals differing less than 1 percent in ash content. Minor inconsistencies in the data are just as likely to have been caused by errors in sampling and chemical analysis as by errors in the nuclear method.

Conclusion. In static measurements, the concentration of several of the elements in coal was determined with varying degrees of accuracy by means of gamma rays produced by neutrons from radioisotope sources. Spectra peaks were readily identifiable for carbon, hydrogen, silicon, aluminum, iron; smaller peaks were found for other elements in coal.

The results were promising enough to warrant extension of the work to a pilot-scale system for measurement of the ash content of coal flowing at rates of 1 to 20 tons per hour. Indications are that the concentrations of ash in moving coal can be measured continuously within 1 percent, and perhaps within 1/2 percent.

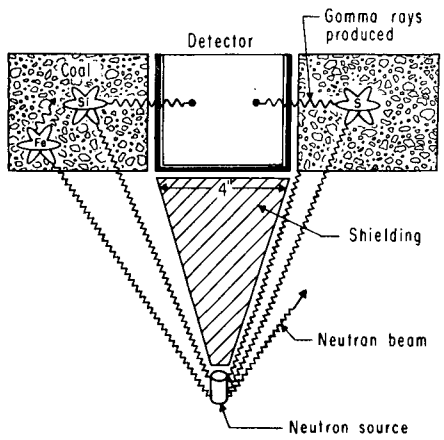

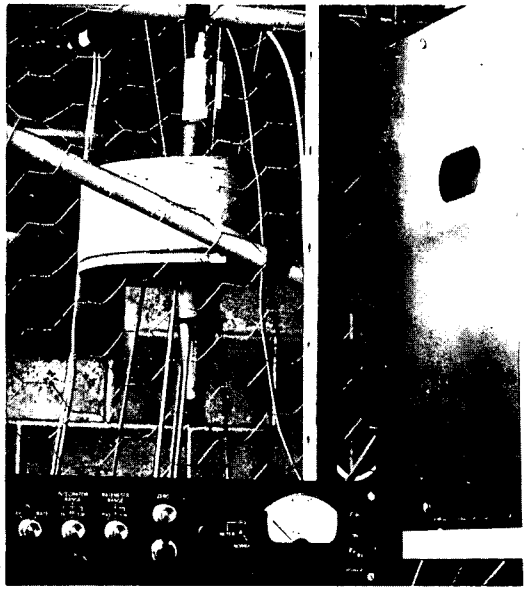

FIGURE 1-Apparatus for Measuring the Gamma Rays Produced by Neutrons Reacting With Ash Elements in Coal

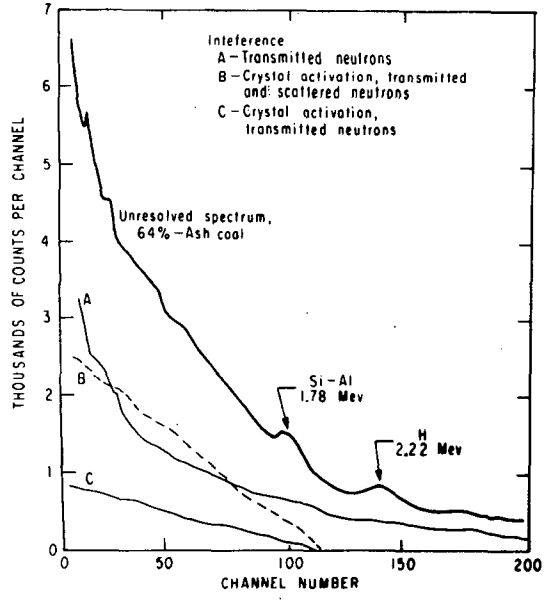

FIGURE 2 – Gamma Ray Spectra and Interference Components of High – Ash Coal

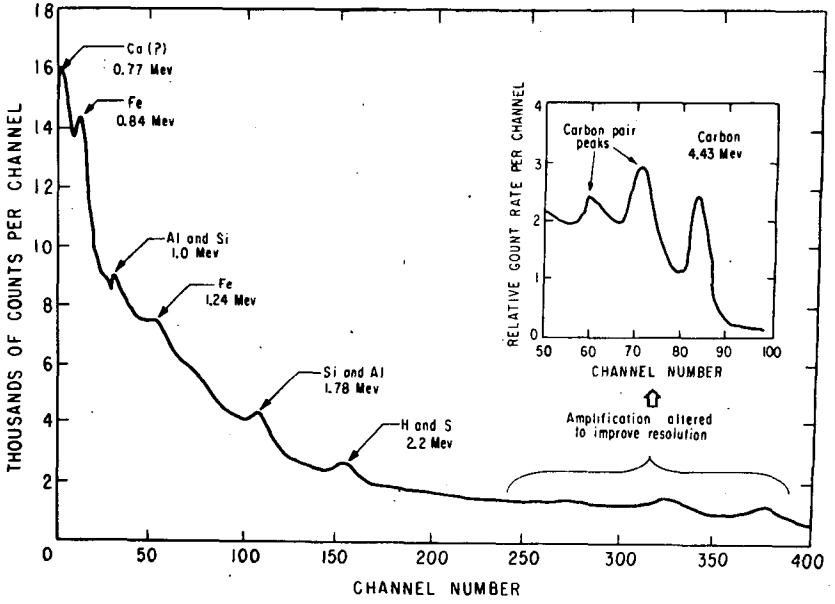

FIGURE 3 – Gamma Ray Spectra from Coal Containing 23% Ash

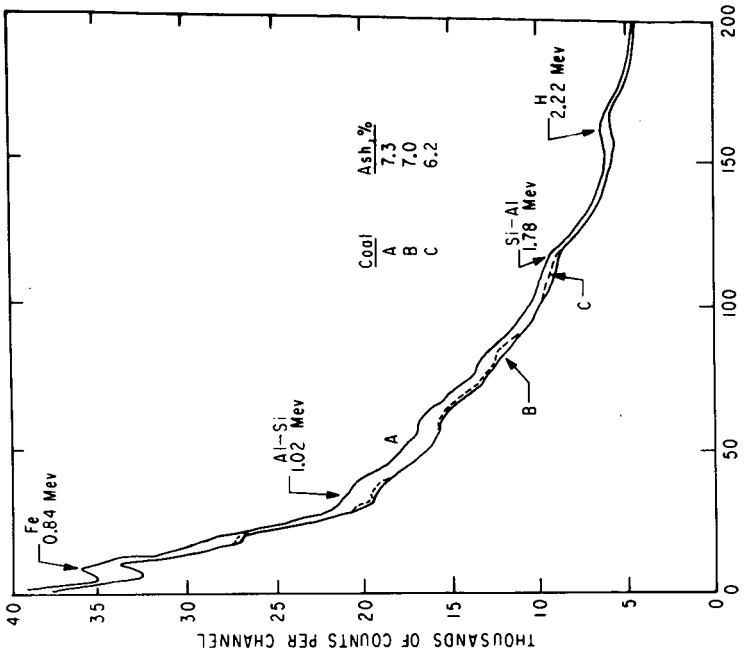

FIGURE 5 — Gamma Ray Spectra from Three Anthracite Samples

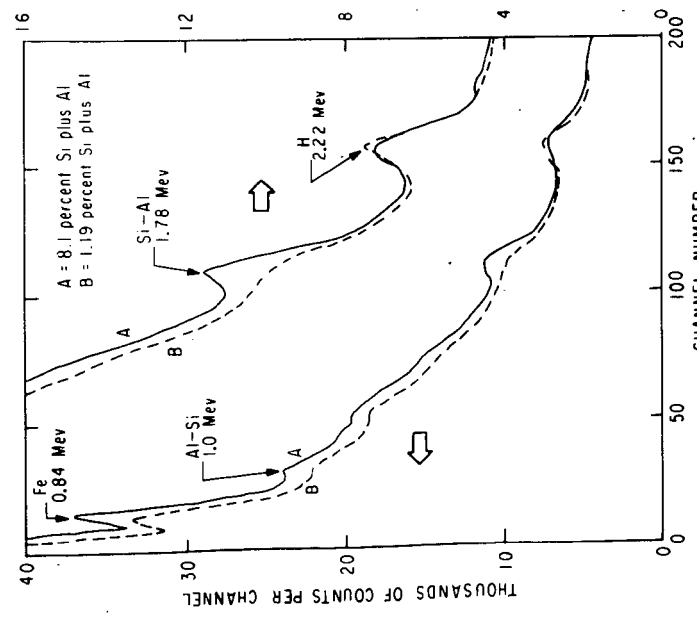

FIGURE 4 – Gamma Ray Spectra of High- and Low-Ash Coals

A NEW APPROACH TO THE PRODUCTION OF FLY ASH BASED STRUCTURAL MATERIALS

Harry E. Shafer, Jr. and Charles F. Cockrell

Coal Research Bureau, West Virginia University
Morgantown, West Virginia

INTRODUCTION

Fly ash, a major by-product from the combustion of pulverized coal, has become a problem of substantial proportion at coal burning power plants. The distribution and magnitude of fly ash production in 1962 is illustrated in Figure 1. During that year fly ash production exceeded 12 million tons. It is estimated that by 1980 approximately 28 million tons of fly ash will be produced annually.[1] At present, the major portion of fly ash is dumped in a slurry in rapidly dwindling storage areas while in other locations fly ash may be sold for as much as $4.00 per ton or carried away at a cost to the power plant of as much as $2.00 per ton. Major commercial uses for fly ash today are soil stabilization in which the fly ash is utilized as a grout; asphalt paving mixes in which the fly ash acts as a filler; and light-weight aggregate in which the fly ash is pelletized and then sintered.[2]

As one facet of many involved in a United States Department of Interior, Office of Coal Research contract for the investigation of coal-associated minerals, work was initiated by West Virginia University's Coal Research Bureau with the objective of utilizing fly ash to reduce the disposal problem at power plants attributable to the lack of adequate markets. The use of a mixture of fly ash and sodium silicate as a means to make structures is documented in previous literature.[3] Early attempts to process a fly ash-sodium silicate mix experienced difficulty because the material set too rapidly for handling, produced blocks with cracks, and gave low compressive strengths. Because of these difficulties a new approach to the production of fly ash-based structural materials was sought which involves in part the use of sand in the fly ash-sodium silicate mix as an agent to increase workability and to decrease fissuring by providing a path for moisture release. Therefore, the objective of this paper is to introduce a method for using a combination of low cost materials in conjunction with modest forming pressures to produce a superior structural product which may be technically feasible. The initial phases of this work have given encouraging results and the United States Department of Interior has recently filed a patent application covering this disclosure.

MATERIALS AND EXPERIMENTAL WORK

The origin and screen analysis of fly ash used in these experiments are given in Table 1. Chemical composition of fly ash is provided in Table 2. Admixed Ohio River sand used to reduce fissuring was screened to pass 28 mesh size. Sodium silicate solution was obtained from the Philadelphia Quartz Company, the composition and properties of which are given in Table 3.

All specimens were formed by use of a floating die into the shape of a brick as a means to facilitate testing. Forming as well as breaking pressures were measured with a Baldwin Model Universal Testing Machine. For firing at high temperatures, a Hoskins electric muffle furnace was used.

In the preparation of test specimens, sand and fly ash in proper proportions were dry mixed for five minutes to insure homogeneity. This mixture was then transferred to vessels where sodium silicate was added in small increments and mixed to form pellets. A quantity of pellets was chosen which would yield a desired brick thickness when formed in the die at a specified pressure.

Generally 400 gram pellet charges were used in order to produce a 2 X 4 X 1-5/8 inch brick test specimen formed at 1000 pounds per square inch pressure (p.s.i.). Cored test specimens were two and later three 1/2 inch diameter holes were adopted as a means to increase surface area, drying, and structural strength.

The newly formed test specimens were subsequently air-dried. Next, compressive breaking strength tests were run on the air-dried bricks or on bricks which were air-dried and then fired at 1100°C.

The final firing temperature of 1100°C was reached through programmed temperature increases over a period of 8 to 10 hours, maintained for four to six hours, and then gradually cooled to room temperature.

Specimens were tested in accordance with the American Society of Testing and Materials (ASTM) method C67-60 entitled "Standard Methods of Sampling and Testing Brick".

RESULTS AND DISCUSSION

Five basic batch test compositions designated A,B,C,D and E and their proportions are given in Table 4. Fly ash weight percentage ranges from 64.7 to 84.5; sand from 0.0 to 22.7 and sodium silicate solution from 9.1 to 15.5.

The foregoing ranges of composition were chosen as a result of exploratory tests, some of which are not listed, which demonstrated that coarser batch compositions with less than approximately 60 percent fly ash resulted in a marked decrease in specimen strength. This observation is indicated in Table 5 with composition E (tests 16 to 24)where breaking strengths were all 4150 p.s.i. or less. On the other hand, finer batch compositions with greater than approximately 72 percent fly ash showed evidence of good breaking strength, 5060 p.s.i. or more, when air-dried for ten days (See tests 13 and 15, Table 5). However, when these batches were fired, uniform moisture release was obstructed because of their fine consistency which caused fissures and decrepitation. Also, fine compositions tended to be initially unworkable and rapidly hardened in thin superficial layers.

It is apparent from these tests that increased compressive breaking strengths resulted for specimens that could be fired. It would appear that the stronger bricks obtained by firing resulted from a solution reaction whereby the specimen underwent partial vitrification.

Results also indicate that for superior breaking strengths above 5100 p.s.i., less binder is required when using the concentrated RU (See tests 1 to 4) in place of the dilute N-type sodium silicate (See tests 5 to 24) solution. Specimens where the RU-type binder was used with modest pressure (1080 p.s.i.) gave peak breaking strengths when fired (See test 1) and superior breaking strengths when unfired (See test 4). Low (790 p.s.i.) forming pressures also yielded superior breaking strengths when fired (See tests 2 and 3).

Within the limited scope of data, variations in breaking strengths due to different fly ash composition did not appear to be significant. Thus, tests 2 and 3 which were prepared under the same conditions using high silica, high alumina Appalachian and lower silica, lower alumina Willow Island Power Plant fly ash yielded essentially the same breaking strengths (5225 versus 5150 p.s.i.).

Because of the exploratory nature of this initial test work, the effect of the number of cores, forming pressure, water addition and bulk density on breaking strengths is not indicated. The correlation of these factors is currently being investigated over more confined ranges of variation than those presented in Table V.

Additional observations indicate that the bulk density of raw fly ash in compositions A,B, and C for varying test conditions were not significantly different, ranging from 104 to 107 pounds per cubic foot. However, when portions of iron were removed from raw fly ash by magnetic separation, the bulk density of composition B decreased to 96 to 98 pounds per cubic foot. This desirable reduction in bulk density is more than likely accompanied by a decrease in breaking strengths. There is also some reason to believe, based on observations made during testing, that the reduction of iron content in fly ash is accompanied by a favorable increase in workability and a decrease in binder consumption.

In order to examine individual requirements other than physical strength, ASTM tests were undertaken on several typical specimens produced from composition B.[4] Five hour boiling tests were conducted and in no instance did the water absorbed exceed 12 percent of the original weight as compared to a permissible 17 percent for optimum grade SW brick and 22 percent for high grade MW brick. The saturation coefficient was found to be 0.79. This compares favorably with an allowable 0.78 and 0.88 in grades SW and MW bricks respectively. Additional firing shrinkage tests were also conducted and in no case did the shrinkage exceed 1/64-inch for a 4-inch test specimen (0.39% shrinkage). This is well within the allowance of standard ASTM specifications. A severe test to determine the durability of the specimens was designed and undertaken. For a period of 24 hours specimens were alternated between a steam chamber (98°C) and a freezer (-25°C) at hourly intervals in order to test their resistance to thermal and moisture decomposition under extreme temperature change. The specimens were tested while still cold and the compressive breaking strengths were found to be comparable to other test specimens of the same compositions which did not undergo the repeated freezing and heating. No such thermal gradient (123°C) exists in nature over a short period of time, the purpose of this test being only to demonstrate the durability of the specimens.

Since fly ash-based structures may, among other applications, find use as a building material some comparisons are in order. The breaking strengths of the fly ash-based test specimens compare favorably with those of common face, clay based, brick. The measured breaking strengths of six specially prepared common face bricks of dimensions similar to those of the fly ash-based test specimens exceeded approximately 2600 p.s.i. Thus, seventy-five percent of the fired and 58 percent of the unfired fly ash-based test specimens exceeded the minimum breaking strength (2600 p.s.i.) of the common faced brick. The favorable similarities in strength are further enhanced when comparing the relative bulk densities. Bulk density of the best grade pressed brick is approximately 150 pounds per cubic foot while common brick has a bulk density of 125 pounds per cubic foot.[5,6] The highest bulk density obtained from the fly ash-based test specimens did not exceed 107 pounds per cubic foot and indications are that by the removal of magnetic material the bulk density can be further reduced to less than one hundred pounds per cubic foot.

In the absence of scale-up information, a complete cost estimate for the production of fly ash-based structural products is not possible at this time. However, on the basis of information obtained from both inquiries and published sources it is possible to estimate the cost of material.[7,8,9,10,11,12,13,14] At typical prices of $1.00 per ton of fly ash, $2.29 per ton of screened sand, and $2.30 per CWT of RU-type sodium silicate, the cost of materials per thousand fly ash-based bricks amounts to $11.30. This estimate is based on brick bulk densities of 105 pounds per cubic foot for the fired test specimen of composition A. Thus, $43.70 per thousand bricks is available for costs of amortization, depreciation, labor, plant operating cost and profit from the $55.00 per thousand realization value obtainable from the sale of bricks. Work is currently directed at obtaining more detailed information on the factors which affect breaking

strength and bulk density of the bricks. Such factors as materials handling, involving the effect of water additions and mixing time; forming pressure; drying time; firing rates; and firing temperature are critical and a series of factorial design experiments are currently underway.

CONCLUSIONS

Study of test results shows that the fired test specimens of composition A compare well with ASTM specifications on specimens tested. The acquisition cost of fly ash-based structural material is attractive in that cost is low for the material and long distance transportation is not involved (See Figure 1).

No definite conclusions can be drawn concerning the relationship existing between the effect of water addition, forming pressure, drying rate, and bulk density on breaking strength. The relationship between the number of coring holes and drying rate has not been determined.

BIBLIOGRAPHY

1. Weinheimer, C. M., "Fly Ash Disposal - A Mountainous Problem," Electric Light and Power, Vol. 32, 90, Apr., 54.

2. Snyder, M. Jack, "Properties and Uses of Fly Ash," Battelle Technical Review, Vol. 13 (2), 15, Feb., 1964.

3. Littlejohn, Charles E., "Literature Survey of the Utilization of Fly Ash," Engineering Experiment Station Bulletin 6, Engineering Experiment Station, Clemson A & M College (1954).

4. American Society of Testing and Materials Specification C 62-58, "Standard Specifications for Clay Building Brick."

5. Merritt, Fredericks, Building Construction Handbook, p. 2-18, McGraw-Hill Book Company, Inc., New York, 1958.

6. McNally Pittsburgh Coal Preparation Manual 561, McNally Pittsburgh Co., p. 129.

7. Personal Communication, American Power Co., New York, N. Y.

8. Personal Communication, Pennsylvania Power & Light Co., Allentown, Pa.

9. Personal Communication, Cleveland Electric Illuminating Co., Cleveland, Ohio.

10. Personal Communication, Commonwealth Edison Co., Chicago, Illinois..

11. Personal Communication, Duquesne Power Co., Pittsburgh, Pa.

12. Personal Communication, Appalachian Power Co., Glasgow, W. Va.

13. "Quarterly Report on Current Prices," Chemical and Engineering News, Vol. 42 (5), Feb. 3, 1964.

14. "Metals and Minerals," Minerals Yearbook 1962, Vol. 1, 1070, U. S. Department of Interior, U. S. Government Printing Office, 1963.

Table 1
Fly Ash and Screen Analysis

Percentage Retained of Given Mesh Size

Source	Designation	80	100	150	200	270	325	-325
Monongahela Power Company Willow Island Station	Willow Island	0.45	0.40	2.11	3.90	7.70	5.00	80.14
Appalachian Power Company Kanawha River Plant Glasgow, West Virginia	Appalachian (Electric)	0.12	0.01	0.07	0.12	0.24	3.02	95.42

Table 2
Spectrochemical Analysis of Fly Ash (%)

Designation	SiO_2	Al_2O_3	Fe_2O_3	TiO_2	CaO	MgO	Na_2O	Carbon
Willow Island	50.1	22.4	18.5	1.3	1.9	1.0	1.0	1.0
Appalachian (Electric)	58.1	27.5	6.0	1.7	1.6	1.0	1.0	2.5

Table 3
Composition and Properties of Sodium Silicate Solution

Type	$Na_2O:SiO_2$	$\%Na_2O$	$\%SiO_2$	$\%H_2O$	Specific Gravity	°Baume 68°F	Viscosity (Poises-20°C)	lbs/Gal.
N	1:3.22	8.9	28.7	62.4	1.394	41.0	1.8	11.6
RU	1:2.40	13.85	33.2	53.0	1.559	52.0	21.0	13.0

Table 4
Percentage Composition of Fly Ash-Sand-Sodium Silicate Mixtures

Composition	Fly Ash (% Weight)	Sand (% Weight)	Sodium Silicate Solution (% Weight)	Sodium Silicate (Type)
A	68.2	22.7	9.1	RU
B	65.8	21.9	12.3	N
C	84.5	0.0	15.5	N
D	74.0	13.0	13.0	N
E	64.7	21.6	13.7	N

Table 5
Compilation of Test Results in Order of Decreasing Breaking Strengths According to Composition

Test Number	Composition[1]	Breaking[2] Strength	Bulk[3] Density	Method of[4] Hardening	Number[5] Cores	Forming[6] Pressures	Water[7] Addition
1.	A-WI	9190	105-107	F	3	1080	60
2.	A-WI	5225		F	3	790	60
3.	A-AP	5150		F	3	790	60
4.	A-WI	5100	105-107	10 AD	3	1080	60
5.	B-WI	6780	104-106	F	2	1080	0
6.	B-WI-IR	5400	96-98	F	3	1080	0
7.	B-WI	5260		F	2	790	0
8.	B-WI-IR	4500		F	3	1080	0
9.	B-WI-IR	3590	96-98	7 AD	3	1080	0
10.	B-WI	3560	104-106	7 AD	2	1080	0
11.	B-AP	3520		7 AD	2	790	0
12.	B-WI-IR	2800		7 AD	3	790	0
13.	C-WI	5570	104-106	10 AD	3	1080	0
14.	C-AP	1500		7 AD	2	790	0
15.	D-AP	5060		10 AD	3	790	0
16.	E-AP	4150		F	3	790	0
17.	E-AP	3200		F	2	790	0
18.	E-WI	2460		F	2	1370	100
19.	E-Wi	2440		F	2	1900	100

Table 5 (Continued)

Test Number	Composition[1]	Breaking[2] Strength	Bulk[3] Density	Method of[4] Hardening	Number[5] Cores	Forming[6] Pressures	Water[7] Addition
20.	E-WI	1900		F	2	960	100
21.	E-AP	1525		10 AD	2	530	0
22.	E-AP	1400		21 AD	2	790	0
23.	E-AP	1220		7 AD	2	790	0
24.	E-AP	1260		7 AD	2	530	0

1. WI = Willow Island Power Plant Fly Ash
   AP = Appalachian Power Plant Fly Ash
   IR = Iron reduced by magnetic separation to approximately 5.6 percent.

2. Breaking strength in pounds per square inch (p.s.i.).

3. Bulk density in pounds per cubic foot.

4. F = Fired at 1100°C
   10 AD = Air-dried for ten days
   7 AD = Air dried for seven days

5. Number of evenly spaced holes of 1/2- inch diameter in test specimen.

6. Forming pressure in pounds per square inch (p.s.i.).

7. Water addition in milliliters.

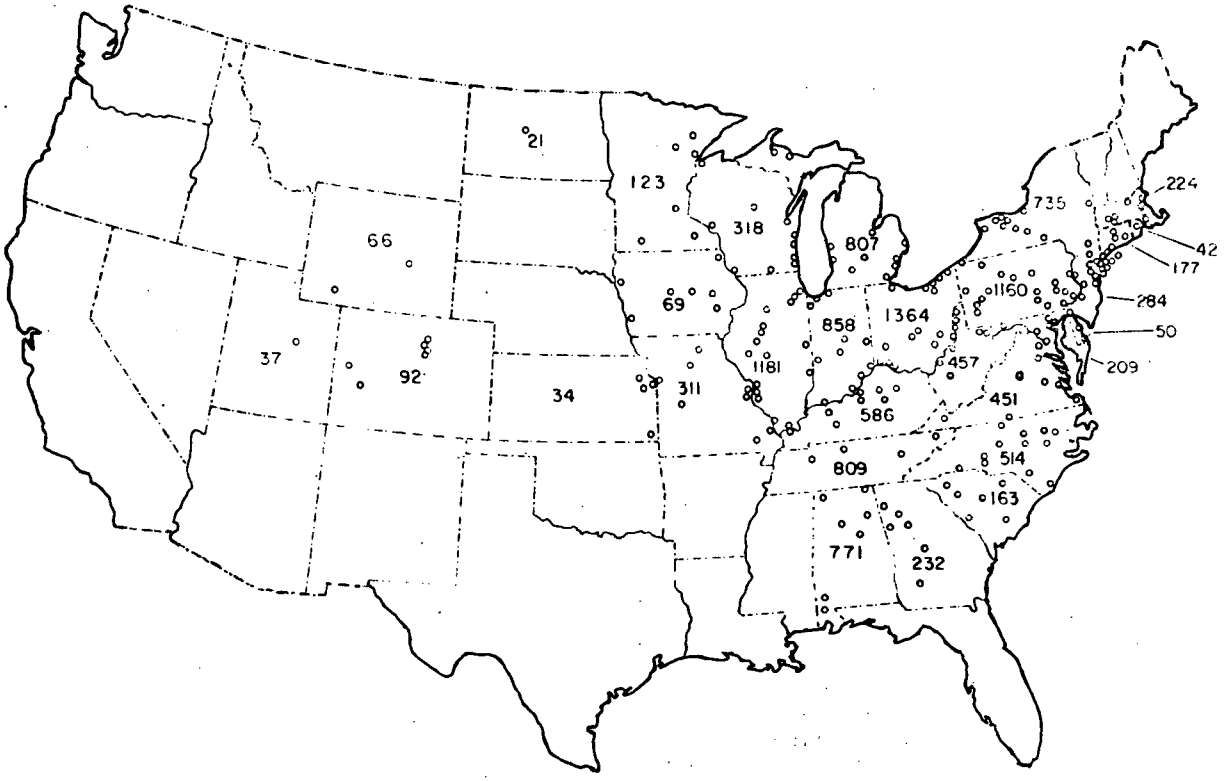

FIGURE 1
Location of Pulverized Coal Units
and Fly Ash Production of Individual
States (in thousands of tons)
1962

Aromatic Molecules Containing Substituents Internal to the π-Electron Cloud

V. Boekelheide

Department of Chemistry, University of Oregon, Eugene, Oregon

A discussion of the synthesis and chemistry of molecules having groups internal to the π-electron cloud will be presented. The 15,16-dihydropyrene system will be used to illustrate the properties of molecules of this type.

Synthesis and Properties of Intramolecularly Overcrowded Hydrocarbons

Melvin S. Newman

Department of Chemistry, The Ohio State University, Columbus, Ohio

For many years the question of the degree of coplanarity needed for existence of certain polycyclic aromatic hydrocarbons has been of interest. The most strained hydrocarbon of this type that has been made to date is hexahelicene, I. The origin of the problems relating to the synthesis and resolution of I will be described as well as related research which has been stimulated by the above work.

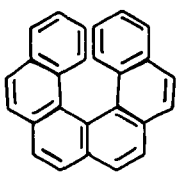

I

Aromatic Molecules Containing Substituents Internal to the π-Electron Cloud

V. Boekelheide

Department of Chemistry, University of Oregon, Eugene, Oregon

A discussion of the synthesis and chemistry of molecules having groups internal to the π-electron cloud will be presented. The 15,16-dihydropyrene system will be used to illustrate the properties of molecules of this type.

Synthesis and Properties of Intramolecularly Overcrowded Hydrocarbons

Melvin S. Newman

Department of Chemistry, The Ohio State University, Columbus, Ohio

For many years the question of the degree of coplanarity needed for existence of certain polycyclic aromatic hydrocarbons has been of interest. The most strained hydrocarbon of this type that has been made to date is hexahelicene, I. The origin of the problems relating to the synthesis and resolution of I will be described as well as related research which has been stimulated by the above work.

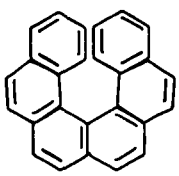

I

Action of Nitrous Acid on Borazaro Compounds

M.J.S. Dewar, Department of Chemistry, University of Chicago
W.H. Poesche, University of Alberta, Edmonton, Alberta, Canada

Diazotisation of borazaro compounds with subsequent treatment with base (sodium acetate) gives boron-free products. Two different reaction paths have been recognised for this reaction: The first leads to the corresponding 1,2-diaza compounds by electrophilic displacement of the boronic acid group by the diazonium ion, the second to a product with twice its molecular weight. Which of the two paths is followed seems to depend on the borazaro compound and the reaction medium employed. Thus when diazotisation is carried out in acetic acid/hydrochloric acid, 10-methoxy-10,9-borazarophenanthrene gives the path 1 product exclusively; 6-methoxy-6,5-borazarobenz[a]anthracene and 5-methoxy-5,6-borazarobenz[a]anthracene give the path 1 product in 50% yield. Under the same conditions 6-methoxy-6,5-borazarochysene gives only the path 2 product.

The synthesis of halogeno compounds will be described, which have been prepared to obtain information about the factors which determine the course of the reaction and the structure of the path 2 reaction product.

$B_{10}H_{10}^{-2}$ and $B_{12}H_{12}^{-2}$: Inorganic Aromatic Species

W.H. Knoth, J.C. Sauer, W.R. Hertler, E.L. Muetterties and H.C. Miller

Central Research Department, Experimental Station
E.I. du Pont de Nemours and Company, Wilmington, Delaware

$B_{10}H_{10}^{-2}$ and $B_{12}H_{12}^{-2}$ are extremely stable species with a derivative chemistry of sufficient scope to rival that of organic aromatic systems. $B_{10}H_{10}^{-2}$ and $B_{12}H_{12}^{-2}$ form stable conjugate acids of somewhat greater strength than sulfuric acid, and are not readily degraded by base. Derivatives containing the following substituents directly on boron, either singly or in combination, have been prepared: halogen, COOH, CN, COOEt, $CONH_2$, COR, R, NH_2, NCO, N_3, OH, OR, OCOR SH, carbon monoxide, nitrogen, organic sulfides, amines, nitriles, and amides. Specific examples include: $B_{12}H_{10}(COOH)_2^{-2}$, $B_{10}H_8(NCO)_2^{-2}$, $B_{10}Cl_8(N_2)_2$, $B_{10}H_8(CO)_2$ and $B_{10}H_9COC_6H_5^{-2}$. Synthetic methods and properties will be described, together with observations on stereochemistry, isomer formation and separation, directive effects of substituents and inferences on possible mechanisms of substitution.

Action of Nitrous Acid on Borazaro Compounds

M.J.S. Dewar, Department of Chemistry, University of Chicago
W.H. Poesche, University of Alberta, Edmonton, Alberta, Canada

Diazotisation of borazaro compounds with subsequent treatment with base (sodium acetate) gives boron-free products. Two different reaction paths have been recognised for this reaction: The first leads to the corresponding 1,2-diaza compounds by electrophilic displacement of the boronic acid group by the diazonium ion, the second to a product with twice its molecular weight. Which of the two paths is followed seems to depend on the borazaro compound and the reaction medium employed. Thus when diazotisation is carried out in acetic acid/hydrochloric acid, 10-methoxy-10,9-borazarophenanthrene gives the path 1 product exclusively; 6-methoxy-6,5-borazarobenz[a]anthracene and 5-methoxy-5,6-borazarobenz[a]anthracene give the path 1 product in 50% yield. Under the same conditions 6-methoxy-6,5-borazarochysene gives only the path 2 product.

The synthesis of halogeno compounds will be described, which have been prepared to obtain information about the factors which determine the course of the reaction and the structure of the path 2 reaction product.

$B_{10}H_{10}^{-2}$ and $B_{12}H_{12}^{-2}$: Inorganic Aromatic Species

W.H. Knoth, J.C. Sauer, W.R. Hertler, E.L. Muetterties and H.C. Miller

Central Research Department, Experimental Station
E.I. du Pont de Nemours and Company, Wilmington, Delaware

$B_{10}H_{10}^{-2}$ and $B_{12}H_{12}^{-2}$ are extremely stable species with a derivative chemistry of sufficient scope to rival that of organic aromatic systems. $B_{10}H_{10}^{-2}$ and $B_{12}H_{12}^{-2}$ form stable conjugate acids of somewhat greater strength than sulfuric acid, and are not readily degraded by base. Derivatives containing the following substituents directly on boron, either singly or in combination, have been prepared: halogen, COOH, CN, COOEt, $CONH_2$, COR, R, NH_2, NCO, N_3, OH, OR, OCOR SH, carbon monoxide, nitrogen, organic sulfides, amines, nitriles, and amides. Specific examples include: $B_{12}H_{10}(COOH)_2^{-2}$, $B_{10}H_8(NCO)_2^{-2}$, $B_{10}Cl_8(N_2)_2$, $B_{10}H_8(CO)_2$ and $B_{10}H_9COC_6H_5^{-2}$. Synthetic methods and properties will be described, together with observations on stereochemistry, isomer formation and separation, directive effects of substituents and inferences on possible mechanisms of substitution.

Investigations on the Use of NMR Spectroscopy for Structural Determinations in the Field of Polycyclic Aromatic Substances

R.H. Martin

Universite Libre de Bruxelles, Service de Chimie Organique,
50, Av. F.D. Roosevelt, Bruxelles, Belgium

Up to now, very little use has been made of NMR spectroscopy in the field of polycondensed aromatics.

A systematic investigation of

1--unsubstituted polycyclic aromatic hydrocarbons,
2--polycondensed aza-aromatic systems,
3--monosubstituted derivatives of triphenylene, phenanthrene, biphenylene, benzo[a]biphenylene, pyrene, benzo[c]phenanthrene, dibenzo[g,p]chrysene (tetrabenzonapthalene), fluorene and acenaphthene,
4--aromatic cyclic ketones,

has yielded information which can be used to solve many structural problems resulting from ambiguous syntheses.

Screening effects (shielding and deshielding of aromatic protons) due to substituents and cyclic heteroatoms are particularly important in ortho, meta, para, peri and "angular" positions. The precise knowledge of these effects and of their magnitude is, of course, of great importance for the interpretation of integrated spectra of unknown substances.

The scope and limitations of this technique will be discussed and illustrated by examples drawn from the chemistry of polycyclic aromatic hydrocarbons and polycondensed heterocyclic compounds.

Presented Before the Division of Fuel Chemistry
American Chemical Society
Chicago, Ill., Aug. 30-Sept. 4, 1964

ALKALI METALS AS HYDROGENATION CATALYSTS FOR AROMATIC MOLECULES

Sidney Friedman, Marvin L. Kaufman, and Irving Wender

U. S. Bureau of Mines, 4800 Forbes Avenue
Pittsburgh, Pa. 15213

Sodium in liquid ammonia has been used for many years as a reducing system for aromatic systems,[1,2] and more recently both sodium and lithium in amines have become increasingly important.[3,4] In these reductions, the amines serve as proton donors; in liquid ammonia, an alcohol is usually added to furnish the hydrogen.[1] There are also a few cases known where ethers are used as solvents for reductions with alkali metals;[5,6] in these reactions, the alkali metal salt of the hydrocarbon is undoubtedly formed. Addition of water or alcohol then provides the necessary hydrogen to decompose the salt and form the reduced hydrocarbon. In every one of these reactions, the alkali metal is used stoichiometrically, and is eventually converted to $M^+ B^-$, where M = Na or Li and B = OH, OR, or NR_2. In each of these reactions, the equivalent of an ionic carbon-metal bond is formed at some stage of the reaction.

Carbon-metal bonds, such as those formed in alkali metal reductions, are known to be readily hydrogenated.[7] Thus, if such a bond is formed in an atmosphere of hydrogen, reduction can take place to regenerate the metal or to form its hydride.

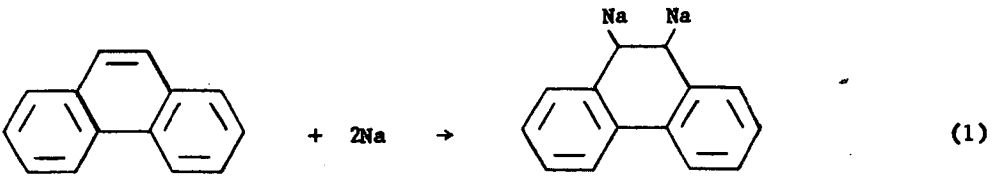

(1)

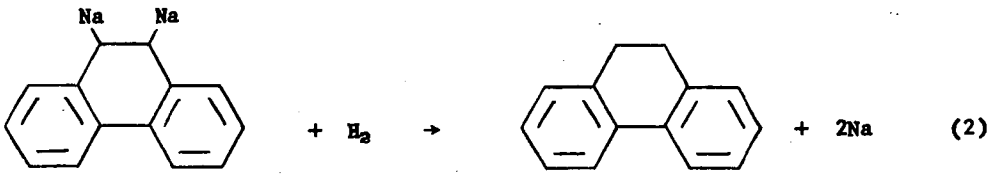

(2)

or

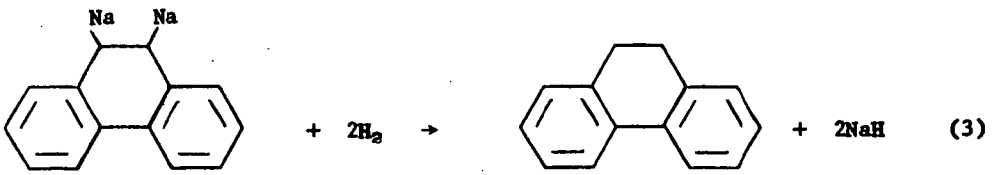

(3)

(4)

The sodium hydride formed in (3) or (4) might also be capable of adding to a double bond, providing an alternate pathway to the reduction product.

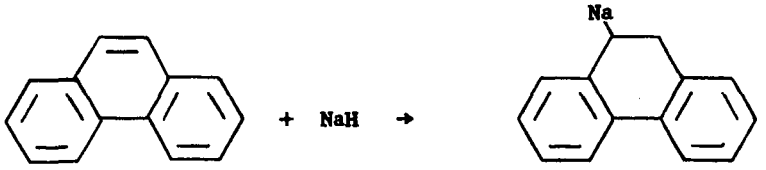

(5)

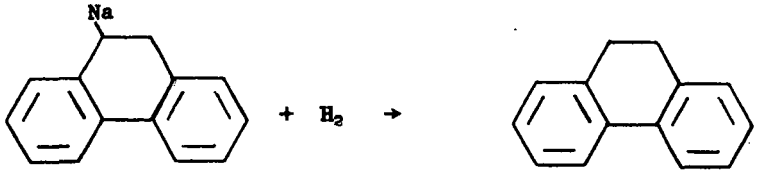

(6)

In either case, the series of reactions would constitute a catalytic hydrogenation.

Several investigations have been carried out to explore this catalytic system, using both alkali metals[8-10] and sodium hydride[11] as the initial catalysts, and in all cases hydrogenations have been achieved. However, very little has been done toward exploring this system in detail; most of the reported work has been confined to the reduction of naphthalene to tetrahydronaphthalene. We wished to investigate the system in more detail; to study the effects of other alkali metals and of other solvents and to apply it to compounds other than naphthalene, especially compounds of the type one might find in coal or coal tar.

Initially, a series of reactions was conducted in which an alkali metal, an aromatic hydrocarbon, and a solvent (benzene or toluene) were heated with hydrogen in a rocking autoclave to a specified temperature. As an example, 10 grams of naphthalene, 1 gram of sodium, and 80 ml of toluene were placed in an autoclave with hydrogen at 1,000 psi and heated to 300° C with rocking. After five hours at temperature, the autoclave was allowed to cool overnight and then opened. The reaction product contained some white solid in suspension. Addition of isopropyl alcohol caused considerable reaction, with the evolution of gas, presumed to be hydrogen from decomposition of sodium hydride. The solution was extracted with water, and solvent removed from the organic layer by distillation. Examination of the product by mass spectrometry and gas chromatography showed it to be 62 percent tetrahydronaphthalene and 36 percent unreacted naphthalene, with 2 percent of dihydronaphthalene.

Similar experiments showed that lithium, which is a better reducing agent than sodium in metal-amine systems,[4] is a much poorer catalyst than sodium for hydrogenation. Even at 325° C, only 4 percent of the naphthalene was reduced.

Further experiments with sodium at 250° gave reductions of anthracene and phenanthrene to mixtures of dihydro- and tetrahydro-derivatives. There was evidence that careful control of temperature and pressure might allow the hydrogenation to be carried out selectively.

Experiments using sodium were extended to an investigation of sodium-potassium alloy (NaK) as a catalyst. This was found to be more active than sodium, the alloy probably behaving more like potassium. At 250° C, naphthalene is reduced to tetrahydronaphthalene in 92 percent yield, with 8 percent of 1,2,3,4,1',2',3',4'-octahydro-2,2'-dinaphthyl being formed by reductive dimerization. Anthracene and phenanthrene are reduced mainly to their symmetrical octahydro derivatives, with small amounts of intermediate reduction products also being present among the products. Chrysene is reduced to a mixture of products, chief among them being hexahydro-, octahydro-, and dodecahydrochrysenes. The major reduction product of triphenylene is sym-dodecahydrotriphenylene. Both pyrene and naphthacene, however, are reduced only to the dihydro stage at 250° C. At 350° C, pyrene is reduced to a mixture of products including hexahydro- and decahydropyrenes. At 350° C, biphenyl is hydrogenated to phenylcyclohexane in good yield and p-terphenyl yields both trans-1,4-diphenylcyclohexane and dodecahydroterphenyl, corresponding to the reduction of either one or two of the three rings. The reduction of o-terphenyl is similar, except that cyclization occurs to give sym-dodecahydrotriphenylene as a major product.

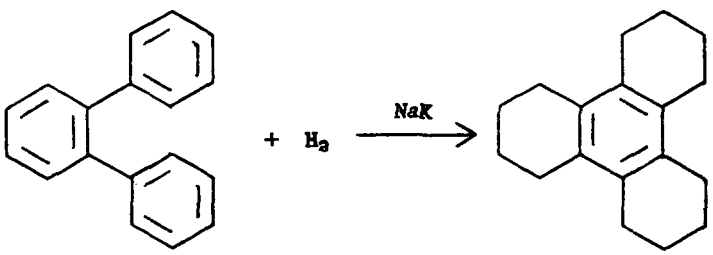

(7)

This is probably the best available method for preparation of the latter compound.

In the reduction of the polyaryls, scission of the bonds between the rings is indicated by the formation of benzene, biphenyl, phenylcyclohexane, and traces of higher polyaryls. When benzene or toluene is heated to 350° C with NaK and hydrogen, hydrogen is absorbed with the formation of hydrogenated dimers and higher polymers, as well as coal-like chars.

Since the reaction of alkali metals and alkali metal salts is an equilibrium reaction,

$$2Na + KX \rightleftharpoons NaX + NaK \qquad (8)$$

it was felt that NaK could be formed in situ in a reaction vessel at elevated temperatures by using sodium metal and the appropriate potassium salt. Potassium chloride-sodium mixtures fail to give results comparable to NaK when used as a hydrogenation catalyst at 250° C. Instead, the mixture behaves like sodium. When potassium carbonate or hydroxide is used with sodium, however, hydrogenation of naphthalene, phenanthrene, and pyrene proceeds to give products and yields similar to those obtained with NaK.

The success of the potassium salt/sodium metal system suggested that the use of rubidium salts might allow the catalytic behavior equivalent to sodium-rubidium (NaRb) to be studied without the inconvenience of handling metallic rubidium. Experiments have indicated this to be the case.

At 180° C, naphthalene is hydrogenated to tetrahydronaphthalene in 99 percent yield when a mixture of sodium metal and rubidium carbonate is used as catalyst. At temperatures between 200° C and 220° C, anthracene and phenanthrene are rapidly hydrogenated to their octahydro derivatives. Chrysene is hydrogenated to dodecahydrochrysene, i.e., a product containing a single aromatic ring, in 85 percent yield at 250° C. Perylene, at 250° C, is reduced to a mixture of 47 percent octahydroperylene and 30 percent dodecahydroperylene; pyrene similarly forms decahydro- and dodecahydropyrenes. Naphthacene, which is strangely resistant to extensive reduction by this method, nevertheless goes to octahydronaphthacene in 36 percent yield at 300° C.

Fluorene, which seems to have been neglected in the literature on catalytic hydrogenation, is reduced by NaRb to hexahydrofluorene. A smaller amount of tetrahydrofluorene was isolated from a chromatogram and identified by its ultraviolet spectrum.

Both biphenyl and 1,3,5-triphenylbenzene are reduced catalytically by NaRb. Biphenyl forms phenylcyclohexane in greater than 70 percent yield at 250° C. This is comparable to a reduction catalyzed by NaK at 350° C. Triphenylbenzene is hydrogenated and also cleaved to give a mixture of products. These include hexahydro-, dodecahydro-, and octadecahydrotriphenylbenzene, as well as hydrogenated biphenyl and terphenyl.

o-Terphenyl, at 250°, forms both hexahydroterphenyl and sym-dodecahydrotriphenylene, the cyclization product. The most important product, however, is biphenyl, formed as a result of cleavage.

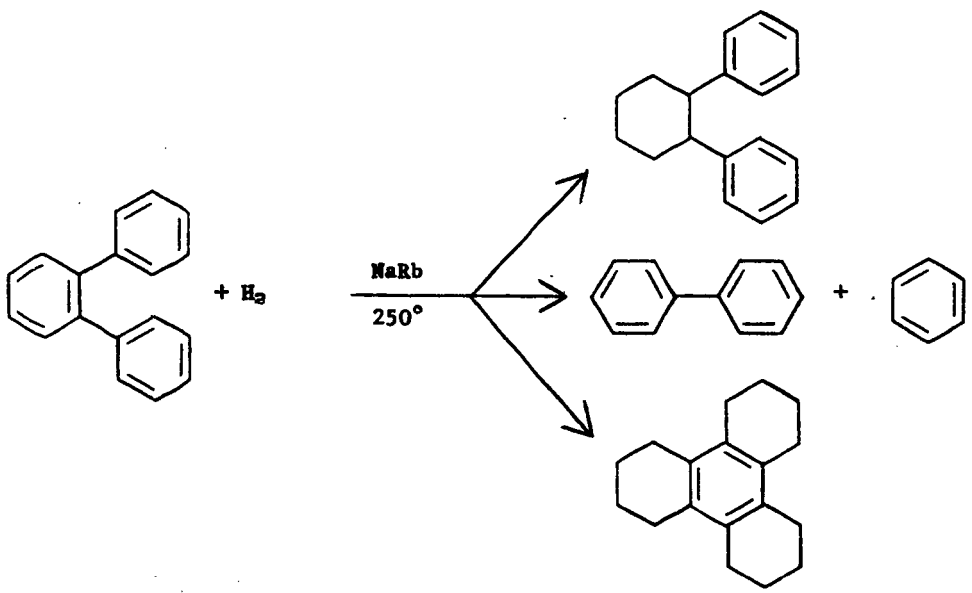

(9)

It thus appears that polyaryls are cleaved under these experimental conditions. In addition, small but measurable quantities of biphenyl appear to be formed by dimerization of the benzene used as solvent, while toluene dimerizes to give ditolyl and methylbiphenyl, the last by loss of a methyl group.

The presence in an aromatic molecule of oxygen-containing functional groups necessitates that sufficient catalyst be present to allow for the formation of an alkali metal salt of the hydroxyl group which may be formed. The major product formed in the NaRb catalyzed hydrogenation of 2-methoxynaphthalene is tetrahydronaphthalene with small amounts of 2-naphthol, dihydronaphthol, and tetrahydronaphthol as other important products. 2-Naphthol, at 220°, is hydrogenated to tetrahydronaphthalene, with a small amount of tetrahydronaphthol being formed, also. p-Phenylphenol, at 250°, forms phenylcyclohexane as the major product. 2-Naphthoic acid, also at 250°, is reduced and decarboxylated to tetrahydronaphthalene.

The reduction of anthraquinone at 250° also demonstrates that NaRb removes oxygen from organic compounds at elevated temperature and hydrogen pressure. In this case, octahydroanthracene is the principal product, with sym-octahydroanthranol as the only other important product.

Diphenylene oxide is converted primarily to phenylcyclohexane at 250° with small amounts of biphenyl and hexahydroterphenyl. This last product again indicates involvement of the solvent benzene.

In contrast to the reactivity of diphenylene oxide, dibenzothiophene, its sulfur analog, is relatively inert toward both hydrogenation and cleavage in the presence of NaRb. At 250°, some phenylthiophenol and biphenyl are formed, but most of the dibenzothiophene is recovered unchanged. This is also in contrast to Raney nickel or lithium-ethylenediamine reductions, both of which bring about desulfurization. The presence of sulfur compounds does not poison the alkali metal catalysts, and this is one important factor in their favor.

When nitrogen-containing heterocyclic aromatic compounds were hydrogenated, some ring cleavage and decomposition was noted. Pyridine, when used as a solvent, forms a variety of products, including tar. Quinoline with NaRb at 220°, is hydrogenated to tetrahydroquinoline, but at the same time it forms large quantities of dimers, in addition to a considerable number of unidentified products. Acridine and phenanthridine, at 250°, are hydrogenated to octahydro derivatives, apparently the unsymmetrical isomers.

Experiments to evaluate cesium as a catalyst were carried out in a manner similar to those involving rubidium, using cesium carbonate and sodium metal. Cesium proved to be a less active hydrogenation catalyst than rubidium, or about equal to potassium in catalytic activity.

Initially, benzene and toluene were used as solvents because of their lack of activity toward alkali metals. Since the work was directed primarily toward reductions of coal, it was apparent that a better coal solvent would be useful. Amines, which are good coal solvents, react with alkali metals to form amides:

$$M + RNH_2 \rightleftharpoons RNH^- + M^+ + \tfrac{1}{2}H_2$$

However, the reaction is probably reversible, so that in the presence of hydrogen, some metal remains, probably in solution. In any event, the catalytic hydrogenation does proceed in amine and in benzene-amine solvents. Whereas 180° is the lowest temperature at which measurable hydrogen uptake occurs with benzene as solvent, at 120° phenanthrene is hydrogenated to octahydrophenanthrene in ethylenediamine and in butylamine-benzene (1:1) with sodium and rubidium carbonate catalyst. By lowering the initial hydrogen pressure to 100 psi it is possible to prepare 1,2,3,4-tetrahydrophenanthrene in butylamine-benzene at 120°.

Similarly, other polycyclic hydrocarbons can be reduced at temperatures up to 200° in ethylenediamine and in ethylenediamine-benzene (1:1). In ethylenediamine, pyrene can be hydrogenated to a mixture containing tetra-, hexa-, and decahydropyrenes; in ethylenediamine-benzene, naphthacene is converted to a mixture of di-, hexa-, and octahydronaphthacenes. These results are roughly comparable to those obtained at 250° when benzene is used as solvent.

The use of alkali metals as catalysts for hydrogenation of coal tar and its fractions and of coal itself is currently under investigation. For example, a pitch which originally had a H_{arom}/H_{aliph} ratio of 4.26 was hydrogenated in toluene at 250°, using NaRb as catalyst. This ratio was reduced from 4.26 to 0.75. At 350°, in the absence of solvent, the ratio of H_{arom}/H_{aliph} was further reduced to 0.61.

Experimental

Reagents. The hydrocarbon solvents were dried over sodium. The ethylenediamine was refluxed with sodium and freshly distilled before use.

The reactants were obtained from standard suppliers. Where possible, reagent grade material was used.

The NaK (containing 76 percent potassium by weight) was generously provided by the Mine Safety Appliance Research Corp. The liquid NaK was transferred by means of a hypodermic syringe.

Analyses of products. Products were analyzed by gas-liquid chromatography where possible, and by low-voltage mass spectrometry routinely. This latter procedure provides a molecular weight distribution of products. In certain experiments, it was possible to isolate a specific component and identify it by infrared and ultraviolet spectrometry.

The procedure for all experiments was similar. Several examples will be given to illustrate the procedure. Results are tabulated in tables I-V.

Hydrogenation of Naphthalene

A solution of 30 grams of naphthalene in 150 milliliters of toluene was placed in an 0.5 liter Aminco rocking autoclave with 2 grams of NaK. The autoclave was pressured to 1,250 psig with hydrogen, and then heated to 250° C. It took 2-1/2 hours for the autoclave to reach this temperature. The autoclave was kept at 250° for 4-1/2 hours. The autoclave was allowed to cool overnight and isopropyl alcohol added to decompose the residual NaK and metal hydrides. The solution was

extracted with water to remove the sodium and potassium hydroxides, and the organic layer extracted with ether. The ether solution was distilled through a Helipack packed column to remove all solvents. The residue, containing the naphthalene and its reduction products, was examined by mass spectrometry and gas chromatography. It was found to consist of 91 percent tetrahydronaphthalene and 8 percent of dimeric products of molecular weights 260 and 262.

Hydrogenation of Phenanthrene

A solution of 5 grams of phenanthrene in 80 milliliters of benzene was placed in an Aminco rocking autoclave with 1.5 grams of sodium and 2.0 grams of rubidium carbonate. The autoclave was pressured to 1,400 psig with hydrogen, and then heated to 200° C. It took two hours for the autoclave to reach this temperature, which was maintained for 5 hours. The autoclave was allowed to cool overnight, and isopropyl alcohol added to decompose the metal hydrides. The solution was extracted with water to remove the metal hydroxides, and the organic layer extracted with ether. The ether and benzene were removed by distillation and the residue was examined by mass spectrometry. The product contained 10 percent dihydrophenanthrene and 78 percent octahydrophenanthrene, as well as smaller amounts of tetrahydrophenanthrene and phenanthrene. Traces of dimeric products were also present.

1. Birch, A. J., Quart. Revs., 4, 69 (1950).

2. Watt, G. W., Chem. Revs., 46, 317 (1950).

3. Benkeser, R. A., Advances in Chem. Ser., 23, 58 (1959).

4. Reggel, L., Friedel, R. A., and Wender, I., J. Org. Chem., 22, 891 (1957).

5. Mohler, H. and Sorge, J., Helv. Chim. Acta, 22, 229 (1939).

6. Hunt, S. E. and Lindsey, A. S., J. Chem. Soc., 1958, 2227.

7. Chu, T. L. and Yu, S. C., J. Am. Chem. Soc., 76, 3367 (1954).

8. Guyot, Chim et Ind. Spec. No. 410 (April 1928); C.A. 22, 4522 (1928).

9. Orlov, N. A. and Likhachev, N. D., Ber. 63B, 2179 (1930).

10. Bergstrom, F. W. and Carson, J. F., J. Am. Chem. Soc., 63, 2934 (1941).

11. Hügel, S. and Friess, J., Bull. Soc. Chim., 49, 1042 (1931).

Table I. Alkali metal catalyzed hydrogenations of polycyclic aromatic hydrocarbons

Compound	Catalyst	Temp., °C	Principal products[a]
Naphthalene	Li	325	Very little hydrogenation
	Na	300	Tetrahydronaphthalene
	NaK	250	Tetrahydronaphthalene
	NaRb	180	Tetrahydronaphthalene
Anthracene	Na	250	Dihydro-, tetrahydroanthracene
	NaK	250	Octahydro-, tetrahydroanthracene
	NaRb	220	Octahydroanthracene
Phenanthrene	Na	250	Tetrahydro-, dihydrophenanthrene
	NaK	250	Octahydrophenanthrene
	NaRb	200	Octahydrophenanthrene
Naphthacene	NaK	250	Dihydronaphthacene
	NaRb	300	Octahydronaphthacene
Chrysene	NaK	250	Hexahydro-, octahydro-, dodecahydrochrysene
	NaRb	250	Dodecahydrochrysene
Triphenylene	NaK	250	Dodecahydrotriphenylene
Pyrene	NaK	250	Dihydropyrene
	NaK	350	Decahydro-, hexahydropyrene
	NaRb	250	Decahydro-, dodecahydropyrene
Perylene	NaRb	250	Octahydro-, dodecahydroperylene
Fluorene	NaRb	250	Hexahydrofluorene, tetrahydrofluorene

[a] In order of decreasing yield.

Table II. Alkali metal catalyzed hydrogenations of polyaryl hydrocarbons

Compound	Catalyst	Temp., °C	Principal products[a/]
Biphenyl	NaK	350	Phenylcyclohexane
	NaRb	250	Phenylcyclohexane
o-Terphenyl	NaK	350	sym.-Dodecahydrotriphenylene
	NaRb	250	Biphenyl, sym.-dodecahydrotriphenylene, hexahydroterphenyl
1,3,5-Triphenylbenzene	NaRb	250	Hexahydro-, dodecahydro-, octadecahydrotriphenylbenzene, phenylcyclohexane

a/ In order of decreasing yield.

Table III. NaRb catalyzed hydrogenations of oxygenated aromatic compounds

Compound	Catalyst	Temp., °C	Principal products[a/]
2-Methoxynaphthalene	NaRb	250	Tetrahydronaphthalene, 2-naphthol, dihydro- and tetrahydronaphthol
2-Naphthol	NaRb	220	Tetrahydronaphthalene, tetrahydro-2-naphthol
p-Phenylphenol	NaRb	250	Phenylcyclohexane
2-Naphthoic acid	NaRb	250	Tetrahydronaphthalene
Anthraquinone	NaRb	250	Octahydroanthracene, sym.-octahydroanthranol

a/ In order of decreasing yield.

Table IV. NaRb catalyzed hydrogenations of heterocyclic aromatic compounds

Compound	Catalyst	Temp., °C	Principal products[a/]
Diphenylene oxide	NaRb	250	Phenylcyclohexane, biphenyl, hexahydroterphenyl
Dibenzothiophene	NaRb	250	Phenylthiophenol, biphenyl
Quinoline	NaRb	220	Tetrahydroquinoline, dimers
Acridine	NaRb	250	Octahydroacridine
Phenanthridine	NaRb	250	Octahydrophenanthridine

a/ In order of decreasing yield.

Table V. NaRb catalyzed hydrogenations in amine solvents

Compound	Catalyst	Temp., °C	Solvent	Principal products[a/]
Phenanthrene	NaRb	120	Ethylenediamine	Octahydrophenanthrene
	NaRb	120	Butylamine-benzene (1:1)	Octahydrophenanthrene
Pyrene	NaRb	200	Ethylenediamine	Tetrahydro-, hexahydro-, decahydropyrene
Naphthacene	NaRb	200	Ethylenediamine-benzene (1:1)	Dihydro-, octahydro-, hexahydronaphthacene

a/ In order of decreasing yield.

Chemistry of Benzologs of 4-Thiopyrone

P.H. Given, R.W. Wedel, S. Guha and J.R. Jones

Department of Fuel Technology, The Pennsylvania State University, University Park, Pennsylvania

The six compounds studied contained one, two or three benzene rings fused to each other or to the thiopyrone ring. Of the six, three have not been previously reported. The M.O.-L.C.A.O. method with the Hückel approximation has been used to calculate the π-electronic energy levels, bond orders, electron densities, localization energies and super-delocalizabilities. The calculations were made both assuming and neglecting participation of the d-orbital of the sulfur. Reasonably good straight line relationships were found between the calculated and experimental $N \rightarrow V_1$ transition energies (spectra determined in cyclohexane).

The calculated bond orders and charge densities indicated that there is a considerable degree of delocalization in the thiopyrone ring, and strong conjugation between sulfur and oxygen, with a greater separation of charge than in the oxygen analogs. The carbonyl vibrations are found at unusually low frequencies (1615-1640 cm^{-1}), again showing strong conjugation. The carbonyl frequency of 5,6-benzothiochromone is exceptionally low at 1615 cm^{-1}, suggesting the possibility of C-H-O hydrogen bonding with the 6' position; the proton in this position has a distinctive and very high chemical shift in the n.m.r. spectrum, at 10.1 p.p.m (TMS = 0).

The low bond order of the C=O bond suggests that the oxygen could be considered as an integral part of the π-electronic system. It therefore seems permissible to regard the polarographic half--wave potential in aprotic conditions as a measure of the energy required to put one electron in the lowest vacant π orbital. Accordingly, measured half wave potentials (dimethylformamide) were plotted against calculated LV orbital energies, and satisfactory correlation was found.

A comparison of the pyrolysis of dibenzothiophene and thioxanthen-9-one at 600°and 800° showed the former compound to be much more stable thermally; whereas the sulfur in the thiophene derivative was mostly retained in the carbonaceous char, in the pyrolysis of the thioxanthenone it was mostly released as sulfur dioxide.

Competing Reactions in Ozonation of Polycyclic Aromatic Hydrocarbons

Philip S. Bailey

Department of Chemistry, The University of Texas, Austin, Texas

Anthracene undergoes attack by ozone predominantly at the atoms of lowest atom or para localization energy. This occurs by two competing routes. The first involves one mole-equivalent of ozone and the formation of a trans-annular ozonide which affords either anthraquinone or ring rupture products, depending on the solvent and work-up conditions. The second route involves three mole-equivalents of ozone and results in anthraquinone and three mole-equivalents of molecular oxygen. Initial bond attack is a minor reaction.

Benz[a]anthracene undergoes the same competing reactions; bond attack competes more favorably than with anthracene, although it does not predominate over atom attack. The solvent appears to play a role in the competition.

From a survey of the recent literature regarding the ozonation of various polycyclic aromatic hydrocarbons, it can be seen that if the hydrocarbons are arranged in the order of decreasing differences between bond and atom localization energies, those in the upper part of the list undergo predominant atom attack, whereas those in the lower part of the list undergo predominant bond attack by ozone.

MO Studies of Aromatic Systems

Michael J.S. Dewar, Alice L.-H. Chung, Gerald J. Gleicher and Clifton C. Thompson

Department of Chemistry, The University of Texas, Austin, Texas

This paper will discuss the problem or aromaticity, and the calculation of physical and chemical properties of aromatic systems by quantum mechanical methods. A new approach based on the use of various modifications of the Pople SCF MO method will be described.

Competing Reactions in Ozonation of Polycyclic Aromatic Hydrocarbons

Philip S. Bailey

Department of Chemistry, The University of Texas, Austin, Texas

Anthracene undergoes attack by ozone predominantly at the atoms of lowest atom or para localization energy. This occurs by two competing routes. The first involves one mole-equivalent of ozone and the formation of a trans-annular ozonide which affords either anthraquinone or ring rupture products, depending on the solvent and work-up conditions. The second route involves three mole-equivalents of ozone and results in anthraquinone and three mole-equivalents of molecular oxygen. Initial bond attack is a minor reaction.

Benz[a]anthracene undergoes the same competing reactions; bond attack competes more favorably than with anthracene, although it does not predominate over atom attack. The solvent appears to play a role in the competition.

From a survey of the recent literature regarding the ozonation of various polycyclic aromatic hydrocarbons, it can be seen that if the hydrocarbons are arranged in the order of decreasing differences between bond and atom localization energies, those in the upper part of the list undergo predominant atom attack, whereas those in the lower part of the list undergo predominant bond attack by ozone.

MO Studies of Aromatic Systems

Michael J.S. Dewar, Alice L.-H. Chung, Gerald J. Gleicher and Clifton C. Thompson

Department of Chemistry, The University of Texas, Austin, Texas

This paper will discuss the problem or aromaticity, and the calculation of physical and chemical properties of aromatic systems by quantum mechanical methods. A new approach based on the use of various modifications of the Pople SCF MO method will be described.

Thermodynamic Studies of Polycyclic Aromatic Compounds

Brian D. Kybett and John L. Margrave

Department of Chemistry, Rice University, Houston, Texas

Available data for heats of combustion and vapor pressures of poly-- cyclic aromatic compounds will be presented and evaluated. Special attention will be directed toward cases where large strain energies are involved and toward heterocyclic systems.

Electronic Interactions in Paramagnetic Polycyclic Substances

S.I. Weissman

Department of Chemistry, Washington University, St. Louis, Missouri

All odd electron polycyclic substances and some even electron ones are paramagnetic. The paramagnetism permits detailed investigation of electronic interactions by magnetic resonance spectroscopy. The following properties will be discussed: spin distribution, rate of spin migration, spin-spin interactions, and inter-electron correlations.

The phenomena are illustrated by the behavior of hydrocarbon radicals, ketyls, and chelate compounds.

ESR Examination of the Electronic Distribution in Polycyclic Triplets

E. Wasserman, G. Smolinsky, A.M. Trozzolo and W.A. Yager

Bell Telephone Laboratories, Murray Hill, New Jersey

The parameters describing the magnetic dipole interaction of the unpaired electrons in a triplet state are easily obtained using randomly oriented samples. The values of D and E are sensitive measures of an averaged distance between the electrons. In the metastable π-π^* triplets responsible for the phosphorescence of aromatic hydrocarbons, both electrons are delocalized over the π- system. In many ground state triplets one electron may be effectively localized at one atom and serve as a probe of the density of the other electron at that center. Applications are made to determine the effect of substituents on delocalization in nitrenes and methylenes.

Thermodynamic Studies of Polycyclic Aromatic Compounds

Brian D. Kybett and John L. Margrave

Department of Chemistry, Rice University, Houston, Texas

Available data for heats of combustion and vapor pressures of poly-- cyclic aromatic compounds will be presented and evaluated. Special attention will be directed toward cases where large strain energies are involved and toward heterocyclic systems.

Electronic Interactions in Paramagnetic Polycyclic Substances

S.I. Weissman

Department of Chemistry, Washington University, St. Louis, Missouri

All odd electron polycyclic substances and some even electron ones are paramagnetic. The paramagnetism permits detailed investigation of electronic interactions by magnetic resonance spectroscopy. The following properties will be discussed: spin distribution, rate of spin migration, spin-spin interactions, and inter-electron correlations.

The phenomena are illustrated by the behavior of hydrocarbon radicals, ketyls, and chelate compounds.

ESR Examination of the Electronic Distribution in Polycyclic Triplets

E. Wasserman, G. Smolinsky, A.M. Trozzolo and W.A. Yager

Bell Telephone Laboratories, Murray Hill, New Jersey

The parameters describing the magnetic dipole interaction of the unpaired electrons in a triplet state are easily obtained using randomly oriented samples. The values of D and E are sensitive measures of an averaged distance between the electrons. In the metastable π-π^* triplets responsible for the phosphorescence of aromatic hydrocarbons, both electrons are delocalized over the π- system. In many ground state triplets one electron may be effectively localized at one atom and serve as a probe of the density of the other electron at that center. Applications are made to determine the effect of substituents on delocalization in nitrenes and methylenes.

Thermodynamic Studies of Polycyclic Aromatic Compounds

Brian D. Kybett and John L. Margrave

Department of Chemistry, Rice University, Houston, Texas

Available data for heats of combustion and vapor pressures of poly-- cyclic aromatic compounds will be presented and evaluated. Special attention will be directed toward cases where large strain energies are involved and toward heterocyclic systems.

Electronic Interactions in Paramagnetic Polycyclic Substances

S.I. Weissman

Department of Chemistry, Washington University, St. Louis, Missouri

All odd electron polycyclic substances and some even electron ones are paramagnetic. The paramagnetism permits detailed investigation of electronic interactions by magnetic resonance spectroscopy. The following properties will be discussed: spin distribution, rate of spin migration, spin-spin interactions, and inter-electron correlations.

The phenomena are illustrated by the behavior of hydrocarbon radicals, ketyls, and chelate compounds.

ESR Examination of the Electronic Distribution in Polycyclic Triplets

E. Wasserman, G. Smolinsky, A.M. Trozzolo and W.A. Yager

Bell Telephone Laboratories, Murray Hill, New Jersey

The parameters describing the magnetic dipole interaction of the unpaired electrons in a triplet state are easily obtained using randomly oriented samples. The values of D and E are sensitive measures of an averaged distance between the electrons. In the metastable π-π^* triplets responsible for the phosphorescence of aromatic hydrocarbons, both electrons are delocalized over the π- system. In many ground state triplets one electron may be effectively localized at one atom and serve as a probe of the density of the other electron at that center. Applications are made to determine the effect of substituents on delocalization in nitrenes and methylenes.